Phytochemical and Biological Studies of Extracts from Selected South African Indigenous Medicinal Plants: *Bulbine* and *Helichrysum* species

By

MASIXOLE MAKHABA

BSc. Chemistry, BSc. Honours Chemistry, and MSc. Chemistry (University of the Western Cape)

A thesis submitted in fulfilment of the requirements for the degree

Doctor of Philosophy

Department of Chemistry
Faculty of Natural Sciences
University of the Western Cape

Supervisor: Prof. W.T. Mabusela

December 2021

Abstract

Medicinal plants from the Asteraceae and Asphodelaceae families are among the most widely recognized in South African traditional medicine for managing diabetes mellitus. Diabetes mellitus is a universal epidemic, yet there are no permanent treatments for this disease. Three South African indigenous medicinal plants, namely *Helichrysum petiolare* (Asteraceae), *H. splendidum* (Asteraceae), and *Bulbine frutescens* (Asphodelaceae) which have reported ethnobotanical usage in the management of diabetes were investigated in this study. Despite the increasing scientific evidence using the extracts that supports the ethnobotanical claims of these medicinal plants, the active metabolites, or their mechanism of action is not considered. Phytochemical studies of leaf extracts (employing sequential extraction with solvents of different polarity) of the selected plants led to the isolation and characterization of twenty-six compounds (**1**-**26**); two of which are new from natural sources and were named petiolactone A (**1**) and B (**2**). Structural characterization of the isolated compounds was achieved by means of spectroscopic techniques (1D and 2D NMR, HRESIMS, and UV-vis). Biological screening of the extracts and isolated compounds in the α-glucosidase and α-amylase assays displayed no significant activity compared to the control. Cytotoxicity effects of the isolated compounds were also assessed using cell viability assay 3-(4, 5-dimethylthiazolyl-2)-2, 5-diphenyltetrazolium bromine (MTT) against triple the negative breast cancer cell line (MDA-MB-231). Compound **1** (petiolactone A) was found to be more active (IC_{50} = 107.8 and 43.65 µg/mL, respectively, after 24- and 72-hours exposure) compared to compound **2** (petiolactone B) its derivative, which proved to be toxic to the cells. It was proposed that this may be due to the differences in the substitution patterns of the pyrone-moiety. Other compounds that were found to be active included **21** and **22** (both with IC_{50} of 24.05 µg/mL), **16** (IC_{50} =38.04 µg/mL), **5**, (IC_{50} = 40.03 µg/mL), **17** (IC_{50} = 40.27 µg/mL), **3** (IC_{50} = 41.32 µg/mL), **19** (IC_{50} =48.79 µg/mL), as well as **14** and **15** mixtures (both with IC_{50} of 67.83 µg/mL). It was suggested that the lack of antidiabetic effect might be that the active metabolites towards diabetes have not been isolated or are not present in appreciable amounts in the leaves or there's a synergistic effect that occurs when the whole plant and/or extract is used. Future studies will be considered to target the active compounds and determine the possible mechanism of action in diabetes as well as cytotoxicity.

Keywords: *Helichrysum* genus. *Bulbine* genus. Novel pyrone-containing flavones. Cytotoxicity. α-Glucosidase. α-Amylase.

Declaration

I, **Masixole Makhaba** hereby declare that the "Phytochemical and biological studies of extracts from selected South African indigenous medicinal plants: *Bulbine* and *Helichrysum* species" is my original dissertation and to my knowledge, it has not been submitted anywhere else for the award of a degree at any other University. Where other written sources have been quoted, then their words have been re-written, but the general information attributed to them has been referenced. I further declare that ethical guidelines were complied with in conducting this study.

Date ……..…… Signed …M. Makhaba.....

Acknowledgements

I would like to take this opportunity to express my sincere gratitude and respect to my supervisor **Prof. W.T. Mabusela** for opening his doors and welcoming me with warmth since I joined in honors. To you Prof., I salute you for being a great mentor and father throughout the years.

To my "Organic A Laboratory" family, **Masande N. Yalo, Ndikho Nako, Zandile Mthembu, Olusola I. Watti, Kelly L.V. Correia, Sazi S. Thwala**, and **Dr. M. Koki** thank you for all the fun memories and shared experiences over the years.

A special thanks to the following great and special people: **Prof. E. Beukes** for the assistance with acquiring the NMR data, **Prof. A. Hussein Mohammed** for opening your laboratory, **Dr. J. Sagbo** and **Dr. R. Sharma** for all your efforts lastly, **Prof M. Onani** for everything (too many to count).

To the entire Chemistry Department, thank you! Thank you to the National Research Foundation (NRF) for the financial support.

Finally, to all my family and loved ones thank you so much for your prayers, love, and patience - I have done it!

Dedication

Let perseverance finish its work so that you may be mature and complete, not lacking anything." (Declares the Lord) – **James 1:4.**

To my whole family, the "**Makhaba Clan**", I hope this inspires a generation that is well rooted in education!

"**Tolo, Dlangamandla, Zulu, Mchenge, Mabhanekazi**, **Nongwandla**, **Ngwenyankomo**…"

Table of Contents

Chapter 5

Phytochemistry of *Helichrysum splendidum* (Thunb.) Less.

Chapter 6

Literature Review of the *Bulbine* Genus.

Chapter 7

Phytochemistry of *Bulbine frutescens* (L.) Willd.

List of Figures

List of Tables

List of Schemes

List of Plates

List of Abbreviations

Hex	Hexane
DCM	Dichloromethane
EtOAc	Ethyl acetate
BuOH	Butanol
MeOH	Methanol
DMSO-d_6	Deuterated dimethyl sulfoxide
J	Coupling constant
s	Singlet
d	Doublet
t	Triplet
m	Multiplet
brs	Broad Singlet
brt	Broad Triplet
brd	Broad Doublet
brq	Broad Quartet
ddd	Doublet-of-Doublet-of-Doublets
brdd	Broad-Doublet-of-Doublets
δ_C	Carbon Chemical Shift
δ_H	Proton Chemical Shift
NMR	Nuclear Magnetic Resonance
^{1}H-NMR	Proton Nuclear Magnetic Resonance
^{13}C-NMR	Carbon Thirteen Nuclear Magnetic Resonance
HSQC	Heteronuclear Single Quantum Coherence
HMBC	Heteronuclear Multiple Bond Correlation
COSY	Correlation Spectroscopy
NOE	Nuclear Overhauser Effect
TLC	Thin Layer Chromatography
LC-MS	Liquid Chromatography-Mass Spectroscopy
HRESIMS	High Resolution Electrospray Ionization Mass Spectrometry
DEPT-135	Distortionless Enhancement by Polarization

CD_3OD	Deuterated Methanol
$CDCl_3$	Deuterated Chloroform
D_2O	Deuterated Oxide
1D	One Dimension
2D	Two Dimension
MHz	Mega Hertz
Hz	Hertz
Fig.	Figure
Spp.	Species
mg	Milligram
g	Gram
UV	Ultraviolet

List of Isolated Compounds

Plant 1: *Helichrysum petiolare*

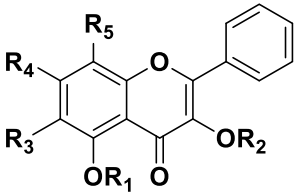

3 R_1 = H, R_2 = Me, R_3 = H, R_4 = OH, R_5 = H

4 R_1 = H, R_2 = H, R_3 = R_4 = R_5 = OMe

5 R_1 = H, R_2 = Me, R_3 = OH, R_4 = OMe, R_5 =H

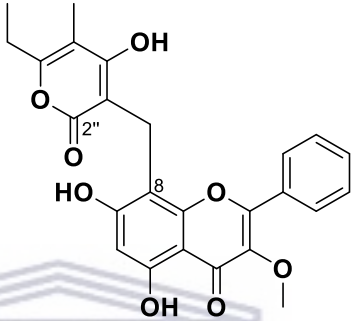

1

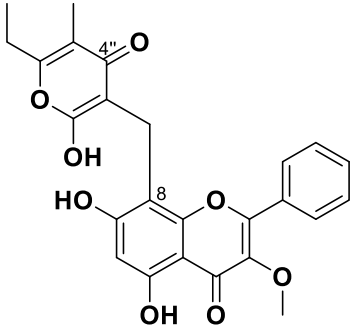

2

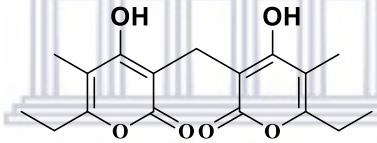

6

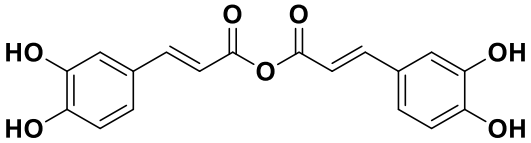

7

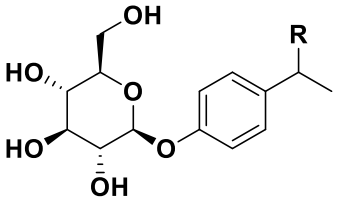

8 R = CO
9 R = OH

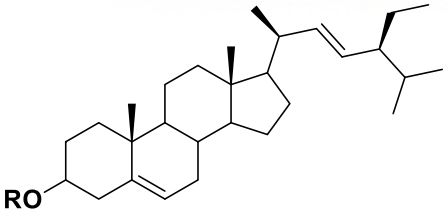

10 R = beta-D-glucoside
11a R = H

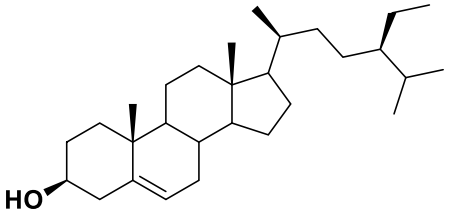

11b

Plant 2: *H. splendidum*

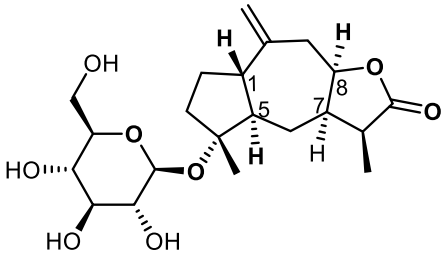

14

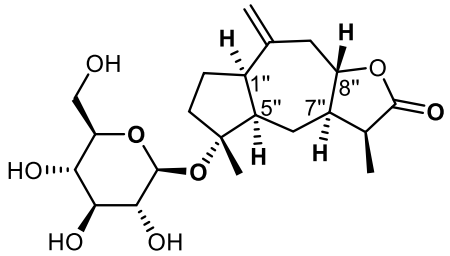

15

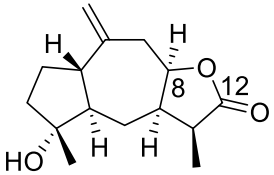

12

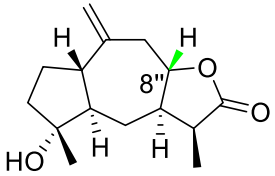

13

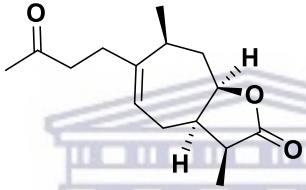

16

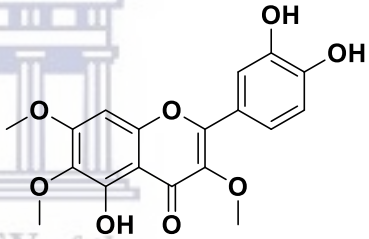

19

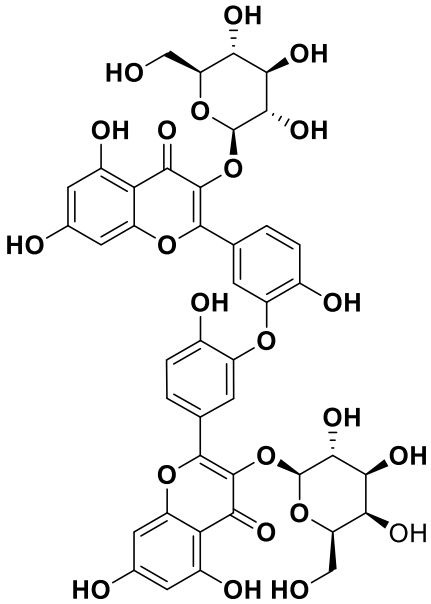

18

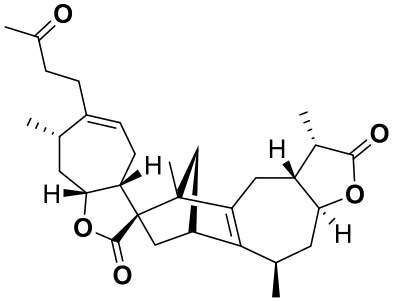

17

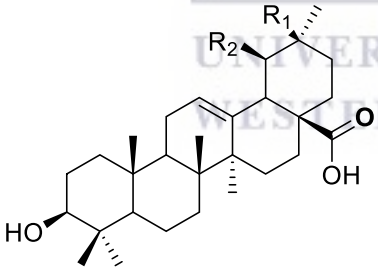

21 R_1 = Me, R_2 = H_2
22 R_1 = H, R_2 = Me

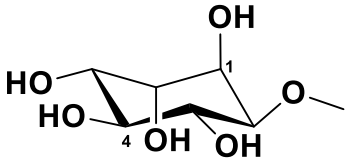

20

Plant 3: *Bulbine frutescens*

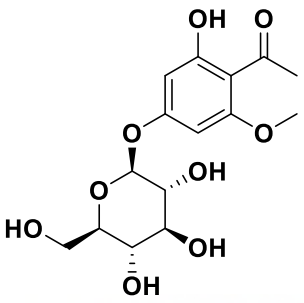

23

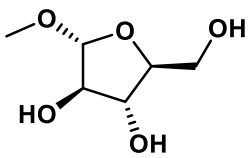

24

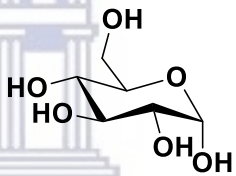

25

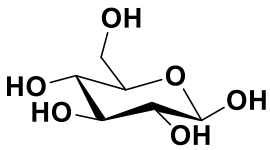

26

List of Proposed Publications

1. *Helichrysum* genus and compounds activities in the management of diabetes mellitus (doi.org/10.3390/plants11101386).
2. Isolation and identification of pyrone-containing flavone from *Helichrysum petiolare* (Manuscript submitted to *Plants Journal*).
3. Characterization of four new compounds from *Protea cynaroides* leaves and their tyrosinase inhibitory potential (Manuscript submitted to *Plants Journal*).

Chapter 1

Background of the Study.

1.1.Introduction

This chapter discusses diabetes mellitus and highlights the challenges that are associated with oral antidiabetic drugs. The later part of this chapter explores some South African indigenous medicinal plants as alternative strategies in the management of diabetes.

1.1.1. Diabetes Mellitus

Diabetes mellitus (DM) is one of the most common and very prevalent chronic diseases that are a major cause of global morbidity and mortality in both developing and developed countries (Erasto et al., 2005). It is a condition that arises "when there are raised levels of glucose in a person's blood because their body cannot produce any or enough of the hormone insulin or cannot effectively use the insulin it produces" (International Diabetes Federation, 2019). Epidemiological studies have shown that the chronic hyperglycaemia of diabetes is associated with various long-term and life-threatening complications such as dysfunction, and failure of different organs, especially the eyes, kidneys, nerves, heart, and blood vessels (Deshpande, Harris-Hayes and Schootman, 2008; American Diabetes Association, 2014). According to the International Diabetes Federation (2019), the estimated number of people globally who had diabetes between the years 2000 and 2019 was approximately 177 and 463 million, respectively. This number is projected to increase further to 552 million by the year 2030 (70% increase in developing countries and 20% in developed countries) (International Diabetes Federation, 2019; Mohiuddin et al., 2016).

Africa has a total population of approximately 1.37 billion people, from which South Africa accounts for close to 60.1 million (Stats S.A., 2021). In 2019 the recorded number of people aged between 20–79 years in Africa diagnosed with diabetes was 19.4 million. In South Africa, close to 4.6 million people had diabetes in the same year (Atlas, 2015; International Diabetes Federation, 2019). Therefore, this suggests that diabetes is emerging as a significant health problem in Africa, including South Africa (Mbanya, Bonicci and Nagan, 1996). In addition, due to its association with several microvascular (nephropathy, retinopathy, and nephropathy) and macrovascular complications (heart attacks, stroke, and peripheral vascular disease) (Bradshaw et al., 2007), it places a significant burden on the South African health

system. Thus, two common aetiological types of DM have been identified and are discussed below: the insulin dependent (type 1) and non-insulin dependent DM (type 2).

i. Type 1 DM

Type 1 DM is a disorder that occurs most frequently in children and young adults. This catabolic disorder arises from a cellular-mediated ($CD4^+$ and $CD8^+$ T-cells) autoimmune destruction of the β-cells of the islets of Langerhans in the pancreas with consequent insulin deficiency (Zimmet et al., 2003; Filippi and von Herrath, 2008). Markers of the immune destruction of the β-cell include islet cell autoantibodies (ICA), autoantibodies to insulin, autoantibodies to glutamic acid decarboxylase (GAD65), and autoantibodies to the tyrosine phosphatases IA-2 and IA-2β (American Diabetes Association, 2014). As such, the onset of type 1 DM becomes clinically apparent only after significant destruction of the β-cell mass, which reduces the ability to maintain glycaemic control and metabolic function (Lebastchi and Herold, 2012). This means that in type 1 DM the body produces very little or not enough insulin (thus a diagnosed person depends on insulin for survival), which may ultimately lead to severe chronic hyperglycaemia. Furthermore, autoimmune destruction of β-cells is associated with multiple genetic predispositions, such as the human leukocyte antigen (HLA) on chromosome 6p21 and the insulin gene on chromosome 11p1 (Sirdah and Reading, 2020). The clinical presentation of type 1 DM varies significantly but may include polyuria, polydipsia, and polyphagia, nausea, thirst, and blurred vision (International Diabetes Federation, 2019).

ii. Type 2 DM

Type 2 DM is a heterogeneous disorder that is strongly allied with insulin resistance (mainly in the skeletal muscle and liver) and impaired insulin secretion which is caused by pancreatic β-cell dysfunction (Atlas, 2015). Notably, insulin resistance is associated with obesity, dyslipidaemia, and hypertension, which are considered early signs in most patients who eventually develop type 2 DM (Collins, 2002). Furthermore, type 2 diabetes is characterized by hyperglycaemia during fasting and after eating. Type 2 DM has been found to be the most predominant form of diabetes globally, accounting for over 90% of all reported cases (Levitt, 2008). In the year 2000, it was estimated that 87% of diabetes cases in South Africa were attributed to excess body weight, from which boys and girls (<20 years) accounted for approximately 16.6%, while men and

women (20< years) were about 55.5% (Ng et al., 2014). Type 2 DM can be managed through diet control and consumption of oral drugs containing hypoglycaemic agents.

1.1.2. Treatment and Challenges Associated with Oral Antidiabetic Drugs

As previously stated, DM can be defined as a chronic or heterogeneous group of diseases which result in hyperglycaemia. There are several oral antidiabetic drugs which are currently accessible to manage this chronic disease via different modes of action. For instance, *α*-glucosidase and *α*-amylase inhibiting agents which act by delaying digestion and absorption of the intestinal carbohydrate in type 2 DM (Etsassala et al., 2019). Biguanides, another group of oral antidiabetic drugs, reduce hepatic glucose production, and sulfonylureas which stimulate insulin secretion (Sena et al., 2010). Others include thiazolidinediones which function by improving the insulin action (Rizos et al., 2009). Despite this, the usefulness of these drugs is hindered by their adverse side effects and exorbitant prices. In addition, some show limited efficacy, failure in metabolism adjustment, and the prevention of diabetic complications (Chen et al., 2020). These are briefly discussed in Table 1.1 below.

Table 1.1: Treatment and challenges associated with oral antidiabetic drugs

Antidiabetic drug	Route of glycaemic control	Disadvantages
i. *α*-Glucosidase and *α*-amylase inhibition		
❖ Acarbose, miglitol, voglibose	❖ Postprandial glucose levels.	❖ Associated with frequent gastrointestinal side effects such as diarrhoea, abdominal pain, flatulence, and increased transaminase (Uwaifo and Ratner, 2007). ❖ Expensive (Nathan et al., 2006)
ii. Biguanides		
❖ Metformin, buformin	❖ Fasting glucose, and insulin sensitivity.	❖ Although rare, they are known to cause lactic acidosis in people with severe kidney impairment, heart failure, and gastrointestinal effects (Uwaifo and Ratner, 2007).

		❖ Continued use, overtime, may interfere (block) with vitamin B12 absorption in the body (Ting et al., 2006).
iii. Sulfonylureas		
❖ Chlorpropamide, tolazamide, tolbutamide, glibenclamide (glyburide)	❖ Fasting glucose, and postprandial glucose.	❖ Generally, cause weight gain and hypoglycaemia (Uwaifo and Ratner, 2007). ❖ They have limited durability of effect (Sena et al., 2010).
iv. Thiazolidinedione		
❖ Rosiglitazone (Avandia), pioglitazone (Actos)	❖ Insulin sensitivity, postprandial, and fasting glucose.	❖ Weight gain (Nathan et al., 2006). ❖ Causes fluid retention which can aggravate cardiac status in patients with heart failure (Guan et al., 2005). ❖ Generally, they may cause hepatotoxicity (fatal in the case of troglitazone) in patients with impaired liver function (Marcy, Britton and Blevins, 2004).
v. Others		
❖ DPP-4 inhibitors (Sitagliptin)	❖ Postprandial glucose.	❖ Upper respiratory infection, nasopharyngitis, and headache (Sena et al., 2010). ❖ Expensive (Uwaifo and Ratner, 2007).

1.1.3. **Traditional Medicine**: *a summary of some South African medicinal plants traditionally used to manage diabetes*

According to World Health Organization (2005), traditional medicine (TM) or known locally as '*muthi*' can be define as:

> 'The sum total of the knowledge, skills and practices based on the theories, beliefs and experiences indigenous to different cultures, whether explicable or not, used in the maintenance of health, as well as in the prevention, diagnosis, improvement or treatment of physical and mental illnesses.'

Despite the strides in modern medicine for the treatment of diabetes mellitus, TM is still very popular in South Africa. It is estimated that there are approximately 500 medicinally recognized plants that are traded on the day-to-day in informal medicinal plant markets across the country (Arnold and De Wet, 1993; Mander, 1998; Mulholland, 2005; Mander et al., 2007). Among these medicinal plants, some of the most studied with known antidiabetic activity include *Hypoxis argentae*, *H. hemerocallidea*, *Tarchonanthus camphoratus*, *Euclea undulata*, *Strychnos henningsii*, *Cissampelo campensis*, *Elaeodendron transvaalense*, *Schkuria pinnata*, *Vernonia amygdalina*, *Catharanthus roseus*, *Senna alexandri*, *Cymbopogon citrutus*, *Nuxia floribunda*, and *Curcubita pepo*, and *Sutherlandia frutescens* (Nyakudya et al., 2020). The use of these medicinal plants, particularly in the treatment of diabetes, is strongly influenced by inaccessibility, cultural importance, exorbitant prices, and undesirable side effects of western medicines (Light et al., 2005). Plants contain a plethora of secondary metabolites (flavonoids, phenolics, sesquiterpene lactone, triterpene, diterpene, alkaloids) which render them useful in treating ailments such as diabetes. Nevertheless, the challenges associated with most plants that are used in South African TM for the management of diabetes are that many of them are yet to be scientifically investigated or that their modes of action are not well reported. Since the investigated plant species in this study are from the Asteraceae and Asphodelaceae families, thus this section will only highlight South African indigenous species from these families which are used in TM to manage diabetes along with their known mechanism of action (Table 1.2).

Table 1.2: Some South African indigenous medicinal plants from Asteraceae and Asphodelaceae families that are used in traditional medicine to manage diabetes with reported antidiabetic activity

Scientific name [vernacular names]	Methods of preparation	Route of administration	Antidiabetic activity	Reference
❖ *Aloe arborescens* Mill. [Ikalene (*isiXh.); inkalane, umhlabana (*isiZu.); tshikhopha (*V.); kransaalwyn (*Afr.)]	❖ Decoction.	❖ Orally.	❖ The aqueous leaf gel extract using alloxan-induced diabetic rats via inhibition on the destruction of islets of Langerhans.	❖ Mogale et al. (2011)[#] ❖ Semenya and Maroyi, (2019)
❖ *Aloe ferox* Mill. [Ikhala (*isiXh.); inhlaba (*isiZ.); bitteraalwyn, bergaalwyn (*Afr.)]	❖ Decoction.	❖ Orally.	❖ The ethanol leaf gel extract in (STZ)-induced type 2 diabetes rat model through increased insulin secretion.	❖ Cock, Ndlovu and Van Vuuren (2021) ❖ Loots et al. (2011)[#]
❖ *Aloe greatheadii* var. *davyana* (Schonland) ¨ Glen & D.S.Hardy [Kgopane (*Ts.); transvaalaalwyn, grasaalwyn (*Afr.)]	❖ Decoction.	❖ Not specified.	❖ The ethanol leaf gel extract in (STZ)-induced type 2 diabetes rat model through increased insulin secretion.	❖ Cock, Ndlovu and Van Vuuren (2021) ❖ Loots et al. (2011)[#]

❖ *Artemisia afra* Jacq. ex Willd. [Umhlonyane (*isiXh.); mhlonyane (*isiZu.); lengana (*T.); zengana (*S.S.); wilde-als (*Afr.)]	❖ Decoction (mixed with sugar to mask bitterness)	❖ Orally	❖ The aqueous leaf extract (50, 100, and 200 mg/kg body weight) against STZ-induced diabetic rats promotes insulin secretion).	❖ Erasto et al. (2005) ❖ Sunmonu and Afolayan (2013)[#]
❖ [a]***Bulbine spp.***			**This genus is discussed separately in** chapter 6.	
❖ *Brachylaena discolor* DC. [Umphahla (*isiXh.); phahla, isiduli, isiphahluka (*isiZu.); mphahla (*N.S.); kusvaalbos (*Afr.)]	❖ Infusion.	❖ Orally.	❖ Glucose utilisation activity of the DCM:MeOH (1:1) extract (leaf, stem and root) against Chang liver, 3T3-L1 adipose, and C2C12 muscle cell.	❖ Erasto et al. (2005) ❖ van de Venter et al. (2008)[#]
❖ *Brachylaena elliptica* (Thunb.) DC. [Isiduli, isagqeba, umphahla (*isiXh.); isiduli-ehlathi, igqeba-elimnyama, iphahle,	❖ Infusion.	❖ Orally or gargle.	❖ The aqueous leaf extract had potent glucose utilization in HepG2 cells via activation of the MAPK and P13K pathways.	❖ Palgrave (2015) ❖ Sagbo et al. (2018)[#]

uhlunguhlungu (*isiZu.); bitterblaar, suurbos (*Afr.)]				
❖ *Brachylaena ilicifolia* (Lam.) E.Phillips and Schweick. [Bitterblaar, hulsbitterblaar (*Afr.); igqeba (*isiXh.)]	❖ Decoction.	❖ Orally.	❖ The aqueous leaf extract had potent glucose utilization in HepG2 cells via activation of the MAPK and P13K pathways.	❖ Cock, Ndlovu and Van Vuuren (2021) ❖ Sagbo (2017)[#]
❖ *Dicoma anomala* Sond. [Inyongana (*isiXh.); isihlabamakhondlwane, umuna (*isiZu.); hloenya, mohlasetse (*S.S.); maagbitterwortel, kalwerbossie, koorsbossie, gryshout, maagbossie (*Afr.)]	❖ Decoction.	❖ Orally.	❖ The DCM:MeOH root extract exhibited potent inhibitory effect on DPP-IV, and potent modulatory effects on hepatic cells glucose utilization in 3T3-L1 adipocytes.	❖ Moteetee, Moffett and Seleteng-Kose (2019) ❖ Matsabisa et al. (2020)[#]
❖ ***[b]Helichrysum spp.***	**This genus is discussed separately in chapter 3**.			

❖ *Pteronia divaricata* (P.J.Bergius) Less. [Geelgombos, geelknopbos, spalkpenbos (*Afr.)]	❖ Decoction.	❖ Orally.	❖ Whole acetone plant extract showed inhibition of α-glucosidase (IC_{50} = 31.22 ± 0.35µg/mL) and α-amylase (IC_{50} = 36.30 ± 4.62 µg/mL).	❖ Deutschländer, Lall and Van De Venter (2009a) ❖ Deutschländer et al. (2009b)[#]
❖ *Tarchonanthus camphoratus* L. [Moologa (*V.); mofahlana (S.S.); igqeba emLimhlophe (*isiZu.); wildekanferbos (*Afr.); mofathla (*T.)]	❖ Not specified.	❖ Not specified.	❖ The aqueous whole leaf extract had significant glucose utilisation activity in Chang liver cells (131.5%). The ethanol extract moderate in C2C12 muscle cells.	❖ van Huyssteen et al., (2011)
❖ *Tagetes minuta* L. [Kakiebos, khakibos, langkakiebos, stinkbos, stinkkhakibos, transvaalse kakiebos (*Afr.), mbanje (*isiNd.)]	❖ Not specified.	❖ Not specified.	❖ The aerial EtOAc plant extract showed inhibition in the α-amylase enzyme assay (IC_{50} not given).	❖ Davids, Gibson and Johnson (2016) ❖ Ibrahim et al. (2015)[#]

❖ *Vernonia amygdalina* (Delile) Sch.Bip. ex Walp.	❖ Infusion.	❖ Orally.	❖ The ethanol leaf extract (300 mg/kg) against STZ-induced diabetic rats. Results showed regeneration of the β-cells of the pancreas.	❖ Asante et al. (2016)[#] ❖ Erasto et al. (2005)

[a] -*Bulbine spp.* = see chapter 6 for the detailed discussion of the literature. [b] -*Helichrysum spp.* = see chapter 3 for the detailed discussion of the literature. [#] -Reference showing the antidiabetic study of the plants. [*] -isiXh. = isiXhosa. isiZu. = isiZulu. isiNd. = isiNdebele. S.S. = Southern Sotho. N.S. = North Sotho. T. = Tswana. Se. = Sepedi. Afr. = Afrikaans. V. = Venda (or Tshivenda). Ts. = Tsonga. Abbreviation = Streptozotocin (STZ), dipeptidyl peptidase-4 (DPP-IV), ethyl acetate (EtOAc), dichloromethane (DCM), methanol (MeOH), phosphoinositide 3-kinase (P13K), mitogen-activated protein kinase (MAPK), half maximal inhibitory concentration (IC_{50}).

1.1.4. Rational of the Study

Diabetes mellitus is a universal epidemic. It is one of the most common and very prevalent chronic diseases that are a major cause of global morbidity and mortality in both developing and developed countries (Erasto et al., 2005). Epidemiological studies have shown that the chronic hyperglycaemia of diabetes mellitus is associated with various long-term and life-threatening complications such as dysfunction and failure of different organs, especially the eyes, kidneys, nerves, heart, and blood vessels (Deshpande, Harris-Hayes and Schootman, 2008; American Diabetes Association, 2014). Efforts are continuously taken to find lasting curative agents to treat diabetes mellitus. The main problem with current oral antidiabetic drugs includes several undesirable side effects, exorbitant prices, limited efficacy, failure in metabolism adjustment, and the prevention of diabetic complications (Chen et al., 2020). These shortcomings have led to the search for medicinal plants with hypoglycaemic properties and consequently their use in the management of diabetes. Ethnobotanical reports suggest that there are at least 1 200 medicinal plants used traditionally to manage diabetes mellitus in different cultures, globally (Mogale et al., 2011). In South Africa, it is estimated that approximately 80% of the population consult as many as 200 000 indigenous healers for ailments such as diabetes (Gericke, 2002; McKean et al., 2013). Most of the work that is done on South African indigenous medicinal plants, in relation to diabetes mellitus, has only focused on the biological evaluation of the extracts. This means that the antidiabetic activity is inappropriately credited to the extracts and the active metabolites, or their mechanism of action is not considered. In this study, three South African indigenous medicinal plants from the Asteraceae (*Helichrysum petiolare* and *H. splendidum*) and Asphodelaceae (*Bulbine frutescens*) families, which are implicated in the management of diabetes mellitus, were selected to carry out a phytochemical evaluation to provide a rationale for their ethnopharmacological use. The isolation and identification of active compounds of either species will go a long way in promoting the use and acceptance of these medicinal plants (*Helichrysum petiolare, H. splendidum,* and *Bulbine frutescens*) as antidiabetic agents. Furthermore, the results of this study may potentially add value to the ongoing investigations of establishing a complete pharmacopeia of South African indigenous medicinal plants.

1.1.5. Research Aims and Objectives

The aim of this study was to carry-out an extensive phytochemical and biological evaluation of the crude extracts from three South African indigenous medicinal plants (*H. petiolare*, *H. splendidum*, and *Bulbine futescens*) which are used traditionally to manage diabetes.

The specific objectives of the research study were:

a) To prepare the crude extracts of each plant by liquid-liquid extraction (sequentially) using hexane, dichloromethane (DCM), ethyl acetate (EtOAc), and butanol (BuOH).
b) To isolate using column and high-performance liquid chromatography (HPLC), identify (HPLC-mass spectrometry), and characterize the secondary metabolites by nuclear magnetic resonance (NMR), MS, and Fourier-transform infrared spectroscopy (FTIR) spectroscopic techniques.
c) To assess the bioactivity of the extracts and compounds of each plant for inhibiting α-glucosidase and α-amylase enzymes; thereby validating their ethnopharmacological use in the management of diabetes.
d) To assess the cytotoxicity effects of the extracts and compounds against cell viability assay.

References

American Diabetes Association, 2014. Diagnosis and classification of diabetes mellitus. *Diabetes care*, *37*(Supplement 1), pp. S81-S90.

Arnold, T.H. and De Wet, B.C., 1993. *Plants of southern Africa: names and distribution*. National Botanical Institute.

Asante, D.B., Effah-Yeboah, E., Barnes, P., Abban, H.A., Ameyaw, E.O., Boampong, J.N., Ofori, E.G. and Dadzie, J.B., 2016. Antidiabetic effect of young and old ethanolic leaf extracts of *Vernonia amygdalina*: A comparative study. *Journal of diabetes research*, *2016*.

Atlas, D., 2015. International diabetes federation. *IDF Diabetes Atlas, 7th edn. Brussels, Belgium: International Diabetes Federation*.

Bradshaw, D., Norman, R., Pieterse, D. and Levitt, N.S., 2007. Estimating the burden of disease attributable to diabetes South Africa in 2000. *South African Medical Journal*, *97*(8), pp.700-706.

Chen, X., Gao, M., Jian, R., Hong, W.D., Tang, X., Li, Y., Zhao, D., Zhang, K., Chen, W., Zheng, X. and Sheng, Z., 2020. Design, synthesis, and α-glucosidase inhibition study of novel embelin derivatives. *Journal of Enzyme Inhibition and Medicinal Chemistry*, *35*(1), pp.565-573.

Cock, I.E., Ndlovu, N. and Van Vuuren, S.F., 2021. The use of South African botanical species for the control of blood sugar. *Journal of Ethnopharmacology*, *264*, p.113234.

Collins, F.M., 2002. Current treatment approaches to type 2 diabetes mellitus: successes and shortcomings. *American Journal of Managed Care*, *8*, pp. S460-S471.

Davids, D., Gibson, D. and Johnson, Q., 2016. Ethnobotanical survey of medicinal plants used to manage high blood pressure and type 2 diabetes mellitus in Bitterfontein, Western Cape Province, South Africa. *Journal of ethnopharmacology*, *194*, pp.755-766.

Deshpande, A.D., Harris-Hayes, M. and Schootman, M., 2008. Epidemiology of diabetes and diabetes-related complications. *Physical therapy*, *88*(11), pp.1254-1264.

Deutschländer, M.S., Lall, N. and Van De Venter, M., 2009a. Plant species used in the treatment of diabetes by South African traditional healers: An inventory. *Pharmaceutical Biology*, *47*(4), pp.348-365

Deutschländer, M.S., Van de Venter, M., Roux, S., Louw, J. and Lall, N., 2009b. Hypoglycaemic activity of four plant extracts traditionally used in South Africa for diabetes. *Journal of Ethnopharmacology*, *124*(3), pp.619-624.

Erasto, P., Adebola, P.O., Grierson, D.S. and Afolayan, A.J., 2005. An ethnobotanical study of plants used for the treatment of diabetes in the Eastern Cape Province, South Africa. *African Journal of Biotechnology*, *4*(12).

Etsassala, N.G., Badmus, J.A., Waryo, T.T., Marnewick, J.L., Cupido, C.N., Hussein, A.A. and Iwuoha, E.I., 2019. Alpha-glucosidase and alpha-amylase inhibitory activities of novel abietane diterpenes from *Salvia africana-lutea*. *Antioxidants*, *8*(10), p.421.

Filippi, C.M. and von Herrath, M.G., 2008. Viral trigger for type 1 diabetes: pros and cons. *Diabetes*, *57*(11), pp.2863-2871.

Gericke, N., 2002. Plants, products, and people: Southern African perspectives. In *Advances in Phytomedicine* (Vol. 1, pp. 155-162). Elsevier.

Guan, Y., Hao, C., Cha, D.R., Rao, R., Lu, W., Kohan, D.E., Magnuson, M.A., Redha, R., Zhang, Y. and Breyer, M.D., 2005. Thiazolidinediones expand body fluid volume through

PPARγ stimulation of ENaC-mediated renal salt absorption. *Nature medicine*, *11*(8), pp.861-866.

Ibrahim, S.R., Mohamed, G.A., Abdel-Latif, M.M., El-Messery, S.M., Al Musayeib, N.M. and Shehata, I.A., 2015. Minutaside A, new α-amylase inhibitor flavonol glucoside from *Tagetes minuta*: Antidiabetic, antioxidant, and molecular modeling studies. *Starch-Stärke*, *67*(11-12), pp.976-984.

International Diabetes Federation, 2019. IDF diabetes atlas ninth edition 2019.

Lebastchi, J. and Herold, K.C., 2012. Immunologic and metabolic biomarkers of β-cell destruction in the diagnosis of type 1 diabetes. *Cold Spring Harbor perspectives in medicine*, *2*(6), p.a007708.

Levitt, N.S., 2008. Diabetes in Africa: epidemiology, management, and healthcare challenges. *Heart*, *94*(11), pp.1376-1382.

Light, M.E., Sparg, S.G., Stafford, G.I. and Van Staden, J., 2005. Riding the wave: South Africa's contribution to ethnopharmacological research over the last 25 years. *Journal of Ethnopharmacology, 100*(1-2), pp. 127-130.

Loots, D.T., Pieters, M., Islam, M.S. and Botes, L., 2011. Antidiabetic effects of *Aloe ferox* and *Aloe greatheadii* var. davyana leaf gel extracts in a low-dose streptozotocin diabetes rat model. *South African Journal of Science*, *107*(7), pp.1-6.

Mander, M., 1998. Marketing of indigenous medicinal plants in South Africa: a case study in KwaZulu-Natal.

Mander, M., Ntuli, L., Diederichs, N. and Mavundla, K., 2007. Economics of the traditional medicine trade in South Africa: health care delivery. *South African health review*, *2007*(1), pp.189-196.

Marcy, T.R., Britton, M.L. and Blevins, S.M., 2004. Second-generation thiazolidinediones and hepatotoxicity. *Annals of Pharmacotherapy*, *38*(9), pp.1419-1423.

Matsabisa, M.G., Chukwuma, C.I., Chaudhary, S.K., Kumar, C.S., Baleni, R., Javu, M. and Oyedemi, S.O., 2020. *Dicoma anomala* (Sond.) abates glycation and DPP-IV activity and modulates glucose utilization in Chang liver cells and 3T3-L1 adipocytes. *South African Journal of Botany*, *128*, pp.182-188.

Mbanya, J.C., Bonicci, F. and Nagan, K., 1996. Guidelines for the Management of NIDDM in Africa. *A consensus document, Greece, Novo Nordisk A/s*, p.1Á.

McKean, S., Mander, M., Diederichs, N., Ntuli, L., Mavundla, K., Williams, V. and Wakelin, J., 2013. The impact of traditional use on vultures in South Africa. *Vulture News*, *65*, pp.15-36.

Mogale, M.A., Lebelo, S.L., Shai, L.J. and Eloff, J.N., 2011. *Aloe arborescens* aqueous gel extract alters the activities of key hepatic enzymes and blood concentration of triglycerides, glucose, and insulin in alloxan-induced diabetic rats. *African Journal of Biotechnology*, *10*(20), pp.4242-4248.

Mohiuddin, M., Arbain, D., Islam, A.S., Ahmad, M.S. and Ahmad, M.N., 2016. Alpha-glucosidase enzyme biosensor for the electrochemical measurement of antidiabetic potential of medicinal plants. *Nanoscale research letters*, *11*(1), pp.1-12.

Moteetee, A., Moffett, R.O. and Seleteng-Kose, L., 2019. A review of the ethnobotany of the Basotho of Lesotho and the Free State Province of South Africa (South Sotho). *South African Journal of Botany*, *122*, pp.21-56.

Mulholland, D.A., 2005. The future of ethnopharmacology: A southern African perspective. *Journal of ethnopharmacology*, *100*(1-2), pp.124-126.

Nathan, D.M., Buse, J.B., Davidson, M.B., Ferrannini, E., Holman, R.R., Sherwin, R. and Ting, R.Z.W., Szeto, C.C., Chan, M.H.M., Ma, K.K. and Chow, K.M., 2006. Risk factors of vitamin B12 deficiency in patients receiving metformin. *Archives of internal medicine*, *166*(18), pp.1975-1979.

Ng, M., Fleming, T., Robinson, M., Thomson, B., Graetz, N., Margono, C., Mullany, E.C., Biryukov, S., Abbafati, C., Abera, S.F. and Abraham, J.P., 2014. Global, regional, and national prevalence of overweight and obesity in children and adults during 1980–2013: a systematic analysis for the Global Burden of Disease Study 2013. *The lancet*, *384*(9945), pp.766-781.

Nyakudya, T.T., Tshabalala, T., Dangarembizi, R., Erlwanger, K.H. and Ndhlala, A.R., 2020. The potential therapeutic value of medicinal plants in the management of metabolic disorders. *Molecules*, *25*(11), p.2669.

Palgrave, K.C., 2015. *Palgrave's trees of southern Africa*. Penguin Random House South Africa.

Rizos, C.V., Elisaf, M., Mikhailidis, D.P. and Liberopoulos, E.N., 2009. How safe is the use of thiazolidinediones in clinical practice? *Expert opinion on drug safety*, *8*(1), pp.15-32.

Sagbo, I.J., van de Venter, M., Koekemoer, T. and Bradley, G., 2018. In vitro antidiabetic activity and mechanism of action of *Brachylaena elliptica* (Thunb.) DC. *Evidence-Based Complementary and Alternative Medicine*, *2018*.

Sagbo, I.J., 2017. Antidiabetic activity and mechanism of action of extracts of *Brachylaena elliptica* (Thurb.) DC. and *Brachylaena ilicifolia* (Lam) Phill and Schweick.

Sena, C.M., Bento, C.F., Pereira, P. and Seiça, R., 2010. Diabetes mellitus: new challenges and innovative therapies. *EPMA Journal*, *1*(1), pp.138-163.

Semenya, S.S. and Maroyi, A., 2019. A review of plants used against diabetes mellitus by Bapedi and Vhavenda ethnic groups in the Limpopo province, South Africa. *Asian J Pharmaceut Clinical Res*, *12*, pp.44-50.

Sirdah, M.M. and Reading, N.S., 2020. Genetic predisposition in type 2 diabetes: A promising approach toward a personalized management of diabetes. *Clinical genetics*, *98*(6), pp.525-547.

Stats, S.A., 2021. Statistical Release P0302. Mid-year population estimates 2020.

Sunmonu, T.O. and Afolayan, A.J., 2013. Evaluation of antidiabetic activity and associated toxicity of *Artemisia afra* aqueous extract in wistar rats. *Evidence-Based Complementary and Alternative Medicine*, *2013*.

Uwaifo, G.I. and Ratner, R.E., 2007. Differential effects of oral hypoglycaemic agents on glucose control and cardiovascular risk. *The American journal of cardiology*, *99*(4), pp.51-67.

van de Venter, M., Roux, S., Bungu, L.C., Louw, J., Crouch, N.R., Grace, O.M., Maharaj, V., Pillay, P., Sewnarian, P., Bhagwandin, N. and Folb, P., 2008. Antidiabetic screening and scoring of 11 plants traditionally used in South Africa. *Journal of ethnopharmacology*, *119*(1), pp.81-86.

van Huyssteen, M., Milne, P.J., Campbell, E.E. and van de Venter, M., 2011. Antidiabetic and cytotoxicity screening of five medicinal plants used by traditional African health practitioners in the Nelson Mandela Metropole, South Africa. *African Journal of Traditional, Complementary and Alternative Medicines*, *8*(2).

World Health Organization, 2005. *National policy on traditional medicine and regulation of herbal medicines: Report of a WHO global survey*. World Health Organization.

Zimmet, P., Cowie, C., Ekoe, J.M. and Shaw, J., 2003. Classification of diabetes mellitus and other categories of glucose intolerance. *International textbook of diabetes mellitus*.

Chapter 2

Research Methodologies.

2.1.General Experimental Procedures

The 1D (^{1}H, ^{13}C, and DEPT-135) and 2D NMR (COSY, HSQC, HMBC) spectra were recorded on Avance 400 MHz NMR spectrometer (Bruker, Rheinstetten, Germany) at 400 (^{1}H) and 100 (^{13}C) MHz. UV-vis was recorded on Perkin Elmer Lambda 950 UV-Vis-NIR. Chemical shifts were reported in parts per million (ppm) and coupling constants (*J*) in Hz. Proton and carbon values are relative to the internal standard TMS and were acquired in CD_3OD, $CDCl_3$, or DMSO-d_6. LCMS and HRESI-MS were obtained on a Waters Synapt G2 mass spectrometer (Cone Voltage 15 V), which was operated in the negative and/or positive ion mode using direct injection. Column chromatography was performed using Sephadex (LH-20, Sigma-Aldrich) and normal-phase silica gel 60 (70-230 mesh ASTM, Merck). TLC was performed on silica gel aluminum sheets (Silica gel 60 F_{254}, Merck) to monitor the fractions. Visualization was achieved with 10% H_2SO_4 and detection with vanillin sulfuric acid reagent and heating to 105 °C.

2.2.Biological Evaluation

2.2.1. Reagents (α-amylase and α-glucosidase enzymes)

Alpha-glucosidase (*Saccharomyces cerevisiae*), α-amylase (*procaine pancreas*), and 3, 5, di-nitro salicylic acid (DNS), p-nitro-phenyl-α-D-glucopyranoside (pNPG), sodium carbonate (Na_2CO_3), sodium dihydrogen phosphate, and di-sodium hydrogen phosphate were purchased from Sigma-Aldrich, South Africa.

2.2.2. α-Amylase Activity

The α-amylase assay was carried out according to the method by Telagari and Hullatti (2015), with slight modification. In a 96-well plate, the reaction mixture containing 40 µl of phosphate buffer (100 mM, pH = 6.8), 20 µl α-amylase (2 U/mL), and 20 µL of 200 µg/mL concentration of the extracts (or isolated compounds) was pre-incubated at 25°C for 20 min. Then, 20 µL of 1% soluble starch (100 mM phosphate buffer pH 6.8) was added as a substrate and incubated further at 25°C for 30 min. A volume of 100 µL of the colour reagent (DNS) was added and then steamed in a 90°C water bath for 10 minutes. The absorbance of the resulting mixture was measured at 540 nm using Multiplate Reader (Multiskan Thermo scientific, version 1.00.40,

Vantaa, Finland) after 10 minutes. Acarbose (200 µg/mL) was used as a standard. Each experiment was repeated three times. The results were expressed as percentage inhibition, which was calculated using equation 1.

$$Inhibitory\ activity = \frac{AC-AS}{AC} x100 \qquad \text{…(equation 1)}$$

Where, AC -absorbance of the substrate control and AS – absorbance of inhibitor/sample control.

2.2.3. α-Glucosidase Activity

The α-glucosidase inhibitory activity of the crude extracts and isolated compounds were adapted, with slight modification, from the standard method previously described by Telagari and Hullatti (2015). In a 96-well plate, the reaction mixture containing 50 µL of phosphate buffer (100 mM, pH = 6.8), 10 µL α-glucosidase (1 U/mL), and 20 µL of 200 µg/mL concentration of the extracts (or isolated compounds) was pre-incubated at 37°C for 15 min. Then, 20 µL of P-NPG (5 mM) was added as a substrate and incubated further at 37°C for 20 min. The reaction was stopped by adding 50 µL of sodium carbonate Na_2CO_3 (0.1 M). The absorbance of the released *p*-nitrophenol was measured at 405 nm using Multiplate Reader (Multiskan Thermo scientific, version 1.00.40, Vantaa, Finland). Acarbose (200 µg/mL) was used as a positive control. Each experiment was repeated three times. The results were expressed as percentage inhibition, which was calculated using equation 2.

$$Inhibitory\ activity = \frac{AC-AS}{AC} x100 \qquad \text{…(equation 2)}$$

Where, AC -absorbance of the substrate control and AS – absorbance of inhibitor/sample control.

2.2.4. Cell Viability Assay (MTT)

The chemicals used in the current study were of the highest possible quality and were purchased from the following companies:

American Type Cell Culture (ATCC), Manassas, USA:

a) Breast cancer cell line MDA-MB-231

Corning Incorporated, New York, USA:

a) Tissue culture flasks (25 and 75 cm^2)
b) Eppendorf vials

c) Pipette Tips 1000, 200, and 10 µL
d) Serological pipettes (10 mL)

Gibco Invitrogen, Karlsruhe, Germany:

a) Dulbecco's Modified Eagle Medium
b) Fetal Bovine Serum (FBS)
c) Trypsin/Ethyl Diamine Tetra Acetic acid (EDTA) (0.25%)

Greiner Bio-One, Frickenhausen, Germany:

a) Tissue culture plates (6-, 24- and 96-well plates)
b) Test tubes (15 mL and 50 mL)

Lasec, Cape Town, South Africa:

a) Syringes (5, 10, and 25 mL)

Oxoid, Basingstoke, Hampshire, RG24 SPW, England:

a) Phosphate Buffered Saline (PBS) with $Ca^{2+/}Mg^{2+}$

Sigma-Aldrich, Steinheim, Germany:

a) Dimethylsulphoxide (DMSO)
b) Penicillin
c) Streptomycin
d) 3-(4, 5-dimethylthiazolyl-2)-2, 5-diphenyltetrazolium bromine (MTT)
e) Trypan Blue (TB)
f) Millex syringe filter units (0.22 and 0.45 µm)

i. Equipment and Supply. The type of equipment used included ELISA-reader (Labtech System LT 4000 microplate reader, Lasec, Cape Town, South Africa), Laminar Flow (LN Series, Nuve, Ankara, Turkey), Incubator (Series 2000, Lasec, Cape Town, South Africa), and Microscope (inverted System Microscope, Lasec, Cape Town, South Africa).

ii. Sample Preparation. Stock solutions were prepared by carefully weighing and dissolving isolated compounds in DMSO to yield a final concentration of 10000 µg/mL. Subsequently, stocks were further diluted in a complete growth medium to the desired concentration range. Finally, DMSO concentration in working solutions was accounted for in control groups.

iii. Cell Culture. The MDA-MB-321 breast cancer cell line was used for the purpose of the study. They were cultivated at 37°C in 95% air and 5% CO_2, following standard aseptic work

procedures. Cells were cultured in a complete DMEM growth medium, supplemented with 10% fatal bovine serum, 1% penicillin (100 IU/mL), and streptomycin (100 µg/mL), in 75 cm^2 culture flasks.

iv. Culture of MDA-MB-231 Cells. Cells were cultured in 75 cm^2 flasks, allowed to grow to 80% confluency, and finally passaged once this was reached. To remove compounds that may interfere with the actions of trypsin, the growth medium was discarded, and the cells were rinsed with 5 mL sterile PBS. Subsequently, 1-2 mL of 0.25% trypsin were added, allowed to cover the surface of the flask, and incubated at 37ºC until cells began to detach. This took approximately 5 minutes and was performed under intermittent visual control. Once cells detached, 2 mL of complete growth medium was added to neutralize the action of the trypsin. Cells were then carefully re-suspended by repeated aspiration and then finally transferred to a 15 mL conical tube to be centrifuged at 125 x g for 5-10 minutes. Following this, the supernatant was removed, and the cell pellet was re-suspended in a 5 mL complete growth medium. Thereafter, 1 mL of the resulting suspension was transferred into a new 75 cm^2 flask, containing a complete growth medium, and the passage was recorded to track the age and physiology of the cells. Additionally, cell morphology was observed and compared with cell viability.

v. Cell Counting and Seeding. Following the detachment of the cells with trypsin and re-suspension in a fresh growth medium, cell counts were performed using a hemocytometer so that a specific cell concentration could be reached in 6-well plates or 96-well plates. This was achieved by combining 50 µl of cell suspension with an equal volume of 2% trypan blue and transferring 10 µl of this mixture to a hemocytometer counting chamber. The chamber was viewed under a microscope and the total cell count for each experiment was calculated according to equation 3. Following this, a dilution of cells was made according to the final cell number needed for each experiment as needed.

$$Volume\ of\ cells\ required\ (\mu l) = \frac{number\ of\ cells\ needed}{total\ number\ of\ cells\ counted} x100 \qquad \text{...(equation 3)}$$

vi. Determination of Cell Viability. Cell viability was determined using the 3-(4, 5-dimethylthiazolyl-2)-2, 5-diphenyltetrazolium bromine (MTT) assay. This is a colorimetric assay, which allows for the detection of viable and dead cells. In short, cultures were removed from the incubator at the appropriate times and the MTT working solution was prepared by

dissolving the MTT salt in PBS at a concentration of 5 mg/mL. If sediment appeared, the solution was heated to 37°C and swirled until no longer opaque. Then, 10 µl of this solution were added to each well and placed into the incubator for 4 hours. Next, the growth medium and MTT were removed and DMSO was added to each well to solubilize the remaining crystals. Finally, the absorbance was read at 570 nm Labtech System LT 4000 microplate reader (Lasec, Cape Town, South Africa) and results were expressed as percentage viability. This was calculated according to the absorbance of treated cells versus the absorbance of the controls, according to equation 4.

$$Percentage\ viability = \frac{Absorbance\ (sample)}{Absorbance\ (control)} x100 \qquad \text{…(equation 4)}$$

vii. MDA-MB-231 Cell Viability. MDA-MB-231 cells were grown to 80% confluency and were then trypsinated with 1-2 mL 0.25% trypsin. Thereafter, the trypsin was inactivated by adding 2 mL of complete growth medium and a cell count was performed. Following this, cells were seeded into sterile 96-well plates at 5×10^3 cells/well in 100 µl of complete growth medium. After exposing cells to various concentrations of the isolated compounds for 24 hours and 72 hours, respectively, 10 µl of MTT were added to each well. The plates were incubated at 37ºC for an additional 4 hours. Subsequently, the growth medium and MTT were removed from each well, and the remaining crystals were solubilized with 100 µl of DMSO. Finally, the absorbance of the samples was measured at 570 nm with an ELISA reader (Labtech System LT 4000 microplate reader).

viii. Statistical Analysis. Data generated in the present study were recorded and analyzed statistically using MedCalc for Windows, version 20.014 (MedCalc Software, Mariakerke, Belgium). Experiments were run in triplicate. After calculating the summary stats, including the Kolmogorov-Smirnov test for normal distribution, data were analyzed by means of the independent t-test if normally distributed. If the samples were not normally distributed, the Mann-Whitney test was used. To test for a trend between parameters, repeated measures and one-way ANOVA was performed. A P-value of less than 0.05 was considered significant.

References

Telagari, M. and Hullatti, K., 2015. In-vitro α-amylase and α-glucosidase inhibitory activity of *Adiantum caudatum* Linn. and *Celosia argentea* Linn. extracts and fractions. *Indian journal of pharmacology*, *47*(4), p.425.

Chapter 3

Literature Review of the *Helichrysum* Genus.

3.1.Introduction

This chapter aims to summarize the existing literature (using SciFinder, Google Scholar, PubMed, and Scopus search engines) regarding South African indigenous *Helichrysum* species that are traditionally used to manage diabetes. The chemistry and known biological activity (of extracts or pure isolates) as applicable to this study are also described.

3.1.1. *Helichrysum* Genus

The genus *Helichrysum* Miller (family = Asteraceae, tribe = Inuleae, subtribe = Gnaphalieae) is highly diverse and most distributed in the family Asteraceae – consisting of over 500 species worldwide (Hilliard, 1983). Species of this genus occur throughout the African continent, southwest Asia, India, Sri Lanka, Australia, and southern Europe (Lourens et al., 2004; Mashigo et al., 2015). About 245 are indigenous to South Africa and they display enormous morphological diversity (Hilliard, 1983; Akinyede et al., 2021). These fast-growing aromatic shrubs have remained popular among South African cultures. According to Lourens, Viljoen, and Van Heerden (2008), "the uses are well documented although renaming of species and the resulting confusing taxonomic nomenclature may cause uncertainty as to which specific species was referred to in some reports." Nevertheless, the Khoi-San people have used them to anoint their bodies (Hutchings, 1996), in other cultures (Sotho/Xhosa/Zulu) the smoke is inhaled to invoke the goodwill of the ancestors, and decoction of the leaves is used to treat respiratory conditions, including wound dressing (Van Wyk and Gericke, 2000; Lourens, Viljoen and Van Heerden, 2008). As a result, this multipurpose use has since attracted the interest of many scientists and various biological studies have been undertaken. For example, antibacterial activity (Mathekga and Meyer, 1998), antimicrobial activity (Lourens et al., 2011), anti-proliferative activity (Sagbo and Otang-Mbeng, 2020), and antidiabetic activity (Aladejana, Bradley and Afolayan, 2020). There are also a plethora of reports concerning the phytochemistry of this genus, and the most reported compounds include flavonoids, acylphloroglucinols, chalcones, sesquiterpenes, etc.

3.1.2. Ethnopharmacology and Biological Activity: *on diabetes mellitus*

As stated earlier, several *Helichrysum* species are widely used in South African traditional medicine for various reasons (wound dressing, digestive, and respiratory problems, cold, and fever, etc.). However, regarding their use in diabetes mellitus, a comprehensive literature search revealed only six species with documented use in the traditional treatment of diabetes: *H. gymnocomum* (Oyedemi, Bradley and Afolayan, 2009), *H. crispum* (L.) D. Don. (Hulley and Van Wyk, 2019), *H. caespititium* (DC.) Harv. (Semenya, Potgieter and Erasmus, 2012), as well as *H. nudifolium* L., *H. odoratissimum* L., and *H. petiolare* Hilliard & B.L. Burtt (Erasto et al., 2005). Interestingly, only *H. odoratissimum* (Njagi et al., 2015) and *H. petiolare* (Aladejana, Bradley and Afolayan, 2020) have been scientifically evaluated to corroborate the ethnobotanical usage. Table 3.1 discusses the known information of each species in relation to the management of diabetes as it is used in traditional medicine, including any reported antidiabetic studies.

Table 3.1: South African indigenous *Helichrysum* species (Asteraceae) used in traditional medicine for treating diabetes, with information on the plant parts used, methods of preparation/route of administration, and type of antidiabetic study

Scientific name [Local names]	Plant part used	Preparation and mode of administration	Type of anti-diabetic study (*in vitro/in vivo*)	References
❖ *H. gymnocomum* DC. [Impepho (*isiXh. /*isiZu.); phefo Ea Setlolo (*S.S.)]	❖ Leaves.	❖ Decoction of the leaves (fresh) is taken orally (two-teaspoonfuls).	❖ Not available.	❖ Oyedemi, Bradley and Afolayan (2009)
❖ *H. nudifolium* (L.) Less. [Isicwe (*isiXh.), umadotsheni, isicwe; umaphephesa (*isiZu.); bolebo, boleba-ba-liliba, leboko, papetloane-ea-liliba, papetloane-e-kholo, tsebe-litelele (*SS)]	❖ Leaves, roots.	❖ Decoction of the leaves (fresh) or roots is taken orally.	❖ Not available.	❖ Erasto et al. (2005)

❖ *H. odoratissimum* (L.) Sweet. [Imphepho (isiXh. /isiZu.); kooigoed, kruie (*Afr.)]	❖ Whole plant.	❖ A fresh plant is crushed, boiled (with water) and the infusion taken orally.	❖ Boiled aqueous leaf (dry) extract *in vivo* against alloxan-induced diabetic Swiss albino mice (P<0.05 at150 mg/kg body weight dose).	❖ Erasto et al. (2005) ❖ Njagi et al. (2015)#
❖ *H. caespititium* (DC.) Harv. [Boriba, botsiki-nyane, lelula-phooko, moriri-oa-lefatse, phate-ea-naha (*S.S.); mokgata (*S.); sewejaartjies and speelwonderboom (*Afr.)]	❖ Whole pant.	❖ Whole plant is cooked for 10–20 min or pounded and taken with warm water or soft porridge.	❖ Not available.	❖ Semenya, Potgieter and Erasmus (2012)
❖ *H. crispum* (L.) D. Don. [Hotnotskooigoed, hottentotskooigoed, hottentotskruie, kooigoed (*Afr.)]	❖ Not specified.	❖ Infusion is taken orally.	❖ Not available.	❖ Hulley and Van Wyk (2019)

❖ ***H. petiolare* Hilliard & B.L. Burtt** [Imphepho (*isiXh. /*isiZu.), kooigoed, kruie (*Afr.)]	❖ Whole plant.	❖ A fresh plant is crushed, boiled and the concentrated solution (infusion) is taken orally.	❖ Whole plant cold and boiled aqueous extracts *in vitro* using α-glucosidase, α-amylase, and glucose utilization assays.	❖ Aladejana, Bradley and Afolayan (2020)# ❖ Erasto et al. (2005)

* -isiXh. = isiXhosa. isiZu. = isiZulu. S.S. = Southern Sotho. S. = Sepedi. Afr. = Afrikaans. # -Author showing the antidiabetic activity.

***H. petiolare* Hilliard & B.L. Burtt** is investigated in this study and its literature is discussed in detail in chapter 4.

3.1.3. Phytochemistry

Numerous studies concerning the chemistry of the *Helichrysum* (Asteraceae) genus have been previously reported (Bohlmann et al., 1978; Bohlmann and Suwita, 1979; Bohlmann and Mahanta, 1979; Jakupovic et al., 1989; Jakupovic et al., 1986), of which flavonoids, chalcones, phenolic acids, terpenes, and essential oils, pyrones (both homo- and heterodimeric), benzofurans (bitalin esters), and acylated phloroglucinols (prenyl/geranyl and acyl groups) were predominant. A detailed review of the phytochemistry (including biological activities, and traditional uses) of the South African indigenous species was provided by Lourens, Viljoen, and Van Heerden (2008). While another study, which focused on the bioactive compounds from *Helichrysum* spp. with antimicrobial activity, was recently reported (Akaberi et al., 2019). Nevertheless, Table 3.2 only highlights the metabolites from South African indigenous *Helichrysum* species used traditionally to manage diabetes (see above in Table 3.1) with reported antidiabetic activity (whether reported from this genus or species from other genera). Interestingly, the active metabolites showing antidiabetic activity are yet to be identified in some species (*H. crispum* and *H. caespititium*). Whereas flavonoids with various structural backbones (flavanols, flavone, and chalcones) have been identified in other species. Thus, there is still more work that needs to be done to identify the active metabolites towards diabetes.

Table 3.2: Secondary metabolites isolated from South African indigenous *Helichrysum* species (used to manage diabetes mellitus) with reported anti-diabetic activities

Species	Structure and name of the compound (class)	Anti-diabetic activity /mechanism of action	Study type (*in vitro**/*in vivo***)	References
❖ *H. gymnocomum* DC.	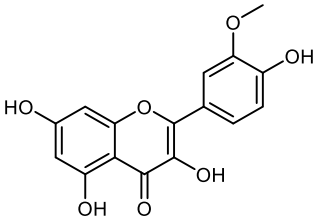 Isorhamnetin (flavanol)	❖ High fat-diet/STZ-induced diabetic Male Wistar rats. The mechanism of action is via modulation of the insulin resistance signaling pathway-related RNA.** ❖ Glucose-uptake in L6 myotubes at 1 nM concentration via translocation of GLUT-4.* ❖ α-Amylase inhibition *in silico*.*	❖ *In vivo*.** ❖ *In vitro*.*	❖ Drewes and Van Vuuren (2008) ❖ Jiang et al. (2019) ❖ Matboli et al. (2021) ❖ Metibemu et al. (2016)
	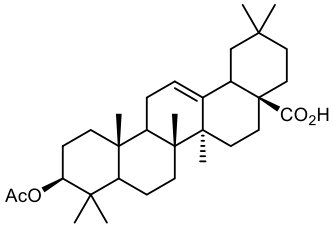 3-*O*-acetyloleanolic acid (sesquiterpene)	❖ The compound showed a significant decrease (31 mg/kg of b.w., $P < 0.05$) in the glucose levels against STZ-induced diabetic Male Wistar rats.**	❖ *In vivo*.**	❖ Bohlmann and Mahanta (1979) ❖ Narváez-Mastache et al. (2006)

❖ *H. nudifolium* L.	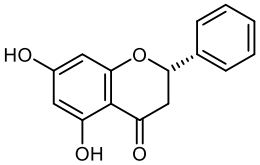 (+)-Pinocembrin (flavanone)	❖ Against STZ-induced diabetic rats in diabetic neuropathy.** ❖ The compound increased neuronal survival and restored the expression of the inflammatory factors NF-κB and TNF-a to normal levels against STZ-induced diabetic rats (in diabetic encephalopathy).**	❖ *In vivo.***	❖ Bohlmann and Zdero (1980) ❖ Granados-Pineda et al. (2018) ❖ Pei and Sun (2018)
	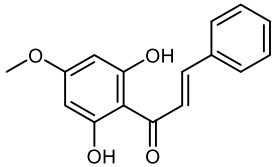 2`,6`-dihydroxy-4`-methoxychalcone (chalcone)	❖ The compound showed reduction in blood glucose levels from 277.4±7.7 mg/dl before treatment to 158.8±9.2 mg/dl after 12 days (P <0.05) in STZ-induced diabetic Male Wistar rats.**	❖ *In vivo.***	❖ Bohlmann and Zdero (1980) ❖ Marques et al. (2015
	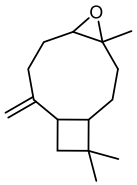 Caryophyllene oxide (sesquiterpene)	❖ Administration of 200 mg/kg b.w. of the compound significantly increased insulin levels (P < 0.05) and lowered blood glucose levels via oxidative and inflammatory stress against STZ-induced diabetic rats.**	❖ *In vivo.***	❖ Basha and Sankaranarayanan 2016) ❖ Jakupovic et al. (1986)

❖ *H. odoratissimum* L.	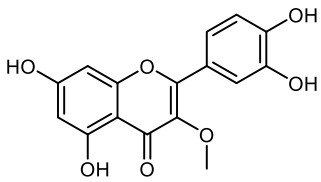 3-*O*-methylquercetin (flavonoid)	❖ *α*-Glucosidase inhibition (the compound showed an IC_{50} = 0.292 mM).*	❖ *In vitro.**	❖ Phoopha et al. (2020) ❖ Van Puyvelde et al. (1989)
	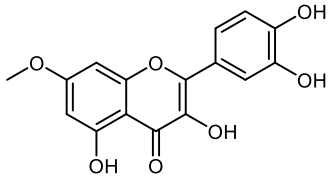 Rhamnetin (flavonol)	❖ *α*-Amylase inhibition (IC_{50} = 73.9 µM, compared to 26.3 µM of acarbose).*	❖ *In vitro.**	❖ Legoale, Mashimbye and van Ree (2013) ❖ Milella et al. (2016)
	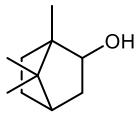 Borneol (monoterpene)	❖ Administration of 50 mg/kg body weight/day significantly reduced glucose levels, enhanced insulin secretion, and amended the disrupted islets of Langerhans in STZ-induced diabetic Wistar rats.**	❖ *In vivo.***	❖ Asekun, Grierson and Afolayan (2007) ❖ Madhuri and Naik 2017)

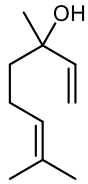 Linalool (monoterpene)	❖ Administration of the compound at 3 mM demonstrated 1.3 mg/g tissue glucose uptake in 30 min compared to 1.5 mg/g uptake by 2-unit insulin in rat hemi-diaphragm diaphragm tissue.*	❖ *In vitro.**	❖ Lawal et al. (2015) ❖ More et al. (2014)
❖ ***H. petiolare* Hilliard & B.L. Burtt**	Discussed in detail in chapter 4.		

Abbreviation = streptozotocin (STZ), oral glucose tolerance test (OGTT), body weight (b.w.), ribonucleic acid (RNA), glucose transporter type 4 (GLUT-4). **Hilliard & B.L. Burtt** is investigated in this study and its phytochemistry is discussed in detail in chapter 4.

References

Akaberi, M., Sahebkar, A., Azizi, N. and Emami, S.A., 2019. Everlasting flowers: Phytochemistry and pharmacology of the genus *Helichrysum*. *Industrial Crops and Products*, *138*, p.111471.

Akinyede, K.A., Cupido, C.N., Hughes, G.D., Oguntibeju, O.O. and Ekpo, O.E., 2021. Medicinal Properties and *In vitro* Biological Activities of Selected *Helichrysum* Species from South Africa: A Review. *Plants*, *10*(8), p.1566.

Aladejana, A.E., Bradley, G. and Afolayan, A.J., 2020. *In vitro* evaluation of the anti-diabetic potential of *Helichrysum petiolare* Hilliard & BL Burtt using HepG2 (C3A) and L6 cell lines. *F1000Research*, *9*.

Asekun, O.T., Grierson, D.S. and Afolayan, A.J., 2007. Characterization of essential oils from *Helichrysum odoratissimum* using different drying methods.

Basha, R.H. and Sankaranarayanan, C., 2016. β-Caryophyllene, a natural sesquiterpene lactone attenuates hyperglycemia mediated oxidative and inflammatory stress in experimental diabetic rats. *Chemico-Biological Interactions*, *245*, pp.50-58.

Bohlmann, F., Zdero, C., Hoffmann, E., Mahanta, P.K. and Dorner, W., 1978. Neue diterpene und sesquiterpene aus südafrikanischen *Helichrysum*-arten. *Phytochemistry*, *17*(11), pp.1917-1922.

Bohlmann, F. and Mahanta, P.K., 1979. Weitere Phloroglucin-derivate aus *Helichrysum gymnoconum*. *Phytochemistry*, *18*(2), pp.348-350.

Bohlmann, F. and Suwita, A., 1979. Weitere phloroglucin-derivate aus *Helichrysum*-arten. *Phytochemistry*, *18*(12), pp.2046-2049.

Bohlmann, F. and Zdero, C., 1980. Neue geranylphloroglucin-derivate aus *Helichrysum monticola*. *Phytochemistry*.

Drewes, S.E. and van Vuuren, S.F., 2008. Antimicrobial acylphloroglucinols and dibenzyloxy flavonoids from flowers of *Helichrysum gymnocomum*. *Phytochemistry*, *69*(8), pp.1745-1749.

Erasto, P., Adebola, P.O., Grierson, D.S. and Afolayan, A.J., 2005. An ethnobotanical study of plants used for the treatment of diabetes in the Eastern Cape Province, South Africa. *African Journal of Biotechnology*, *4*(12).

Granados-Pineda, J., Uribe-Uribe, N., García-López, P., Ramos-Godinez, M.D.P., Rivero-Cruz, J.F. and Pérez-Rojas, J.M., 2018. Effect of pinocembrin isolated from Mexican brown propolis on diabetic nephropathy. *Molecules*, *23*(4), p.852.

Hulley, I.M. and Van Wyk, B.E., 2019. Quantitative medicinal ethnobotany of Kannaland (western Little Karoo, South Africa): Non-homogeneity amongst villages. *South African Journal of Botany*, *122*, pp.225-265.

Hutchings, A., 1996. *Zulu medicinal plants: An inventory*. University of Natal press.

Jakupovic, J., Kuhnke, J., Schuster, A., Metwally, M.A. and Bohlmann, F., 1986. Phloroglucinol derivatives and other constituents from South African *Helichrysum* species. *Phytochemistry*, *25*(5), pp.1133-1142.

Jakupovic, J., Zdero, C., Grenz, M., Tsichritzis, F., Lehmann, L., Hashemi-Nejad, S.M. and Bohlmann, F., 1989. Twenty-one acylphloroglucinol derivatives and further constituents from South African *Helichrysum* species. *Phytochemistry*, *28*(4), pp.1119-1131.

Jiang, H., Yamashita, Y., Nakamura, A., Croft, K. and Ashida, H., 2019. Quercetin and its metabolite isorhamnetin promote glucose uptake through different signalling pathways in myotubes. *Scientific reports*, *9*(1), pp.1-15.

Lawal, O.A., Ogunwande, I.A., Kasali, A.A., Opoku, A.R. and Oyedeji, A.O., 2015. Chemical composition, antibacterial and cytotoxic activities of essential oil from the leaves of *Helichrysum odoratissimum* grown in South Africa. *Journal of Essential Oil-Bearing Plants*, *18*(1), pp.236-241.

Legoale, P.B., Mashimbye, M.J. and van Ree, T., 2013. Antiinflammatory and antioxidant flavonoids from *Helichrysum kraussii* and *H. odoratissimum* flowers. *Natural product communications*, *8*(10), p.1934578X1300801015.

Lourens, A.C.U., Viljoen, A.M. and Van Heerden, F.R., 2008. South African *Helichrysum* species: a review of the traditional uses, biological activity and phytochemistry. *Journal of Ethnopharmacology*, *119*(3), pp.630-652.

Lourens, A.C.U., Van Vuuren, S.F., Viljoen, A.M., Davids, H. and Van Heerden, F.R., 2011. Antimicrobial activity and *in vitro* cytotoxicity of selected South African *Helichrysum* species. *South African Journal of Botany*, *77*(1), pp.229-235.

Madhuri, K. and Naik, P.R., 2017. Ameliorative effect of borneol, a natural bicyclic monoterpene against hyperglycemia, hyperlipidemia and oxidative stress in streptozotocin-induced diabetic Wistar rats. *Biomedicine & Pharmacotherapy*, *96*, pp.336-347.

Marques, A.M., Pereira, S.L., Paiva, R.A., Cavalcante, C.V., Sudo, S.Z., Tinoco, L.W., Moreira, D.L., Guimaraes, E.F., Sudo, R.T., Kaplan, M.A.C. and Sudo, G.Z., 2015. Hypoglycemic effect of the methanol flower extract of *Piper claussenianum* and the major constituent 2′, 6′-dihydroxy-4′-methoxychalcone in streptozotocin diabetic rats. *Indian journal of pharmaceutical sciences*, *77*(2), p.237.

Matboli, M., Saad, M., Hasanin, A.H., Saleh, L.A., Baher, W., Bekhet, M.M. and Eissa, S., 2021. New insight into the role of isorhamnetin as a regulator of insulin signalling pathway in type 2 diabetes mellitus rat model: Molecular and computational approach. *Biomedicine & Pharmacotherapy*, *135*, p.111176.

Mathekga, A.D.M. and Meyer, J.J.M., 1998. Antibacterial activity of South African *Helichrysum* species. *South African Journal of Botany*, *64*(5), pp.293-295.

Metibemu, D.S., Saliu, J.A., Metibemu, A.O., Oluwadahunsi, O.J., Oboh, G., Omotuyi, I.O. and Akinloye, O.A., 2016. Molecular docking studies of isorhamnetin from *Corchorus olitorius* with target alpha-amylase related to Type 2 diabetes. *Journal of Chemical and Pharmaceutical Research*, *8*(4), pp.1262-1266.

Milella, L., Milazzo, S., De Leo, M., Vera Saltos, M.B., Faraone, I., Tuccinardi, T., Lapillo, M., De Tommasi, N. and Braca, A., 2016. α-Glucosidase and α-amylase inhibitors from *Arcytophyllum thymifolium*. *Journal of natural products*, *79*(8), pp.2104-2112.

More, T.A., Kulkarni, B.R., Nalawade, M.L. and Arvindekar, A.U., 2014. Antidiabetic activity of linalool and limonene in streptozotocin-induced diabetic rat: a combinatorial therapy approach. *Int J Pharm Pharm Sci*, *6*(8), pp.159-63.

Narváez-Mastache, J.M., Garduño-Ramírez, M.L., Alvarez, L. and Delgado, G., 2006. Antihyperglycemic activity and chemical constituents of *Eysenhardtia platycarpa*. *Journal of natural products*, *69*(12), pp.1687-1691.

Njagi, J.M., Ngugi, M.P., Kibiti, C.M., Ngeranwa, J., Njue, W., Gathumbi, P. and Njagi, E., 2015. Hypoglycemic effect of *Helichrysum odoratissimum* in alloxan induced diabetic mice.

Oyedemi, S.O., Bradley, G. and Afolayan, A.J., 2009. Ethnobotanical survey of medicinal plants used for the management of diabetes mellitus in the Nkonkobe municipality of South Africa. *Journal of Medicinal Plants Research*, *3*(12), pp.1040-1044.

Pei, B. and Sun, J., 2018. Pinocembrin alleviates cognition deficits by inhibiting inflammation in diabetic mice. *Journal of neuroimmunology*, *314*, pp.42-49.

Phoopha, S., Wattanapiromsakul, C., Pitakbut, T. and Dej-Adisai, S., 2020. A new stilbene derivative and isolated compounds from *Bauhinia pottsii* var. *pottsii* with their anti-alpha-glucosidase activity. *Pharmacognosy Magazine*, *16*(68), p.161.

Sagbo, I.J. and Otang-Mbeng, W., 2020. Anti-proliferative and genotoxic activities of the *Helichrysum petiolare* Hilliard & BL Burtt. *Scientia Pharmaceutica*, *88*(4), p.49.

Semenya, S., Potgieter, M. and Erasmus, L., 2012. Ethnobotanical survey of medicinal plants used by Bapedi healers to treat diabetes mellitus in the Limpopo Province, South Africa. *Journal of Ethnopharmacology*, *141*(1), pp.440-445.

Van Puyvelde, L., De Kimpe, N., Costa, J., Munyjabo, V., Nyirankuliza, S., Hakizamungu, E. and Schamp, N., 1989. Isolation of flavonoids and a chalcone from *Helichrysum odoratissimum* and synthesis of helichrysetin. *Journal of Natural Products*, *52*(3), pp.629-633.

Chapter 4

Phytochemistry of *Helichrysum petiolare* Hilliard & B.L. Burtt.

4.1. Introduction

This chapter focuses on the phytochemistry of *Helichrysum petiolare* Hilliard & B.L. Burtt., which is a plant that has been selected for investigation. Section A briefly discusses the literature of the plant, while section B are results and discussions.

4.2. General Experimental Procedures. See chapter 2.

4.3. Plant Material

The leaves of *Helichrysum petiolare* were collected in Kirstenbosch National Botanical Gardens, South Africa, Cape Town (-33° 59' 13.19" S, 18° 25' 29.39" E) on 31 August 2018, and the identity of the species was confirmed by the curator of the herbarium.

4.4. Extraction and Isolation

The air-dried and ground leaves of *H. petiolare* (264 g) were extracted by maceration with 80% MeOH at room temperature (3.0 L x 48 h x 3). The combined MeOH extracts were concentrated *in vacuo* using a rotary evaporator (under 45 ºC) to obtain approximately 39.0 g of the total dry extract, which was suspended in water and extracted sequentially to furnish the crude extracts: hexane (3.63 g), DCM (1.75 g), EtOAc (1.75 g), and BuOH (7.87 g). The DCM extract was chromatographed on silica gel (gel 60, 70-230 mesh ASTM, Merck, dry packing), eluting with a $CHCl_3$:EtOAc stepwise gradient (100 :0→50: 50) to give one hundred and twenty-seven fractions (1-127). TLC was used to monitor the fractions (silica gel aluminum sheets, visualization with vanillin sulfuric acid reagent and heating to 105 °C), eluting with $CHCl_3$:EtOAc (90:10 → 50:50) gradient. Fractions 51-76 upon standing for two days (at room temperature) produced yellow needle-like crystals which were washed successively by $CHCl_3$ and MeOH to result in compound **1** (44.0 mg). The combined fractions 29-32 (32.0 mg) were concentrated as described above and chromatographed on flash silica gel column, eluting isocratic with $CHCl_3$:EtOAc (50:50) to obtain compound **2** (24 mg). In addition, compound **3** precipitated out directly from fractions 15-18 of the main column (DCM). The hexane extract was chromatographed on silica gel (dry packing), eluting with hexane:DCM stepwise gradient (100 :0 → 0: 100) to obtain two hundred and fifty fractions (1-250). TLC was once again used

to monitor the fractions, eluting with hexane:EtOAc (80:20 →50:50) gradient. Fraction 220 (250 mg) was chromatographed on flash silica gel column, eluting isocratic with $CHCl_3$:EtOAc (90:10) to yield compounds **4** (15.0 mg), **6** (32.0 mg), and **11** (32.0 mg). Fraction 244 upon standing overnight (at room temperature) produced white crystals which were washed successively by DCM and MeOH to result in compound **5**. The BuOH extract was fractionated by column chromatography on silica gel (dry packing), eluting with a DCM:MeOH stepwise gradient (100:0 → 50:50) to obtain one hundred and eighty-two fractions (1-182). The fractions were monitored by TLC using various solvents (DCM:MeOH, 100:0 → 50:50; EtOAc:MeOH, 90:10). Fractions 90-101 (40.0 mg) were concentrated and chromatographed on Sephadex (LH-20) column chromatography, eluting isocratic with ethanol:deionized water (90:10) to give compound **7** (32.0 mg). While fractions 30-35 (50.5 mg) were combined and subjected to repeated column chromatography on silica gel, eluting with DCM:MeOH (95:5 → 90:10) gradient to give compound **8** (36 mg). Compound **9** (14.2 mg) was obtained after successful purification of fractions 50-60 (20.0 mg) on flash silica gel column, eluting isocratic with EtOAc:MeOH (90:10). The EtOAc extract was fractionated by column chromatography on silica gel (dry packing), eluting with an EtOAc:MeOH stepwise gradient (100 :0→50: 50) to obtain fifty fractions (1-50). TLC was used to monitor the fractions (EtOAc:MeOH, 95:5 →90:10). Fractions 30-35 upon standing for two days produced a white precipitate, which was washed successively with $CHCl_3$ and MeOH to obtain compound **10**.

4.5. Biological Evaluation

i. α-Glucosidase and α-amylase enzyme inhibition assays. See chapter 2.

ii. Cell viability assay (MTT). See chapter 2.

Scheme 4.1: A summary of the experimental procedure for the isolation of compounds from *H. petiolare*

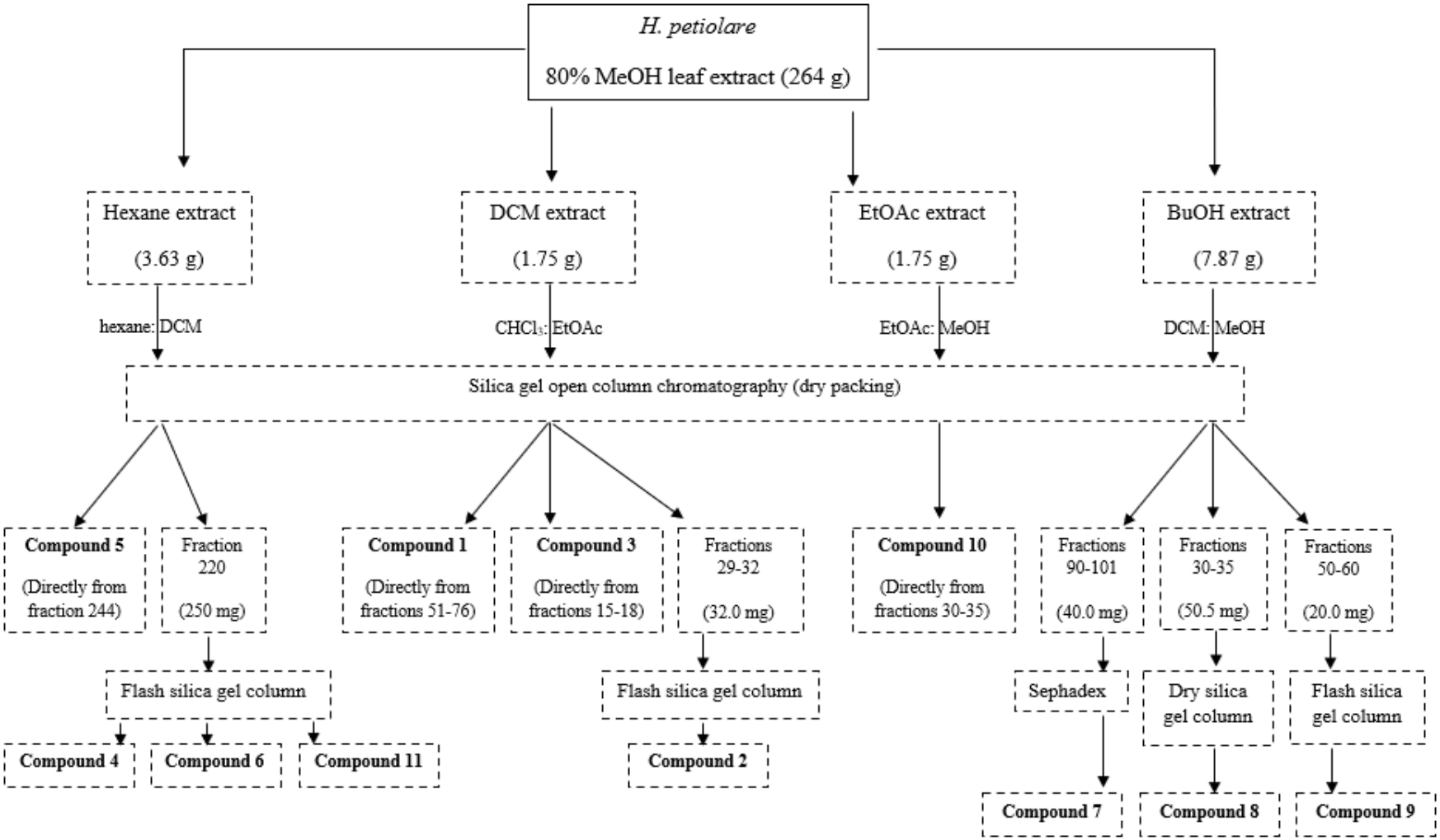

4.6. Section A

4.6.1. Taxonomy

Kingdom: Plantae

Division: Magnoliophyta

Class: Magnoliopsida

Order: Asterales

Family: Asteraceae (or Compositae)

Genus: *Helichrysum* Mill

Species: *H. petiolare* Hilliard & B.L. Burtt, (Hilliard and Burtt, 1983)

Fig. 4.1: Leaves of *H. petiolare* (source: http://pza.sanbi.org/helichrysum-petiolare**)**

4.6.2. Background

Helichrysum petiolare Hilliard & B.L. Burtt (Asteraceae) also known as *'kooigoed'* in Afrikaans or *'impepho'* in isiXhosa is an indigenous South African medicinal plant, which occurs in the drier inland parts, sheltered slopes, and forest margins of the Western Cape (Cederburg and Jonkershoek Mountains), Eastern Cape, and KwaZulu-Natal (Hilliard, 1983). It is a ground covering shrub and it belongs to group 18 according to the Hilliard classification system. The main interests of this multipurpose medicinal plant are the leaves (Fig. 4.1), which have significant use in ethnomedicine.

4.6.3. Ethnopharmacology

The use of medicinal plants to treat ailments is still a widely accepted phenomenon among the population of South Africa, particularly, in rural communities where at least 80% still rely on the benefits of traditional medicines (Vasisht and Kumar, 2004). For instance, infusions/decoctions of the leaves of *Helichrysum petiolare* (like most species in the genus) are used topically for wound dressing (Scott, Springfield and Coldrey, 2004; Lourens, Viljoen and Van Heerden, 2008), including respiratory-related conditions such as coughs, colds, and asthma (Lourens, Viljoen and Van Heerden, 2008). Other uses involve the treatment of diabetes (Odeyemi and Bradley, 2018). As such, this has attracted interest and various research groups have reported many biological activities to validate these claims.

4.6.4. Biological Activity: *on diabetes mellitus*

i. In vitro

Enzyme

Aladejana, Bradley and Afolayan, 2020 recently showed the anti-diabetic activity of the whole plant cold and boiled aqueous extracts using α-glucosidase, and α-amylase assays. The boiled aqueous extract exhibited significant inhibition effects in both assays in a concentration-dependent manner. An IC_{50} value of 844.27 ± 36.81 µg/mL was recorded in the α-glucosidase assay, compared to 804.01 ± 27.09 µg/mL of the acarbose-control. While the α-amylase had an IC_{50} of 0.361 ± 0.0210 µg/mL (IC_{50} = 0.378 ± 0.0084 µg/mL for the control).

Cell-lines

The whole plant ethanol, cold aqueous, and boiled aqueous extracts were evaluated using a glucose utilization assay in L6 myocytes and HepG2 (C3A) hepatocytes (Aladejana, Bradley and Afolayan, 2020). It was found that the cold aqueous extract was more superior (dose-dependent increase) out of the tested extracts, particularly, in the L6 cell-lines myocytes.

ii. In vivo (mice)

No data was available in the literature.

4.6.5. Other Bioactivities

The antibacterial activity of the aqueous extract, against a Gram-positive bacterium (*Staphylococcus aureus*) was reported by Scott, Springfield and Coldrey 2004. Lourens et al. (2004) showed the anti-inflammatory of the acetone and methanol leaf extracts. While the

cytotoxicity (*in vitro*) of the chloroform:methanol (1:1) leaf and stem extracts against transformed human kidney epithelial (Graham) cells, MCF-7 breast adenocarcinoma, and SF-268 glioblastoma cells was shown by Lourens et al. (2011). Furthermore, the antigenotoxicity of the dichloromethane and 90% methanol leaf extracts against aflatoxin B1-induced mutagenicity in S9 rat liver fraction (Makhuvele et al., 2018), and antityrosinase activity of the crude extracts (Sonka, 2018) were also reported. Table 4.1 shows a summary of some known biological activities (whether reported directly from this plant or other sources) that are associated with the individual constituents of *Helichrysum petiolare.*

4.6.6. **Previous Work**: *phytochemistry*

The chemistry of this species has been previously studied but is limited. The major publication(s) of its phytochemistry was reported by Jakupovic et al. (1989), and the main phytoconstituents that have been isolated (from the aerial parts) include flavonoids, chalcones, pyrones, as well as sesquiterpenes (Table 4.1). The essential oil content was evaluated by Lourens et al. (2004). Interestingly, 7,8-dimethoxy-5-hydroxyflavone is the only flavonoid that was reported by Jakupovic et al. (1989), though *Helichrysum* species are known sources of flavonoids. Therefore, this prompted us to re-investigate further the phytochemistry of this species (discussed later in this chapter, section B).

Table 4.1: Secondary metabolites isolated from *Helichrysum petiolare* (including plant part from which it was isolated) and their known biological activities

Name and structure (class)	Part of the plant	Biological Activity	Study type (*in vitro**/*in vivo***)	References
❖ **7,8-dimethoxy-5-hydroxyflavone (flavone)** 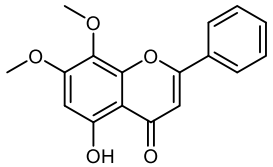	❖ Aerial parts.	❖ Antiviral activity (showed IC_{50} = 2.322 µg/mL againsy MDCK cells).*	❖ *In vitro.**	❖ Jakupovic et al. (1989) ❖ Wu et al. (2010)
❖ **Pinostrobin chalcone (flavonoids)** 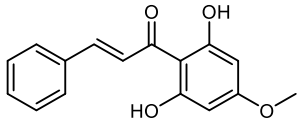	❖ Aerial parts.	❖ Cytotoxic activity (IC_{50} = 20.42 ± 2.23 and 22.51 ± 0.42 µg/mL).* ❖ Antioxidant activity (showed IC_{50} = 11. 66 ± 0. 61 in DPPH, 24. 38 ± 1. 24 in LPO, and 86. 74 ± 7. 89 mg/L in PCO assays).*	❖ *In vitro.**	❖ Jakupovic et al. (1989) ❖ Mohammed et al. (2019) ❖ Xu et al. (2013)
❖ **Ocimepyrone (pyrone)** 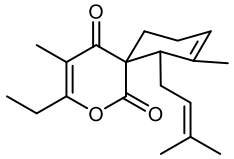	❖ Aerial parts.	-	-	❖ Jakupovic et al. (1989)

❖ **Humulone methyl ether (alpha acids)** 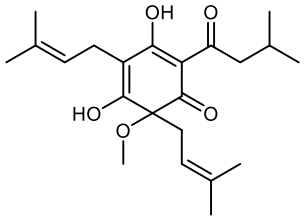	❖ Aerial parts.	-	-	❖ Jakupovic et al. (1989)
❖ **3-Oxo-cadina-1,9-diene (cadinane)** 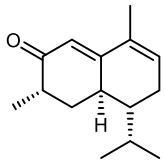	❖ Aerial parts.	-	-	❖ Jakupovic et al. (1989)
❖ ***α*-Humulene (sesquiterpene)** 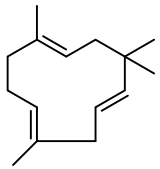	❖ Aerial parts.	❖ Anticancer activity (the compound had 50 ± 6% inhibition in MCF-7 human tumor cell lines).* ❖ Anti-inflammatory activity (in female BALB/c mice).**	❖ *In vitro.** ❖ *In vivo.***	❖ Jakupovic et al. (1989) ❖ Legault and Pichette (2007) ❖ Rogerio et al. (2009)

❖ **Spathulenol (sesquiterpene)** 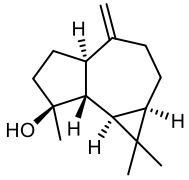	❖ Aerial parts.	❖ Antifungal activity (showed MIC = 32 µg/mL in *Tricophyton mentagrophytes*).* ❖ Anti-inflammatory Activity (in Cg-induced mice paw oedema).** ❖ Antioxidant activity (IC_{50} = 26.13 µg/mL in DPPH assay).* ❖ Antimycobacterial (MIC = 231.9 µg/mL in ovarian cancer cells).*	❖ *In vitro*.* ❖ *In vivo*.**	❖ Al-Ja'fari et al. (2011) ❖ do Nascimento et al. (2018) ❖ Jakupovic et al. (1989)
❖ **Ledol (sesquiterpene)** 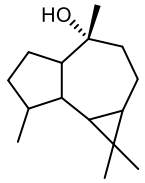	❖ Aerial parts.	❖ Anticancer activity (moderate inhibition in cultured human lymphoblastoid Raji cells).*	❖ *In vitro*.*	❖ Jakupovic et al. (1989) ❖ Spiridonov, Konovalov and Arkhipov (2005)
❖ **Caryophyllene oxide (sesquiterpene)** 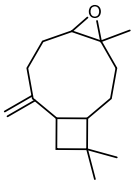	❖ Aerial parts.	❖ Anti-inflammatory activity ($P < 0.05$ in Cg-induced mice paw oedema).** ❖ Cytotoxicity (showed IC_{50} = 2.1 ± 0.9 µg/mL against BALB/c mice macrophages).* ❖ Antifungal activity.*	❖ *In vitro*.* ❖ *In vitro*.**	❖ Chavan, Wakte and Shinde (2010) ❖ Jakupovic et al. (1989) ❖ Monzote et al. (2009) ❖ Yang et al. (2000)

❖ ***β*-Caryophyllene**[a] **(sesquiterpene)**	❖ Aerial parts.	❖ Anti-inflammatory activity ($P < 0.0001$ in Cg-induced mice paw oedema).** ❖ Antimicrobial activity (showed MIC = 3 ± 1.0 µM, in *Staphylococcus aureus*).* ❖ Antioxidant activity (showed IC_{50} = 1.25 ± 0.06 in DPPH and 3.23 ± 0.07 in FRAP assays).* ❖ Anti-proliferative (had an IC_{50} = 19 µM in HCT 116 cell lines).*	❖ *In vitro*.* ❖ *In vivo*.**	❖ Brito et al. (2019) ❖ Dahham et al. (2015) ❖ Lourens et al. (2004)
❖ ***α*-Humulene epoxide (sesquiterpene)**	❖ Aerial parts.	❖ Anticarcinogenic activity (had significant inhibition at 20 mg dose in the liver of A/J Mice).**	❖ *In vivo*.**	❖ Jakupovic et al. (1989) ❖ Zheng et al. (1992)
❖ **γ-Muurolene**[a] **(sesquiterpene)**	❖ Aerial parts.	-	-	❖ Lourens et al. (2004)

❖ ***α*-Muurolene[a] (sesquiterpene)**	❖ Aerial parts.	-	-	❖ Lourens et al. (2004)
❖ **1,8-Cineole[a] (monoterpene)**	❖ Aerial parts.	❖ Anti-proliferative activity (showed inhibitions between 5–50 mM against HCT116 and 5–25 mM in RKO cell lines).* ❖ Antimicrobial activity (had an MIC = 2.0 mg/mL in *Bacillus cereus* and *Cryptococcus neoformans*).*	❖ *In vitro*.*	❖ Lourens et al. (2004) ❖ Murata et al. (2013) ❖ Vuuren and Viljoen (2007)
❖ ***α*-Pinene[a] (monoterpene)**	❖ Aerial parts.	❖ Anti-osteoarthritic activity (had a 33.6 ± 3.1% reduction in human chondrocyte cell lines C-28/I2).* ❖ Antimicrobial activity (showed MIC = 3.125 µg/mL in *Cryptococcus neoformans*).*	❖ *In vitro*.*	❖ Lourens et al. (2004) ❖ Rufino et al. (2014) ❖ Silva et al. (2012)

❖ **Borneol[a] (monoterpene)** 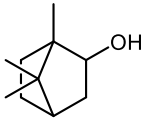	❖ Aerial parts.	❖ Anti-inflammatory activity ($P < 0.01$ in Cg-induced peritonitis against male albino Swiss mice).[**] ❖ Anticonvulsant (by modulation of GABAergic system through enhancement of GABAA-BZD receptor).[**] ❖ Antimicrobial activity (MIC = 125 – 250 µg/mL).[*]	❖ *In vitro*.[*] ❖ *In vivo*.[**]	❖ Almeida et al. (2013) ❖ Lourens et al. (2004) ❖ Quintans-Júnior et al. (2010) ❖ Tabanca et al. (2001)
❖ **Limonene[a] (monoterpene)** 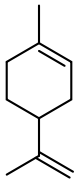	❖ Aerial parts.	❖ Antimicrobial activity (had an MIC = 3.0 mg/mL in *Bacillus cereus* and *Cryptococcus neoformans*).[*] ❖ Anticancer activity (had 72% reduction at 10000 ppm doses after 18 weeks on DMBA-induce mammary cancer in rodents).[**]	❖ *In vitro*.[*] ❖ *In vivo*.[**]	❖ Elegbede et al. (1984) ❖ Lourens et al. (2004) ❖ Vuuren and Viljoen (2007)

❖ ***p*-Cymene**[a] **(alkylbenzene)** 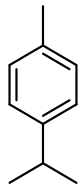	❖ Aerial parts.	❖ Anti-inflammatory activity ($P < 0.05$ on LPS-induced acute lung injury in rodents).**	❖ *In vivo*.**	❖ Lourens et al. (2004) ❖ Xie et al. (2012)
❖ ***α*-Terpineol**[a] **(monoterpene)** 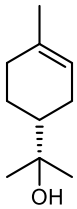	❖ Aerial parts.	❖ Anti-inflammatory activity ($P < 0.001$ on LPS-induced murine macrophages).* ❖ Antitumour activity (had potency against NCI-H69 cell line, IC_{50} = 0.26 mM).* ❖ Antimicrobial activity (had MIC = 0.1–0.8 and MBC = 0.1–1.6 mg/mL against bacterial strains).*	❖ *In vitro*.*	❖ de Oliveira et al. (2012) ❖ Hassan et al. (2010) ❖ Lourens et al. (2004) ❖ Park et al. (2012)

[a] -Major oil contents were reported in the study. Abbreviations = 2,2-diphenyl-1-picrylhydrazyl (DPPH), malonaldehyde (MDA), minimal inhibitory concentrations (MIC), minimum bactericidal concentration (MBC), inhibitory concentration 50% (IC_{50}), glutathione 51- transferase (GST), ferric reducing antioxidant power (FRAP), lipid peroxide (LPO), and protein carbonylation (PCO), 7,12-dimethylbenz[a]anthracene (DMBA), carrageenan (Cg), methadone (MTD), lipopolysaccharide (LPS), madin-darby canine kidney (MDCK), gamma-aminobutyric acid (GABAergic), benzodiazepine gamma-aminobutyric acid type A (GABAA-BZD)

4.7. Section B

4.7.1. Results and Discussion

The treatment and extraction of the plant material (*Helichrysum petiolare*) were carried out as outlined below in the experimental subsection. Phytochemical study of the leaf extracts from *H. petiolare* resulted in isolation and identification of 11 compounds, two of them (**1** and **2**) are described for the first time from natural source.

Compound 1: Petiolactone A

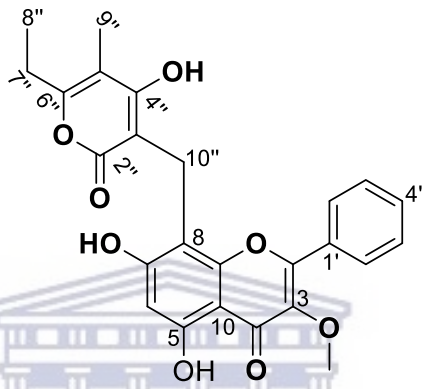

Fig. 4.2: Chemical structure of compound **1**

Compound **1** (Fig. 4.2) was obtained as a yellow precipitate from fraction 51-76 (44.0 mg) of the main-column on silica gel, eluting with $CHCl_3$:EtOAc (100 :0 → 50: 50) stepwise gradient. Its structural characterization followed from an extensive evaluation of the nuclear magnetic resonance (NMR) and high-resolution electrospray ionization mass spectrometry (HRESIMS) experiments. The HRESIMS (Fig. 4.10) gave a molecular ion peak [M^+] at *m*/*z* 449.1232, which was calculated for $C_{25}H_{22}O_8$.

The proton (^{1}H) NMR spectrum (Fig. 4.4) of compound **1** showed proton signals that resonated at δ_H: 1.05 (3H, *t*, *J* = 7.5 Hz, H-8``), 1.86 (3H, *s*, H-9``), 2.43 (2H, *q*, *J* = 7.5 Hz, H-7``), and 3.80[a] (2H, *s*, H-10``), which were characteristic of a 6``-ethyl-4``-hydroxy-5``-methyl-*α*-pyrone moiety found in *Helichrysum* species (Jakupovic et al., 1989). Whereas the splitting pattern and the integration of the signals at δ_H 7.57[a] (3H, *t*, *J* = 3.2 Hz, H-3`/4`/5`) and 8.10[a] (2H, *m*, H-2`/6`) were indicative of an unsubstituted B-ring. Additionally, a strong aromatic singlet appeared at δ_H 6.22 (1H, *s*, H-6). Carbon thirteen (^{13}C) NMR (Fig. 4.6) and distortionless enhancement by polarization transfer (DEPT-135) spectra (Fig. 4.7) of compound **1** displayed 25 carbons resonances, which included three methyl at δ_C 10.2 (C-9``),

11.9 (C-8``), and 60.0 (C-3), two methylene at $\delta_C$ 17.8 (C-1`), and 24.1 (C-7``), including six methine at δ_C 98.8 (C-6), 128.9 (C-2`/4`), 129.1 (C-3`/5`), and 131.3 (C-4`), as well as 14 *quartery* carbons at δ_C 100.3 (C-3``), 104.6 (C-10), 105.1 (C-8), 106.6 (C-5``), 130.8 (C-1`), 138.7 (C-3), 154.6 (C-2), 155.8 (C-9), 159.4 (C-5), 159.6 (C-6``), 163.0 (C-7), 164.3 (C-2``), 166.2 (C-4``), and 178.8 (C-4). Extensive interrogation of the (^{1}H - ^{13}C) heteronuclear single quantum correlation (HSQC) (Fig. 4.8) and heteronuclear multiple bond correlation (HMBC) experiments (Fig. 4.9) revealed important correlations (^3J) that assisted in assigning the peaks. The proton signal of the methylene bridge (H-10``) at $\delta_H$ 3.80$^a$ showed correlations with C-3`` (δ_C = 100.3), C-2`` ($\delta_C$ = 164.3), C-4`` (δ_C = 166.2), C-7 (δ_C = 163.0), C-8 (δ_C = 105.1), and C-9 (δ_C = 154.6), thereby confirming the linkage of the *α*-pyrone moiety at C-8 of the flavone unit. In addition, the aromatic singlet placed on H-6 (δ_H = 6.22) had correlations (^3J) with C-5 (δ_C = 159.4), C-7 (δ_C = 163.0), C-8 (δ_C = 105.1), and C-10 (δ_C = 104.6) on HMBC, which further supported this assignment. Furthermore, the position of the methoxy group was located at C-3 based on its HMBC correlation with the resonance at δ_C 138.7. Since only one aromatic proton was placed on the A-ring, it was proposed that two hydroxyl substituents were present in this ring. To confirm this, acetylation was carried out. As such, the ^{13}C NMR (Fig. 4.12, Table 4.8 in the appendix) of the acetylated derivative revealed six additional resonance (δ_C = 19.6, 21.0, 21.1, 166.4, 168.0, and 169.4) which were indicative of the three acetyl groups at C-5 and C-7. While the other acetyl unit replaced the hydroxyl group placed at C-4`` of the α-pyrone moiety.

The structure of compound **1** was compared to two known compounds, lepidissipyrone previously isolated from *Helichrysum lepidissimum* (Jakupovic et al., 1989) and *H. excisum* (Lourens et al., 2011), as well as obstusifolin obtained from *Pseudognaphalium obtusifolium* (formerly *Gnaphalium obtusifolium*) (Hänsel, Ohlendorf and Pelter, 1970). In our compound **1**, the signal at δ_C 138.7 (C-3) was assigned to the 3-methoxy group (this signal is absent in both lepidissipyrone and obstusifolin), while the attachment of the α-pyrone moiety, confirmed through HMBC correlation, was placed at C-8 (placed at C-6 in lepidissipyrone). Nevertheless, all the above data agreed with the structure of compound **1**, which is novel, having been assigned as 6``-ethyl-4``-hydroxy-5``-methyl-2-oxo-2*H*-pyran-3-yl-5,7-dihydroxy-3-methoxyflavone; and is hereby given the trivial name petiolactone A (Fig. 4.2). This flavonoid is one of the major compounds found in this plant (*H. petiolare*). Table 4.2 shows the NMR spectroscopic data of this compound and Fig. 4.3 shows significant HMBC and (^{1}H-^{1}H) correlation spectroscopy (COSY) correlations. The UV-visible spectrum is shown in Fig. 4.11.

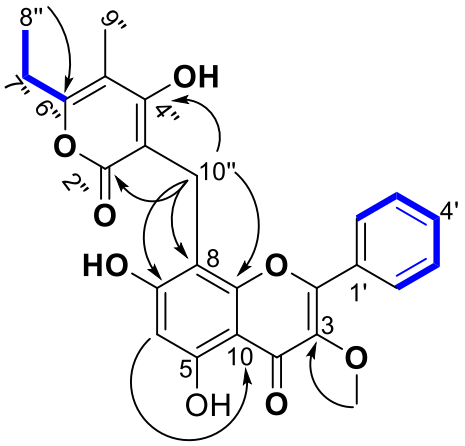

Fig. 4.3: Selected HMBC (black arrows) and COSY (blue) correlations of compound **1**

Table 4.2: NMR spectroscopic data (400 MHz, DMSO-d_6) of compound **1**

#	δC, type	δH (*J* in Hz)	HMBC
2	155.8, C	-	-
3	138.7, C	-	-
4	178.8, C	-	-
5	159.4, C	-	-
6	98.8, CH	6.22, *s*	C-10, C-5, C-4[b], C-7, C-8
7	163.0, C	-	-
8	105.1, C	-	-
9	154.6, C	-	-
10	104.6, C	-	-
1`	130.8, C	-	-
2`, 6`	128.9[a], CH	8.10[a], *m*	C-4`, C-3`, 5`, C-2
3`, 5`	129.1[a], CH	7.57[a], *t* (3.2)	C-2`, 6`, C-1`
4`	131.3, CH	7.57[a], *t* (3.2)	C-2`,6`, C-3`, 5`
2``	164.3, C	-	-
3``	100.3, C	-	-
4``	166.2, C	-	-
5``	106.6, C	-	-
6``	159.6, C	-	-
7``	24.1, CH_2	2.43, *q* (7.5)	C-8``, C-5``, C-6``
8``	11.9, CH_3	1.05, *t* (7.5)	C-6``, C-7``
9``	10.2, CH_3	1.86, *s*	C-5``, C-6``, C-4``
10``	17.8, CH_2	3.80[a], *s*	C-3``, C-2``, C-4``, C-7, C-8, C-9
3-OMe	60.0, CH_3	3.80[a], *s*	C-3
5-OH	–	12.65, *s*	C-5, C-6, C-10

[a] -Overlapping ^{1}H and ^{13}C-NMR signals. [b] -long range correlation on HMBC.

Fig. 4.4: ^{1}H-NMR spectrum (DMSO-d$_6$, 400 MHz) of compound **1**

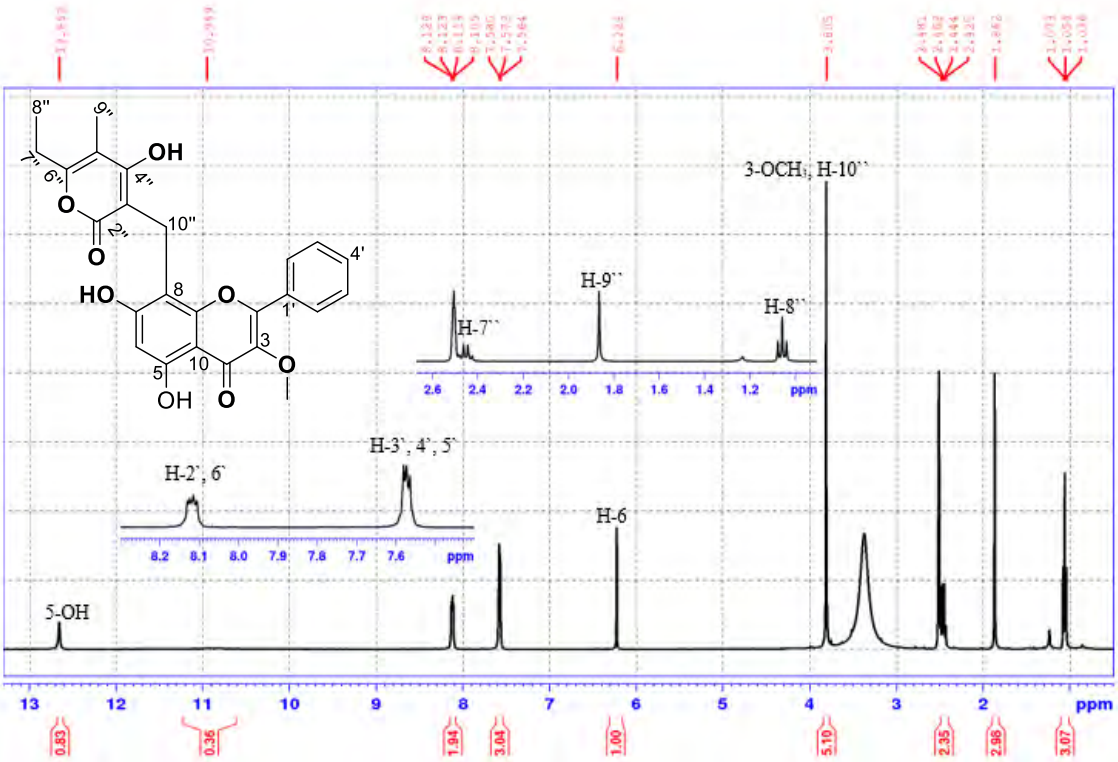

Fig. 4.5: COSY spectrum (DMSO-d_6) of compound **1**

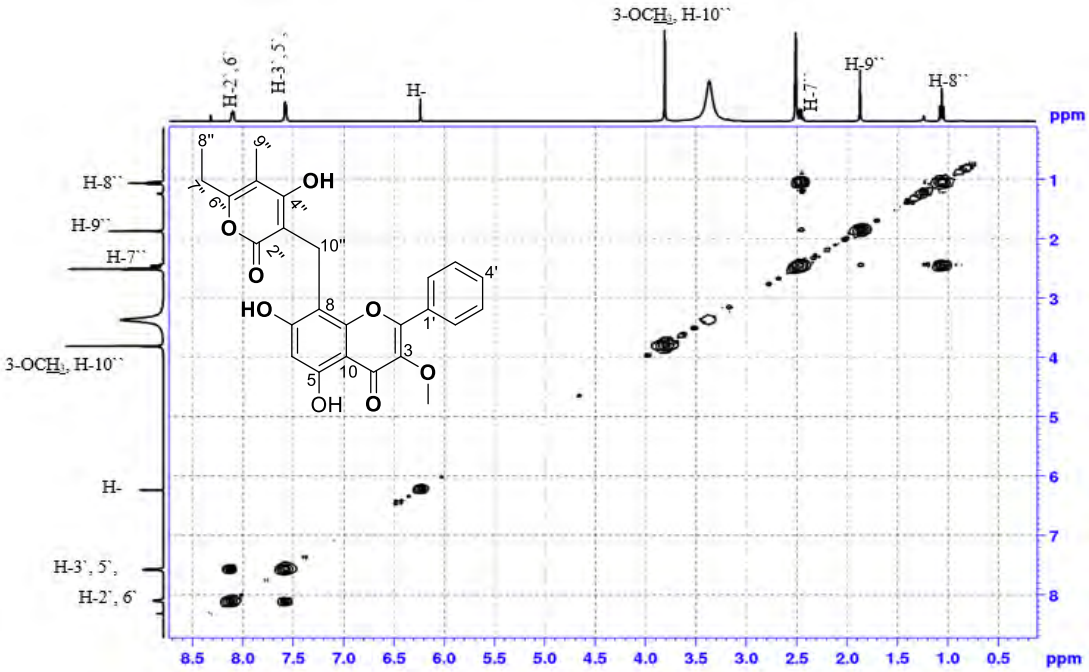

Fig. 4.6: ^{13}C-NMR spectrum (DMSO-d_6, 100 MHz) of compound **1**

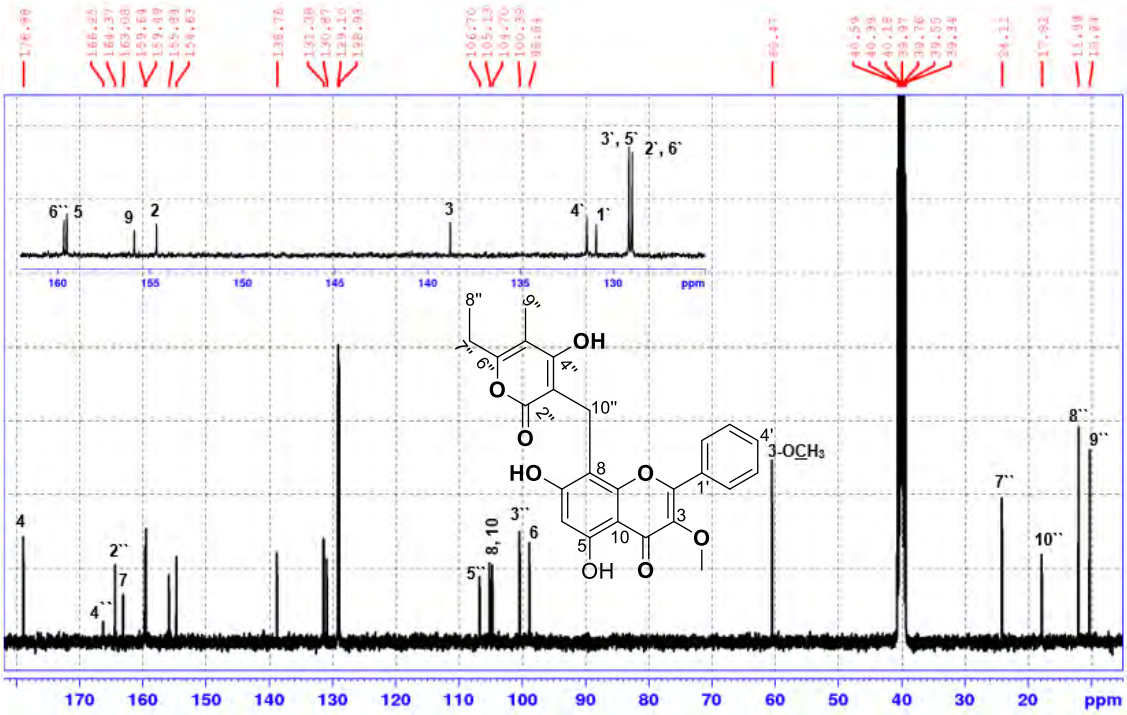

Fig. 4.7: DEPT-135 spectrum (DMSO-d_6) of compound **1**

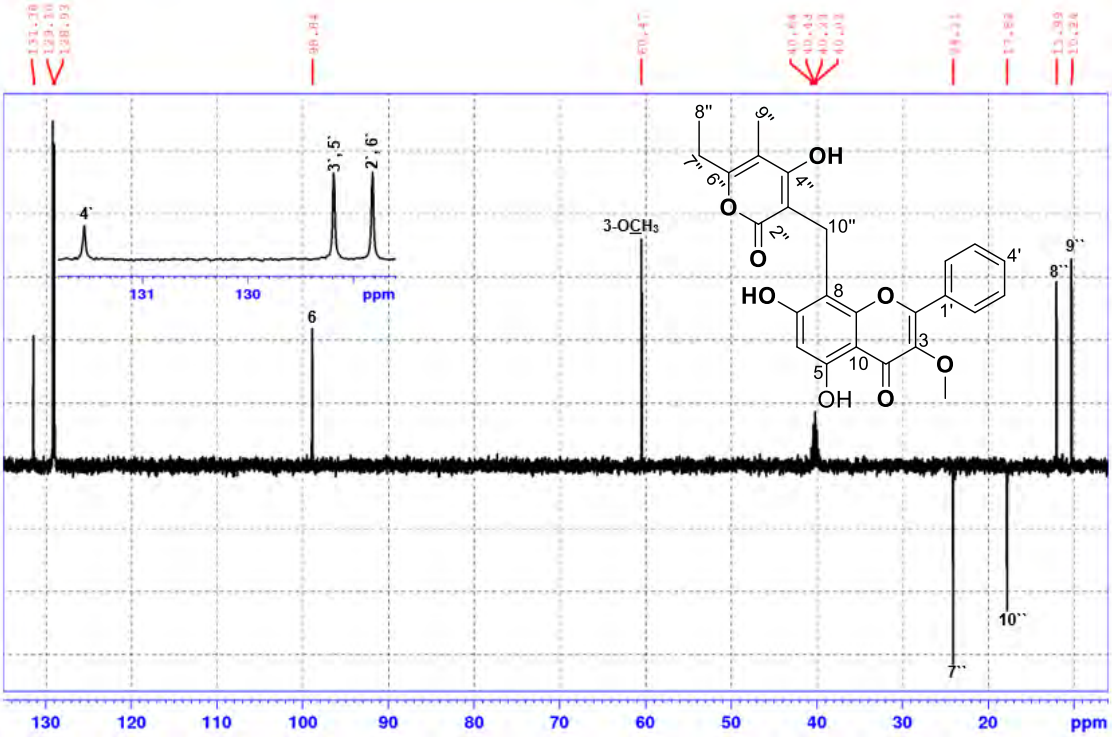

Fig. 4.8: HSQC spectrum (DMSO-d_6) of compound **1**

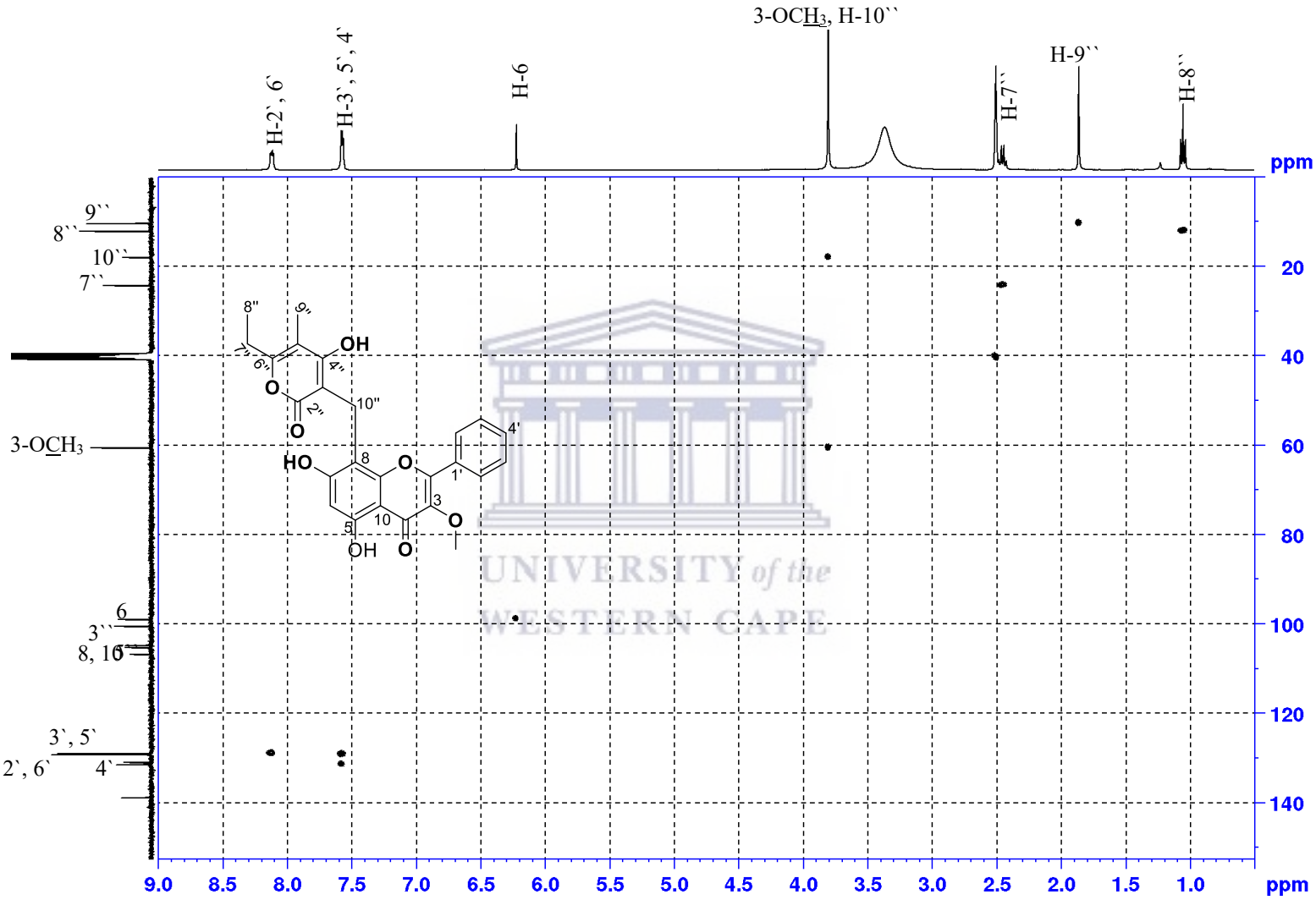

Fig. 4.9: HMBC spectrum (DMSO-d_6) of compound **1**

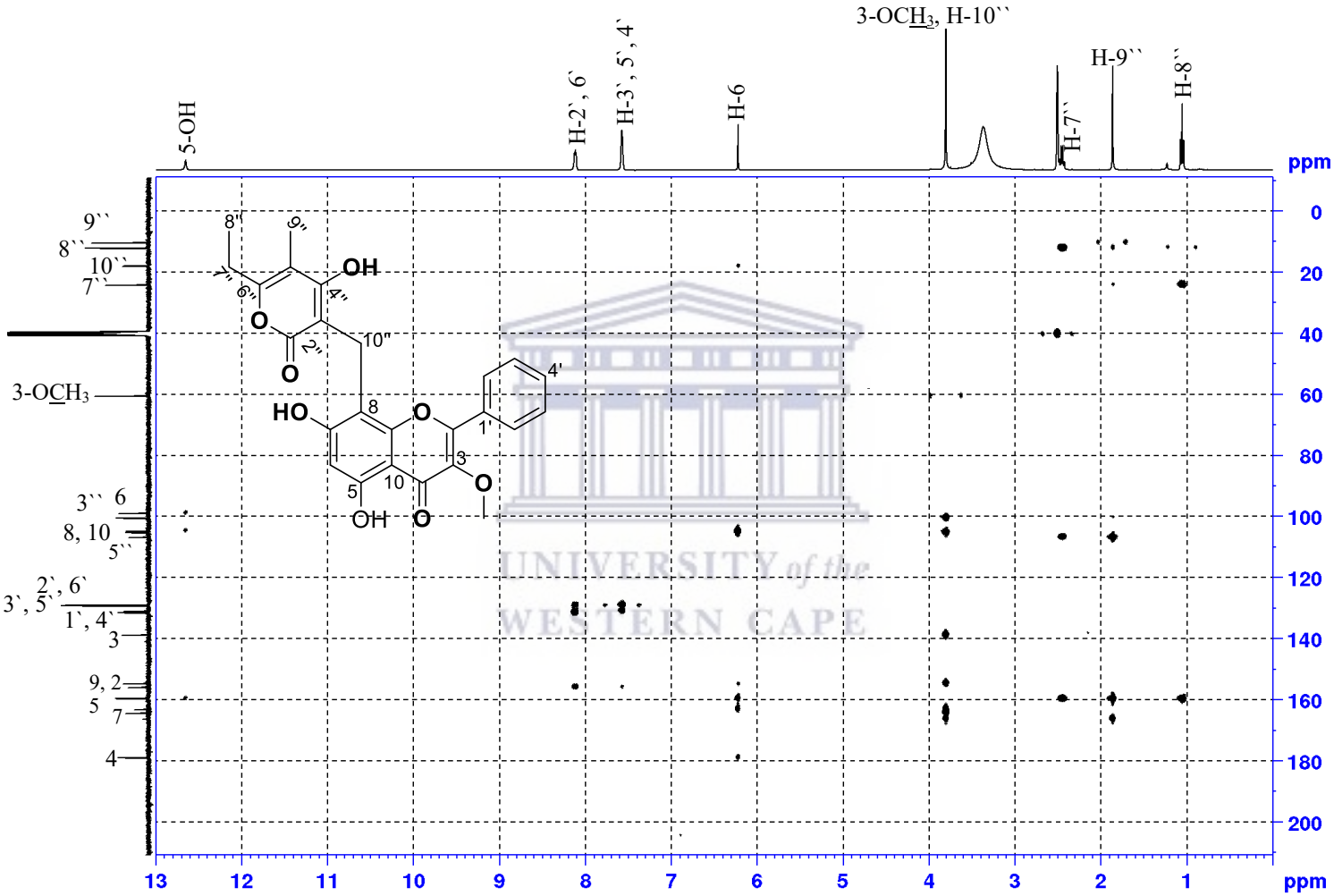

Fig. 4.10: HR-ESI-MS spectrum of compound **1**

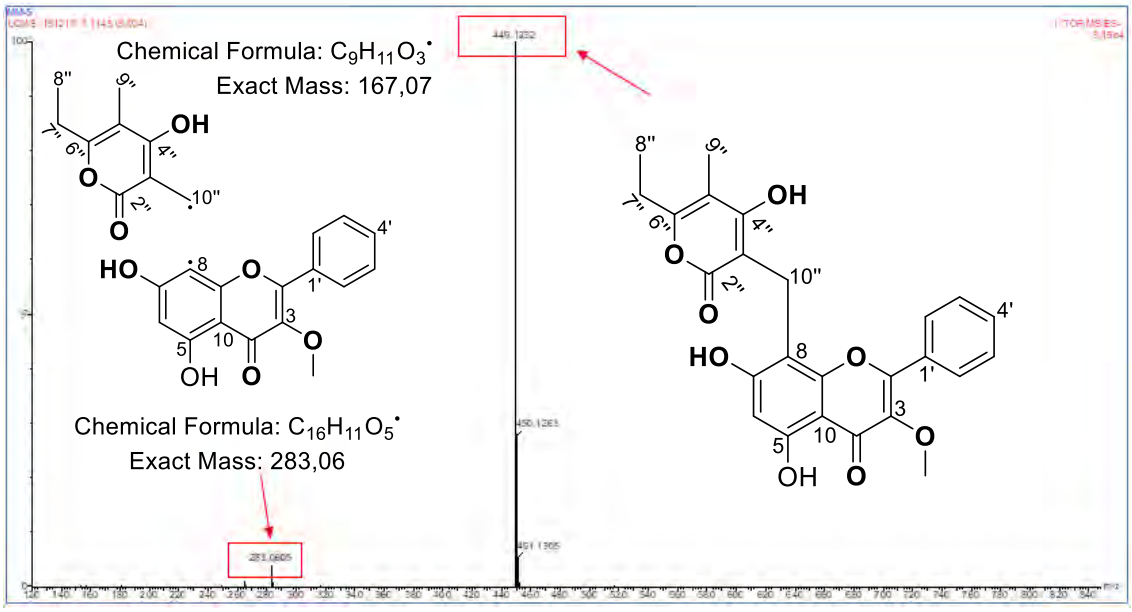

Fig. 4.11: UV-vis spectrum (MeOH) of compound **1**

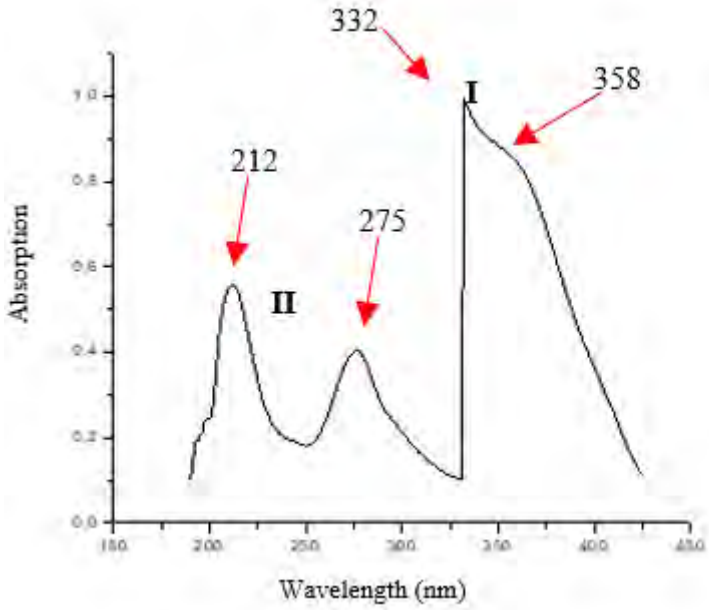

Fig. 4.12: ^{13}C NMR spectrum (100 MHz, $CDCl_3$) of the acetylated derivative of compound **1**

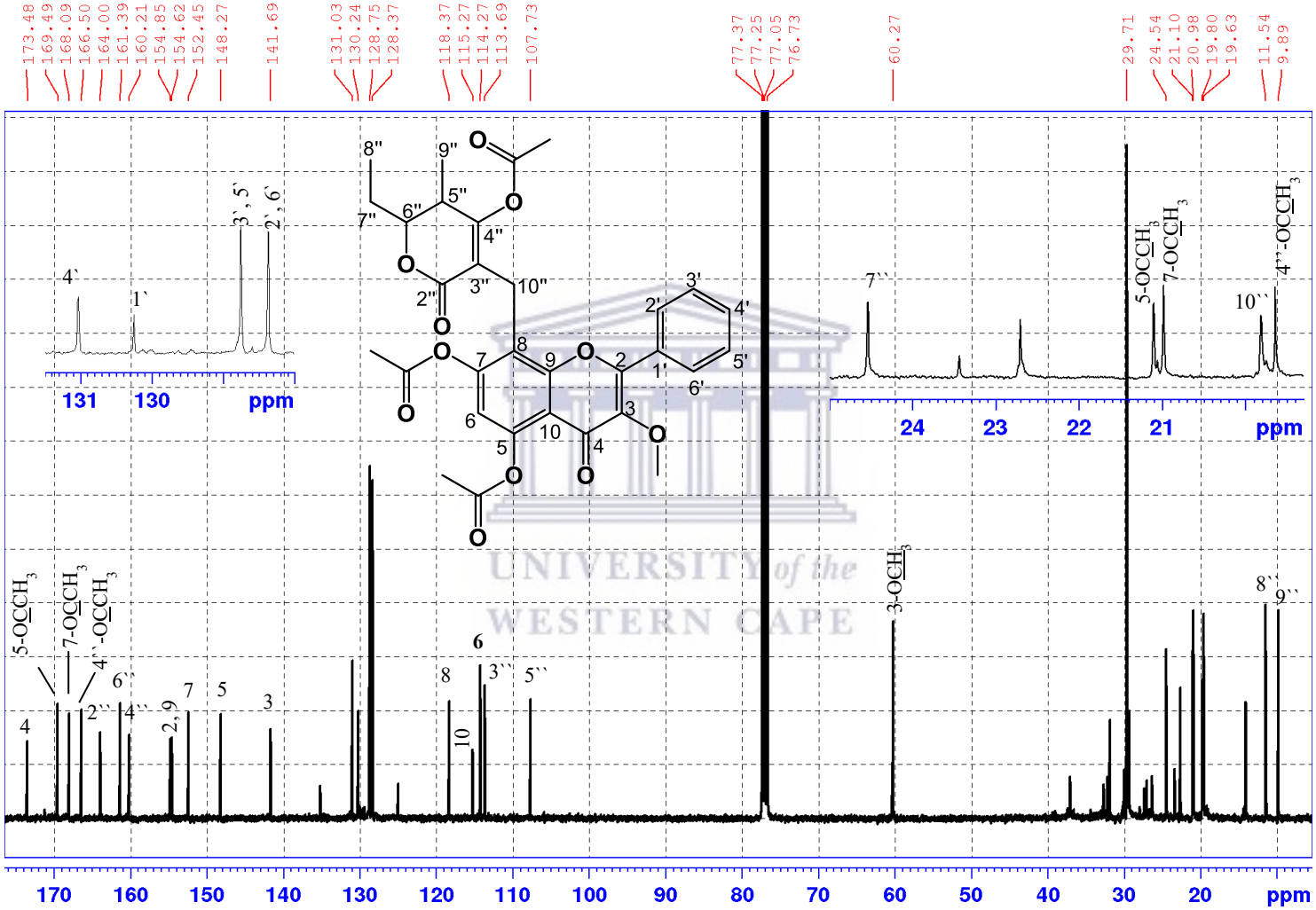

Compound 2: Petiolactone B

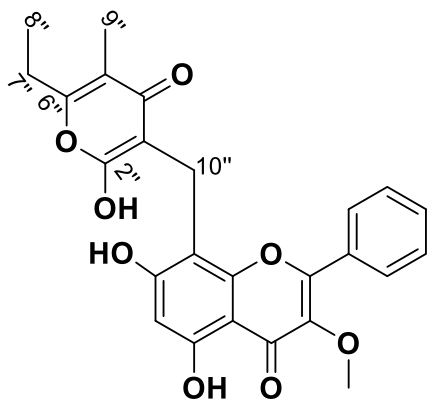

Fig. 4.13: Chemical structure of compound **2**

Compound **2** (Fig. 4.13) was isolated as a yellow amorphous powder after successful purification of fractions 29-32 (32.0 mg) of the main silica gel column using flash silica gel column chromatography, eluting isocratically with $CHCl_3$:EtOAc (50:50). Its structural characterization followed from an extensive evaluation of the NMR (one and two-dimensional) and HRESIMS experiments. The HRESIMS (Fig. 4.20) showed a fragment peak with *m/z* at 437.1215 corresponding to $[(M+2H) – 15]^-$ (calculated for $C_{25}H_{22}O_8$).

The ^{1}H (Fig. 4.15) and ^{13}C NMR (Fig. 4.17) spectra of compound **2** resembled those of compound ***1***, with a few exceptions. The following key differences were noted: the proton signals of the pyrone moiety all shifted significantly upfield, δ_H: 0.75 (3H, *t*, *J* = 7.6 Hz, H-8``), 1.41 (3H, *s*, H-9``), 2.22 (2H, *q*, *J* = 7.5 Hz, H-7``). In fact, the corresponding carbon resonances were also shifted, $\delta_C$ 5.6 (C-9``), 9.9 (C-8``), 21.7 (C-7``), and 29.7 (C-10``). In addition, a deshielded signal appeared at $\delta_C$ 201.6 and could only be assigned to the carbonyl unit located at C-4``. While the signals for C-2`` and C-6``, respectively, appeared at δ_C 104.0 (this was 164.3 in compound **1**) and 186.4 (this was 159.6 in compound **1**). Evidently, the substitution pattern had to be different. Therefore, a γ-pyrone (or 4-pyrone) ring system was assigned to the pyrone moiety. To further corroborate this, an HMBC experiment (Fig. 4.20) was employed, from which the following correlations were observed: the proton signal at δ_H 1.41 (H-9``) with C-4`` (δ_C = 201.6) or 3.18 (H-10``) with C-4`` (δ_C = 201.6). The attachment of the γ-pyrone moiety and substitution pattern of the flavonoid remained unchanged (confirmed by HMBC). Similarly, to confirm the number of hydroxyl groups in this compound

acetylation was carried out. As such, the ^{13}C NMR (Fig. 4.23, Table 4.9 in the appendix) of the acetylated derivative revealed six additional resonance (δ_C = 20.4, 21.1, 21.1, 167.3, 167.9, and 169.4) that were indicative of the three acetyl groups located at C-5, C-7, and C-2``. Therefore, the structure of compound **2** was readily established as 6``-ethyl-4``-hydroxy-5``-methyl-4-oxo-4*H*-pyran-3-yl-5,7-dihydroxy-3-methoxyflavone and is hereby given the trivial name petiolactone B. Table 4.3 shows the NMR spectroscopic data of this compound and Fig. 4.14 shows significant HMBC and (^1H-^1H) correlation spectroscopy (COSY) correlations. The UV-visible spectrum is shown in Fig. 4.22.

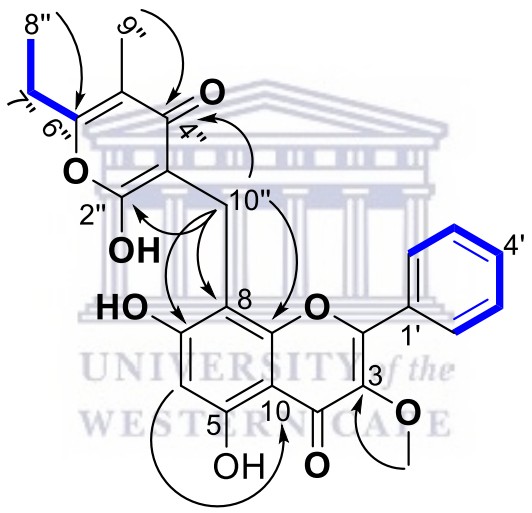

Fig. 4.14: Selected HMBC (black arrows) and COSY (blue) correlations of compound **2**

Table 4.3: NMR spectroscopic data (400 MHz, DMSO-d_6) for compound ***2***

#	δ_C, type	δ_H (*J* in Hz)	HMBC
2	155. 3, C	-	–
3	138.9, C	-	–
4	178.6, C	-	–
5	160.0, C	-	–
6	98.4, CH	6.24, *s*	C-10, C-5, C-4[b], C-7, C-8
7	163.6, C	-	–
8	100.3, C	-	–
9	155.4, C	-	–
10	104.7, C	-	–
1`	130.7, C	-	–
2`, 6`	128.8[a], CH	8.21[a], *m*	C-4`, C-3`, 5`, C-2
3`, 5`	129.1[a], CH	7.56[a], *brt* (3.3)	C-2`, 6`, C-1`
4`	131.5, CH	7.56[a], *brt* (3.3)	C-2`,6`, C-3`, 5`
2``	104.0[a], C	-	–
3``	104.0[a], C	-	-
4``	201.6, C	-	-
5``	107.1, C	-	-
6``	186.4, C	-	-
7``	21.7, CH_2	2.22, *q* (7.7)	C-8``, C-5``, C-6``
8``	9.9, CH_3	0.75, *t* (7.6)	C-6``, C-7``
9``	5.6, CH_3	1.41, *s*	C-5``, C-6``, C-4``
10``	29.7, CH_2	3.18, *m*	C-3``, C-2``, C-4``, C-7, C-8, C-9
3-OMe	60.0, CH_3	3.80[a], *s*	C-3
5-OH	–	12.65, *s*	C-5, C-6, C-10

[a] -Overlapping ^{1}H and ^{13}C-NMR signals. [b] -long range correlation on HMBC.

Although compounds 1 and 2 are structural isomers, from an organic reaction mechanisms point of view they may readily interchange via tautomerism, but the exposure of one of the isomers to basic or acidic conditions showed no evidence of such phenomenon, thus suggesting some inherent stability of each isomer (scheme 4.2). Interestingly, there is hardly anything in the literature about tautomerism between these two molecular frameworks except one paper which claims it happens only at the melting point (<168 ºC) of one 4-hydroxy-2-pyrone system (4-OH-2-P) where it becomes converted to a 2-hydroxy-4-pyrone (2-OH-4-P) system (Butt and Elvidge, 1963).

Scheme 4.2: Proposed tautomerism (mechanism) of compounds **1** and **2**

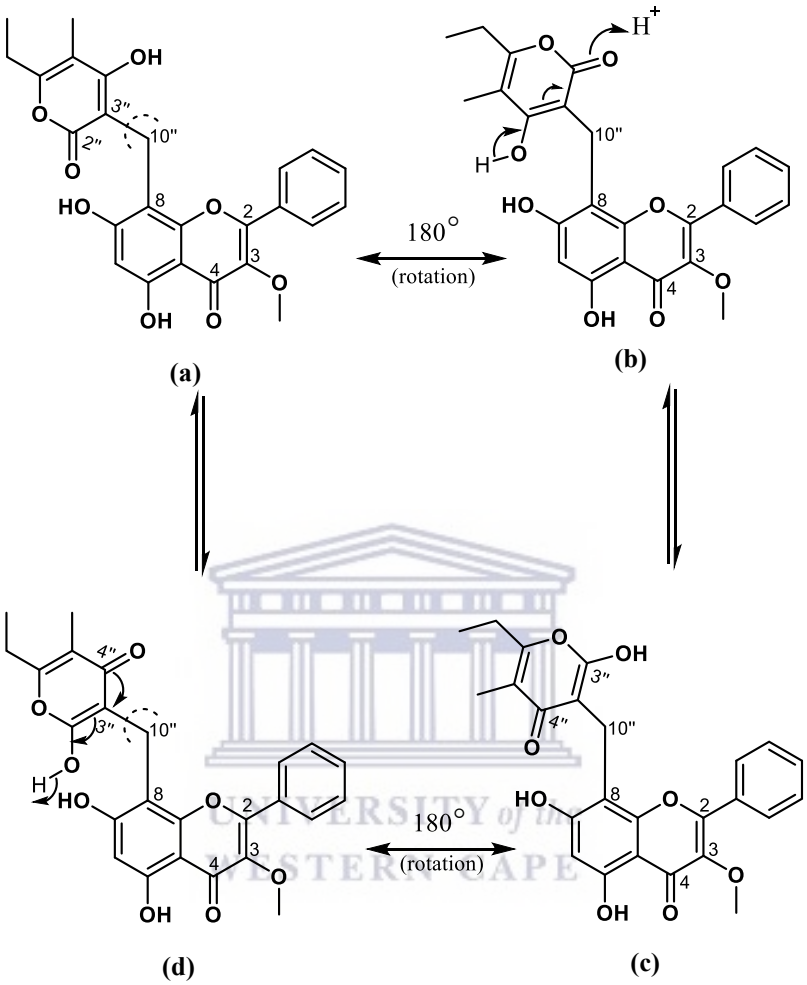

Nevertheless, further probing of the literature provided evidence that may support our hypothesis of the independent existence of the two molecular frameworks. According to the literature, there is evidence to the effect that while the 4-OH-2-P system prefers participating in Diels-alder reactions as dienes and do not engage in the formation of hydrazones with, for instance, phenylhydrazine (Cai, 2019), 2-OH-4-P system readily participates in the latter (Mishrikey, 1992). In other words, the two frameworks will not be present together because of tautomeric equilibrium, but each one enjoys its own stability and with a larger energy barrier.

Fig. 4.15: ^{1}H-NMR spectrum (DMSO-d_6, 400 MHz) of compound **2**

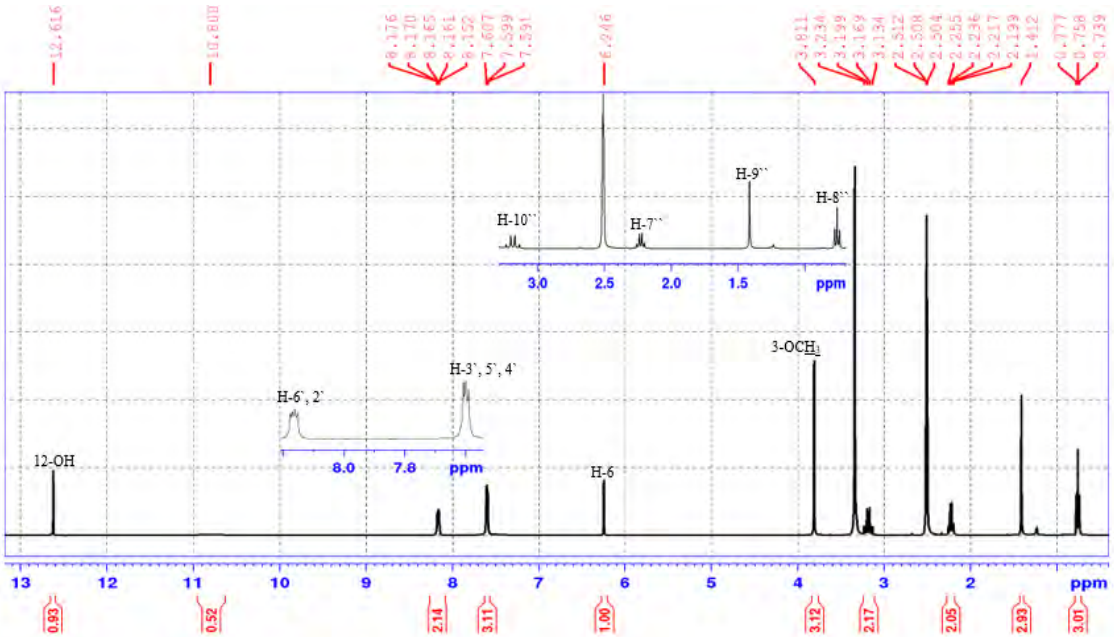

Fig. 4.16: COSY spectrum (DMSO-d_6) of compound **2**

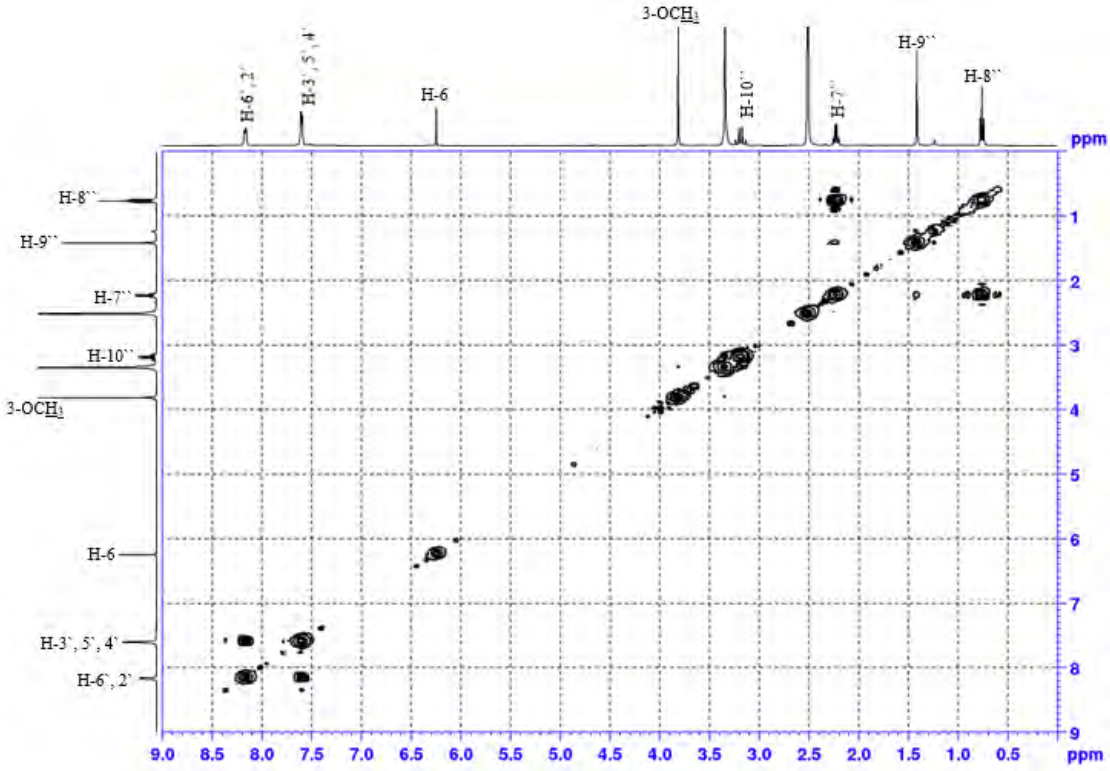

Fig. 4.17: ^{13}C-NMR spectrum (DMSO-d_6, 100 MHz) of compound **2**

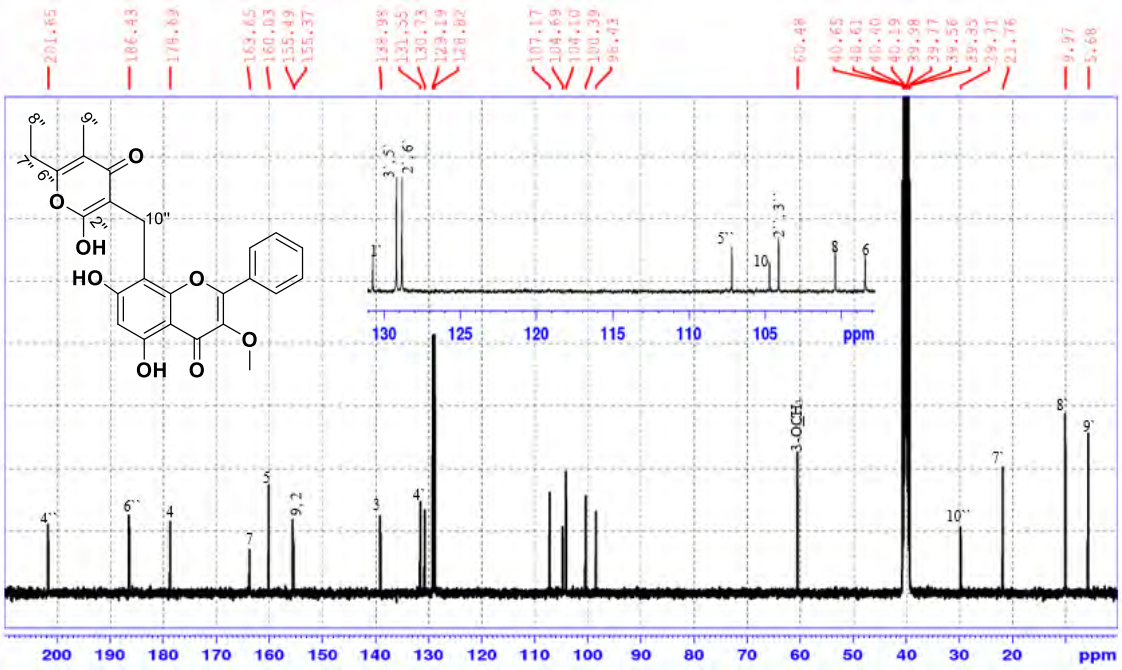

Fig. 4.18: DEPT-135 spectrum (DMSO-d_6) of compound **2**

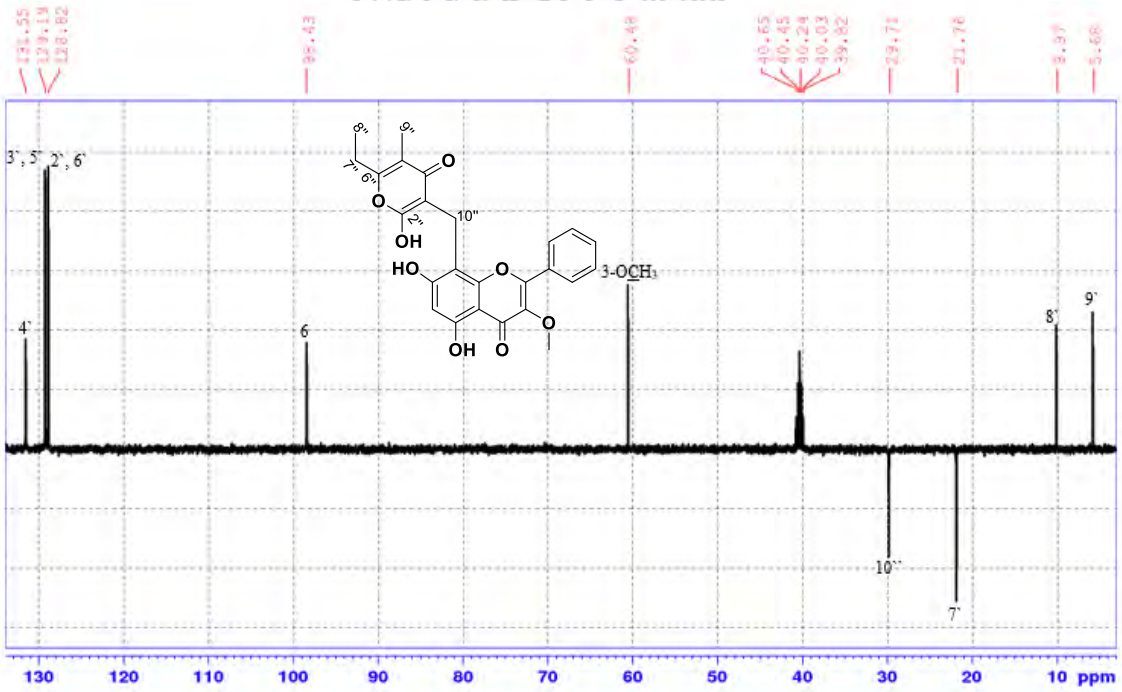

Fig. 4.19: HSQC spectrum (DMSO-d_6) of compound **2**

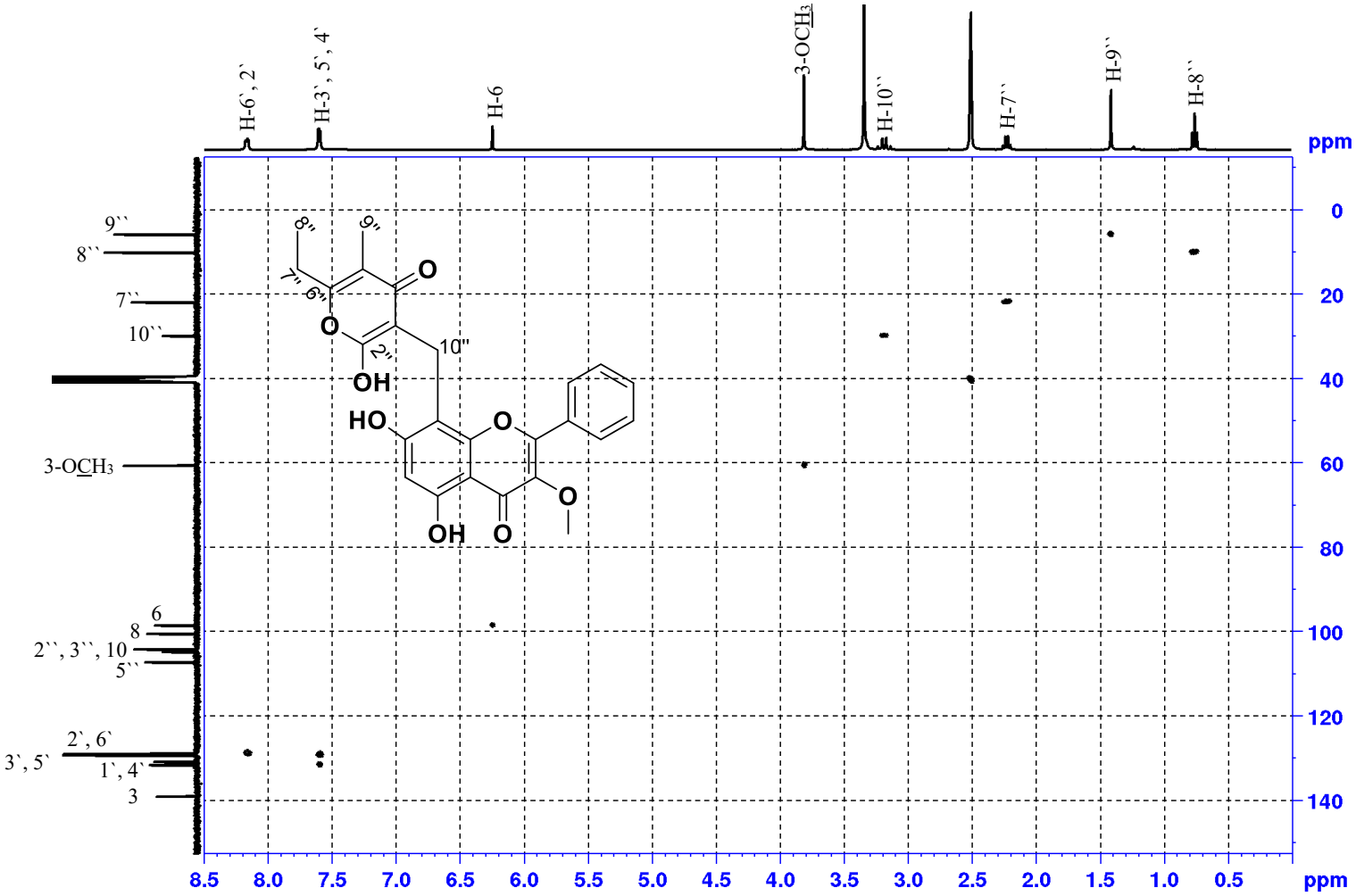

Fig. 4.20: HMBC spectrum (DMSO-d_6) of compound **2**

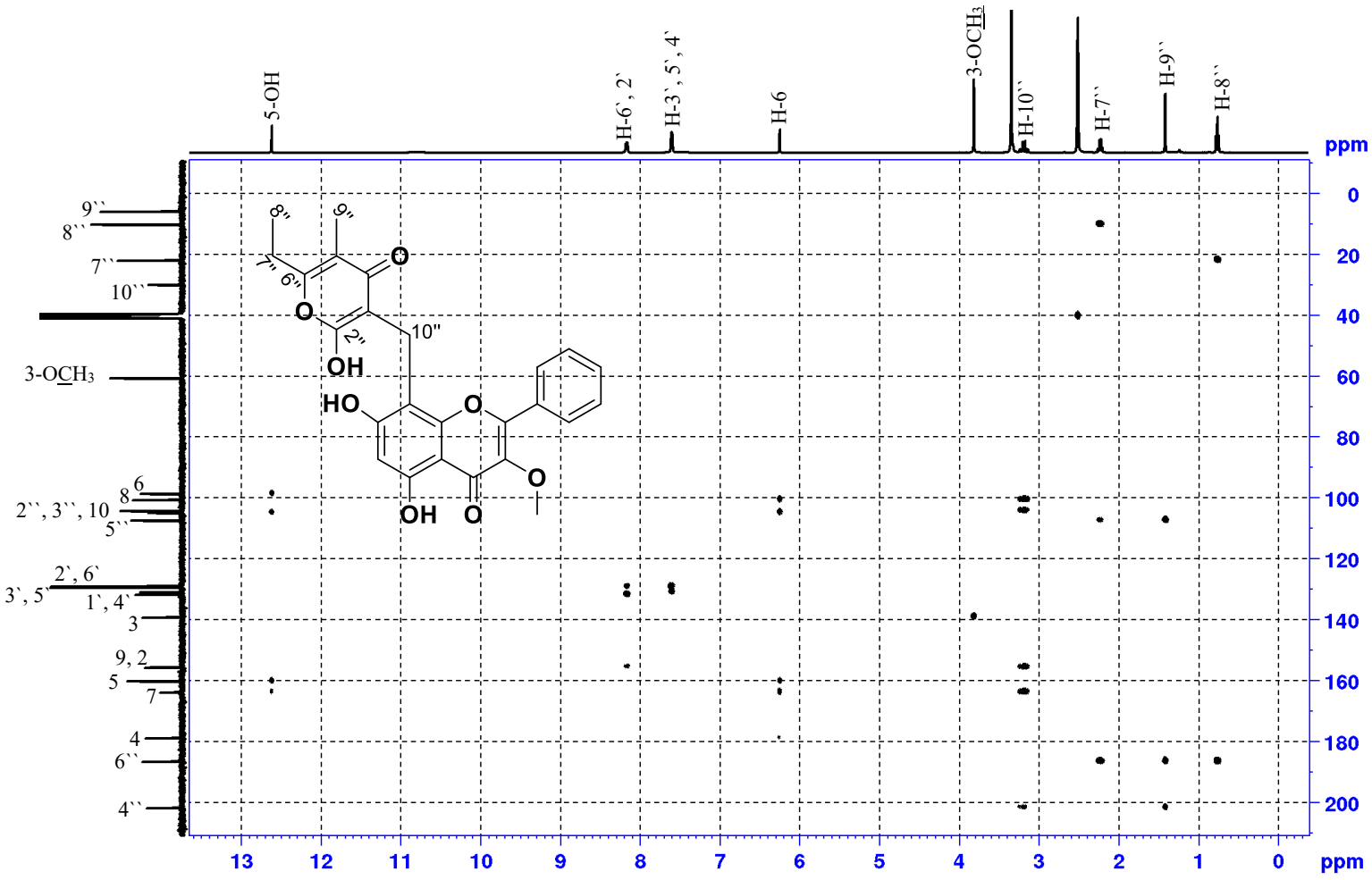

Fig. 4.21: HR-ESI-MS spectrum of compound **2**

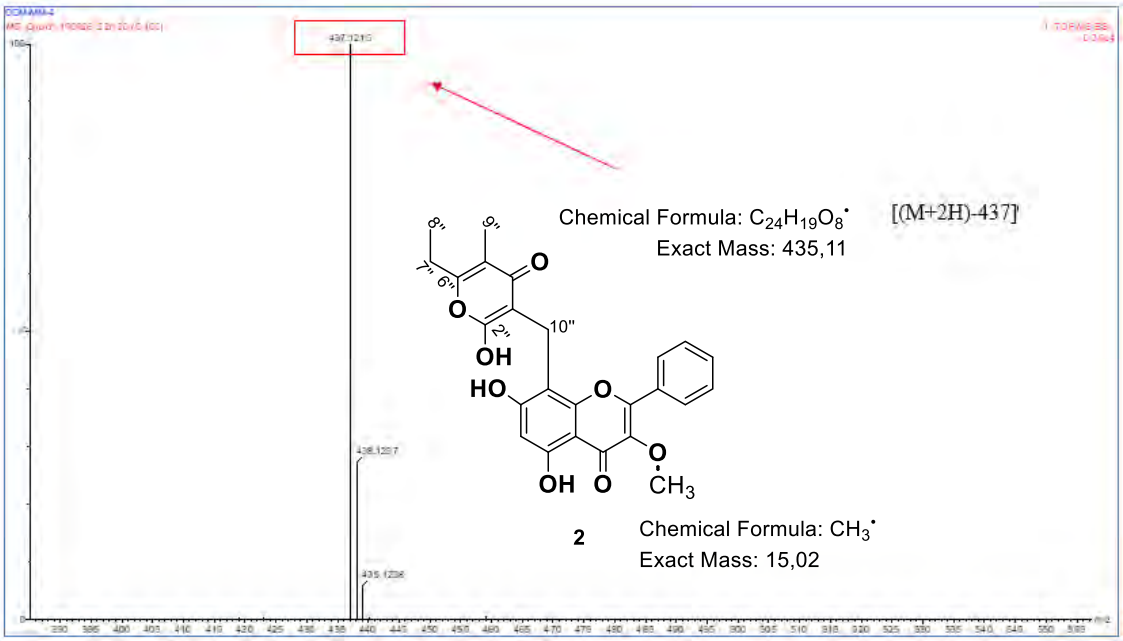

Fig. 4.22: UV-vis spectrum (MeOH) of compound **2**

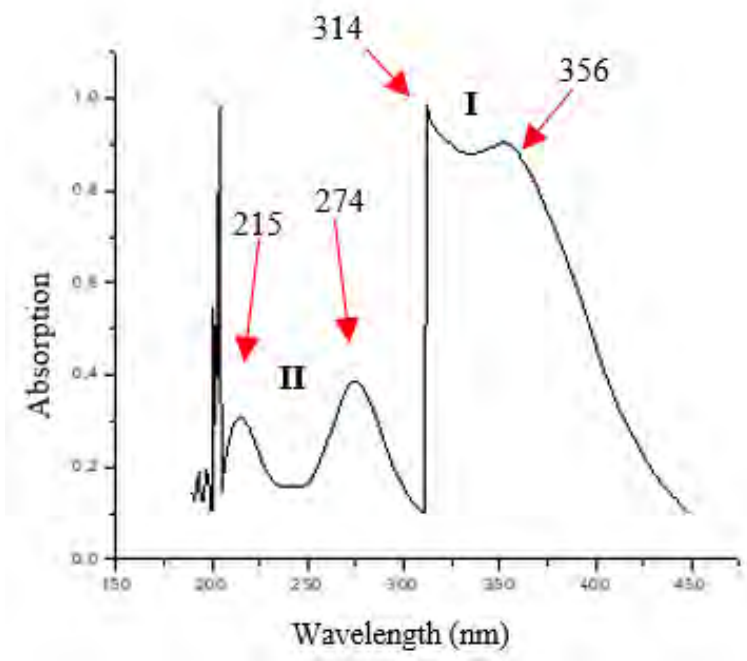

Fig. 4.23: ^{13}C NMR spectrum (100 MHz, $CDCl_3$) of the acetylated derivative of compound **2**

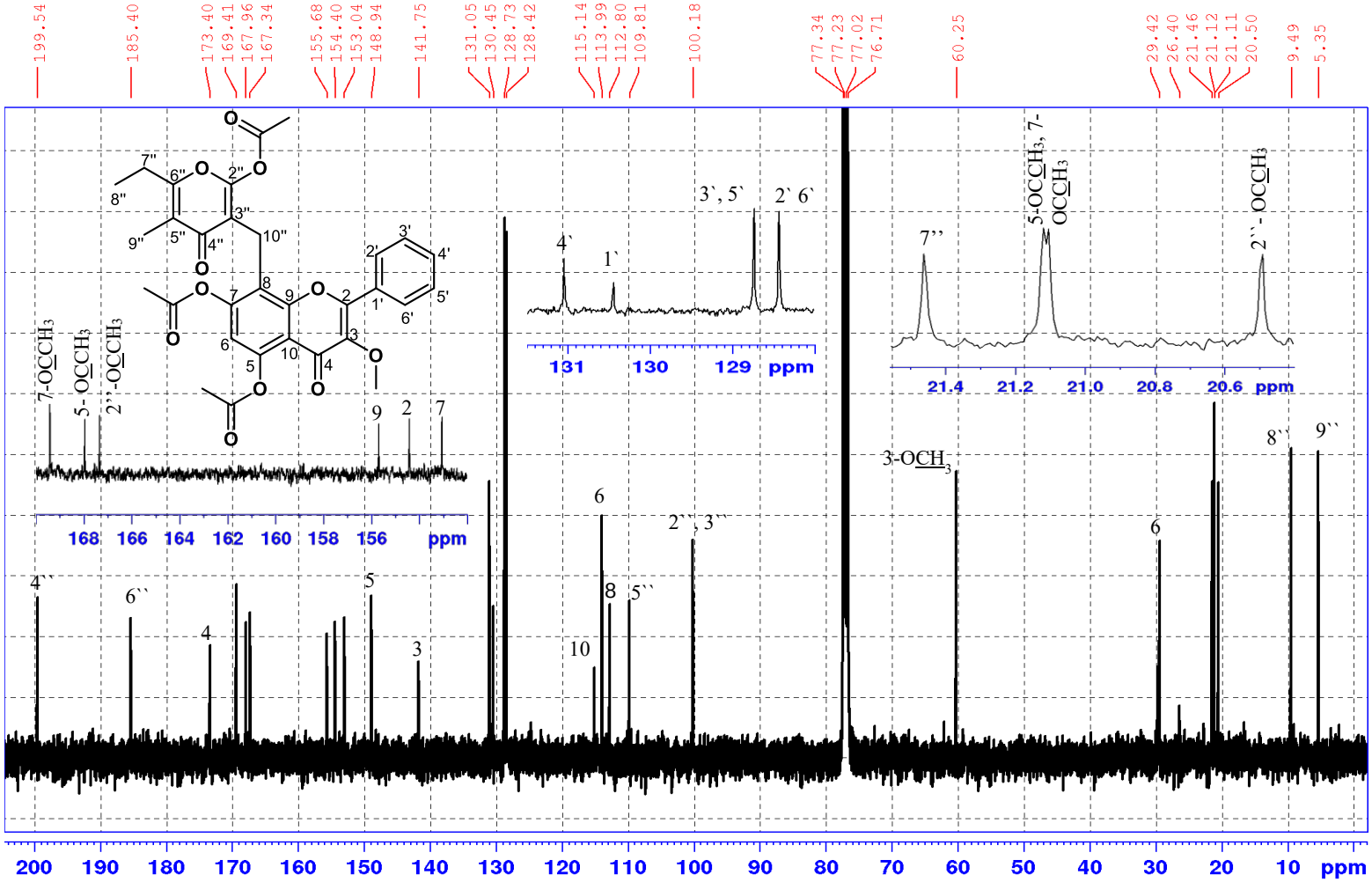

Compounds 3, 4, and 5: galanin-3-methyl ether (**3**), 3,5-dihydroxy-6,7,8-trimethoxyflavone (**4**), and 5,6-dihydroxy-3,7-demethoxyflavone (**5**)

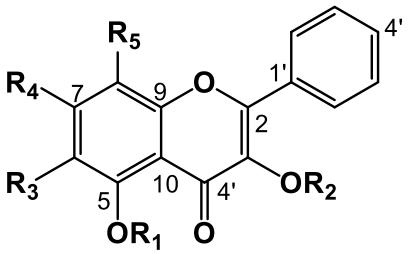

3 R_1 = H, R_2 = Me, R_3 = H, R_4 = OH, R_5 = H

4 R_1 = H, R_2 = H, R_3 = R_4 = R_5 = OMe

5 R_1 = H, R_2 = Me, R_3 = OH, R_4 = OMe, R_5 =H

Fig. 4.24: Chemical structures of compounds **3**, **4**, and **5**

Compound **3** (Fig. 4.24) was obtained as a yellow amorphous powder from fractions 15-18 (9.00 mg) of the main silica gel column, eluting with $CHCl_3$:EtOAc gradient (100 :0→50: 50). Interrogation of the spectroscopic data showed that it was identical to the compound that is already reported in the literature; thus, its characterization was established using both one dimensional (1D) and two-dimensional (2D) NMR spectra (^{1}H, ^{13}C, DEPT-135, COSY, HMBC, HSQC) and by direct comparison with the literature (Xin et al., 2017). The ^{1}H NMR spectrum (Plate 3A in the appendix) showed resonances assignable to two *meta*-coupled aromatic protons at δ_H 6.23 (1H, *d*, *J* = 2.0 Hz, H-6) and 6.46 (1H, *d*, *J* = 2.0 Hz, H-8). Furthermore, the integration and substitution pattern of the signals at δ_H 8.01 (2H, *m*, H-2`/6`) and 7.58 (3H, *t*, *J* = 3.24 Hz, H-3`/4`/5`) indicated an unsubstituted B-ring (Jakupovic et al., 1989). The remainder of the spectrum showed a strong singlet at δ_H 3.80 that was indicative of the methoxy protons, whose connectivity at C-3 (δ_C 139.2) was confirmed by (^{1}H–^{13}C) HMBC correlation (Plate 3F in the appendix). The ^{13}C NMR (Plate 3C in the appendix) and DEPT-135 (Plate 3D in the appendix) spectra showed 16 signals: indicative of one methyl at δ_C 61.5, seven methine at δ_C 98.7 (C-6), 93.9 (C-8), 128.2 (C-2`/6`), 128.8 (C-3`/5`) and 131.1 (C-4`), including eight *quaternary* carbons as shown in Table 4.4. The ^{1}H-NMR and ^{13}C-NMR spectroscopic data of compound **3** was found to resemble the known compound galangin (Vrkoc, Ubik and Sedmera, 1973), except the absence of the signal at δ_C 139.2 (C-3) in

galangin. Nevertheless, compound **3** was identified as 5,7-dihydroxy-3-methoxyflavone (galangin-3-methyl ether), which to the best of our knowledge is reported for the first time from *Helichrysum petiolare*. This compound has been previously isolated from *Helichrysum armenium* (Cubukcu and Yüksel, 1982), *H. italicum* (D'Abrosca et al., 2016), *H. kraussii* (Legoalea and Mashimbyeb, 2013), and *H. odoratissimum* (Legoalea and Mashimbyeb, 2013).

Compound **4** (Fig. 4.24) was isolated as yellow needles/platelets after successful purification of fraction 220 (250 mg) of the main silica gel column using flash silica gel column chromatography, eluting isocratic with $CHCl_3$:EtOAc (50:50). It was readily identified as 3,5-dihydroxy-6,7,8-trimethoxyflavone based on its 1D and 2D NMR data, in conjunction with HRESIMS (Plate 4G in the appendix), which showed a molecular ion peak $[M - H]^-$ at *m/z* 343.0823 corresponding to $C_{18}H_{16}O_7$. The ^1H NMR (Plate 4A in the appendix) spectrum showed three intense singlets at δ_H 3.96, 3.98, and 4.13 assignable to the three methoxy groups. Other resonances of note include the signal at δ_H 6.68 for the hydroxyl proton (which in compound **3** was replaced by a methoxy) showing cross-peaks in HMBC (Plate 4F in the appendix) with C-3 (δ_C = 136.4), C-4 (δ_C = 176.0) and C-2 (δ_C = 145.6). ^{13}C NMR (Plate 4C in the appendix) and DEPT-135 (Plate 4D in the appendix) suggested a *maximum* substitution of the A-ring. The integration and substitution pattern of the B-ring was found to be the same as in compound **3** (Table 2). Finally, the NMR data of compound **4** was identical to those published in the literature (Wollenweber et al., 1993). Therefore, based on this evidence, compound **4** was determined as 3,5-dihydroxy-6,7,8-trimethoxyflavone, which to the best of our knowledge is isolated for the first in *H. petiolare.* This compound has been previously isolated from several *Helichrysum* species, including *H. graveolens* (Hansel and Cubukcu, 1972), *H. arenarium* (Vrkoc, Ubik and Sedmera, 1973), *H. kraussii* (Candy and Wright, 1975), *H. pallasii* (Cubukcu and Bingol, 1984), *H. noeanum* (Bingöl and Çubukçu, 1984), *H. decumbens* (Tomás-Lorente et al., 1989), *H. odoratissimum* (Van Puyvelde et al., 1989), *H. stoechas* (Lavault and Richomme, 2004), *H. compactum* (Süzgeç et al., 2005) and *H. chasmolycicum* (Süzgeç-Selçuk and Birteksöz, 2011).

Compound **5** (Fig. 4.24) was isolated as white crystals from fraction 244 (36 mg) of the main silica gel column, eluting with hexane:DCM (100:0 → 0: 100) gradient. The molecular formula of ***5*** was determined as $C_{17}H_{14}O_6$ by the HRESIMS experiment (Plate 5G in the appendix), which provided a molecular ion peak $[M - H]^-$ at *m/z* 313.0710. Its structure was deduced by direct comparison of its ^1H (Plate 5A in the appendix) and ^{13}C NMR (Plate 5C in the appendix) spectra with compounds **3** and **4**, which immediately suggested a demethylated derivative. This was confirmed as follows. The ^1H NMR spectral data showed two intense singlets at δ_H 4.04 (3H, s, 7-OCH_3) and 3.86 (3H, *s*, 3-OCH_3) corresponding to the two methoxy groups, whose attachments were confirmed by (^1H-^{13}C) HMBC (Plate 5F in the appendix) correlation. The singlet at δ_H 6.57 (H-8) for the aromatic proton was assigned based on its HMBC correlation with C-9 (δ_C = 155.1), C-7 (δ_C =130.0), C-6 (δ_C = 152.4[a]), C-4 (δ_C = 179.4), and C-10 (δ_C = 106.3). Since the positions of the two methoxy-groups (3-OCH_3 and 7-OCH_3) and that of the aromatic proton (H-8) was already confirmed by cross-peaks on HMBC, it was tentatively proposed that two OH-groups with chemical shifts at δ_H 12.85 (1H, *s*) and 5.30 (1H, *s*) were present in the A-ring. According to the literature (Wollenweber et al., 1993), the de-shielded singlet at δ_H 12.4 is typical for a hydrogen-bonded OH-group, implying that this downfield resonance must be placed at C-5. As such, the other resonance (δ_H 5.30) was assigned to the hydroxyl group placed at C-6. The ^{13}C NMR spectrum of compound **5** showed slight differences in comparison to compound **3**, with the signals at δ_C 130.0 and 152, respectively, being assigned as a 7-methoxy and 6-hydroxy group, according to HMBC. It is worth pointing out that to the best of our knowledge the ^{13}C NMR data (Table 2) of compound **5** is presented here for the first time. Nevertheless, based on the obtained spectroscopic evidence and comparison of the available ^1H NMR data (Wollenweber et al., 1993), compound **5** was established as 5,6-dihydroxy-3,7-demethoxyflavone. Although this compound has been previously isolated from three natural sources *Helichrysum chrysargyrum* (Bohlmann, Zdero and Ziesche, 1979), *Achyrocline alata* (Bohlmann et al., 1980), and *Gnaphalium affine* (Morimoto, Kumeda and Komai., 2000), to the best of our knowledge, it is hereby reported for the first time in *H. petiolare*.

Table 4.4. NMR spectroscopic data (400 MHz, $CDCl_3$, DMSO-d_6) of compounds **3**, **4**, and **5**

	3[$]		**4**[*]		**5**[*]		
#	**δ_C, type**	**δ_H (*J* in Hz)**	**δ_C, type**	**δ_H (*J* in Hz)**	**δ_C, type**	**δ_H (*J* in Hz)**	**HMBC**
2	155.6, C	-	145.6, C	-	156.0, C	-	-
3	139.2, C	-	136.4, C	-	139.2, C	-	-
4	178.6, C	-	176.0, C	-	179.4, C	-	-
5	161.7, C	-	147.8, C	-	151.7[a], C	-	-
6	98.7, CH	6.23, *d* (2.0)	136.0, C	-	152.4[a], C	-	C-8, C-6, C-5, C-7
7	164.9, C	-	153.4, C	-	130.0, C	-	-
8	94.3, CH	6.46, *d* (2.0)	133.2, C	-	93.1, CH	6.57, *s*	C-6, C-10, C-9, C-7, C-4
9	157.0, C	-	145.2, C	-	155.1, C	–	-
10	104.9, C	-	105.3, C	-	106.3, C	–	-
1`	130.5, C	-	130.7, C	-	130.4, C	–	-
2`, 6`	128.6, CH	8.01, *m*	127.7, CH	8.27, *m*	128.4, CH	8.06, *m*	C-4`, C-3`, C-5`, C-2
3`, 5`	129.2, CH	7.58, *t* (3.2)	128.7, CH	7.55, *m*	128.6, CH	7.51, *t* (3.6)	C-2`, 6`, C-1`, C-4`
4`	131.5, CH	7.58, *t* (3.2)	130.5, CH	7.50, *m*	130.9, CH	7.51, *t* (3.6)	C-2`, 6`, C-3`, C-5`
3-OH, O<u>Me</u>	60.0, CH_3	3.88, *s*	-	6.68, *s*	60.4, CH_3	3.86, s	C-3
5-OH	-	12.57, *s*	-	11.44, *s*	-	12.85, *s*	C-5, C-6, C-10
6-OH, O<u>Me</u>	-	-	61.2, CH_3	3.96, *s*	-	5.30, *s*	-
7-OH, O<u>Me</u>	-	10.93, *brs*	61.8, CH_3	4.13, *s*	60.9, CH_3	4.04, *s*	-
8-O<u>Me</u>	-	-	62.1, CH_3	3.99, *s*	-	-	-

[a] -Signals may be interchangeable. [$] -measured in DMSO-$d_6$. [*] -measured in $CDCl_3$

Compound 6: Helipyrone

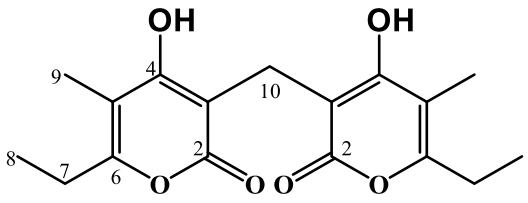

Fig. 4.25: Chemical structure of compound **6**

Compound **6** (Fig. 4.25) was isolated as a white amorphous powder after successful purification of fraction 220 (250 mg) of the main silica gel column using flash silica gel column chromatography, eluting isocratic with $CHCl_3$:EtOAc (50:50). Its structure was readily deduced to be helipyrone by comparison with the available literature (Ali, Bagch and Pakrashi, 1982). High-resolution mass spectrometry, HRMS (Plate 6G in appendix), confirmed the molecular formula $C_{17}H_{20}O_6$ (with two characteristic fragments $[M – H]^+$ at *m/z* = 167.03 and 153.0550).

Briefly, the ^{1}H NMR spectrum (Plate 6A in appendix) showed the following resonances at δ_H: 3.55 (2H, *s*, H-10), 1.20 (3H, *t*, *J* = 7.5 Hz, H-8), 2.56 (2H, *q*, *J* = 7.4 Hz, H-7), and 1.96 (3H, *s*, H-9). The ^{13}C NMR spectrum (Plate 6C in appendix) exhibited nine carbon signals at δ_C 169.7 (C-2), 101.7 (C-3), 168.7 (C-4), 108.8 (C-5), 161.4 (C-6), 24.3 (C-7), 19.1 (C-10), 11.6 (C-8), and 9.4 (C-9), which were assigned through HSQC (Plate 6E in appendix) and HMBC (Plate 6F in appendix) experiments. Our data agreed to the known helipyrone structure that has been previously reported from *Helichrysum italicum* (Opitz and Hansel, 1970), *H. arenarium* (Vrkcoč, Dolejš and Buděšínský, 1975), *H. stoechas* (Rios, Recio and Villar, 1991), *H. microphyllum* (Venditti et al., 2016), *Anaphalis araneosa* (Ali, Bagch and Pakrashi, 1982), and *A. sinica* (Hua and Wang, 2004). To the best of our knowledge, this is the first report of compound **6** from *H. petiolare*. Table 4.5 shows the fully assigned NMR data of compound **6** (alongside the reported literature data).

Table 4.5: ^{1}H and ^{13}C-NMR spectroscopic data ($CDCl_3$, 400 MHz) of compound **6**

#	δC, type		δH (*J* in Hz)		HMBC
2	169.7 (C)	169.1[ǂ] (C)	–	–	–
3	101.7 (C)	101.5[ǂ] (C)	–	–	–
4	168.7 (C)	168.3[ǂ] (C)	–	–	–
5	108.8 (C)	108.5[ǂ] (C)	–	–	–
6	161.4 (C)	160.9[ǂ] (C)	–	–	–
7	24.3 (CH_2)	24.3[ǂ] (CH_2)	2.56, *q* (7.4)	2.57[ǂ], *q*	C-8, C-6, C-5
8	11.6 (CH_3)	11.4[ǂ] (CH_3)	1.20, *t* (7.5 Hz)	1.20[ǂ], *t*	C-7, C-6
9	9.4 (CH_3)	9.2[ǂ] (CH_3)	1.96, *s*	1.98[ǂ], *s*	C-6, C-5, C-4
10	19.1 (CH_2)	19.2[ǂ] (CH_2)	3.55, *s*	3.53, *s*[ǂ]	C-4, C-3, C-2
4-OH			11.2, *s*	11.1[ǂ], *s*	

[ǂ] -Literature data (Ali et al., 1982; $CDCl_3$, 100 MHz)

Compound 7: Caffeic anhydride

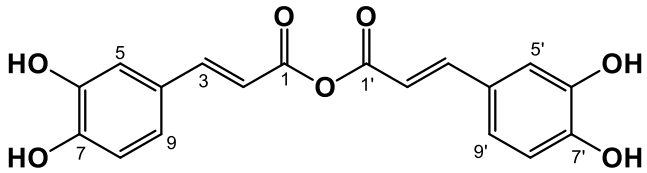

Fig. 4.26: Chemical structure of compound **7**

Compound **7** (Fig. 4.26) was obtained as a yellow solid after successful purification of fractions 90-101 (40.0 mg) of the main silica gel column on Sephadex column chromatography, eluting isocratic with ethanol:deionized water (90:10). Its structural characterization followed from 1D and 2D NMR experiments (Plates 7A-7F in the appendix), as well as comparison with the available literature (Elabbaraa et al., 2014).

The ^{1}H NMR spectrum (Plate 7A in the appendix) displayed prominent peaks (with some impurities) in the aromatic region (δ_H = 6.18–7.47) which appeared as duplicates. Interrogation of the spectrum revealed that the signals at δ_H 6.75 (1H, *d*, *J* = 3.0 Hz, H-8), 6.96 (1H, *d*, *J* = 8.3 Hz, H-9), and 7.10 (1H, *m*) were indicative of a trisubstituted benzene ring (Elabbaraa et al., 2014). Furthermore, the *trans*-configured olefinic protons H-2 and H-3, respectively, appeared as doublets at δ_H 6.25 (1H, *d*, *J* = 15.7 Hz) and 7.47 (1H, *d*, *J* = 15.7 Hz). Though this

compound would be expected to display 9 carbon signals (since it is symmetrical), in the ^{13}C NMR spectrum (Plate 7C in the appendix) certain peaks were resolved, which may be due to the influence of the solvent (DMSO-d_6) and/ or experimental conditions. Nonetheless, the peaks were assigned through HSQC (Plate 7E in the appendix), HMBC (Plate 7F in the appendix), and COSY (Plate 7B in the appendix) experiments. Table 4.6 shows a summary of the NMR spectroscopic data of compound **7**. Thus, based on this evidence and comparison with the available literature (Elabbaraa et al., 2014), compound **7** was determined as caffeic anhydride. To the best of our knowledge, this compound is isolated for the first time from *H. petiolare*.

Table 4.6: ^{1}H and ^{13}C-NMR spectroscopic data (DMSO-d_6, 400 MHz) of compound **7**

#	δ_C, type		δ_H (*J* in Hz)		HMBC
1	166.8 (C)	168.6[ǂ] (C)	-	-	-
2	114.8 (CH)	115.3[ǂ] (CH)	6.25, *d* (15.7)	6.19[ǂ], *d*, (15.6)	C-4, C-1
3	145.3 (CH)	145.2[ǂ] (CH)	7.47, *d* (15.7)	7.45[ǂ], *d*, (15.6)	C-1, C-4, C-9, C-5
4	125.8 (C)	126.6[ǂ] (C)	-	-	-
5	115.4[a] (CH)	115.9[ǂ] (CH)	7.10, *m*	7.05[ǂ], *d* (1.9)	C-7, C-3, C-6, C-9
6	146.3[a] (C)	146.1[ǂ] (C)	-	-	-
7	149.3 (C)	148.6[ǂ] (C)	-	-	-
8	116.4 (CH)	116.5[ǂ] (CH)	6.75, *d* (3.0)	6.77[ǂ]	C-7, C-6, C-4, C-9
9	121.8 (CH)	121.8[ǂ] (CH)	6.96, *d* (8.3)	6.92[ǂ], *d* (8.1)	C-7, C-3, C-5
1`	165.5 (C)	168.6[ǂ] (C)	-	-	-
2`	116.5 (CH)	115.3[ǂ] (CH)	6.18, *d* (15.8)	6.19[ǂ], *d* (15.6)	C-4`, C-1`
3`	144.1 (CH)	145.2[ǂ] (CH)	7.41, *d* (15.8)	7.45[ǂ], *d* (15.6)	C-1`, C-4`, C-9`, C-5`
4`	126.2 (C)	126.6[ǂ] (C)	-	-	-
5`	115.4[a] (CH)	115.9[ǂ] (CH)	7.04, *m*	7.05[ǂ], *d* (1.9)	C-7`, C-3`, C-6`, C-9`
6`	146.3[a] (C)	146.1[ǂ] (C)	-	-	-
7`	148.6 (C)	148.6[ǂ] (C)	-	-	-
8`	116.3 (CH)	116.5[ǂ] (CH)	6.73, *d* (3.0)	6.77[ǂ]	C-7`, C-6`, C-4`, C-9`
9`	120.7 (CH)	121.8[ǂ] (CH)	6.92, *d* (8.4)	6.92[ǂ], *d* (8.1)	C-7`, C-3`, C-5`

[a] -Overlapping signals. [ǂ] -Literature data (Elabbaraa et al., 2014, DMSO-d_6, 300 MHz).

Compounds 8 and 9: Picein (**8**) and *p*-Vinylphenyl glycoside (**9**)

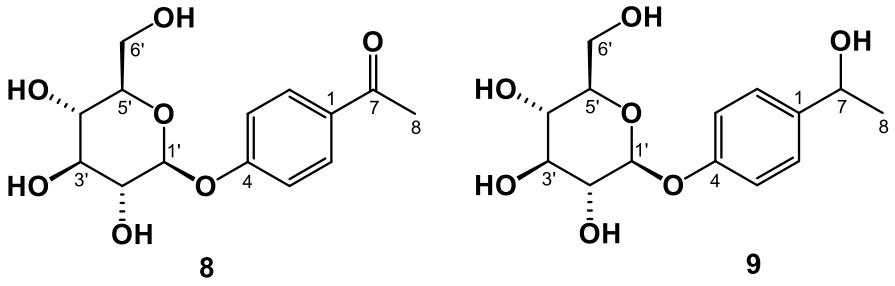

Fig. 4.27: Chemical structures of compounds **8** and **9**

Compound **8** (Fig. 4.27) was obtained as colourless needles after subjecting fractions 30-35 (50.5 mg) of the main silica gel column to repeated column chromatography, eluting with DCM:MeOH (95:5 → 90:10) gradient. Analysis of the ^{1}H-NMR (Plate 8A in the appendix) showed two intense doublets at δ_H 7.99 (2H, *d*, *J* = 8.9 Hz, H-2/6) and 7.18 (2H, *d*, *J* = 8.9 Hz, H-3/5), a strong singlet 2.58 (3H, *s*, H-8). The anomeric proton appeared as a doublet (broad) at δ_H 5.04 (1H, *brd*, *J* = 7.5 Hz) and was assigned a β-orientation based on its *J* coupling (Ushiyama and Furuya, 1989). ^{13}C-NMR (Plate 8C in the appendix) spectrum revealed the presence of fourteen signals, from which six belonged to the sugar unit (δ_C = 61.0, 69.8, 73.3, 76.5, 76.9, and 100.1), while the remaining were assigned to the aglycone moiety (25.0, 117.6^{a}, 130.2^{a}, 131.2, 161.6, and 198.0). The complete assignment of the peaks was achieved through HSQC (Plate 8E in appendix) and HMBC (Plate 8F in appendix) experiments, as well as by comparison with the available literature (Ushiyama and Furuya, 1989; Chemam et al., 2017; Dou et al., 2018). Therefore, the structural identity of this compound, which to the best of our knowledge is isolated for the first time in the *Helichrysum* genus, was determined as picein. Table 4.7 shows the fully assigned NMR data of compound **8**.

Compound **9** (Fig. 4.27) was obtained as white crystals after successful purification of fractions 50-60 (20.0 mg) of the main silica gel column using flash silica gel column chromatography, eluting isocratically with EtOAc:MeOH (90:10). Its structural characterization was compared to compound **8**. The major difference was observed in the ^{1}H NMR (Plate 9A in the appendix) where a proton signal appeared at δ_H 4.80 (1H, *q*, *J* = 6.4 Hz), which was absent in the compound **8**. The ^{13}C NMR (Plate 9C in the appendix) showed a peak

at δ_C: 69.0 and was placed at C-7 (due to the hydroxy group) in compound **9**, while this signal appeared at δ_C 198 (due to the carbonyl group) in compound **8**. The signals placed at C-1 (140.1) and C-2/6 (126.2[a]) also shifted downfield, due to a different alkyl substituent. The sugar unit remained unchanged (though its anomeric proton was overlapping with the solvent peak). Therefore, based on this evidence and comparison with the available literature (Zhao et al., 2007; Socolsky et al., 2008), compound **9** was determined as *p*-vinylphenyl glycoside. To the best of our knowledge, this compound is hereby reported for the first time from the *Helichrysum* genus. **Table 4.7** shows the complete assignment of all ^{1}H and ^{13}C-NMR signals. HSQC (Plate 9E), HMBC (Plate 9F), DEPT-135 (Plate 9D), and COSY (Plate 9B) experiments are shown in the appendix.

Table 4.7: ^{1}H and ^{13}C-NMR spectroscopic data (CD_3OD, 400 MHz) of compounds **8** and **9**

	Compound 8			**Compound 9**	
#	**δ_C, type**	**δ_H (*J* in Hz)**	**HMBC[#, b]**	**δ_C, type**	**δ_H (*J* in Hz)**
1	131.2 (C)	-	-	140.1 (C)	-
2, 6	130.2[a] (CH)	7.99, *d* (8.9)	C-4[#], C-7[#]	126.2[a] (CH)	7.30, *d* (8.5)
3, 5	115.8[a]	7.18, *d* (8.9)	C-1[#], C-4[#]	116.1[a] (CH)	7.08, *d* (8.6)
4	161.6 (C)	-	-	156.8 (C)	-
7	198.0 (C)	-	C-2/6[b], C-1[b]	69.0 (CH)	4.80, *q* (6.4)
8	25.0 (CH_3)	2.58, *s*	C-7[#], C-1[#]	24.1 (CH_3)	1.42, *d* (6.4)
Sugar moiety					
1`	100.1 (CH)	5.04, *brd* (7.5)	C-1`	101.0 (CH)	4.90, *m*
2`	76.9 (CH)	3.42–3.5, *m*	-	73.5 (CH)	3.40–3.48, *m*
3`	76.5 (CH)		-	76.5 (CH)	
4`	73.3 (CH)		-	70.0 (CH)	
5`	69.8 (CH)		-	76.7 (CH)	
6`	61.0 (CH_2)	3.92, *dd* (12.0, 2.1) 3.72, *dd* (12.0, 5.5)	-	61.1 (CH_2)	3.90, *dd* (12.1, 1.8) 3.71, *dd* (12.0, 5.1)

[a] -Overlapping signals due to symmetry. [b] -HMBC correlation is only for compound **9**. [#] -HMBC correlation is for both compounds.

Compound 10: β-sitosterol-3-*O*-β-D-glucoside (or daucosterol)

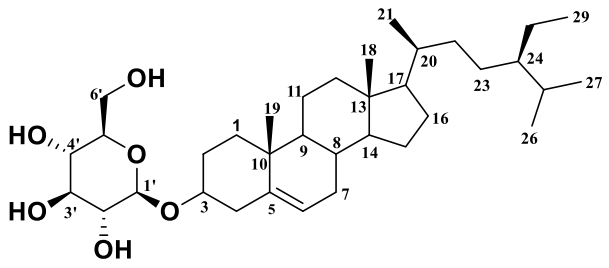

Fig. 4.28: Chemical structure of compound **10**

Compound **10** (Fig. 4.28) was obtained as a light-yellow amorphous powder directly from fractions 30-35 (50.9 mg) of the main silica gel column. Its structure was immediately identified as β-sitosterol-3-*O*-β-D-glucoside (also called daucosterol) based on its spectroscopic data (Plates 10A-10F in the appendix) and by direct comparison with literature data (Ahmed et al., 2000; Peshin and Kar, 2017). The anomeric proton appeared as a doublet at δ_H 4.22 (1H, *d*, *J* = 7,7 Hz, H-1`) and was assigned a β-orientation due to its *J* coupling constant. The NMR of β-sitosterol-3-*O*-β-D-glucoside has been extensively discussed from various plant sources, the roots of *Ipomoea digitata* (Khan and Hossain, 2015), aerial parts of *Alhagi pseudalhagi* (Sultan, Moohammadnor and Eshbakova, 2011), and *Pergularia tomentosa* (Gohar et al., 2000). Therefore, warrants no further exploration in this thesis but the spectroscopic data is given in the appendix. To the best of our knowledge, this compound is hereby reported for the first time from *H. petiolare*. However, it was reported from the aerial parts of *H. arenarium* (Eshbakova and Aisa, 2009) and flowers of *H. plicatum* (Aydin, 2020).

Compound 11: β-sitosterol (**11a**) and stigmasterol (**11b**) mixture

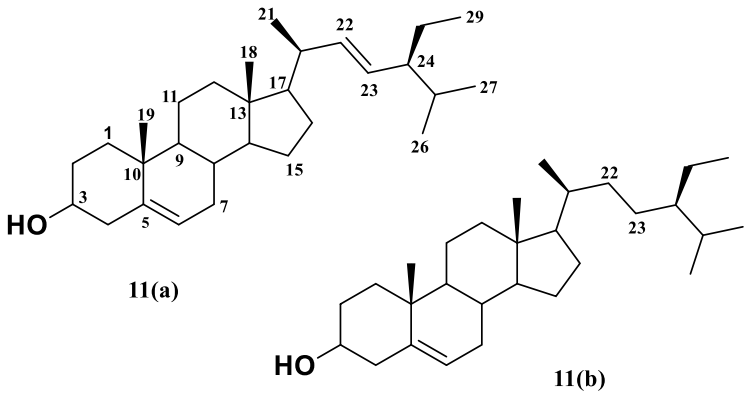

Fig. 4.29: Chemical structure of compound **11**

Compound **11** (Fig. 4.29) was isolated as an inseparable mixture (white amorphous powder) containing two triterpenoid isomers after successful purification of fraction 220 (250 mg) on flash silica gel column chromatography, eluting isocratic with $CHCl_3$:EtOAc (50:50). Gas column chromatography (GCMS) confirmed the presence of two peaks at *m/z* 412.69 (corresponding to $C_{29}H_{48}O$) and 414.71 (corresponding to $C_{29}H_{50}O$). The structural assignment of this compound was readily determined as a mixture of β-sitosterol (**11a**) and stigmasterol (**11b**) through NMR (Plates 11A-11B in the appendix) and GCMS (Plate 11C in the appendix) experiments, as well as comparison with the available literature (Jamaluddin, Mohamed and Lajis, 1994; Pateh et al., 2009; Pierre and Moses, 2015; Okoro et al., 2017). Therefore, warrants no further exploration in this thesis but the spectroscopic data is given in the appendix. The major difference between the two compounds is the presence of a carbon-carbon double bond (C_{22}=C_{23}) between C-22 and C-23 in stigmasterol, while this is absent in β-**s**itosterol (Pateh et al., 2009). To the best of our knowledge, this is the first report of the isolation of compound **11** from *H. petiolare*.

4.7.2. Biological Evaluation of the Isolated Compounds

i. α-Glucosidase and α-amylase assays

Helichrysum petiolare is one of many South African indigenous medicinal plants that are used traditionally to treat and/or manage diabetes. Various techniques have been developed to assess the antidiabetic activity. In this study, the mechanism of this plant towards diabetes was explored (α-glucosidase and α-amylase assays) to provide the rationale for its use in the treatment of diabetes. The extracts (DCM, EtOAc, BuOH, and aqueous extract) and isolated

compounds did not show any significant activity at the screening concentration (200 µg/mL) in the α-glucosidase and α-amylase assay (IC_{50} values were not determined). The hexane extract displayed a 92 % inhibition in α-glucosidase assay at the same concentration (200 µg/mL), even better than acarbose control (35,6 %). However, since none of the isolated compounds (**6, 4, 11, 5**) from this extract showed activity (Table 4.8), it was suggested that there may be a synergistic effect between the compounds that enhances the antidiabetic activity or that the compound(s) responsible for the antidiabetic was not isolated. Other studies have shown that the whole plant boiled aqueous extract of *H. petiolare* had superior inhibition activity (over the cold aqueous extract) against α-glucosidase and α-amylase assays (Aladejana, Bradley and Afolayan, 2020). Therefore, since our study only focused on the leaves (using 80% MeOH or cold extraction) this may suggest that either the active metabolites towards diabetes are not present in appreciable amounts in the leaves or there is a synergistic effect that occurs when the whole plant and/or extract is used (this will be explored further in future studies).

Table 4.8: α-Amylase and α-glucosidase enzymes inhibition of compounds and extracts from *H. petiolare*

	Percentage Inhibition (%) at 200 µg/mL	
	α-amylase	α-glucosidase
Compound 2	19.8	14.8
Compound 9	18.1	*
Compound 1	14.3	6.1
Compound 8	12.8	*
Compound 6	11.3	*
Compound 7	10.2	11.7
Compound 10	6.9	1.3
Compound 4	5.2	*
Compound 11	3.5	*
Compound 5	*	*
Compound 3	*	*
Hexane Extract	*	**92.1**
DCM Extract	*	49.6
Aqueous Extract	*	23.1
EtOAc Extract	*	14.5
BuOH Extract	*	*
Acarbose**	**88.0**	**35.6**

***Not active. **Control.**

ii. Cell viability (MTT) assay - MDA-MB-231 cells

Diabetes mellitus is one of the leading causes of global morbidity and mortality in the world (Erasto et al., 2005). Research shows that women suffering from diabetes have a 40% higher risk of mortality after a breast cancer diagnosis than women without diabetes-diagnosed with breast cancer (Lega et al., 2018). Cytotoxic effects of compounds isolated from *H. petiolare* were evaluated against MDA-MB-231 cells to assess cell viability. Compounds were initially screened for activity prior to more in-depth testing. To achieve this, cells were exposed to 0.1, 10, and 100 µg/mL of each compound over 24 hours, and the MTT assay was performed (Fig. 4.30). Codes used to denote each compound, for the purpose of activity screening, are shown in Table 4.9.

Table 4.9: Isolated compounds (and their designated codes) used for activity screening

Designated code	Compound
A1	1
A2	7
A3	4
A4	2
A5	10
A6	11
A7	8
A8	3
A9	5
A10	9
A11	6

Following 24 hours of exposure, the greatest reduction in MDA-MB-231 cell viability was observed at 100 µg/mL of three compounds, namely **1**, **3**, and **5**. These compounds (**1**, **3**, and **5**) were subsequently selected for further testing.

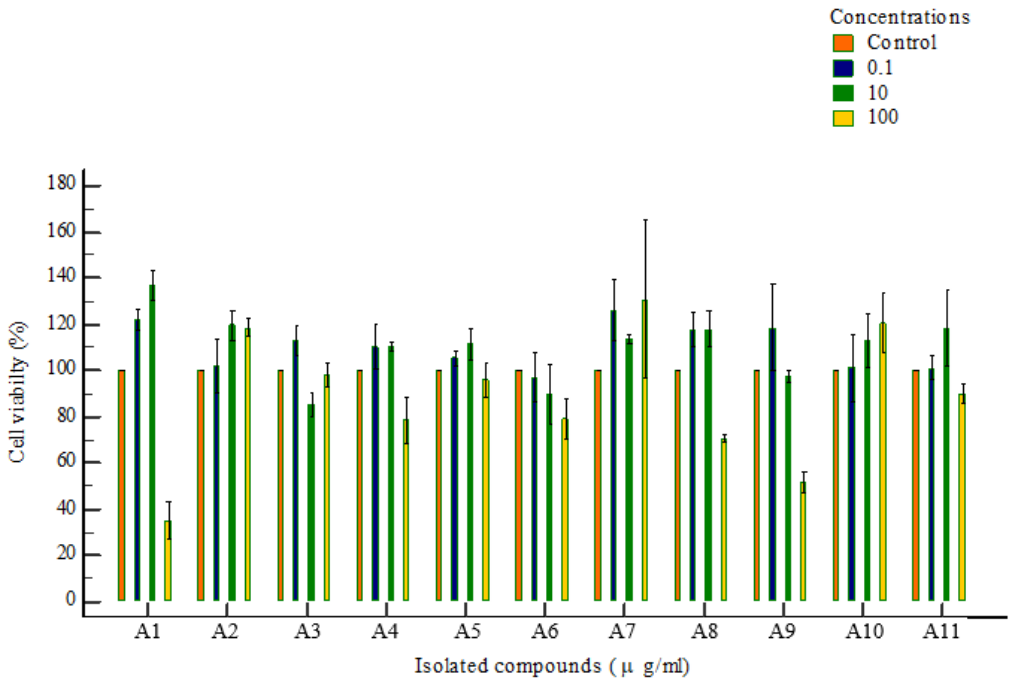

Fig. 4.30: Compound activity screening in MDA-MB-231 cells, as determined by the MTT assay over 24-hours of exposure to isolated compounds (A1-A11)

Compound 1. Following 24-hours (Fig. 4.31) and 72-hours (Fig. 4.32) of exposure to the isolated compound **1**, the MTT assay was performed. Over 24-hours, the compound yielded a dose-dependent effect between the control and highest concentration, yielding slight increases in cell viability between the control and 25 µg/mL, followed by a significant ($P = 0.0036$ and $P<0.0001$) stepwise reduction on cell viability at 50 and 100 µg/mL, respectively. The repeated-measures ANOVA yielded a significant ($P<0.00001$) negative linear trend between control and 100 µg/mL concentration. One-way ANOVA revealed a similar significant ($P<0.001$) trend. Following 72-hours of exposure, the compound revealed a clear dose-depended reduction in cell viability at each concentration used, exhibiting a significant ($P = 0.0002$ and $P<0.0001$) reduction in cell viability at 12.5 µg/mL and 25-100 µg/mL, respectively. Repeated-measure ANOVA revealed a significant ($P<0.0001$) negative linear trend between the control and highest concentration. Similarly, one-way ANOVA yielded a significant ($P<0.001$) trend between control and 100 µg/mL. The calculated IC_{50} values were recorded in Table 4.10

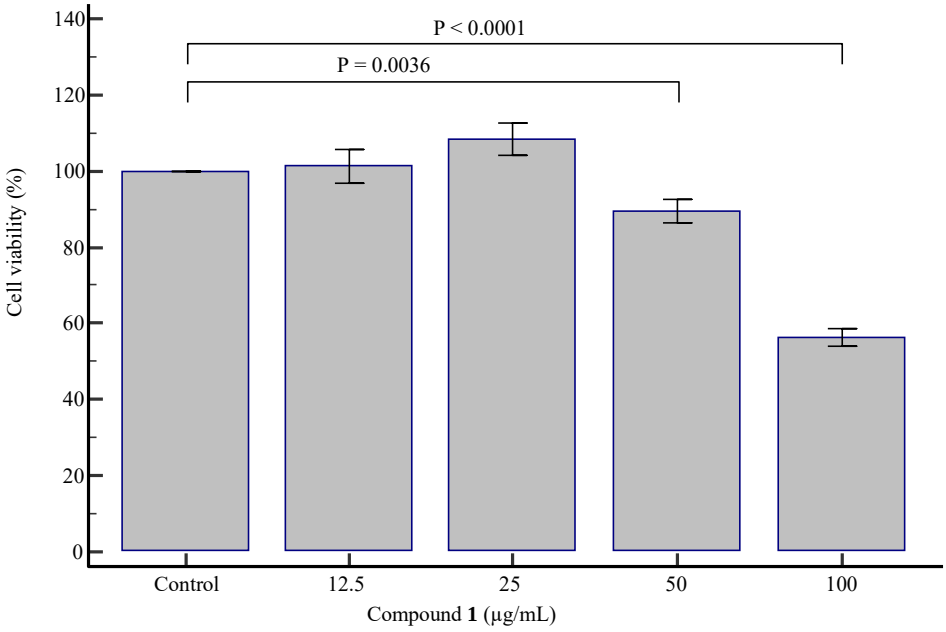

Fig. 4.31: MDA-MB-231 cell viability as determined by the MTT assay over 24-hours of exposure to the isolated compound **1**

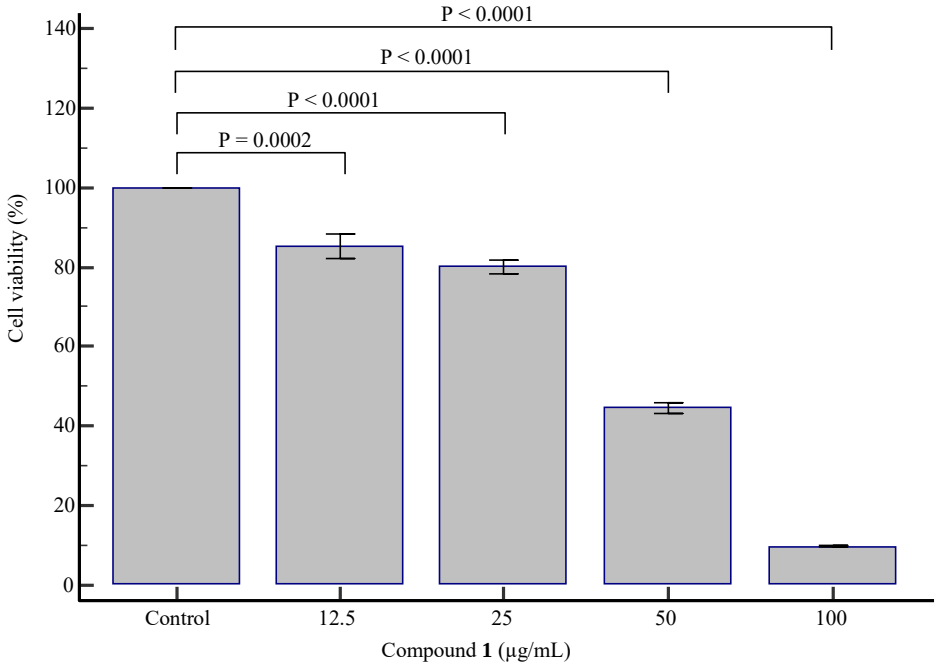

Fig. 4.32: MDA-MB-231 cell viability as determined by the MTT assay over 72-hours of exposure to the isolated compound **1**

Compound 3. Following 24-hours (Fig. 4.33) and 72-hours (Fig. 4.34) of exposure to the isolated compound **3**, the MTT assay was performed. Over 24-hours, the compound yielded significant (P = 0.0076 and P = 0.0003) reductions in cell viability at 12.5 and 100 µg/mL, respectively. Nevertheless, the repeated-measures ANOVA yielded a significant (P = 0.0103) negative linear trend between control and 100 µg/mL. One-way ANOVA revealed a similar significant (P<0.001) trend. Following 72-hours of exposure, the compound revealed similar reductions in cell viability at each concentration used, being significant (P<0.0001) at 12.5, 25, 50, and 100 µg/mL, respectively. Repeated-measure ANOVA revealed a significant (P<0.0001) negative linear trend between the control and highest concentration. Similarly, one-way ANOVA yielded a significant (P<0.001) trend between control and 100 µg/mL. The calculated IC_{50} values were recorded in Table 4.10

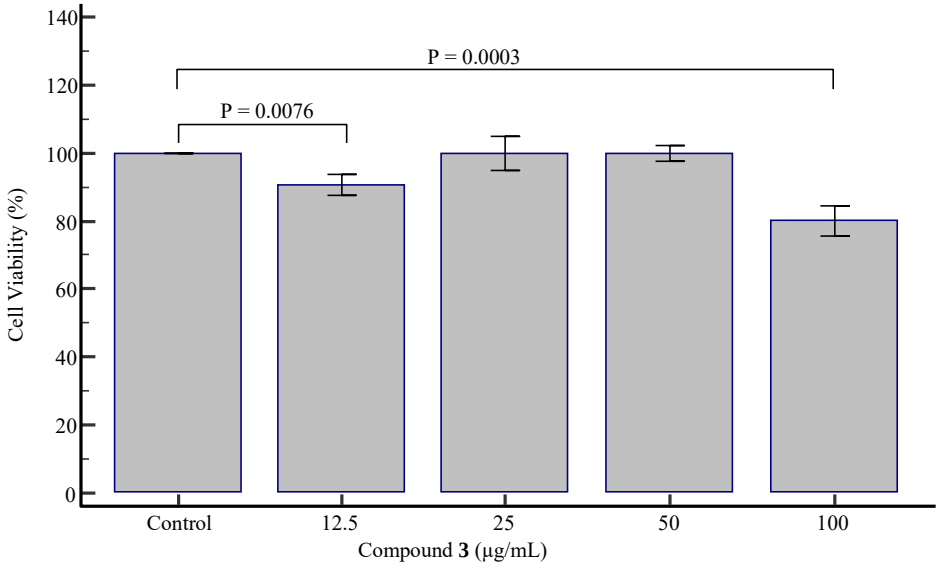

Fig. 4.33: MDA-MB-231 cell viability as determined by the MTT assay over 24-hours of exposure to the isolated compound **3**

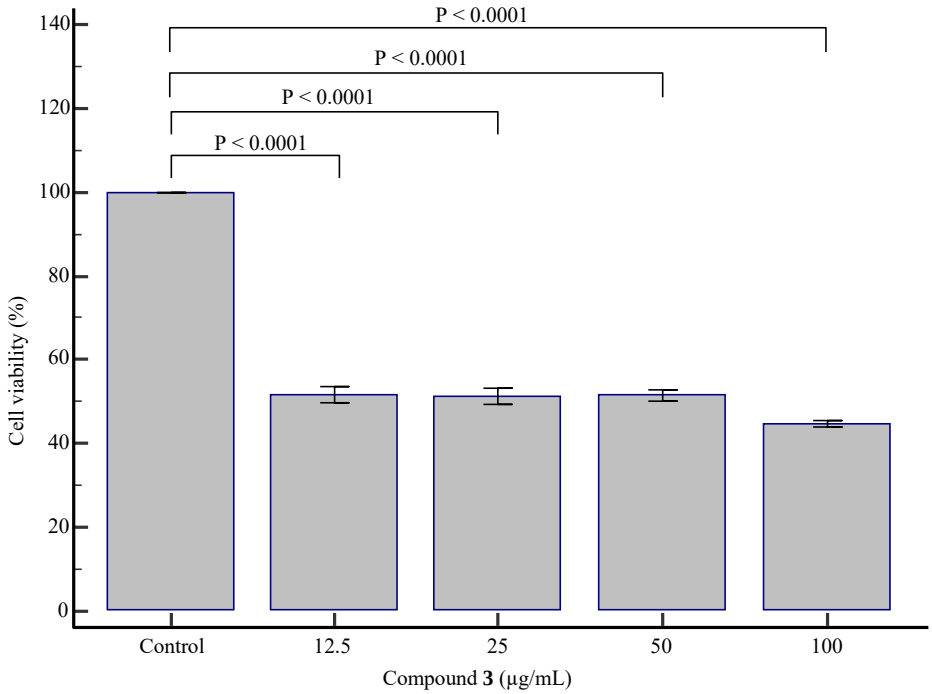

Fig. 4.34: MDA-MB-231 cell viability as determined by the MTT assay over 72-hours of exposure to the isolated compound **3**

Compound 5. Following 24-hours (Fig. 4.35) and 72-hours (Fig. 4.36) of exposure to the isolated compound **5**, the MTT assay was performed. Over 24-hours, the compound yielded a consistent, dose-dependent effect between the control and highest concentration, yielding significant (P = 0.0066, P = 0.0001, P=0.0007 and P<0.0001) incremental decreases in cell viability between the control and 100 µg/mL, respectively. The repeated-measures ANOVA yielded a significant (P<0.00001) negative linear trend between control and 100 µg/mL. One-way ANOVA revealed a similar significant (P<0.001) trend. Following 72-hours of exposure, the compound revealed clear dose-depended reductions in cell viability at each concentration used, exhibiting a significant (P<0.0001) reduction in cell viability at 12.5-100 µg/mL, respectively. Repeated-measure ANOVA revealed a significant (P<0.0001) negative linear trend between the control and highest concentration. Similarly, one-way ANOVA yielded a significant (P<0.001) trend between control and 100 µg/mL. The calculated IC_{50} values were recorded in Table 4.10.

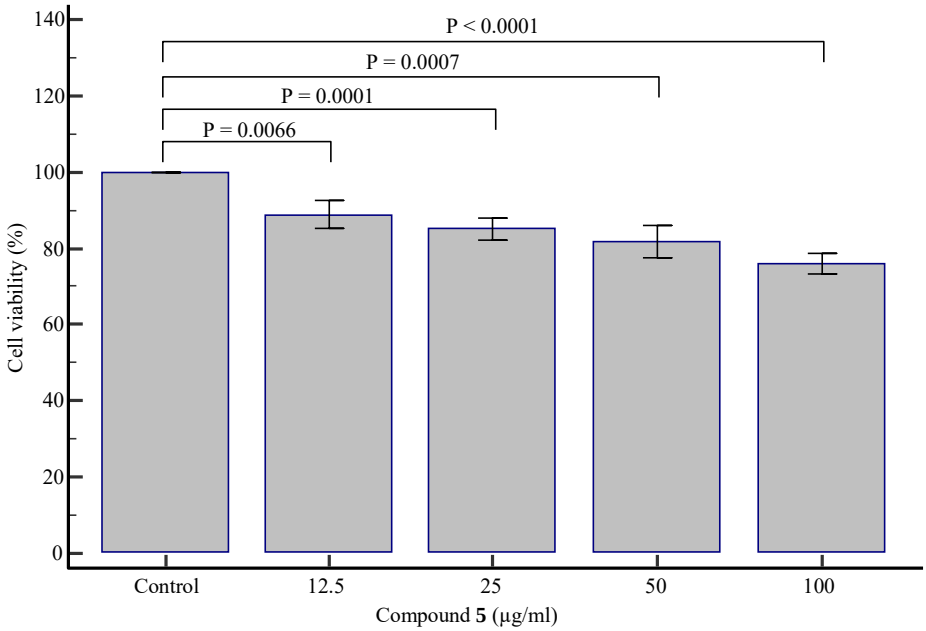

Fig. 4.35: MDA-MB-231 cell viability as determined by the MTT assay over 24-hours of exposure to the isolated compound **5**

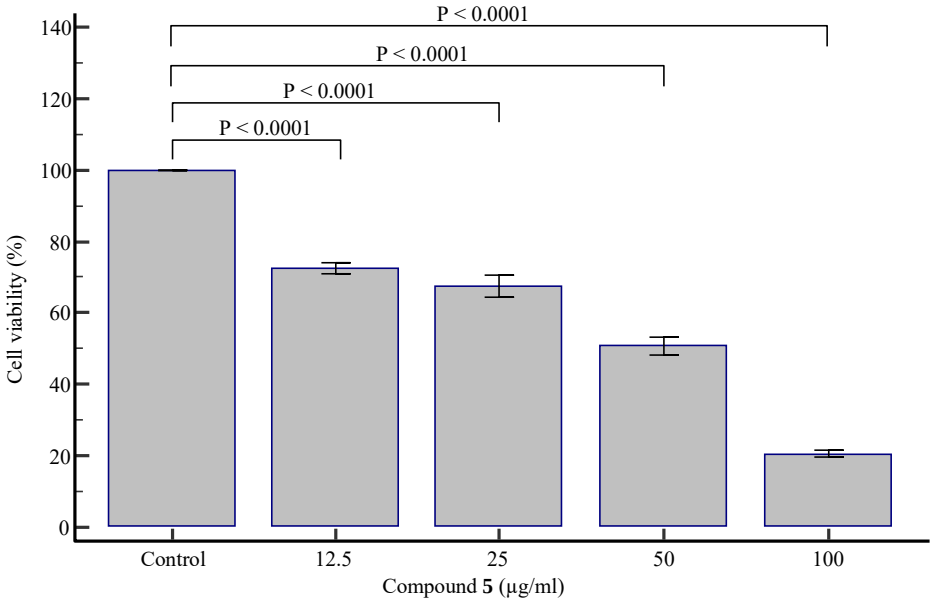

Fig. 4.36: MDA-MB-231 cell viability as determined by the MTT assay over 72-hours of exposure to the isolated compound **5**

Table 4.10: Calculated IC_{50} values over 24 and 72 hours for the isolated compounds

	IC_{50} (µg/mL)	
Compound	**24-hours exposure**	**72-hours exposure**
1	107.8	43.65
3	853.2	41.32
5	121.8	40.03

R-squared values:
-Compounds **1**, 0.8390 (24 hours exposure) and 0.9747 (72 hours exposure)
-Compounds **3**, 0.5316 (24 hours exposure) and 0.9450 (72 hours exposure)
-Compounds **5**, 0.3764 (24 hours exposure) and 0.7878 (72 hours exposure)

4.7.3 Conclusion

Phytochemical study of a leaf methanolic extract (80%) of *Helichrysum petiolare* resulted in the isolation and identification of eleven compounds, two of which are new and were named petiolactone A (**1**) and B (**2**). Compounds **3**–**11** are reported for the first time from this plant. The chemical structures of the isolated compounds were identified based on chemical and spectroscopic methods (and comparison of the known compounds to the available literature). This study has also provided for the first time the ^{13}C NMR data of compound **5**.

Since *H. petiolare* is linked with the ethnopharmacological use in the management of diabetes mellitus, the antidiabetic activity of the compounds and extracts was explored to determine the mechanism of action. However, none of the compounds or extracts (except hexane extract) showed any significant activity in the α-glucosidase and α-amylase assays at the tested concentration. It was suggested that either the active metabolites towards diabetes have not been isolated or are not present in appreciable amounts in the leaves or there's a synergistic effect that occurs when the whole plant and/or extract is used (this will be explored further in future studies). Furthermore, the cytotoxicity of the isolated compounds was also evaluated to assess the cell viability against the triple-negative MDA-MB-231 cell lines. Compound **1** was found to be the most active (IC_{50} = 107.8 and 43.65 µg/mL, respectively, after 24- and 72-hours exposure) showing a clear dose-depended reduction in cell viability at 100 µg/mL ($P<0.001$). Interestingly, the derivative of this compound (**2**) was more toxic to the cell, which may speak heavily about their differences in chemistry. Compounds **3** and **5** were also active at the same concentration. Further studies involving other types of cell lines still need to be done to establish the mechanism of cytotoxicity of the compounds.

References

Ahmed, G.A., El-Olemy, M.M., Abdel-Sattar, E., El-Said, M. and Niwa, M., 2000. Cardenolides and β-Sitosterol Glucoside from *Pergularia Tomentosa*. *Nat. Prod. Sci*, *6*(3), pp.142-146.

Al-Ja'fari, A.H., Vila, R., Freixa, B., Tomi, F., Casanova, J., Costa, J. and Cañigueral, S., 2011. Composition and antifungal activity of the essential oil from the rhizome and roots of *Ferula hermonis*. *Phytochemistry*, *72*(11-12), pp.1406-1413.

Aladejana, A.E., Bradley, G. and Afolayan, A.J., 2020. In vitro evaluation of the anti-diabetic potential of *Helichrysum petiolare* Hilliard & BL Burtt using HepG2 (C3A) and L6 cell lines. *F1000Research*, *9*.

Ali, E., Bagchi, D. and Pakrashi, S.C., 1982. Helipyrone from *Anaphalis araneosa* and its synthesis. *Phytochemistry*.

Almeida, J.R.G.D.S., Souza, G.R., Silva, J.C., Saraiva, S.R.G.D.L., Júnior, R.G.D.O., Quintans, J.D.S.S., Barreto, R.D.S.S., Bonjardim, L.R., Cavalcanti, S.C.D.H. and Junior, L.J.Q., 2013. Borneol, a bicyclic monoterpene alcohol, reduces nociceptive behaviour and inflammatory response in mice. *The Scientific World Journal*, *2013*.

Aydin, T., 2020. Secondary metabolites of *Helichrysum plicatum* DC. subsp. plicatum flowers as strong carbonic anhydrase, cholinesterase, and α-glycosidase inhibitors. *Zeitschrift für Naturforschung C*, *75*(5-6), pp.153-159.

Bohlmann, F., Abraham, W.R., Robinson, H. and King, R.M., 1980. A new labdane derivative and geranylphloroglucinols from *Achyrocline alata*. *Phytochemistry*, *19*(11), pp.2475-2477.

Bohlmann, F., Zdero, C. and Ziesche, J., 1979. Neue flavone und phloroglucin-derivate aus *Helichrysum herbaceum* und *Helichrysum chrysargyrum*. *Phytochemistry*, *18*(8), pp.1375-1378.

Bingöl, S. and Çubukçu, B., 1984. Flavonoids of *Helichrysum noeanum* Boiss. (Asteraceae). *Sci Pharm*, *52*, pp.127-130.

Butt, M.A. and Elvidge, J.A., 1963. 858. Heterocyclic syntheses with malonyl chloride. Part VIII. Hydroxypyrones from 1, 3-diketones. *Journal of the Chemical Society (Resumed)*, pp.4483-4489.

Brito, L.F., Oliveira, H.B.M., das Neves Selis, N., e Souza, C.L.S., Júnior, M.N.S., de Souza, E.P., Silva, L.S.C.D., de Souza Nascimento, F., Amorim, A.T., Campos, G.B. and de Oliveira, M.V., 2019. Anti-inflammatory activity of β-caryophyllene combined with

docosahexaenoic acid in a model of sepsis induced by *Staphylococcus aureus* in mice. *Journal of the Science of Food and Agriculture*, *99*(13), pp.5870-5880.

Cai, Q., 2019. The [4+ 2] cycloaddition of 2-pyrone in total synthesis. *Chinese Journal of Chemistry*, *37*(9), pp.946-976.

Candy, H.A. and Wright, W., 1975. Helichrysoside: A New Acylated Flavonoid Glycoside from *Helichrysum Kraussu* Sgh-Bip.

Chavan, M.J., Wakte, P.S. and Shinde, D.B., 2010. Analgesic and anti-inflammatory activity of Caryophyllene oxide from *Annona squamosa* L. bark. *Phytomedicine*, *17*(2), pp.149-151.

Chemam, Y., Benayache, S., Marchioni, E., Zhao, M., Mosset, P. and Benayache, F., 2017. On-line screening, isolation, and identification of antioxidant compounds of *Helianthemum ruficomum*. *Molecules*, *22*(2), p.239.

Cubukcu, B. and Yüksel, V., 1982. Constituents of Anatolian medicinal plants; flavonoids of *Helichrysum armenium*. *Journal of Natural Products*, *45*(2), pp.137-139.

Cubukcu, B. and Bingol, S., 1984. Pharmacognostical investigations on *Helichrysum pallasii* (Sprengel) Ledeb. *Plantes medicinales et phytotherapie*.

D'Abrosca, B., Buommino, E., Caputo, P., Scognamiglio, M., Chambery, A., Donnarumma, G. and Fiorentino, A., 2016. Phytochemical study of *Helichrysum italicum* (Roth) G. Don: Spectroscopic elucidation of unusual amino-phlorogucinols and antimicrobial assessment of secondary metabolites from medium-polar extract. *Phytochemistry*, *132*, pp.86-94.

Dahham, S.S., Tabana, Y.M., Iqbal, M.A., Ahamed, M.B., Ezzat, M.O., Majid, A.S. and Majid, A.M., 2015. The anticancer, antioxidant and antimicrobial properties of the sesquiterpene β-caryophyllene from the essential oil of *Aquilaria crassna*. *Molecules*, *20*(7), pp.11808-11829.

de Oliveira, M.G., Marques, R.B., de Santana, M.F., Santos, A.B., Brito, F.A., Barreto, E.O., De Sousa, D.P., Almeida, F.R., Badauê-Passos Jr, D., Antoniolli, Â.R. and Quintans-Elegbede, J.A., Elson, C.E., Qureshi, A., Tanner, M.A. and Gould, M.N., 1984. Inhibition of DMBA-induced mammary cancer by the monoterpene d-limonene. *Carcinogenesis*, *5*(5), pp.661-664.

do Nascimento, K.F., Moreira, F.M.F., Santos, J.A., Kassuya, C.A.L., Croda, J.H.R., Cardoso, C.A.L., do Carmo Vieira, M., Ruiz, A.L.T.G., Foglio, M.A., de Carvalho, J.E. and Formagio, A.S.N., 2018. Antioxidant, anti-inflammatory, antiproliferative and antimycobacterial activities of the essential oil of *Psidium guineense* Sw. and spathulenol. *Journal of ethnopharmacology*, *210*, pp.351-358.

Dou, J., Xu, W., Koivisto, J.J., Mobley, J.K., Padmakshan, D., Kögler, M., Xu, C., Willför, S., Ralph, J. and Vuorinen, T., 2018. Characteristics of hot water extracts from the bark of cultivated willow (*Salix* sp.). *ACS Sustainable Chemistry & Engineering*, *6*(4), pp.5566-5573.

Elabbaraa, F.A., Habelb, A.M., Bozkeha, N.M.A., El-Tuonsia, A.T.M. and Awina, T.A., 2014. Caffeic anhydride from *Solanum sodomaeum* (Solanaceae). *Asian. J. Plant. Sci. Res*, *4*, pp.19-22.

Erasto, P., Adebola, P.O., Grierson, D.S. and Afolayan, A.J., 2005. An ethnobotanical study of plants used for the treatment of diabetes in the Eastern Cape Province, South Africa. *African Journal of Biotechnology*, *4*(12).

Eshbakova, K.A. and Aisa, H.A., 2009. Components of *Helichrysum arenarium*. *Chemistry of natural compounds*, *45*(6), pp.929-930.

Gohar, A.A., El-Olemy, M.M., Abdel-Sattar, E., El-Said, M. and Niwa, M., 2000. Cardenolides and β-sitosterol-3-*O*-β-D-glucoside from *Pergularia tomentosa* L. *Natural Product Sciences*, *6*(3), pp.142-146.

Hassan, S.B., Gali-Muhtasib, H., Göransson, H. and Larsson, R., 2010. Alpha terpineol: a potential anticancer agent which acts through suppressing NF-κB signalling. *Anticancer Research*, *30*(6), pp.1911-1919.

Hänsel, R., Ohlendorf, D. and Pelter, A., 1970. Obtusifolin, a flavonone with a biogenetically unusual C9-unit. *Zeitschrift fur Naturforschung. Teil B, Chemie, Biochemie, Biophysik, Biologie und verwandte Gebiete*, *25*(9), pp.989-994.

Hilliard, O.M., 1983. *Helichrysum* Mill. *In*: Leistner, O.A. (Ed.) *Flora of southern Africa* 33[7(2)]. Botanical Research Institute, Pretoria, pp. 61–310.

Hua, Y. and Wang, H.Q., 2004. Chemical components of *Anaphalis sinica* Hance. *Journal of the Chinese Chemical Society*, *51*(2), pp.409-415.

Huang, W.P., Huang, Y.F., Chen, J.Z., Jin, B., Tan, J.N. and Ding, Z.S., 2017. Effect of pinostrobin chalcone on adipogenic differentiation of mesenchymal stem cell C3H10T1/2. *Zhongguo Zhong yao za zhi= Zhongguo zhongyao zazhi= China journal of Chinese materia medica*, *42*(12), p.2339.

Jakupovic, J., Zdero, C., Grenz, M., Tsichritzis, F., Lehmann, L., Hashemi-Nejad, S.M. and Bohlmann, F., 1989. Twenty-one acylphloroglucinol derivatives and further constituents from South African *Helichrysum* species. *Phytochemistry*, *28*(4), pp.1119-1131.

Jamaluddin, F., Mohamed, S. and Lajis, M.N., 1994. Hypoglycaemic effect of *Parkia speciosa* seeds due to the synergistic action of β-sitosterol and stigmasterol. *Food Chemistry*, *49*(4), pp.339-345.

Khan, N.M.M.U. and Hossain, M.S., 2015. Scopoletin and β-sitosterol glucoside from roots of *Ipomoea digitata*. *Journal of Pharmacognosy and Phytochemistry*, *4*(2), pp.05-07.

Lavault, M. and Richomme, P., 2004. Constituents of *Helichrysum stoechas* variety olonnense. *Chemistry of natural compounds*, *40*(2).

Lega, I.C., Austin, P.C., Fischer, H.D., Fung, K., Krzyzanowska, M.K., Amir, E. and Lipscombe, L.L., 2018. The impact of diabetes on breast cancer treatments and outcomes: a population-based study. *Diabetes Care*, *41*(4), pp.755-761.

Legault, J. and Pichette, A., 2007. Potentiating effect of β-caryophyllene on anticancer activity of *α*-humulene, isocaryophyllene and paclitaxel. *Journal of Pharmacy and Pharmacology*, *59*(12), pp.1643-1647.

Legoalea, P.B. and Mashimbyeb, M.J., 2013. Antiinflammatory and antioxidant flavonoids from *Helichrysum kraussii* and *H. odoratissimum* flowers. *Natural product communications*, *8*(10), pp.1403-1404.

Lourens, A.C.U., Reddy, D., Başer, K.H.C., Viljoen, A.M. and Van Vuuren, S.F., 2004. *In vitro* biological activity and essential oil composition of four indigenous South African *Helichrysum* species. *Journal of ethnopharmacology*, *95*(2-3), pp.253-258.

Lourens, A.C.U., Viljoen, A.M. and Van Heerden, F.R., 2008. South African *Helichrysum* species: a review of the traditional uses, biological activity and phytochemistry. *Journal of Ethnopharmacology*, *119*(3), pp.630-652.

Lourens, A.C.U., Van Vuuren, S.F., Viljoen, A.M., Davids, H. and Van Heerden, F.R., 2011. Antimicrobial activity and in vitro cytotoxicity of selected South African *Helichrysum* species. *South African journal of botany*, *77*(1), pp.229-235.

Makhuvele, R., Matshoga, R.G., Antonissen, R., Pieters, L., Verschaeve, L. and Elgorashi, E.E., 2018. Genotoxicity and antigenotoxicity of selected South African indigenous plants. *South African Journal of Botany*, *114*, pp.89-99.

Mishrikey, M.M., 1992. Synthesis and Reactions of 4-Pyrone 2, 4-Dinitrophenylhydrazones. *JOURNAL-CHEMICAL SOCIETY OF PAKISTAN*, *14*, pp.73-73.

Morimoto, M., Kumeda, S. and Komai, K., 2000. Insect Antifeedant Flavonoids from *Gnaphalium affine* D. Don. *Journal of agricultural and food chemistry*, *48*(5), pp.1888-1891.

Mohammed, I.A., Akhtar, M.N., Biau, F.J., Tor, Y.S., Zareen, S., Binti Shahabudin, S., Binti Abd Hamid, H., Ul Haq, Z., Khalil, R. and Khalaf, R.M., 2019. Isolation of cardamonin and pinostrobin chalcone from the rhizomes of *Boesenbergia rotunda* (L.) Mansf. and their cytotoxic effects on H-29 and MDA-MB-231 cancer cell lines. *The Natural Products Journal*, *9*(4), pp.341-348.

Monzote, L., Stamberg, W., Staniek, K. and Gille, L., 2009. Toxic effects of carvacrol, caryophyllene oxide, and ascaridole from essential oil of Chenopodium ambrosioides on mitochondria. *Toxicology and applied pharmacology*, *240*(3), pp.337-347.

Odeyemi, S. and Bradley, G., 2018. Medicinal plants used for the traditional management of diabetes in the Eastern Cape, South Africa: Pharmacology and toxicology. *Molecules*, *23*(11), p.2759.

Okoro, I.S., Tor-Anyiin, T.A., Igoli, J.O., Noundou, X.S. and Krause, R.W.M., 2017. Isolation and Characterisation of Stigmasterol and β–Sitosterol from *Anthocleista djalonensis* A. Chev. *Asian Journal of Chemical Sciences*, pp.1-5.

Opitz, L. and Hansel, R., 1970. Helipyron, ein Methylen-bis-Triacetsaurelacton aus *Helichrysum italicum*. *Tetrahedron letters*.

Park, S.N., Lim, Y.K., Freire, M.O., Cho, E., Jin, D. and Kook, J.K., 2012. Antimicrobial effect of linalool and *α*-terpineol against periodontopathic and cariogenic bacteria. *Anaerobe*, *18*(3), pp.369-372.

Pateh, U.U., Haruna, A.K., Garba, M., Iliya, I., Sule, I.M., Abubakar, M.S. and Ambi, A.A., 2009. Isolation of stigmasterol, β-sitosterol and 2-hydroxyhexadecanoic acid methyl ester from the rhizomes of *Stylochiton lancifolius* Pyer and Kotchy (Araceae). *Nigerian Journal of Pharmaceutical Sciences*, *8*(1), pp.19-25.

Peshin, T. and Kar, H.K., 2017. Isolation and Characterization of β-Sitosterol-3-O-β-D-glucoside from the extract of the flowers of *Viola odorata*. *Journal of Pharmaceutical Research International*, pp.1-8.

Pierre, L.L. and Moses, M.N., 2015. Isolation and characterisation of stigmasterol and β-sitosterol from *Odontonema strictum* (acanthaceae). *J. Innov. Pharm. Biol. Sci*, *2*, pp.88-96.

Quintans-Júnior, L.J., Guimarães, A.G., Araújo, B.E., Oliveira, G.F., Santana, M.T., Moreira, F.V., Santos, M.R., Cavalcanti, S.C., Júnior, W.L., Botelho, M.A. and Ribeiro, L.A., 2010. Carvacrol, (-)-borneol and citral reduce convulsant activity in rodents. *African Journal of Biotechnology*, *9*(39), pp.6566-6572.

Rios, J.L., Recio, M.C. and Villar, A., 1991. Isolation and identification of the antibacterial compounds from *Helichrysum stoechas*. *Journal of ethnopharmacology*, *33*(1-2), pp.51-55.

Rogerio, A.P., Andrade, E.L., Leite, D.F., Figueiredo, C.P. and Calixto, J.B., 2009. Preventive and therapeutic anti-inflammatory properties of the sesquiterpene *α*-humulene in experimental airways allergic inflammation. *British journal of pharmacology*, *158*(4), pp.1074-1087.

Rufino, A.T., Ribeiro, M., Judas, F., Salgueiro, L., Lopes, M.C., Cavaleiro, C. and Mendes, A.F., 2014. Anti-inflammatory and chondroprotective activity of (+)-*α*-pinene: structural and enantiomeric selectivity. *Journal of natural products*, *77*(2), pp.264-269.

Scott, G., Springfield, E.P. and Coldrey, N., 2004. A pharmacognostical study of 26 South African plant species used as traditional medicines. *Pharmaceutical Biology*, *42*(3), pp.186-213.

Silva, A.C.R.D., Lopes, P.M., Azevedo, M.M.B.D., Costa, D.C.M., Alviano, C.S. and Alviano, D.S., 2012. Biological activities of a-pinene and β-pinene enantiomers. *Molecules*, *17*(6), pp.6305-6316.

Socolsky, C., Fascio, M.L., D'Accorso, N.B., Salvatore, A., Willink, E., Asakawa, Y. and Bardon, A., 2008. Effects of p-vinylphenyl glycosides and other related compounds on the oviposition behavior of *Ceratitis capitata*. *Journal of chemical ecology*, *34*(4), pp.539-548.

Sultan, A., Moohammadnor, M. and Eshbakova, K.A., 2011. Chemical constituents of *Alhagi pseudalhagi*. *Chemistry of Natural Compounds*, *47*(1), pp.140-141.

Sonka, L., 2018. Exploring anti-tyrosinase bioactive compounds from the Cape flora.

Spiridonov, N.A., Konovalov, D.A. and Arkhipov, V.V., 2005. Cytotoxicity of some Russian ethnomedicinal plants and plant compounds. Phytotherapy Research: *An International Journal Devoted to Pharmacological and Toxicological Evaluation of Natural Product Derivatives, 19*(5), pp.428-432.

Süzgeç, S., Meriçli, A.H., Houghton, P.J. and Çubukçu, B., 2005. Flavonoids of *Helichrysum compactum* and their antioxidant and antibacterial activity. *Fitoterapia*, *76*(2), pp.269-272.

Süzgeç-Selçuk, S. and Birteksöz, A.S., 2011. Flavonoids of *Helichrysum chasmolycicum* and its antioxidant and antimicrobial activities. *South African Journal of Botany*, *77*(1), pp.170-174.

Tabanca, N., Kırımer, N., Demirci, B., Demirci, F. and Başer, K.H.C., 2001. Composition and antimicrobial activity of the essential oils of *Micromeria cristata* subsp. *phrygia* and the enantiomeric distribution of borneol. *Journal of Agricultural and Food chemistry, 49*(9), pp.4300-4303.

Tomás-Lorente, F., Iniesta-Sanmartín, E., Tomás-Barberán, F.A., Trowitzsch-Kienast, W. and Wray, V., 1989. Antifungal phloroglucinol derivatives and lipophilic flavonoids from *Helichrysum decumbens*. *Phytochemistry*, *28*(6), pp.1613-1615.

Ushiyama, M. and Furuya, T., 1989. Glycosylation of phenolic compounds by root culture of *Panax ginseng*. *Phytochemistry*, *28*(11), pp.3009-3013.

Van Puyvelde, L., De Kimpe, N., Costa, J., Munyjabo, V., Nyirankuliza, S., Hakizamungu, E. and Schamp, N., 1989. Isolation of flavonoids and a chalcone from *Helichrysum odoratissimum* and synthesis of helichrysetin. *Journal of Natural Products*, *52*(3), pp.629-633.

Vasisht, K. and Kumar, V., 2004. Compendium of medicinal and aromatic plants, Vol. 1. *Africa: ICS-UNIDO, Trieste*.

Venditti, A., Lattanzi, C., Ornano, L., Maggi, F., Sanna, C., Ballero, M., Alvino, A., Serafini, M. and Bianco, A., 2016. A new glucosidic phthalide from *Helichrysum microphyllum* subsp. *tyrrhenicum* from La Maddalena Island (Sardinia, Italy). *Natural product research*, *30*(7), pp.789-795.

Vrkcoč, J., Dolejš, L. and Buděšínský, M., 1975. Methylene-bis-2H-pyran-2-ones and phenolic constituents from the root of *Helichrysum arenarium*. *Phytochemistry*, *14*(5-6), pp.1383-1384.

Vrkoc, J., Ubik, K. and Sedmera, P., 1973. Phenolic extractives from the achenes of *Helichrysum arenarium*. *Phytochemistry*.

Vuuren, S.V. and Viljoen, A.M., 2007. Antimicrobial activity of limonene enantiomers and 1, 8-cineole alone and in combination. *Flavour and fragrance journal*, *22*(6), pp.540-544.

Wollenweber, E., Fritz, H., Henrich, B., Jakupovic, J., Schilling, G. and Roitman, J.N., 1993. Rare flavonoid aglycones from *Anaphalis margaritacea* and two *Gnaphalium* species. *Zeitschrift für Naturforschung C*, *48*(5-6), pp.420-424.

Wu, Q., Yu, C., Yan, Y., Chen, J., Zhang, C. and Wen, X., 2010. Antiviral flavonoids from *Mosla scabra*. *Fitoterapia*, *81*(5), pp.429-433.

Xie, G., Chen, N., Soromou, L.W., Liu, F., Xiong, Y., Wu, Q., Li, H., Feng, H. and Liu, G., 2012. p-Cymene protects mice against lipopolysaccharide-induced acute lung injury by inhibiting inflammatory cell activation. *Molecules*, *17*(7), pp.8159-8173.

Xin, M., Guo, S., Zhang, W., Geng, Z., Liang, J., Du, S., Deng, Z. and Wang, Y., 2017. Chemical constituents of supercritical extracts from *Alpinia officinarum* and the feeding deterrent activity against *Tribolium castaneum*. *Molecules*, *22*(4), p.647.

Xu, M., Shen, Y., Zhang, K., Liu, N.N., Jiang, F.S. and Ding, Z.S., 2013. Antioxidant activity of total flavonoid aglycones and the main compound pinostrobin chalcone separated from leaves of *Carya cathayensis*. *Chinese Journal of Experimental Traditional Medical Formulae*, *2013*(22), p.59.

Yang, D., Michel, L., Chaumont, J.P. and Millet-Clerc, J., 2000. Use of caryophyllene oxide as an antifungal agent in an *in vitro* experimental model of onychomycosis. *Mycopathologia*, *148*(2), pp.79-82.

Zhao, D.B., Li, L.X., Liu, X.H., Li, M.J. and Wang, W.L., 2007. Two new phenolic compounds from *Artemisia sphaerocephala*. *Chinese Chemical Letters*, *18*(5), pp.551-553.

Zheng, G.Q., Kenney, P.M. and Lam, L.K., 1992. Sesquiterpenes from clove (*Eugenia caryophyllata*) as potential anticarcinogenic agents. *Journal of natural products*, *55*(7), pp.999-1003.

Chapter 5

Phytochemistry of *Helichrysum splendidum* (Thunb.) Less.

5.1. Introduction

This chapter focuses on the phytochemistry of *Helichrysum splendidum* (Thunb.) Less., which is a plant that has been selected for investigation. Section A briefly discusses the literature of the plant, while section B are results and discussions.

5.2. General Experimental Procedures. See chapter 2.

5.3. Plant Material

The leaves of *H. splendidum* were collected from Kirstenbosch National Botanical Gardens, South Africa, Cape Town (-33° 59' 13.19" S, 18° 25' 29.39" E) on 31 August 2018, and the identity of the species was confirmed by the curator of the Compton Herbarium. The leaves were hand-picked, washed with distilled water, and then air-dried at room temperature until further use.

5.4. Extraction and Isolation.

The air-dried leaves were pulverized into powder (339 g) using an electrical blender and then extracted three times for 48 hours with 80% MeOH (3 x 3L). After each extraction, the supernatant was obtained by filtration using a Buchner funnel (Whatman 0.4-micron filter paper), combined, and concentrated (to remove the MeOH) under reduced pressure (at 45 °C) using a Büchi® Rotavapor® R-210 evaporator with jack and water bath, 29/32 joint, 240V. The remnant (brownish) was freeze-dried to obtain approximately 40.0 g of the total extract, which was suspended in water and extracted sequentially to furnish the crude extracts: hexane (4.50 g), DCM (11.4 g), EtOAc (4.53 g), and BuOH (9.18 g). The hexane extract did not yield any pure compounds. The DCM extract was chromatographed on silica gel (gel 60, 70-230 mesh ASTM, Merck, dry packing), eluting with $CHCl_3$:EtOAc (100 :0→50: 50) gradient to obtain twenty-eight fractions (1-28). TLC was used to monitor the fractions for target compounds (silica gel aluminum sheets, visualization with vanillin sulfuric acid reagent and heating to 105 °C): fractions 14-15 (58.0 mg) were eluted isocratic with EtOAc:Hex (90:10) on silica gel column (dry packing) to obtain compounds **12** (12.7 mg) and **13** (12.7 mg) as an inseparable mixture. While fractions 10-12 (196 mg) were purified on silica gel using hexane:EtOAc (100

:0 → 50: 50) gradient to afford compounds **16** (38.0 mg), **17** (20.8 mg), as well as an inseparable mixture containing **21** (94.6 mg) and **22** (94.6 mg). Compound **19** (13.0 mg) was obtained as a yellow amorphous powder, directly from fractions 20-23 (102 mg) of the main silica gel column, after successive washing with $CHCl_3$ and MeOH. The EtOAc extract was chromatographed on silica gel, eluting with hexane:EtOAc gradient (50:50 → 0: 100) to obtain one hundred and fifty-four fractions (1-154). After successful screening on TLC (detection with vanillin-sulfuric acid reagent), fractions showing similar profiles were combined, concentrated, and then purified accordingly: Fractions 110-119 of the main column upon standing for three days (at room temperature) produced white needle-crystals (after washing successively with DCM and MeOH) which was identified as a mixture of compounds **14** (0.672 g) and **15** (0.672 g). While fractions 140-154 (50.0 mg) were chromatographed successively on Sephadex (LH-20), eluting isocratic with ethanol (100%) to yield compound **18** (5.5 mg). Fractions 12-19 (100 mg) were chromatographed on a flash silica gel column, eluting isocratic with $CHCl_3$ (100%) to obtain compound **19** (86.1 mg). The BuOH extract was chromatographed on silica gel, eluting with DCM:MeOH (100 :0→50: 50) gradient to obtain sixty-five (1-65) fractions. The inseparable mixture containing compounds **14** (0.985 g) and **15** (0.985 g) formed white needle crystals upon leaving fractions 10-16 of the main silica gel column to stand for three days (at room temperature). Whereas compound **20** (43.8 mg) was obtained directly from fractions 18-21 of the silica gel main column, after successive washing of the crystals with $CHCl_3$ and MeOH.

5.5. Biological Evaluation

i. α-Glucosidase and α-amylase enzyme inhibition assays. See chapter 2.

ii. Cell viability assay (MTT). See chapter 2.

Scheme 5.1: A summary of the experimental procedure for the isolation of compounds from *H. splendidum*

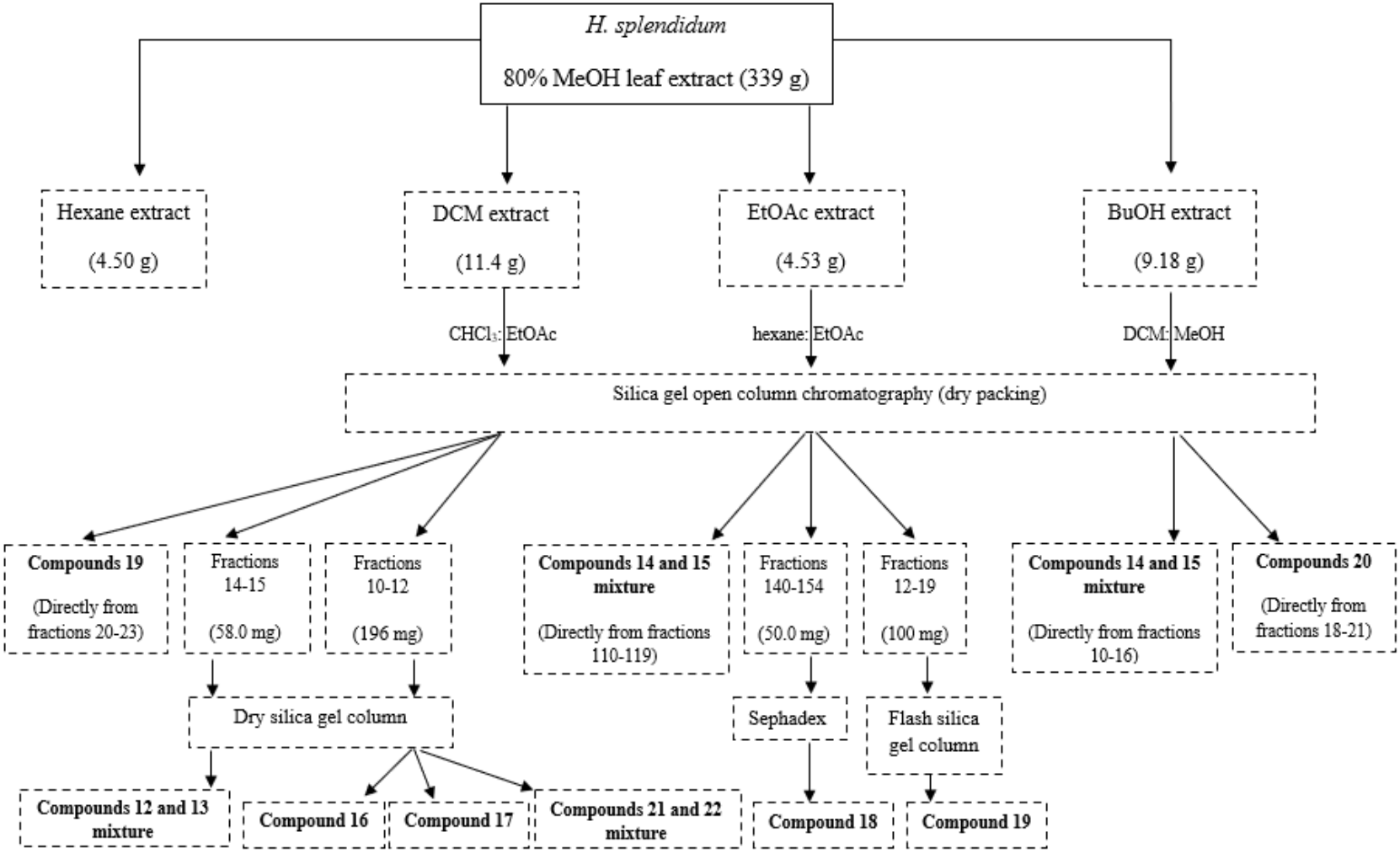

5.6. Section A

5.6.1. Taxonomy

Kingdom: Plantae

Division: Magnoliophyta

Class: Magnoliopsida

Order: Asterales

Family: Asteraceae (or Compositae)

Genus: *Helichrysum* Mill

Species: *H. splendidum* (Thunb.) Less (Hilliard and Burtt, 1983)

Fig. 5.1: Leaves of *H. splendidum* (source: http://pza.sanbi.org/helichrysum-splendidum**)**

5.6.2. Background

Helichrysum splendidum (Thunb.) Less. (*geelsewejaartjie* in Afrikaans, *phefo-ea-loti*, *toanae-moru* in Southern Sotho) is a South African indigenous medicinal plant that is widespread in the summer-rainfall areas; ranging from the Swartberg to Outeniqua mountains in the southern Cape through Eastern Cape, KwaZulu-Natal, Limpopo, Mpumalanga, and Free State (Hilliard, 1983; Chagonda, Makanda and Chalchat, 1999; Pooley, 2003). This fast-growing, evergreen shrub, which belongs to group 22 according to Hilliard's classification system (Hilliard, 1983), is characterized by shinny grey-woolly linear leaves with bright yellow bracts and compact inflorescence (Fig. 5.1). Flowering occurs between October and January/or February.

5.6.3. Ethnopharmacology

According to Van Wyk and Gericke (2000), the use of *Helichrysum* species (*impepho*) in South African traditional medicine is linked to their availability rather than preference. Various parts of *H. splendidum* are used frequently: the roots are used traditionally to treat rheumatism and for fuel (Pooley, 2003), while the leaves are boiled and the steam is inhaled to induce sweating (Lourens, Viljoen and Van Heerden, 2008; Mashigo et al., 2015). Like most species in the genus, the smoke (whole plant) is used during rituals in many cultures (Xhosa/Zulu/Ndebele) to invoke trance and to connect with the ancestors.

5.6.4. Biological Activity: *on diabetes mellitus*

Although *H. splendidum* has no reported use traditionally in the treatment of diabetes mellitus, *Helichrysum* species are known sources of flavonoids, terpenoids, and phenolic compounds which have been shown to possess antidiabetic activities (Milella et al., 2016; Phoopha et al., 2020; Matboli et al., 2021). Therefore, its antidiabetic activity was evaluated in this study (discussed later in this chapter, section B).

5.6.5. Other Bioactivities

The antifungal activity of the essential oils from the South African *H. splendium* population was evaluated *in vitro* by Mashigo et al. (2015) against seven fruit decay pathogen strains (*Alternaria alternata, Colletotrichum gloeosporioides, Fusarium oxysporum, Lasiodiplodia theobromae, Penicillium digitatum, Penicillium expansum*, and *Penicillium italicum*). At 1000 µL/L concentration (the highest tested concentration) *A. alternata* and *C. gloeosporioides* were found to be the most susceptible fungi-exhibiting 84% and 51% inhibition, respectively. Lourens et al. (2011) demonstrated the antibacterial activity of the chloroform:methanol (1:1) leaf and stem extracts at various concentrations (16 to 0.125 mg/mL) against Gram-positive and Gram-negative bacteria, as well as fungi strains. Cytotoxicity was determined against transformed human kidney epithelial (Graham) cells, MCF-7 breast adenocarcinoma and SF-268 glioblastoma cells (at 0.1 mg/mL) using the sulforhodamine B (SRB) assay (Lourens et al., 2011). Table 5.1 shows a summary of some known biological activities (whether reported directly from this plant or other sources) that are associated with the individual constituents isolated from *H. splendidum*.

5.6.6. **Previous Work**: *phytochemistry*

The chemistry of *Helichrysum splendidum* was initially described by Bohlmann and Suwita (1979), Jakupovic et al. (1989), and later by Lourens, Viljoen and Van Heerden (2008). The main constituents that were independently reported by the authors are shown in Table 5.1. According to Jakupovic et al. (1989), this species is characterized by unique/rare sesquiterpene derivatives called guaianolides. Apart from *H. splendidum*, these sesquiterpene derivatives have also been identified from two other species in the genus *H. dasyanthum* (Jakupovic et al., 1989) and *H. montanum* (Lourens, Viljoen and Van Heerden, 2008). In a separate study, Mashigo et al. (2015) described the essential oil content of this species. We have re-investigated the phytochemistry of this species to validate the effects of variable solubility for phytochemical constituents (discussed later in the chapter, section B). Interestingly, in all studies, 5,3′4′-trihydroxy-3,7,8-trimethoxyflavone and phloretin were the only phenolic compounds (flavonoids) reported (Bohlmann and Suwita, 1979), although flavonoids are popular in *Helichrysum* species. This further prompted us to re-investigate the phytochemistry of this plant.

Table 5.1: Secondary metabolites isolated from *Helichrysum splendidum* (including plant part from which it was isolated) and their known biological activities

Name and structure (class)	Part of the plant	Biological Activity	Study type (*in vitro**/*in vivo***)	References
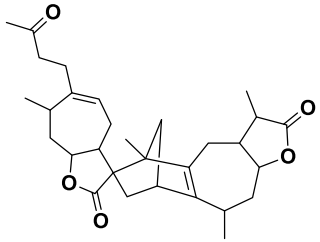	❖ Aerial parts.	-	-	❖ Jakupovic et al. (1989) ❖ Lourens, Viljoen and Van Heerden (2008)
❖ 11*β*,13-dihydroxanthalongin (xanthanolides) 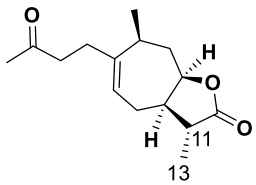	❖ Aerial parts.	-	-	❖ Bohlmann and Suwita (1979) ❖ Lourens, Viljoen and Van Heerden (2008)

❖ 11α,13-dihydroxanthalongin (xanthanolides) 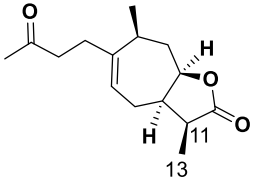	❖ Aerial parts.	❖ Anti-inflammatory (showed IC_{50} = 64.9 µM against RAW264.7 macrophages).*	❖ *In vitro*.*	❖ Cheng et al. (2011) ❖ Jakupovic et al. (1989) ❖ Lourens, Viljoen and Van Heerden (2008)
❖ Spathulenol (sesquiterpene alcohol) 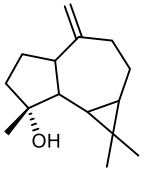	❖ Aerial parts.	❖ Antifungal activity (MIC = 32 µg/mL in *Tricophyton mentagrophytes*).* ❖ Anti-inflammatory Activity (in Cg-induced mice paw oedema).** ❖ Antioxidant activity (IC_{50} = 26.13 µg/mL in DPPH assay).* ❖ Antimycobacterial (MIC = 231.9 µg/mL in ovarian cancer cells).*	❖ *In vitro*.* ❖ *In vivo*.**	❖ Al-Ja'fari et al. (2011) ❖ Bohlmann and Suwita (1979) ❖ do Nascimento et al. (2018)
❖ 11α,13-dihydroinuviscolide (guainolide) 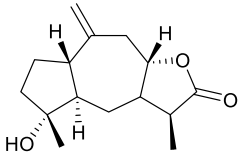	❖ Aerial parts.	❖ Anti-inflammatory (showed IC_{50} = 19.53 µM against RAW264.7 macrophages).*	❖ *In vitro*.*	❖ Cheng et al. (2011) ❖ Jakupovic et al. (1989)

❖ 4α-hydroxy-11αH-guai-9-en-12,8α-olide (guainolide)	❖ Aerial parts.	-	-	❖ Jakupovic et al. (1989)
❖ Helisplendiolide (sesquiterpene)	❖ Aerial parts.	-	-	❖ Bohlmann and Suwita (1979)
❖ (3*S*, 6*E*)-Nerolidol (sesquiterpene alcohol)	❖ Roots.	❖ Antibacterial activity (showed ID_{50} = 5.0-22.0 µg/mL in MSSA 2.6-10.6 µg/mL against MRSA).* ❖ Anti-cancer activity (had an IC_{50} = 2.96 in BT-20 breast cancer and 3.02 µg/mL against HeLa cell lines).* ❖ Anti-malarial activity (IC_{50} = 11.1 µg/mL).*	❖ *In vitro*.*	❖ Bohlmann and Suwita (1979) ❖ Hada et al. (2003) ❖ Kubo and Morimitsu (1995) ❖ Marques et al. (2015) ❖ Pontin et al. (2015) ❖ Vinholes et al. (2014)

		❖ Antifungal activity (inhibited mycelial growth by 85%).* ❖ Antioxidant activity (inhibited hydroxyl radical, IC_{50} = 1.48 mM).*		
❖ Squalene (linear triterpene)	❖ Aerial parts.	❖ Antioxidant activity (had IC_{50} = 0.023 mg/mL in lipid peroxidation of liposomes).* ❖ Chemo-preventive agent (showed a 60 and 12% tumor reduction on NNK-induced lung tumorigenesis in mice).**	❖ *In vitro*.* ❖ *In vivo*.**	❖ Bohlmann and Suwita (1979) ❖ Conforti et al. (2005) ❖ Smith (2000)
❖ τ-Cadinol (sesquiterpene)	❖ Aerial parts.	❖ Antifungal activity (showed IC_{50} = 28.3 µg/mL against *Aspergillus clavatus*).* ❖ Anticancer activity (had moderate inhibition in cancer cell lines).* ❖ Antimicrobial activity (MIC = 62.5 µg/mL).*	❖ *In vitro*.*	❖ Ho et al. (2011) ❖ Mashigo et al. (2015) ❖ Su et al. (2013) ❖ Su et al. (2015)

❖ *α*-Cadinol (sesquiterpene) 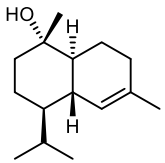	❖ Aerial parts.	❖ Antifungal activity (highest inhibition showed against *Colletotrichum gloeosporioides*, IC_{50} = 11.7 µg/mL).* ❖ Anticancer activity (had moderate inhibition in cancer cell lines).* ❖ Antimicrobial activity (showed MIC = 62.5 µg/mL in *Staphylococcus aureus* and *Staphylococcus epidermidis*).*	❖ *In vitro*.*	❖ Chang et al. (2008) ❖ Guerrini et al. (2016) ❖ Mashigo et al. (2015) ❖ Su et al. (2015)
❖ *α*-Muurolol (sesquiterpene) 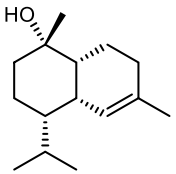	❖ Aerial parts.	❖ Anti-mildew fungal activity (IC_{50} = 41.8–18.6 µg/mL).* ❖ Antibacterial activity (had potent inhibition in DPPH HPTLC bioautography assay).*	❖ *In vitro*.*	❖ Guerrini et al. (2016) ❖ Mashigo et al. (2015) ❖ Su et al. (2018)
❖ *δ*-Cadinene (sesquiterpene) 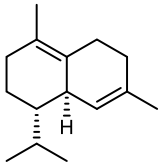	❖ Aerial parts.	❖ Antiproliferative activity (inhibited OVCAR-3 cells).* ❖ Antimicrobial activity (had highest MIC = 31.25 µL/mg against *Streptococcus pneumoniae*).*	❖ *In vitro*.*	❖ Hui, Zhao and Zhao (2015) ❖ Mashigo et al. (2015) ❖ Pérez-López et al. (2011)

❖ *β*-phellandrene (monoterpene) 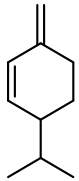	❖ Aerial parts.	❖ Antifungal activity (had highest MIC = 50 ppm in *Candida albicans*).*	❖ *In vitro*.*	❖ Mashigo et al. (2015) ❖ Tampieri et al. (2005)
❖ 1,8-Cineole (monoterpene) 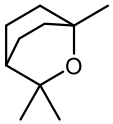	❖ Aerial parts.	❖ Anti-proliferative activity (inhibitions were observed between 5–50 mM in HCT116 and 5–25 mM in RKO cell lines).* ❖ Antimicrobial activity (had highest MIC = 2.0 mg/mL in *Bacillus cereus* and *Cryptococcus neoformans*).*	❖ *In vitro*.*	❖ Mashigo et al. (2015) ❖ Murata et al. (2013) ❖ Santos and Rao (2000) ❖ Vuuren and Viljoen (2007)
❖ *β*-Pinene (monoterpene) 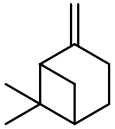	❖ Aerial parts.	❖ Antimicrobial activities (showed MIC =187 µg/mL. against *Candida albicans*). ❖ Antiviral activity (IC_{50} = 1.32 ± 0.11 mM).* ❖ Antioxidant activity (showed IC_{50} = 3116.3 ± 87.4, in DPPH radical scavenging assay).*	❖ *In vitro*.*	❖ Mashigo et al. (2015) ❖ Silva et al. (2012) ❖ Yang et al. (2011) ❖ Sharopov, Wink and Setzer (2015)

❖ Bicyclogermacrene (sesquiterpene) 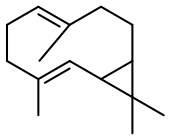	❖ Aerial parts.	❖ Larvicidal activity (showed LC_{50} = 10.3, 11.1, and 12.5 µg/mL, respectively, in *Anopheles subpictus*, *Aedes albopictus,* and *Culex tritaeniorhynchus*).*	❖ *In vitro*.*	❖ Bohlmann and Suwita (1979) ❖ Govindarajan and Benelli (2016)
❖ Germacrene D (sesquiterpene) 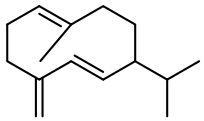	❖ Roots and aerial parts.	❖ Antiproliferative activity (on tumour cell lines, IC_{50} = 21.59–31.94 µg/mL).* ❖ Antioxidant activity (showed IC_{50} = 14.5 ± 0.5 µg/mL in DPPH assay).*	❖ *In vitro*.*	❖ Bohlmann and Suwita (1979) ❖ Casiglia et al. (2017)
❖ α-Terthienyl (thiophenes) 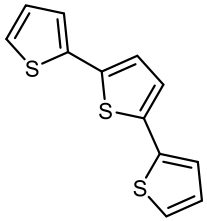	❖ Roots.	❖ Antifungal activity (had 98% growth inhibition of *Colletotrichum gloeosporioides*).* ❖ Antiviral activity (had MIC = 0.028 in SINV and 0.30 µM in MCMV viruses).* ❖ Herbicidal activity (had strong MIC = 1.10 mg/mL in *Chlamydomonas reinhardtii* algae).*	❖ *In vitro*.*	❖ Bohlmann and Suwita (1979) ❖ Fokialakis et al. (2006) ❖ Hudson et al. (1993) ❖ Zhao et al. (2018)

❖ 5,3′4′-trihydroxy-3,7,8-trimethoxyflavone (flavonoid)[1]	❖ Aerial parts.	❖ Antioxidant activity (showed IC_{50} = 17.8 µM in DPPH assay).*	❖ *In vitro*.*	❖ Akimanya et al. (2015) ❖ Bohlmann and Suwita (1979)
❖ Helitenuin (chlorophenol derivative)	❖ Roots.	-	-	❖ Bohlmann and Abraham (1979)
❖ Phloretin (dihydrochalcone flovonoid)	❖ Aerial parts.	❖ Anti-inflammatory activity (inhibited heterodimerization of TLR2/1 receptor in Raw264.7 and HEK293-hTLR2 cells).* ❖ Antimicrobial activity (had MIC = 16–256 µg/mL in *Escherichia coli*, *Staphylococcus aureus,*	❖ *In vitro*.*	❖ Bohlmann and Suwita (1979) ❖ Kim et al. (2018) ❖ Lee et al. (2009) ❖ Rezk et al. (2002)

	Enterococcus faecalis, MRSA, and VRE).*	
	❖ Antioxidant activity (had IC_{50} = 3.1 and 24.0 µM, respectively, in peroxynitrite scavenging and lipid peroxidation assays).*	

Abbreviations = minimal inhibitory concentrations (MIC), inhibitory concentration 50% (IC_{50}), lethal concentration (LC_{50}), inhibitory dose 50% (ID_{50}), carrageenan (Cg), 2,2-diphenyl-1-picrylhydrazyl (DPPH), 4-(methylnitrosamino)-1(3-pyridyl-1-butanone (NNK), murine cytomegalovirus (MCMV), sindbis virus (SINV), methicillin-resistant *Staphylococcus aureus* (MRSA), methicillin-susceptible *Staphylococcus aureus* (MSSA), vancomycin-resistant enterococcus (VRE), high performance thin layer chromatography (HPTLC)

5.7. Section B

5.7.1. Results and Discussion

The treatment and extraction of the plant material (*Helichrysum splendidum*) were carried out as outlined below in the experimental subsection. Phytochemical study of the leaf extracts from *H. splendidum* led to the isolation of eleven compounds, some of which were isolated as inseparable mixtures (**12** and **13**, **14** and **15**, as well as **21** and **22**). Compound **15** (a stereoisomer of compound **14**) was tentatively proposed as a new compound. While compounds **18-22** are reported for the first time from this plant. The characterization of each compound is discussed.

Compounds 12 and 13: 4-hydroxyguai-10(14)-en-12,8-olide isomers

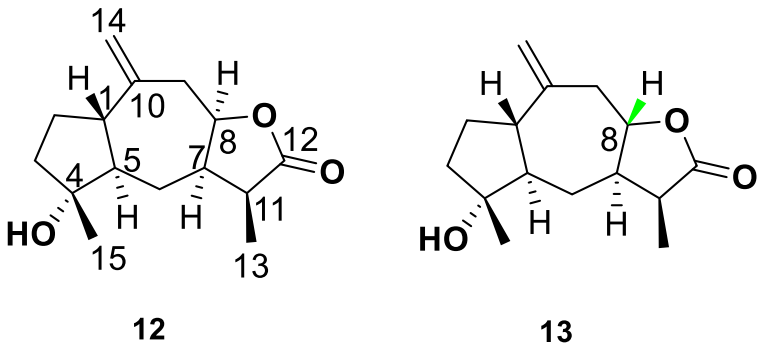

Fig. 5.2: Chemical structures of compounds **12** and **13**

Compounds **12** and **13** (Fig. 5.2) were obtained as an inseparable mixture (yellow solid) after successful purification of the combined fractions 14-15 (58.0 mg) of the main column on silica gel, eluting isocratic with EtOAc:Hex (90:10). Their structures followed from various spectroscopic techniques (^{1}H, ^{13}C, DEPT-135, HSQC, HMBC, COSY, and NOESY NMR) and comparison with the available literature (Jakpovic et al., 1988). Inspection of their ^{1}H (Plate 14A in the appendix) and ^{13}C (Plate 14D in the appendix) NMR spectra revealed them to be a mixture of two close sesquiterpenes, whose structural elucidation will be differentiated and discussed simultaneously.

In the ^{1}H NMR data (Table 5.2) two broad singlets appeared in the olefinic region at δ_H 4.90 and 4.99, which were attributed to the exomethylene group of compounds **12** and **13**, respectively. The signals of the oxymethine appeared at δ_H 4.54 (1H, *ddd*, *J* = 10.3 and 2.5 Hz, H-8) in compounds **12** and 4.37 (1H, *ddd*, *J* = 10.3 and 5.1 Hz, H-8) in **13**. While the methine resonances assigned to H-11 appeared as broad quintes at δ_H 2.84 (1H, *brq*, *J* = 7.5 Hz, H-11) and 2.68 (1H, *brq*, *J* = 7.8 Hz, H-11), respectively, in compounds **12** and **13**. Furthermore, the methylene and methyl proton chemical shifts were confined between δ_H 2.22-1.75, however, they were easily resolved through HSQC (Plate 15F in the appendix), HMBC (Plate 14G in the appendix), and NOSEY (Plate 14C in the appendix) correlations. The observed NOESY correlations in compound **12** were between H-8 with H-7 and H-11 (including H-7 with H-11, and H-5), which was indicative of a 7,8-*cis* configuration of the lactone (Jakupovic et al., 1989). On the other hand, important intermolecular interactions through space were observed between H-8 with H-1 (and H-13) in compound **13**, which suggested a similar orientation was likely at these positions. Since in compound **13** no correlations were observed between H-8 with H-7 and H-11, a 7,8-*trans* configuration was thus assigned for the lactone system. The orientation of H-11 was assigned as *α*-orientation based on literature evidence, which claims that the signal δ_H of H-11*α* appears at ~2.99, while the H-11β would appear at ~2.3 (Gao, Wang and Mabry, 1990). In our case, the chemical shifts were observed at δ_H 2.84 in compound **12** and 2.68 in compound **13**. Evidently, this also permitted the assignment of the relative stereochemistry's at H-1, H-7, H-5, and H-8 (Fig. 5.3). Interrogation of the ^{13}C NMR and DEPT-135 (Plate 14E in the appendix) displayed 30 carbon resonances (with some impurities), including ten CH (δ_C = 82.0, 80.8, 58.9, 57.5, 51.4, 47.7, 45.7, 43.2, 39.8, 39.3), ten CH_2 (δ_C = 111.4, 111.4, 41.2, 41.0, 39.7, 39.6, 27.5, 26.7, 24.8, 21.6), four CH_3 (δ_C = 25.1, 23.9, 11.0, 10.8), and six *quaternary* carbons (δ_C = 179.1, 179.7, 146.7, 143.7, 80.6, 79.7) as shown in Table 5.3. To the best of our knowledge, this is the first report of the ^{13}C NMR of both compounds. Nevertheless, the NMR data of compounds **12** and **13** was consistent with that of similar guaianolides (Table 5.2). Therefore, compound **12** was identified as 11α,13-Dihydroinuviscolide (a 4-hydroxyguai-10(14)-en-12,8-olide isomer), and **13** as the *8-epi* derivative. Both compounds have been previously described in *Helichrysum splendidum* by Jakupovic et al. (1989).

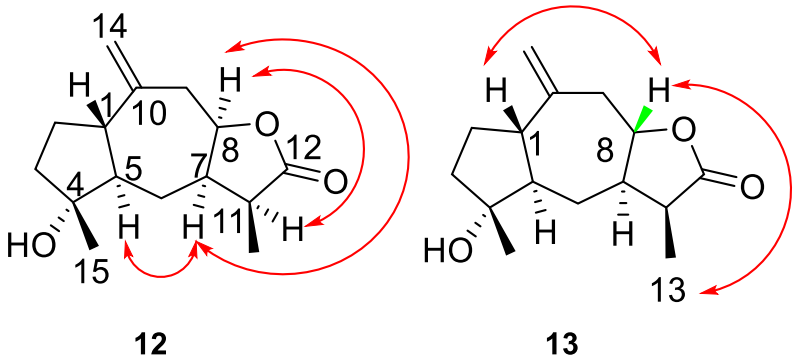

Fig. 5.3: Selected NOESY for compounds **12** and **13**

There are four other known stereoisomers of 4-hydroxyguai-10(14)-en-12,8-olide which have been described in the literature (Bohlmann, Zdero and Ahmed, 1982; Rustaiyan et al., 1987; Blay et al., 2000; Lourens, 2008), as shown in Table 5.2. Guaianolides (sesquiterpenes) represent a special class of metabolites with unique biological properties such as cytotoxicity and antitumor activity owing to the presents of the α-methylene-γ-lactone (Blay et al., 2000).

Table 5.2: ^{1}H NMR spectral data of compounds **12** and **13** ($CDCl_3$, 400MHz) compared to known 4-hydroxyguai-10(14)-en-12,8-olide isomers

#	12	13	Rustaiyan et al. (1987); Bohlmann, Zdero and Ahmed (1982)	Rustaiyan et al. (1987); Blay et al. (2000)	Lourens (2008)	Blay et al. (2000)	Jakupovic et al. (1989)	Jakupovic et al. (1989)
			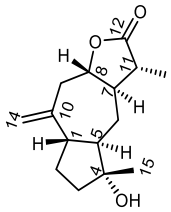	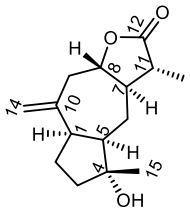	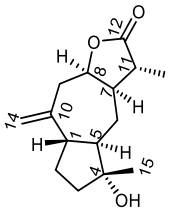	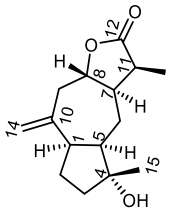	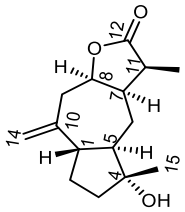	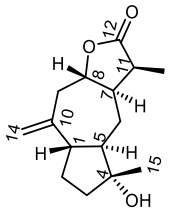
1	2.03, *m*	2.11, *m*	2.18	3.03	2.04		2.05	2.13
2	1.75 and 1.65, *m*	1.88 and 1.78, *m*	1.80	1.75 and 1.89	1.77	1.85-1.60 and 1.92-1.80	1.70	1.78 and 1.92
3	2.95 and 1.82, *m*	1.78 and 1.67, *m*	1.73	1.73	1.77 and 1.72		1.75	1.82, 1.72
4	-	-	-	-	-	-	-	-
5	1.26, *m*	1.57, *m*	1.60	2.13	1.35		1.67	1.60
6	1. 69 and 1.24, *m*	1.91 and 1.95, *m*	2.14 and 1.12	1.80 and 1.08	2.14 and 1.35	2.12 and 1.02	1.85 and 1.70	1.96 and 1.17
7	2.47, *m*	2.21, *m*	1.75	1.71	2.35	2.20-2.08	2.50	2.23
8	4.54, *ddd* (10.3, 2.5)	4.37, *ddd* (10.3, 5.1)	4.26	3.79	4.45	3.97	4.57	4.40
9	2.93 and 2.17, *m*	3.15 and 2.50, *m*	3.17 and 2.51	3.04 and 2.17	2.63 and 2.35	3.04 and 3.00	2.96 and 2.19	3.17 and 2.54
10	-	-	-	-	-	-	-	-
11	2.84, *brq* (7.5)	2.68, *brq* (7.8)	2.30	2.27	2.35	2.65	2.86	2.71
12	-	-	-	-	-	-	-	-
13	1.20, *m*	1.18, *m*	1.25	1.24	1.29	1.16	1.22	1.21
14	4.90, *brs*	4.99, *brs*	4.95 and 5.04	5.05 and 5.09	4.98 and 4.91	5.02 and 5.08	4.93	4.95 and 5.02
15	1.16, *m*	1.17, *m*	1.20	1.16	1.18	1.13	1.20	1.20

Table adapted from Lourens Ph.D. theses (2008).

Table 5.3: ^{13}C NMR spectral data for compounds **12** and **13**

	12	**13**
#	**δ_C, type**	**δ_C, type**
1	51.6, CH	47.8, CH
2	25.0, CH_2	26.9, CH_2
3	39.9, CH_2	41.2, CH_2
4	79.7, C	80.6, C
5	59.0, CH	57.7, CH
6	21.8, CH_2	27.7, CH_2
7	43.4, CH	45.9, CH
8	81.0, CH	82.2 CH
9	39.8, CH_2	41.4, CH_2
10	143.9, C	146.8, C
11	39.5, CH	40.0, CH
12	179.2, C	179.7, C
13	11.0, CH_3	11.2, CH_3
14	111.6[a], CH_2	111.6[a], CH_2
15	25.3, CH_3	24.0, CH_3

[a] –Overlapping signals.

Compounds 14 and 15: Lemmonin C and iso-lemmonin C

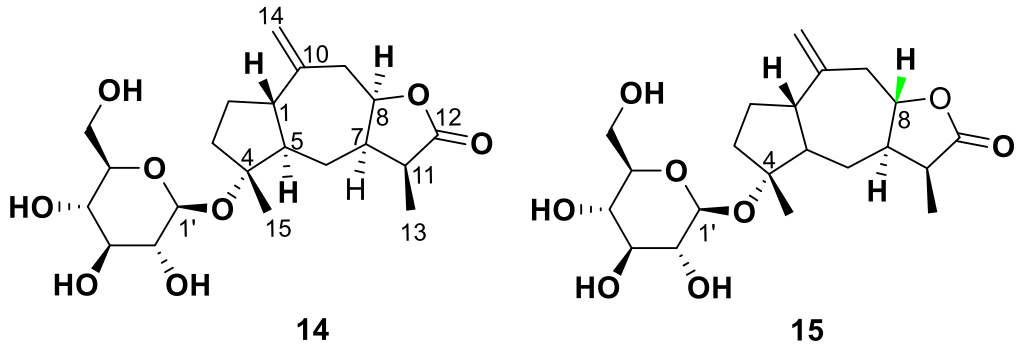

Fig. 5.4: Chemical structures of compounds **14** and **15**

Compounds **14** and **15** (Fig. 5.4) were obtained as an inseparable mixture from the EtOAc and BuOH fractions (only the characterization from BuOH will be discussed). They precipitated out (white needle-crystals) directly from fractions 10-16 (0.985 g) of the main column on silica gel, eluting with DCM:MeOH (100 :0→50: 50) gradient. Inspection of the proton (Fig. 5.6) and carbon thirteen (Fig. 5.7) nuclear magnetic resonance (^{1}H and ^{13}C-NMR) spectra confirmed them to be a mixture of two close sesquiterpenes. This was corroborated by High-Resolution Electrospray Ionisation Mass Spectrometry, HRESIMS, (Fig. 5.11) which gave an *m/z* at 825 $[M]^{+}$, corresponding to and calculated for two $C_{15}H_{21}O_2$ units (they will be discussed separately).

In the ^{1}H NMR spectrum, the proton signals of compound **14** overlapped with compound **15** in the region δ_H 1.09–4.97 and could only be differentiated through a combination of one-dimensional (1D) and two-dimensional (2D) experiments (they were also compared to the aglycones, compounds **12** and **13**). Careful interrogation of the ^{1}H (Table 5.4) and ^{13}C NMR spectroscopic data (Table 5.5) revealed compound **14** to be an exact match to the reported compound (Gao, Wang and Mabry, 1990). 1D selective gradient nuclear overhauser effect spectroscopy (1D NOE) was employed for the unambiguous determination of the relative stereocenters (Fig. 5.8–5.10). The observed 1D NOE correlations of compound **14** were between H-8 with H-7 and H-11 (including H-7 with H-5, H-11, and H-8), which was indicative of a 7,8-*cis* configuration of the lactone (Jakupovic et al., 1989). Since no correlation was observed between H-1 and H-5, then a 1,5-*trans* configuration was proposed. The orientation of H-11 was assigned as α-orientation based on literature evidence, which claims

that the signal δ_H of H-11α appears at ~2.99, while the H-11β would appear at ~2.3 (Gao, Wang and Mabry, 1990). In our case, the chemical shifts were observed at δ_H 2.89, thus, the methyl group was assigned a β-orientation (and H-11 an α-orientation). Furthermore, evidence of a sugar unit was present in the sugar region (δ_H = 3.04–3.81), from which the anomeric proton appeared as a broad doublet at δ_H 4.32 (1H, *brd*, *J* = 7.8 Hz, H1`) and was assigned a β-orientation. In the ^{13}C NMR spectrum, the carbon-carbon double bond signals appeared downfield at δ_C 145.8 (C-10) and 111.9 (C-14). While the signals of the sugar moiety appeared in the region δ_C 62.9-99.9. The remaining peaks were assigned using (^{1}H)–(^{13}C) heteronuclear single quantum correlation, HSQC (Plate 15C in the appendix), and heteronuclear multiple bond correlation, HMBC (Plate 15D in the appendix), experiments. The attachment of the sugar unit was confirmed at C-4 (δ_C = 88.0) by HMBC correlation. Therefore, based on the evidence provided herein and comparison with the literature, compound **14** was determined as a guaianolide, Lemmonin C, a compound previously isolated from *Hymenoxys lemmonii* (Gao, Wang and Mabry, 1990), *H. jamesii* (Ahmed et al., 2002), and *Pulicaria insignis* (Wang et al., 2020). Noteworthy, though its aglycone unit (11α,13-dihydroinuviscolide) has been previously isolated from *H. splendidum* by Jakupovic et al. (1988; 1989), to the best of our knowledge, this is the first account of the isolation of compound **14** from this plant.

On the other hand, compound **15** was tentatively proposed as a new compound and a stereoisomer of **14**. Its structure was elucidated by a comparison of their spectroscopic data (Table 5.4 and 5.5). In the ^{1}H NMR data of compound **15**, the signal of the oxymethine (H-8) appeared at δ_H 4.45 instead of 4.54 as observed in compound **14**, while the methine signal δ_H was assigned to H-1 shifted slightly by approximately +0.09 ppm. Thus, it was clear that a different stereochemistry was plausible, either, at C-8 and/or C-1. 1D NOE experiment was once again employed to assign the relative stereochemistry, from which no intermolecular interactions through space were observed between H-8 with H-7 and/or H-11 (Fig. 5.8). As such, the orientation at H-8 in compound **15** had to be different from compound **14**. Thus, a 7,8-*trans* configuration was assigned for the lactone system. Since compounds **14** and **15** were isolated as mixtures, the remaining stereochemistry's could not be unambiguously assigned due to interferences. Nevertheless, H-1 showed interactions with H-8 (Fig. 5.10), which allowed the determination of the configurations at these positions. The signal and coupling constant *J* 7.8 of the anomeric proton of compound **15** was identical to compound **14** and H-1` was therefore assigned the same stereochemistry. The ^{13}C NMR spectrum also displayed similar resonances of the sugar moiety as observed in compound **14**, which was further

indicative of an equivalent analogue. Similarly, the attachment of the sugar at C-4 was corroborated through HMBC correlation (Fig. 5.5). Furthermore, the signals that were assigned to C-1 and C-8, respectively, appeared at δ_C 48.2 (instead of 52.1 in compound **14**) and 84.0 (instead of 82.8 in compound **14**), which provided additional evidence of a possible change in stereochemistry. The carbon-carbon double bond signals appeared at δ_C 149.9 (C-10) and 111.7 (C-14). HSQC, COSY (Plate 15A in the appendix), DEPT-135 (Plate 15B in the appendix), and HMBC experiments all supported the assignment of a similar carbon backbone of the sesquiterpene moiety assigned in compound **14**. Thus, based on this evidence, compound **15** was tentatively proposed as a new C-8 epimer of compound **14**, iso-lemmonin C.

The aglycone unit (4-hydroxyguai-10(14)-en-12,8-olide, see Table 5.2 above) of compound **15** (and **14**) has been previously isolated from this plant by Jakupovic et al. (1989). However, it is surprising that though this plant has been extensively studied (Bohlmann and Suwita, 1979; Jakupovic et al., 1989; Lourens, 2008), compound **15** was not mentioned by either author. Thus, this emphasizes the caution that needs to be taken when dealing with this class of compounds.

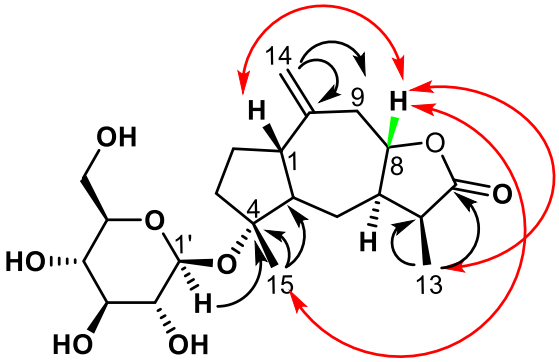

Fig. 5.5: Selected NOE (red) and HMBC (black) correlations for compound **15**

Fig. 5.6: ^{1}H-NMR spectrum (CD_3OD, 400 MHz) of compounds **14** and **15**(#)

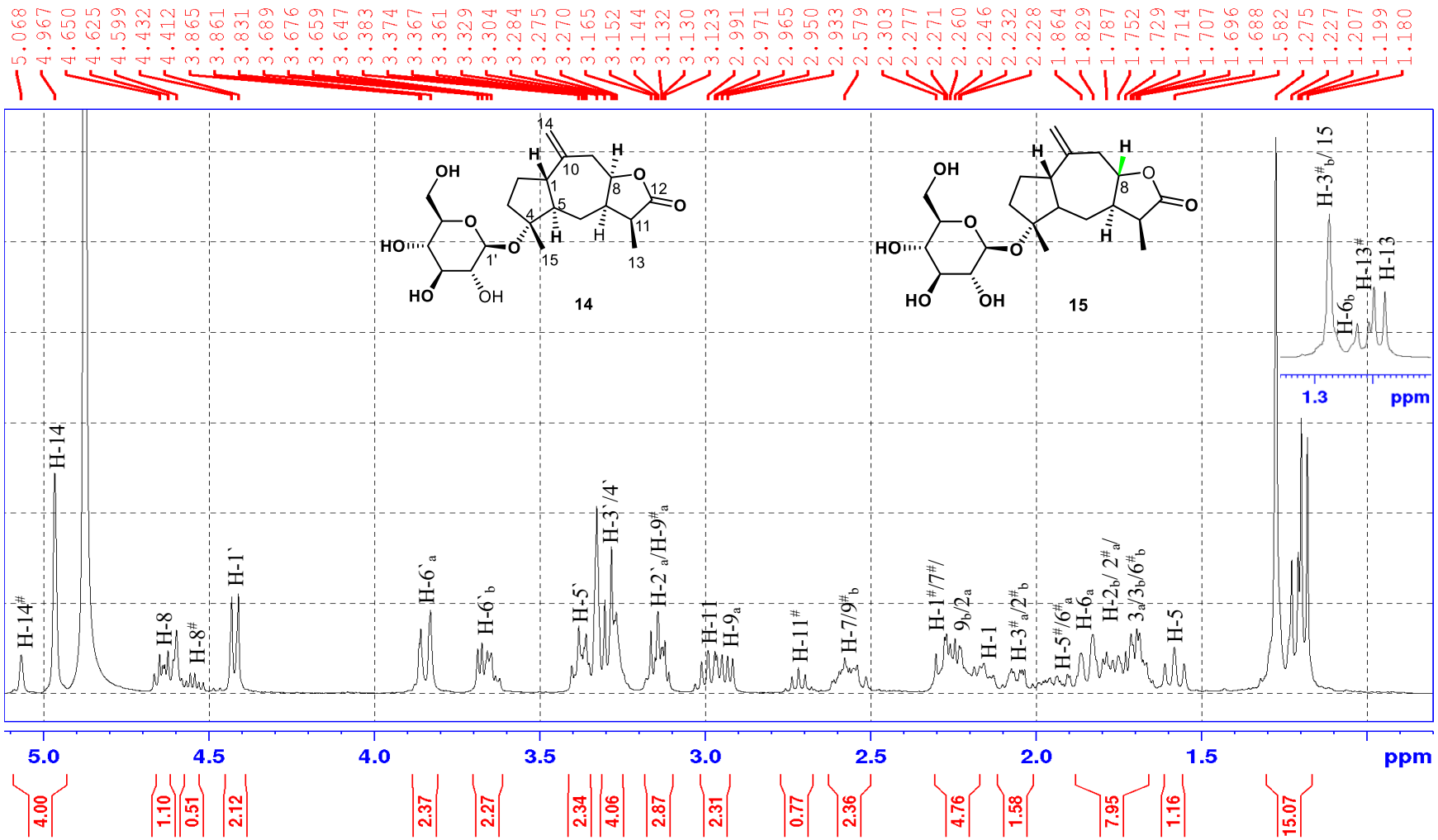

Fig. 5.7: ^{13}C-NMR spectrum (CD_3OD, 100 MHz) of compounds **14** and **15**(#)

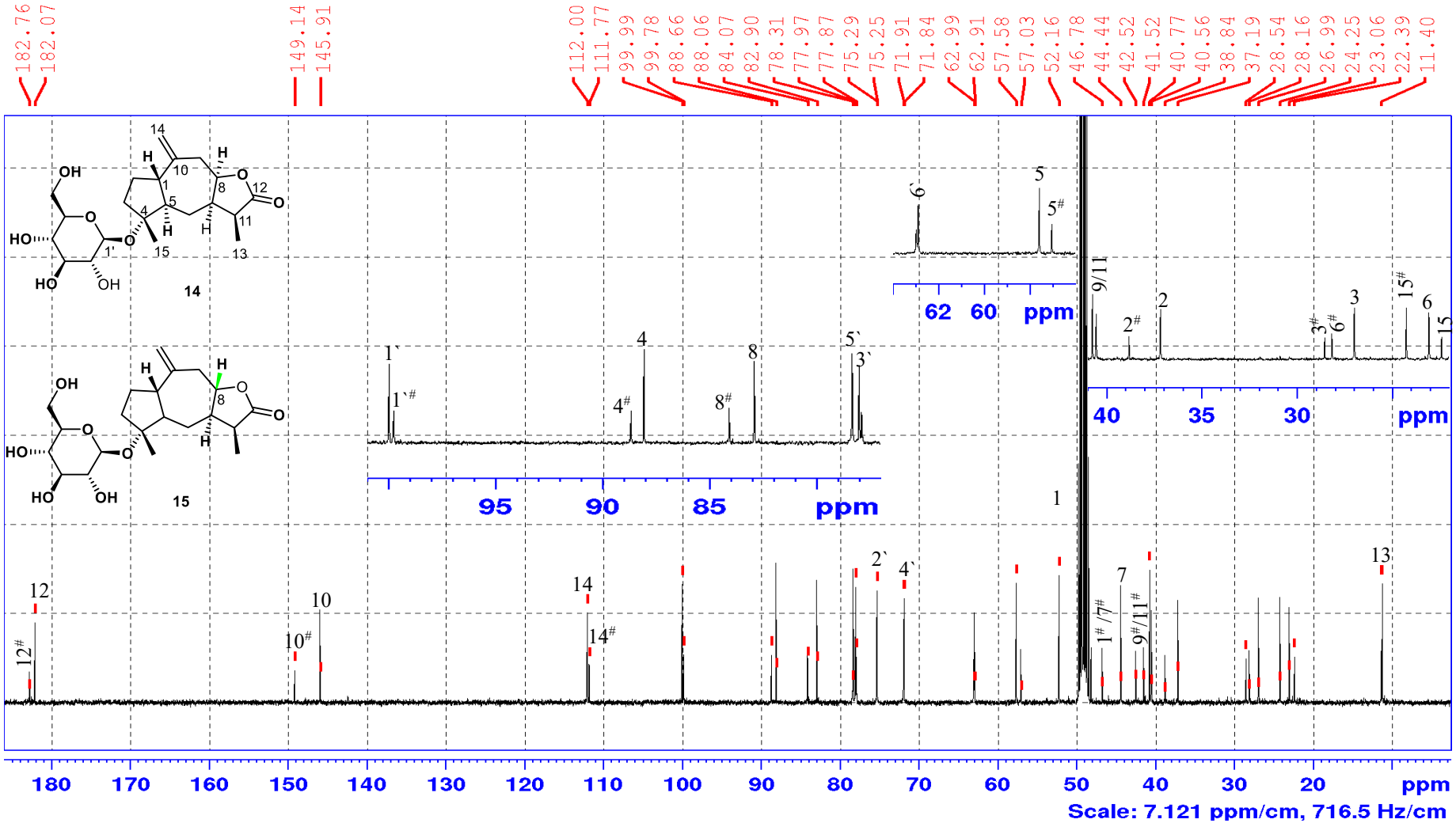

Fig. 5.8: 1D NOE spectrum (CD_3OD) of compounds **14** and **15**(#)

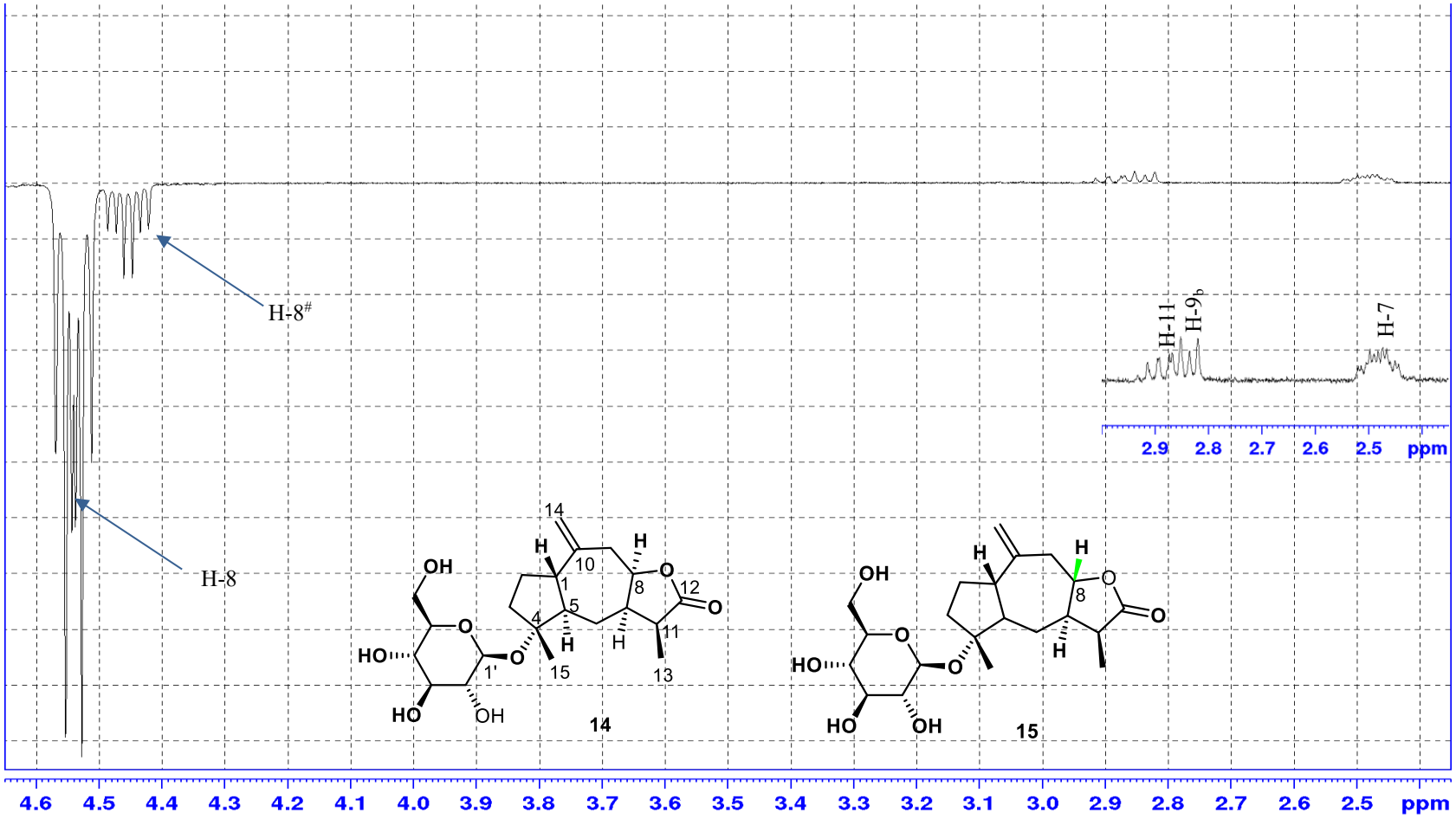

Fig. 5.9: 1D NOE spectrum (CD_3OD) of compounds **14** and **15**

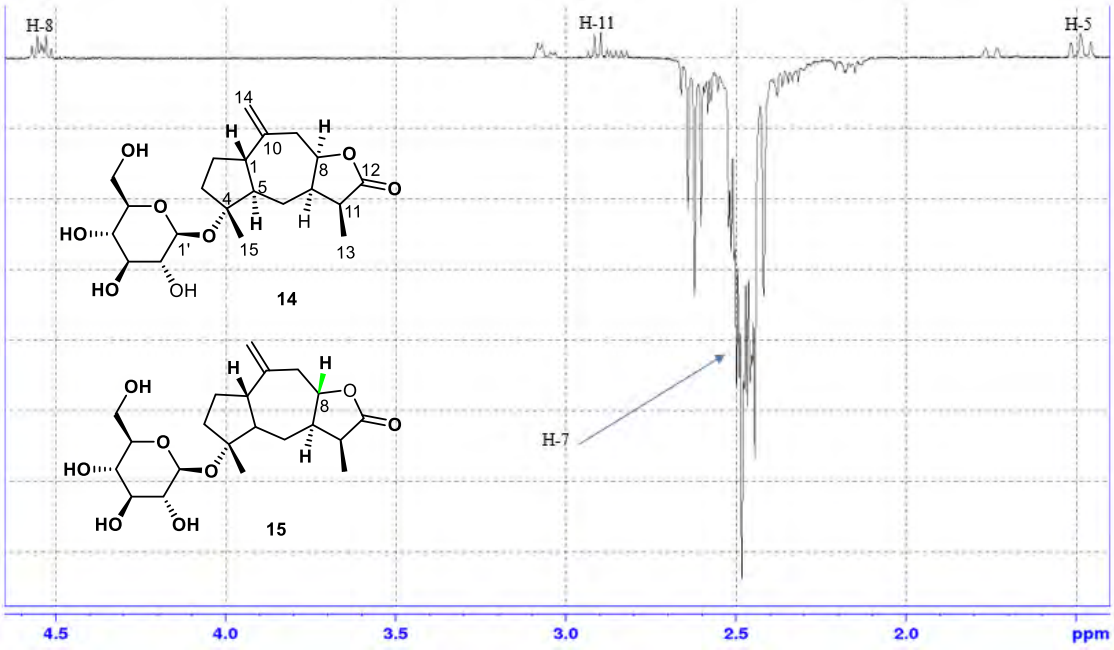

Fig. 5.10: 1D NOE spectrum (CD_3OD) of compounds **14** and **15(#)**

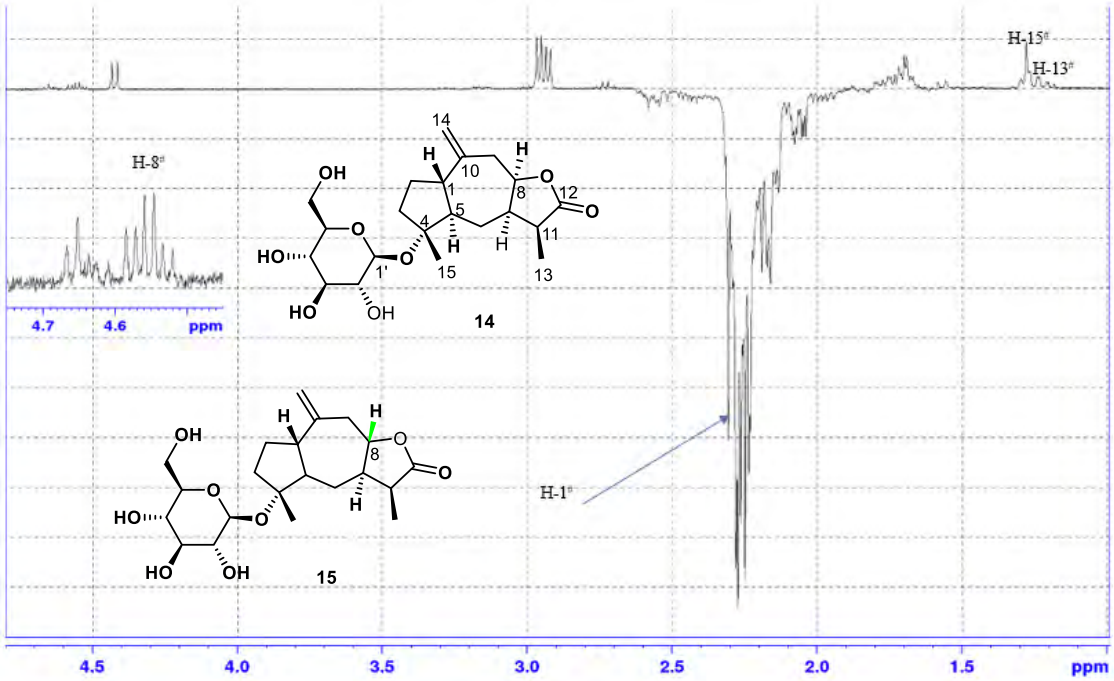

Fig. 5.11: LCMS spectrum of compounds **14** and **15**

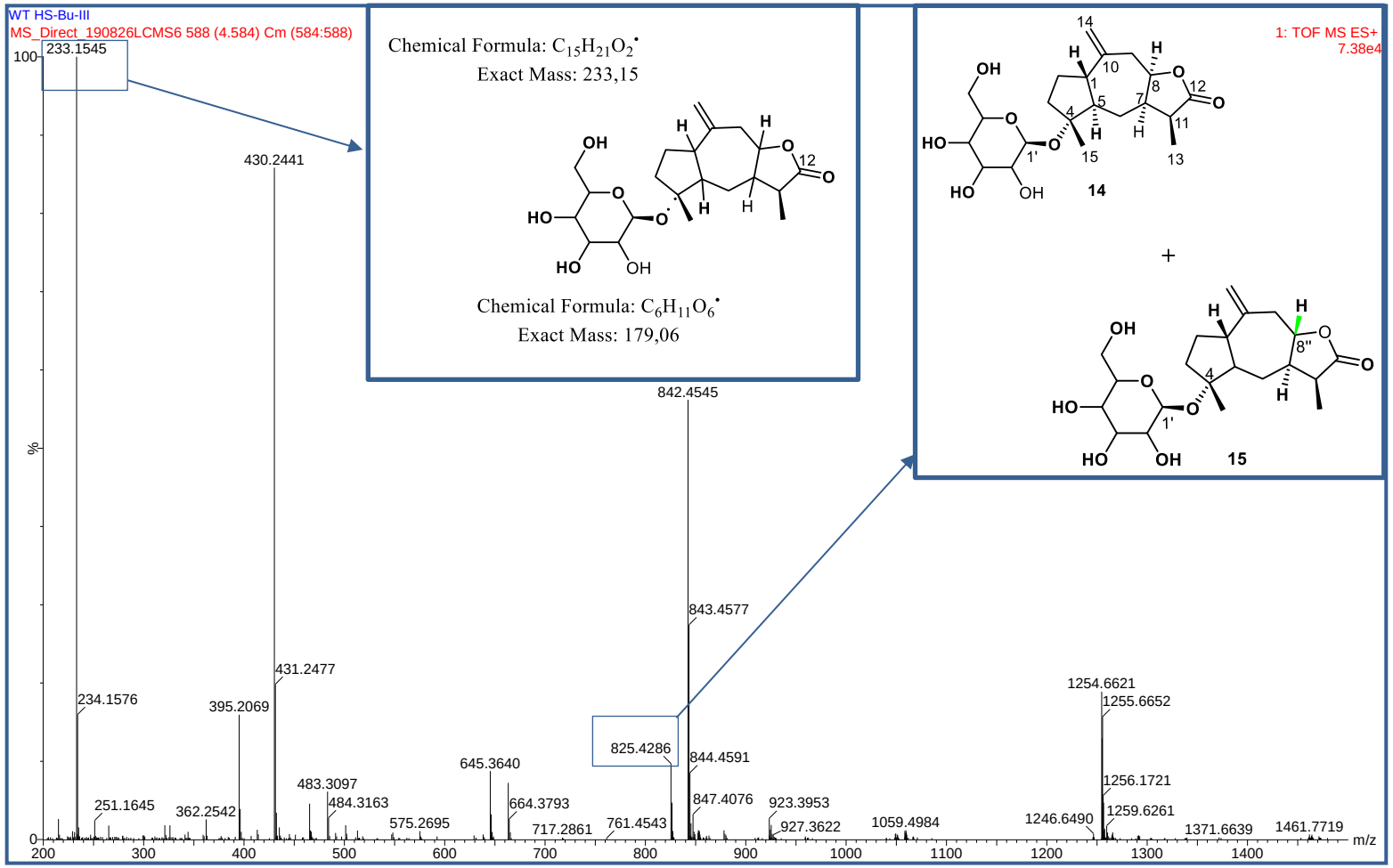

Table 5.4: ^{1}H NMR spectral data (including HMBC and NOESY) of compounds **14** and **15** (CD_3OD), compared to the literature[ǂ]

	δ_H[ǂ] (*J* in Hz)			HMBC[#]	Selected 1D NOE
#	**14**	**15**	(Gao, Wang and Mabry, 1990)[ǂ]		
1	2.06, *m*	2.15, *m*			H-8[c]
2	2.14 and 1.64, *m*	1.97 and 1.58, *m*			
3	1.71 and 1.59, *m*	1.95 and 1.17[a], *m*			
4	-	-	-	-	
5	1.58, *t* (11.5)	1.80, *m*	1.57[ǂ], *br t* (11.0)	C-4, C-1, C-7	
6	1.74 and 1.15, *m*	1.86 and 1.68, *m*	1.83[ǂ], *m*	C-8, C-5, C-1, C-7	
7	2.48, *m*	2.17[a], *m*	2.56[ǂ], *m*	C-12	H-5[b], H-8[b], H-11[b]
8	4.54, *m*	4.45, *m*	4.56[ǂ], *m*	C-6, C-10	H-7[b], H-11[b]
9	2.84 and 2.17[a], *m*	3.05 and 2.44, *m*	2.89[ǂ], *m*	C-10, C-14, C-8, C-1, C-7	
10	-	-	-	-	
11	2.89, *m*	2.62, *m*	2.92[ǂ], *m*	C-12, C-7, C-6, C-13	
12	-	-	-	-	
13	1.09, *d* (7.4)	1.12, *brd* (7.9)	1.13[ǂ], *m*	C-12, C-7, C-11	
14	4.87, *s*	4.97, *s*	4.96[ǂ], *s*	C-10, C-8, C-1, C-9	
15	1.17[a], *s*	1.17[a], *s*	1.24[ǂ], *s*	C-4, C-5, C-2	
Sugar moiety					
1'	4.32, *brd* (7.8)	4.32, *brd* (7.8)	4.47[ǂ], *m*	C-4	-
2'	3.04, *m*	3.04, *m*	3.13[ǂ], *m*	-	-
3'	3.18, *m*	3.18, *m*	3.30[ǂ], *m*	-	-
4'	3.19, *m*	3.19, *m*	3.40[ǂ], *m*	-	-
5'	3.27, *m*	3.27, *m*	3.44[ǂ], *m*	-	-
6'	3.75_{α}, *m*	3.75_{α}, *m*	$3.81^{ǂ}_{\alpha}$, *dd* (2.0, 12.0)	-	-
	3.57_{β}, *m*	3.57_{β}, *m*	$3.64^{ǂ}_{\beta}$, *dd* (5.0, 12.0)		

[a] -Overlapping signals. [b] -Selected 1D NOE correlation for compound **14**. [c] -Selected 1D NOE correlation for compound **15**.[ǂ] -Literature data (Gao, Wang and Mabry, 1990, CD_3OD, 500 MHz). [#] -HMBC correlation for both compounds.

Table 5.5: ^{13}C NMR spectral data of compounds **14** and **15,** compared to literature[ǂ]

	δc[ǂ], type		
#	**14**	**15**	(Gao, Wang and Mabry, 1990)[ǂ]
1	52.1, CH	48.2, CH	51.4[ǂ], CH
2	37.1, CH_2	38.7, CH_2	36.6[ǂ], CH_2
3	26.9, CH_2	28.4, CH_2	26.4[ǂ], CH_2
4	88.0, C	88.6, C	86.8[ǂ], C
5	57.5, CH	56.9, CH	56.6[ǂ], CH
6	23.0, CH_2	28.1, CH_2	24.0[ǂ], CH_2
7	44.3, CH	46.7, CH	43.6[ǂ], CH
8	82.8, CH	84.0, CH	81.2[ǂ], CH
9	40.5, CH_2	42.4, CH_2	39.7[ǂ], CH_2
1	145.8, C	149.0, C	145.9[ǂ], C
11	40.7, CH	41.4, CH	40.2[ǂ], CH
12	182.0, C	182.7, C	179.0[ǂ], C
13	11.1, CH_3	11.3, CH_3	11.2[ǂ], CH_3
14	111.9, CH_2	111.7, CH_2	111.2[ǂ], CH_2
15	22.3, CH_3	24.2, CH_3	22.5[ǂ], CH_3
Sugar moiety			
1'	99.9, CH	99.7, CH	99.2[ǂ], CH
2'	75.2[a], CH	75.2[a], CH	74.9[ǂ], CH
3'	77.9, CH	77.8, CH	77.2[ǂ], CH
4'	71.8, CH	71.9, CH	71.9[ǂ], CH
5'	78.3[a], CH	78.3[a], CH	78.1[ǂ], CH
6'	62.9[a], CH_2	62.9[a], CH_2	63.1[ǂ], CH_2

[a] -Overlapping signals. [ǂ] -Literature (Gao, Wang and Mabry, 1990; CD_3OD, 125 MHz)

Compound 16: 11*α*, 13-Dihydroxanthalongin (or 11*α*, 13-dihydrotomentosin)

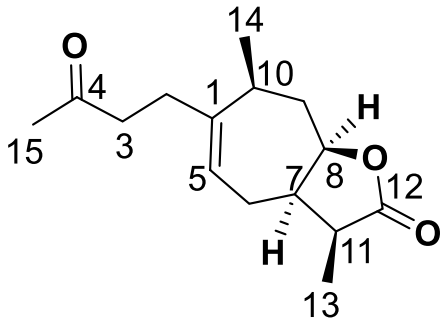

Fig. 5.12: Chemical structure of compound **16**

Compound **16** (Fig. 5.12) was obtained as a yellow-brown gum after successful purification of the combined fractions 10-12 (196 mg) of the main column on flash silica gel column chromatography, eluting with Hex–EtOAc (100 :0→50: 50) stepwise gradient. The characterization of this compound has been previously described from this species by Jakupovic et al. (1989). As such, its structure was readily deduced as 11*α*, 13-Dihydroxanthalongin (*syn*. = 11*α*, 13-dihydrotomentosin), a monomeric guaianolide, using 1D and 2D NMR experiments (Plates 16A-16G in the appendix). In our hands, specific attention was given to the assignment of the relative stereochemistry at the chiral centres.

Noticeable peaks were observed in the ^{1}H NMR (Plate 16A in the appendix, Table 5.6): a deshielded multiplet at δ_H 4.57 (H-8) which was indicative of the proximity of an oxygen atom to this proton, broad doublet of doublets at δ_H 5.40 (1H, *brdd J* = 2.46, 7.13 Hz, H-5) for the non-conjugated double bond, one strong singlet at δ_H 2.10 (H-15) that is distinctive of methyl protons close to a ketone group, two up-field overlapping doublets at δ_H 1.11 (3H, *brd*, *J* = 7.5 Hz, H-13) and 1.09 (3H, *brd*, *J* =7.3 Hz, H-14) for the methyl groups, and a broad triplet at δ_H 2.75 (1H, *brt*, *J* = 7.5 Hz, H-11). The ^{13}C NMR (Plate 16D in the appendix, Table 5.6) and DEPT-135 spectra (Plate 16E in the appendix) exhibited 15 major peaks, which is a distinctive feature for sesquiterpenes. Though the identity of this compound was first described by Jakupovic et al. (1989) from the aerial parts of this species, the ^{13}C NMR data was only given later by Lanzetta et al. (1991). Nevertheless, further inspection of our ^{13}C NMR spectra indicated the presence of three CH_3 (δ_C = 10.8, 21.2 and 29.8), four CH_2 (δ_C = 21.8, 31.0, 36.9 and 42.6), five CH (δ_C = 32.8, 38.8, 80.5, 42.2 and 122.5), and three *quaternary* carbons (δ_C =

144.0, 179.2 and 208.3). The assignments of the peaks were corroborated using HSQC (Plate 16G in the appendix) and HMBC (Plate 16H in the appendix) correlation and are summarized in Table 5.6.

Confirmation of the relative stereochemistry was as follows: assignment of C-11 followed from careful consideration of the literature. According to Lanzetta et al. (1991), a C-11 methyl resonates at δ_C ~10.9 in the 11α,13-dihydroderivative (and at δ_C ~14.0 in the 11β,13-dihydroderivative), owing to the occurrence of a *γ*-gauche effect between the βC-l1 methyl and C-6. In our case, this signal appeared at δ_C 10.8, and therefore, the stereochemistry (of the methyl at C-11) was assigned a β-orientation. A 1D selective gradient NOE correlations (Plate 16F, Fig. 5.13) was run to support this claim and to assign the remaining stereochemistry of the lactone ring. Thus, clear interactions were observed between H-8 (δ_H = 4.57), H-11 (δ_H = 2.75) and H-7 (δ_H = 2.60) confirming the 7,8-*cis* configuration of the lactone. Furthermore, the correlation observed between H-10 (δ_H = 2.29) and H-8 (δ_H = 4.52) was also essential in assigning the α-orientation of H-10. This assignment of the relative stereochemistry of 16 is the same as that proposed by previous authors (Jakupovic et al., 1989; Marcinek-Hüpen-Bestendonk et al., 1990; Lanzetta et al., 1991; Lourens, 2008). Therefore, based on this evidence compound **16** was confirmed as 11α, 13-Dihydroxanthalongin (*syn*. = 11α, 13-dihydrotomentosin) – a stereoisomer of 11β, 13-Dihydroxanthalongin (*syn*. = 11β, 13-dihydrotomentosin) (Bohlmann and Suwita, 1979) and 11,13-dihydroderivative of xanthalogin (*syn*. = tomentosin) (Marcinek-Hüpen-Bestendonk et al., 1990).

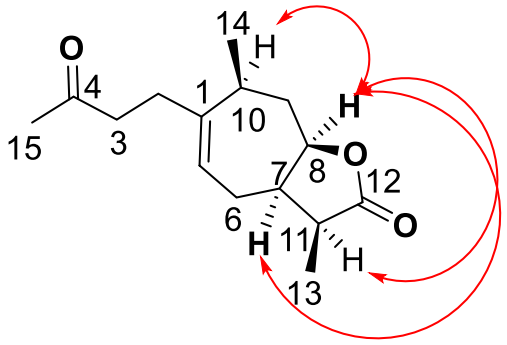

Fig. 5.13: Selected 1D NOE correlations for compound **16**

Table 5.6: ^{1}H and ^{13}C-NMR spectroscopic data ($CDCl_3$, 400 MHz) for compound 16

#	δ_C[ǂ], type		δ_H[ǂ] (*J* in Hz)		HMBC
1	144.0, C	144.1[ǂ], C	-	-	-
2	31.0, CH_2	31.0[ǂ], CH_2	2.28 - 2.18, *m*		C-4, C-10, C-3, C-1, C-5
3	42.6, CH_2	42.7[ǂ], CH_2	2.49 - 2.40, *m*		C-1, C-4, C-2
4	208.3, C	208.2[ǂ], C	-	-	-
5	122.5, CH	122.6[ǂ], CH	5.40, *brdd* (2.46 and 7.13)	5.46[ǂ]	C-10, C-2, C-7
6	21.8, CH_2	21.9[ǂ], CH_2	2.16 - 1.81, *m*		C-1, C-5
7	42.2, CH	42.3[ǂ], CH	2.60, *m*		C-12
8	80.5, CH	80.5[ǂ], CH	4.57, *m*	4.62[ǂ], *m*	C-6
9	36.9, CH_2	36.9[ǂ], CH_2	2.0 - 1.95, *m*		C-1, C-7, C-14, C-10, C-8
10	32.8, CH	32.9[ǂ], CH	2.29, *m*		C-1, C-5
11	38.8, CH	38.9[ǂ], CH	2.75, *brt* (7.5)	2.80[ǂ], *m*	C-6, C-12, C-13, C-7
12	179.2, C	179.1[ǂ], C	-	-	-
13	10.8, CH_3	10.9[ǂ], CH_3	1.11, *brd* (7.5)	1.16[ǂ], *d* (7.3)	C-12, C-7, C-11
14	21.2, CH_3	21.3[ǂ], CH_3	1.09, *brd* (7.3)	1.14[ǂ], *d* (6.7)	C-1, C-9, C-10
15	29.8, CH_3	29.9[ǂ], CH_3	2.10, s	2.16[ǂ], *s*	C-3, C-15

[ǂ] –Literature (Lanzetta et al., 1991; $CDCl_3$, 300 MHz).

Apart from *H. splendidum*, this compound has also been previously identified from the flower heads of *Arnica mollis* (Marcinek-Hüpen-Bestendonk et al., 1990) and *A. amplexicauli* (Passreiter et al., 1996), the aerial parts of the plant *Dittrichia graoeolens* (Desf.) Greuter [(syn. *Inula graueolens*)] (Lanzetta et al., 1991), *Inula japonica* (Yang, Wang and Jia, 2003), *H. montanum* (Lourens, 2008), *I. helianthus-aquatica* (Huang et al., 2011), *I. falconeri* (Cheng et al., 2011), and *I. hupehensis* (Qin et al., 2012), and the whole plants of *I. sericophylla* (Cheng et al., 2012) *I. hookeri* (Cheng et al., 2012).

Compound 17: Helisplendidilactone

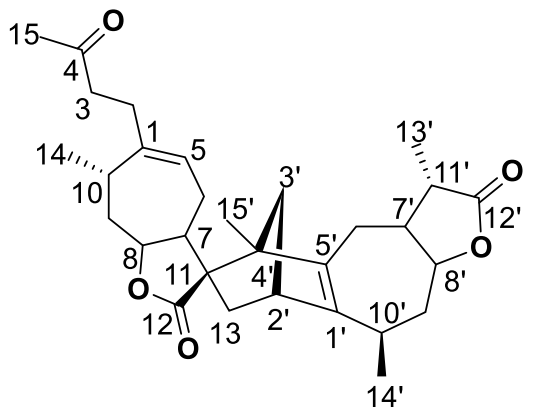

Fig. 5.14: Chemical structure of compound **17**

Compound **17** (Fig. 5.14) was isolated as a yellow gum after successful purification of the combined fractions 10-12 (196 mg) of the main column on flash silica gel column chromatography, eluting with Hex–EtOAc (100 :0→50: 50) stepwise gradient. The characterization of this compound has been previously reported from this species (Jakupovic et al., 1989). Thus, its structure was readily deduced as helisplendidilactone, which is a dimeric guaianolide, using 1D and 2D NMR experiments (Plates 17A-17F in the appendix) and against the known data (Jakupovic et al., 1989; Lourens, 2008).

Inspection of the ^{1}H (Plate 17A in the appendix) and ^{13}C NMR (Plate 17C in the appendix) spectra of compound **17** revealed that certain signals resembled compound **16** (a closely related sesquiterpene lactone that has already been discussed in this thesis, see Table 5.6). As such, in the proton NMR data (Table 5.7) of compound **17,** the broad doublet of doublets for the non-conjugated double bond appeared at δ_H 5.16 (H-5, this was 5.40 in compound **16**), while the oxymethine appeared as multiplet at δ_H 4.45 (H-8, this was 4.57 in compound **16**). A strong doublet of doublet of doublets appeared at δ_H 4.11 integrating for one proton, which was clearly indicative of a second oxymethine placed at H-8` (this δ_H was absent in compound **16**). The ^{13}C NMR of helisplendidilactone was recently revised by Lourens (2008) from the earlier work made by previous authors (Jakupuvic et al., 1989). In our hands, the carbon resonances (δ_C) were assigned as shown in Table 5.7, from which 30 major peaks were displayed. Lourens (2008) corrected the signal (δ_C) assignments of C-9 and C-9`, as well as C-13` and C-15`.

Nonetheless, an inspection of our HMBC (Plate 17F in the appendix, Fig. 5.15) data showed that the broad doublet at δ_H 1.22 (showing an HSQC correlation (Plate 17E in the appendix) with the carbon resonance at δ_C 21.4 assigned to C-14) displayed a correlation with the δ_C 37.1, 35.7, and 144.7. While the doublet at δ_H 1.08 (showing an HSQC correlation with the carbon resonance at δ_C 20.6 assigned to C-14`) had correlations with the $\delta_C$ 40.3, 29.3, and 150.1. Furthermore, the broad doublet at $\delta_H$ 1.20 (showing an HSQC correlation with the carbon resonance at $\delta_C$ 10.6) displayed correlations with $\delta_C$ 179.0 (C-12`), 39.7 (C-11`), and 45.5 (C-7`), whereas the singlet at δ_H 1.18 (showing an HSQC correlation with the carbon resonance at δ_C 13.4) had correlations with δ_C 63.0 (C-11), 140. 6 (C-5`), 50.6 (C-3`), and 54.0 (C-4`). Therefore, it was clear that C-9 should be assigned the signal at 37.1 (previously assigned to C-9' by Jakupuvic et al., 1989) and C-9` the signal at 40.3 (previously assigned to C-9 by Jakupuvic et al., 1989), while δ_C 10.6 be assigned to C-13` (previously assigned to C-15` by Jakupuvic et al., 1989) and δ_C 13.4 to C-15` (previously assigned to C-13` by Jakupuvic et al., 1989). Thus, our assignments confirmed the changes made by Lourens (2008). Other important correlations include the ^{1}H-^{1}H COSY between the triplet at δ_H 2.69 (H-11`) with the broad doublet at $\delta_H$ 1.20 (H-13`) and 2.05 (H-7`) to further support the reassignments of H-13' and H-15`, as well as an HMBC between the broad triplet at δ_H 2.17 with C-1 (δ_C 144.7), which meant that the signal at δ_C 150.1 should be assigned to C-1` (since it showed correlation with H-10` or δ_H 2.27[a]). It is worth pointing out that the assignment of the signal at δ_C 144.7 to C-1 is further corroborated by our previous assignment made in compound **16**.

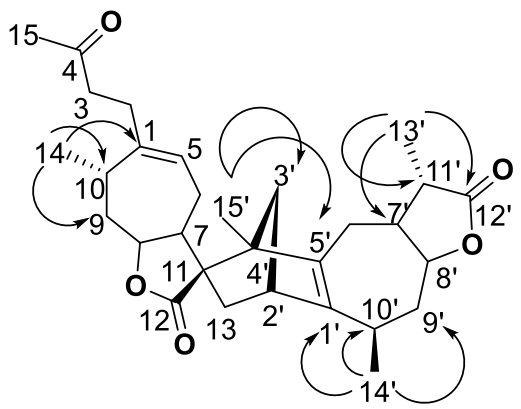

Fig. 5.15: Selected HMBC correlations of compound **17**

Table 5.7: ^{1}H and ^{13}C-NMR spectroscopic data ($CDCl_3$, 400 MHz) for compound **17**

#	δ_C[↓], type		δ_H[↓] (*J* in Hz)		HMBC
1	144.5, C	144.5[↓], C	-	-	-
2	30.3, CH_2	30.3[↓], CH_2	2.17, *brt* (7.6)	2.20[↓], *brt* (7.5)	C-4, C-10, C-3, C-1, C-5
3	42.4, CH_2	42.4[↓], CH_2	2.49 and 2.42[a], *m*	2.54[↓] and 2.44[↓]	C-1, C-4, C-2
4	207.8, C	207.7[↓], C	-	-	-
5	119.7, CH	119.7[↓], CH	5.16, *dd* (5.4, 3.4)	5.19[↓], *brd* (8.5, 5.0)	C-10, C-2, C-7, C-6
6	25.3, CH_2	25.3[↓], CH_2	2.26[a] and 1.13, *m*	2.28[↓] and 1.16[↓], *m*	C-1, C-5, C-8
7	41.8, CH	41.8[↓], CH	2.41[a], *m*	2.44[↓], *m*	C-6, C-11
8	78.5, CH	78.5[↓], CH	4.45, *m*	4.48, *ddd* (9.0, 2.0)	C-12, C-10
9	37.1, CH_2	37.1[↓], CH_2	1.94 and 1.76, *m*	1.98[↓] and 1.78[↓]	C-14, C-10, C-8
10	35.7, CH	35.7[↓], CH	2.27[a], *m*	2.28[↓], *m*	C-14, C-9, C-8, C-5
11	63.0, C	63.0[↓], CH	-	-	-
12	181.7, C	181.6[↓], C	-	-	-
13	36.2, CH_2	36.2[↓], CH_3	1.97 and 1.53, *m*	1.98[↓] and 1.56[↓]	C-2`, C-1`, C-12
14	21.2, CH_3	20.6[↓], CH_3	1.22, *brd* (2.9)	1.26[↓], *d* (7.0)	C-1, C-9, C-10
15	29.8, CH_3	29.8[↓], CH_3	2.10, s	2.13[↓], *s*	C-3, C-4
1`	150.1, C	150.1[↓], C	-	-	-
2`	43.1, CH	43.1[↓], CH	2.91, *m*	2.94[↓] *brs*	C-5`, C-11, C-4`
3`	50.6, CH_2	50.6[↓], CH_2	2.24[a] and 1.05, *m*	2.28[↓] and 1.08[↓]	C-4`
4`	54.0, C	54.0[↓], C	-	-	-
5`	140.6, C	140.7[↓], C	-	-	-
6`	25.0, CH_2	25.0[↓], CH_2	2.41[a] and 1.65, *m*	2.44[↓] and 1.68[↓]	C-7`, C-8`, C-5`, C-1`
7`	45.5, CH	45.5[↓], CH	2.05, *m*	2.08[↓], *ddd* (11.0)	C-13`, C-8`, C-11`, C-9`
8`	84.6, CH	84.5[↓], CH	4.11, *ddd* (11.0, 2.5)	4.14[↓], *ddd* (11.0, 7.5)	C-6`
9`	40.3, CH_2	40.3[↓], CH_2	2.25[a] and 1.46, *m*	2.28[↓] and 1.49	C-14`, C-10`, C-7`, C-8`, C-1`
10`	29.3, CH	29.3[↓], CH	2.27[a], *m*	2.28[↓], *m*	C-8`, C-1`
11`	39.7, CH	39.7[↓], CH	2.69, *t* (7.7)	2.72[↓], *dq* (7.5)	C-12`, C-8`, C-7`, C-13`
12`	179.0, C	179.1[↓], C	-	-	-
13`	10.6, CH_3	10.6[↓], CH_3	1.20, *brd* (2.8)	1.23[↓], *d* (7.5)	C-12`, C-7`, C-11`
14`	20.6, CH_3	21.2[↓], CH_3	1.08, *d* (6.8)	1.11[↓], *d* (~7.0)	C-1`, C-9`, C-10`
15`	13.4, CH_3	13.4[↓], CH_3	1.18, *s*	1.22[↓], *s*	C-5`, C-11, C-4`, C-3`

[a] –Overlapping signals. [↓]–Literature (Jakpovic et al., 1989; $CDCl_3$, 400MHz).

Guaianolides represent one of the largest groups of sesquiterpene lactones, which have chemotaxonomic and biological significance (Jakupovic et al., 1989). Helisplendidilactone is yet to be isolated outside *H. splendidum*, though a similar compound called 13`-epihelisplendidilactone was isolated from *H. montanum* by Lourens (2008). Biosynthetically, these guaianolides have been shown to occur via a Diels-Alder-type dimerization between the cyclopentadiene derivative guaia-1,4-dien-12,8β-olide and xanthalogin (or tomentosin) (Jakpovic et al., 1989).

Compound 18: Quercetin-3-*O*-β-D-glucopyranoside-(3`→*O*-3```)-quercetin-3-*O*-β-D-galactopyranoside

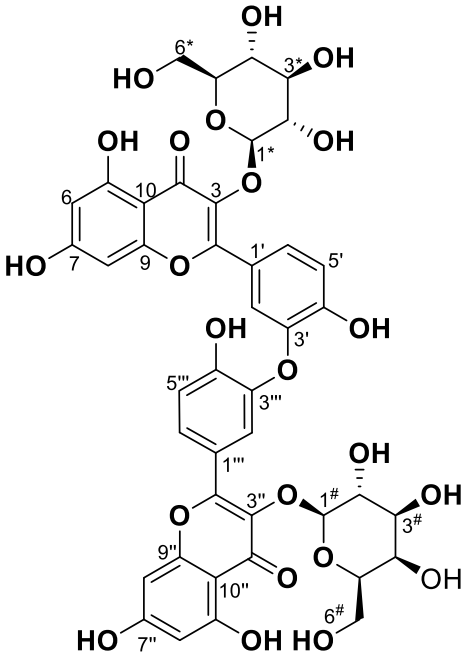

Fig. 5.16: Chemical structure of compound **18**

Compound **18** (Fig. 5.16) was obtained as a brown solid. Its structural elucidation followed from NMR (Plates 18A–18F in the appendix) and HRESIMS (Plate 18G in the appendix) spectroscopy. The HRESIMS showed two significant fragment peaks at m/z 465.1031 $[(M+3H) - C_{21}H_{19}O_{11}]^+$ and 303.0506 $[(M+3H) - C_{27}H_{30}O_{16}]^+$ (calculated for the molecular formula $C_{42}H_{38}O_{23}$), which suggested that it could be a mixture of two flavonoid units with glucose and galactose attached or a biflavonoid glycoside. However, it is hereby proposed to be a biflavonoid glycoside based on the following evidence.

The ^{1}H NMR data (Plate 18A in the appendix, Table 5.8) showed prominent signals δ_H in the aromatic region, whose integration was suggestive of two flavonoid moieties: 5.93^b (2H, *d*, *J* = 2.0 Hz, H-6/6``), 6.10$^b$ (2H, *m*, H-8/8``), 6.64 (1H, *d*, *J* = 2.8 Hz, H-5`), 6.66 (1H, *d*, *J* = 2.8 Hz, H-5```), 7.36^b (2H, *m*, H-6`/6```), 7.51 (1H, *d*, *J* =2.1 Hz, H-2```), and 7.64 (1H, *d*, *J* =2.1 Hz, H-2`). While the ^{13}C NMR (Plate 18C, Table 5.8) of compound **18** exhibited 42 carbon signals δ_C (some overlapped), from which 30 appeared in the aromatic region and were assigned to the two flavonoid units. Furthermore, the ^{1}H and ^{13}C NMR experiments gave

further evidence of two possible sugar units (anomeric protons appeared at δ_H 4.96 (1H, *d*, *J* = 7.4 Hz, H-1*) and 4.88 (1H, *d*, *J* = 7.7 Hz, H-1#)), whose attachments at C-3`/3`` in the C-ring of each flavonoid moiety was confirmed by HMBC correlation (Fig. 5.17). The nature of the sugar units was proposed after detailed interrogation of the NMR data as 3-*O*-galactopyranoside and 3-*O*-glucopyranoside. According to the literature (Bailey and Butterfield, 1981; Bubb, 2003), galactose and glucose isomers can be differentiated from each other by the carbon signal at δ_C C-4 (Table 5.8). In the HMBC spectrum, the proton signal at δ_H 7.36[b] (2H, *m*, H-6`/6```) showed important correlations (^3J) with C-4`/C-4``` and C-2`/C-2```. Since no correlation (^4J) was visible between this proton (δ_H 7.36[b]) and C-3`/3```, the ether linkage of the two flavonoid groups was tentatively placed at C-3`/3```. Clear nuclear Overhauser effect (NOE) through space correlations (Plate 18C in the appendix) were observed between H-2` (δ_H = 7.64) and H-2``` (δ_H = 7.51) to support this assignment. Nonetheless, a comprehensive literature search using SciFinder for known biflavonoids revealed compound **18** to be like that reported from *Machilus zuihoensis* by Mao et al. (2011). Therefore, after successful comparison of their NMR data, compound **18** was tentatively determined as biflavonol glycoside, quercetin-3-*O*-β-D-glucopyranoside-(3`→*O*-3```)-quercetin-3-*O*-β-D-galactopyranoside. To the best of our knowledge, this compound has not been isolated from the *Helichrysum* genus. HSQC (Plate 18E), HMBC (Plate 18F), and COSY (Plate 18B) spectra are shown in the appendix.

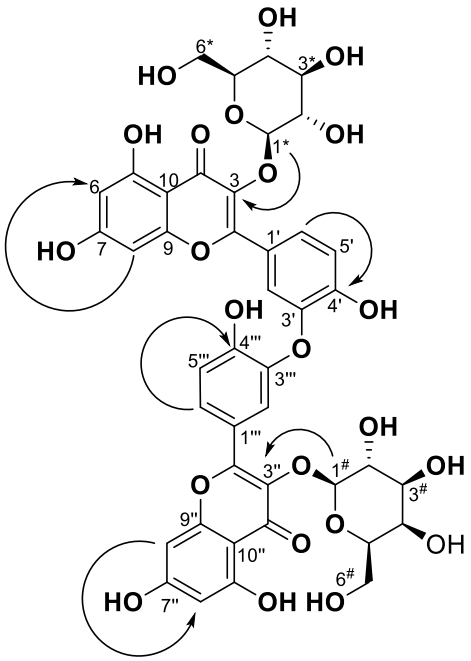

Fig. 5.17: Selected HMBC correlations of compound **18**

Table 5.8: ^{1}H and ^{13}C-NMR spectroscopic data (CD_3OD, 400 MHz) for compound **18**

	Moiety I			Moiety II	
#	**δC, type**	**δH, type**	**HMBC$^{\$}$**	**δC, type**	**δH, type**
2, 2``	157.0[a], C	-	-	157.2[a], C	-
3, 3``	134.1[a], C	-	-	134.3[a], C	-
4, 4``	177.7[a], C	-	-	177.6[a], C	-
5, 5``	161.3[b], C	-	-	161.3[b], C	-
6, 6``	99.4[b], CH	5.93[b], *d* (2.0)	C-8, C-8``; C-10, C-10``; C-7, C-7``; C-5, C-5``	99.4[b], CH	5.93[b], *d* (2.0)
7, 7``	167.3[b], C	-	-	167.3[b], C	-
8, 8``	94.0[b], CH	6.10[b], *m*	C-8, C-8``; C-10, C-10``; C-7, C-7``; C-9, C-9``	94.0[b], CH	6.10[b], *m*
9, 9``	157.2[a], C	-	-	157.1[a], C	-
10, 10``	103.4[b], C	-	-	103.4[b], C	-
1`, 1```	121.4[a], C	-	-	121.5[a], C	-
2`, 2```	116.3[a], CH	7.64, *d* (2.1)	C-6`, C-6```; C-1`, C-1```; C-3`, C-3```; C-2`, C-2```; C-4`, C-4```	116.1[a], CH	7.51, *d* (2.1)
3`, 3```	144.3, C	-	-	144.5, C	-
4`, 4```	148.5[b], C	-	-	148.5[b], C	-
5`, 5```	114.7[a], CH	6.64, *d* (2.8)	C-4`, C-4```; C-3`, C-3```; C-6`, C-6```; C-1`, C-1```	114.6[a], CH	6.66, *d* (2.8)
6`, 6```	121.5, CH	7.36[b], *m*	C-4`, C-4```; C-2`, C-2```; C-9, C-9``	121.8, CH	7.36[b], *m*
Sugar moiety					
1*, 1#	103.3, CH	4.96, *d* (7.4)	C-3 and C-3``	104.3, CH	4.88, *d* (7.7)
2*, 2#	74.2	3.29[b]		69.7	3.17, *m*
3*, 3#	75.6	3.29[b], *m*		71.7	3.63, *m*
4*, 4#	73.7	3.36, *m*		68.6	3.66, *brt* (8.2)
5*, 5#	76.7	3.24, *brt* (8.8)		76.9	3.04, *m*
6*, 6#	60.5	3.37, *m*	C-4#	61.1	3.51, *brdd* (2.1, 1.9)

[a] -Signals maybe interchangeable. [b] -Overlapping signals. $^{\$}$ -HMBC is for both moieties.

The antioxidant (IC_{50} = 30.4 μM in superoxide anion radical scavenging) and anti-inflammatory activity (on high mobility group box 1 (HMGB-1) protein secretion) of this compound was shown by Mao et al. (2011).

Compound 19: Chrysosplenol D

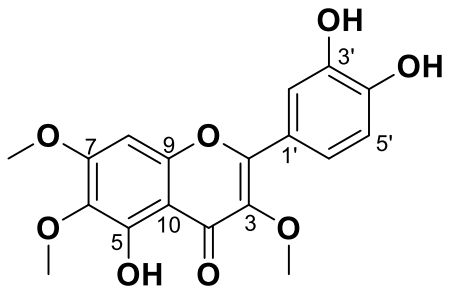

Fig. 5.18: Chemical structure of compound **19**

Compound **19** (Fig. 5.18) was obtained as a yellow amorphous powder from both the DCM and EtOAc extracts (only the characterization from EtOAc will be discussed). Nonetheless, this compound was purified from fractions 12-19 (100 mg) of the main column on flash silica gel column chromatography, eluting isocratic with $CHCl_3$ (100%). The structural assignment of compound **19** was established based on its 1D and 2D NMR spectra (Plates 19A-19F in the appendix) and by direct comparison with the available literature data (Marco et al., 1988).

The ^{1}H-NMR (Plate 19A in the appendix, Table 5.9) showed three intense singlet resonances at δ_H 3.96, 3.90, and 3.81 assignable to the three methoxy protons, whose positions were confirmed by cross-peaks on HMBC (Fig. 5.19). While the singlet at δ_H 6.48 of the aromatic proton was assigned to H-8 according to its HMBC correlation with C-9 (δ_C = 156.9^a), C-7 (δ_C = 158.5), C-6 (δ_C = 128.7), C-4 (δ_C = 179.0) and C-10 (δ_C = 104.8). Since the positions of the three OMe-groups (3-OMe and 7-OMe, and 6-OMe) and the aromatic proton (H-8) was already confirmed, it was tentatively proposed that one OH-group must be present at C-5 of the A-ring. Furthermore, the integration and substitution pattern of the signals at δ_H 7.73 (1H, *d*, *J* = 2.2 Hz, H-2`), 7.63 (1H, *dd*, *J* = 8.4, 2.3 Hz, H-6`) and 6.93 (1H, *d*, *J* = 8.4 Hz, H-5`) provided strong evidence of a quercetin back-bone in the B-ring (Marco et al., 1988). The ^{13}C-NMR (Plate 19C in the appendix, Table 5.9) and DEPT-135 spectra (Plate19D in the appendix) revealed 18 carbon signals which were assigned to three methyl at δ_C 60.9, 59.3, and 55.8, four methine at δ_C 121.2, 115.2^b, 95.2, and eleven quaternary carbons at δ_C 179.0 (C-4), 158.5 (C-7), 156.9^a (C-9), 156.8^a (C-2), 148.7 (C-4`), 148.3 (C-5), 145.1 (C-3`), 138.1 (C-3), 128.7 (C-6), 121.6 (C-1`), and 104.8 (C-10). HMBC correlations were used to corroborate the structure

(Fig. 5.19). Therefore, based on this evidence the identity of compound **19** was determined as chrysosplenol D (or 5,3`,4`-trihydroxy-3,6,7-trimethoxyflavone). Chrysosplenol D has been previously isolated and shown as a maker compound from various Asteraceae species: *Artemisia iwayomogi*, *A. santolinifolia*, *A. molinien*, *A. alba*, and *A. tridentate* (Valant-Vetschera and Wollenweber, 1995), *Achillea biebersteinii*, *A. gerberi*, *A. ageratum*, *A. maura*, and *A. ochroleuca* (Valant-Vetschera and Wollenweber, 1996). To the best of our knowledge, compound **19** is hereby reported for the first time from the *Helichrysum* genus.

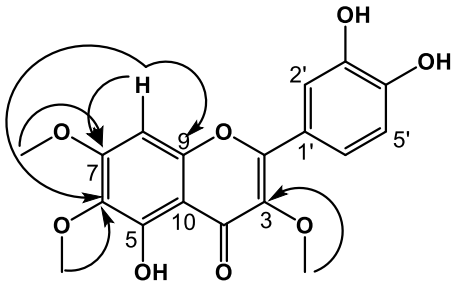

Fig. 5.19: Selected HMBC correlations of compound **19**

Table 5.9: ^{1}H and ^{13}C-NMR spectroscopic data (CD_3OD spiked with $CDCl_3$, 400 MHz) of compound **19**

#	δ_C[↓], type		δ_H[↓] (*J* in Hz)		HMBC
2	156.8, C	155.9[↓], C	-	-	-
3	138.1, C	137.6[↓], C	-	-	-
4	179.0, C	178.1[↓], C	-	-	-
5	148.3, C	151.6[↓], C	-	-	-
6	128.7, C	131.5[↓], C	-	-	-
7	158.5, C	158.5[↓], C	-	-	-
8	95.2, CH	91.2[↓], CH	6.48, *s*	6.86[↓], *s*	C-4, C-7, C-9, C-5, C-6, C-10
9	104.8, C	105.5[↓], C	-	-	-
10	156.9, C	151.6[↓], C	-	-	-
1`	121.6, C	120.7[↓], C	-	-	-
2`	115.2[a], CH	115.6[↓], CH	7.73, *d* (2.2)	7.58[↓], *d* (2.2)	C-2, C-4`, C-3`, C-1`, C-6`
3`	145.1, C	145.2[↓], C	-	-	-
4`	148.7, C	148.8[↓], C	-	-	-
5`	115.2[a], CH	115.5[↓], CH	6.93, *d* (8.4)	6.89[↓], *d* (8.4)	C-4`, C-5`, C-1`, C-6`
6`	121.2, CH	120.6[↓], CH	7.63, *dd* (8.4, 2.3)	7.48[↓], *dd* (8.4, 2.2)	C-2, C-4`, C-2`, C-5`
6-O<u>Me</u>	60.9 CH_3	60.0[↓] CH_3	3.90, *s*	3.71[↓], *s*	C-6
3-O<u>Me</u>	59.3 CH_3	59.6[↓] CH_3	3.81, *s*	3.78[↓], *s*	C-3
7-O<u>Me</u>	55.8 CH_3	56.2[↓] CH_3	3.96, *s*	3.90[↓], *s*	C-7

[a] –Overlapping signals. [↓]–Literature data (Marco et al., 1988; $CDCl_3$, 270 MHz).

Compound 20: L-2-*O*-Methyl-chiroinositol (or L-Quebrachitol)

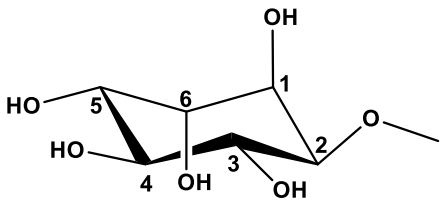

Fig. 5.20: Chemical structure of compound **20**

Compound **20** (Fig. 5.20) was obtained as colourless crystals directly from fractions 18-21 of the main column over silica gel, eluting with DCM:MeOH gradient (100 :0→50: 50). Its structure was characterized as 2-*O*-methyl-L-*chiro*-inositol (*syn* = L-quebrachitol) based on its NMR (Plates 20A–20E in the appendix) and by comparison with previous data (Angyal and Odier, 1983; Abraham et al., 2005; Díaz et al., 2008).

The ^{1}H NMR spectrum (Plate 20A in the appendix) of compound **20** exhibited a strong singlet at δ_H 3.44 assignable to the methoxy protons, whose attachment at C-2 (δ_C = 80.0) was corroborated by HMBC (Fig. 5.21). Further resonances were observed including two distinct downfield triplets at δ_H 4.26 (1H, *t*, *J* = 3.5 Hz, H-1) and 4.05 (1H, *t*, *J* = 3.5 Hz, H-6), two broad doublets of doublets 3.73 (1H, *dd*, *J* = 3.2, 9.6, H-5) and 3.39 (1H, *dd*, *J* = 3.1, 9.5, H-2), as well as a multiplet 3.60[a] (2H, *m*, H-3/4) that integrated for two protons. The coupling constants (*J*) and (^{1}H) – (^{1}H) correlation spectroscopy (COSY) experiment (Plate 20B in the appendix, Fig. 5.20) was essential in assigning the signals: H-2 showed two coupling constants (3.1, 9.5 Hz), which clearly indicated an axial and equatorial orientation of the neighbouring protons (Díaz et al., 2008). It has been shown that the proton (and carbon) chemical shifts are characteristic for the orientation of the methyl group and its neighbouring environment (Angyal and Odier, 1983), such that, equatorial methylation (of the hydroxyl group) at C-2 shifts the H-2 proton up-field to lower frequencies. This results in H-1 (in an equatorial orientation) shifting downfield to higher frequencies while the remaining protons are unchanged (Abraham et al., 2005). Therefore, this evidence permitted the assignments of the remaining proton signals (Table 5.10). The ^{13}C NMR data (Plate 20 C in the appendix) displayed seven carbon resonances with chemical shifts in the region of a heteroatom-linked carbon (Díaz et al., 2008). The signal-bearing the methoxy group appeared at δ_C 80.0 (C-2), whereas the remaining signals were corroborated on HMBC cross-peaks (Plate 20F in the appendix). All chemical shifts

agreed with the literature (Díaz et al., 2008). To the best of our knowledge, this is the first report of this compound in the *Helichrysum* genus.

This optically active cyclitol was first described as a natural product from *Aspidosperma quebracho* (Apocynaceae) by Tanret (1889) and has since been detected in various other species: *Allophylus edulis* (Díaz et al., 2008) and *Hippophaë rhamnoides* (Kallio et al., 2009). Its biosynthetic pathway, in the leaves of *Acer pseudo-platanus* (Schilling, Dittrich and Kandler, 1972) and *Litchi chinensis* (Wu et al., 2018), has been shown to involve first the methylation of *myo*-inositol and then followed by epimerization of the resulting l-O-methyl-myo-inositol (or D-bornesitol). Nonetheless, this is yet to be shown in the *Helichrysum* genus. Furthermore, this compound and its close derivatives (3-*O*-methyl-D-*chiro*-inositol (D-pinitol), 2-*O*-methyl-L-*chiro*-inositol (L-quebrachitol), and *O*-methyl-*scyllo*-inositol (De Almeida et al., 2012)) are known to be responsible for regulating sugar metabolism and protecting cells from oxidative, cytotoxic, and mutagenic damages among many others (Ostlund et al., 1993; Lemos et al., 2006; Junior et al., 2006; De Olinda et al., 2008).

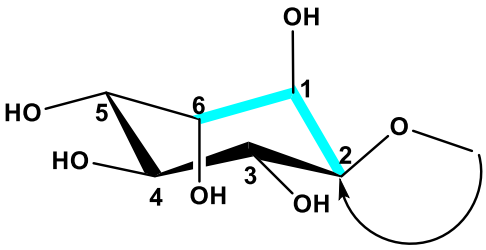

Fig. 5.21: Selected HMBC (black) and COSY (blue) correlations of compound **20**

Table 5.10: ^{1}H and ^{13}C-NMR spectroscopic data (D_2O, 400 MHz) for compound **20**

#	δ_C[ǂ], type		δ_H[ǂ] (*J* in Hz)		HMBC
1	67.0, CH	67.6[ǂ], CH	4.26, *t* (3.5)	4.25[ǂ], *dd* (3.5, 3.6)	C-2, C-6, C-5, C-3
2	80.0, CH	80.6[ǂ], CH	3.39, *dd* (3.1, 9.5)	3.39[ǂ], *dd* (3.2, 9.5)	C-4, C-3, C-1, **OMe**
3	71.8, CH	73.2[ǂ], CH	3.60[a], *m*	3.60[ǂ], *m*	C-2, C-4, C-5
4	72.7, CH	72.3[ǂ], CH	3.60[a], *m*	3.60[ǂ], *m*	C-2, C-3, C-5
5	70.2, CH	70.8[ǂ], CH	3.73, *dd* (3.2, 9.6)	3.73[ǂ], *dd* (3.2, 9.6)	C-8, C-6, C-5, C-7
6	71.3, CH	71.8[ǂ], CH	4.05, *t* (3.5)	4.06[ǂ], *dd* (3.6, 3.7)	C-2, C-4, C-5, C-1
2-OMe	**56.8**	**57.3[ǂ]**	**3.44[ǂ], *s***	**3.44, *s***	**C-2**

[a] –Overlapping signals. [ǂ]–Literature (Díaz et al., 2008; D_2O, 400 MHz).

Compound 21 and 22: Oleanolic (**21**) and ursolic acid (**22**)

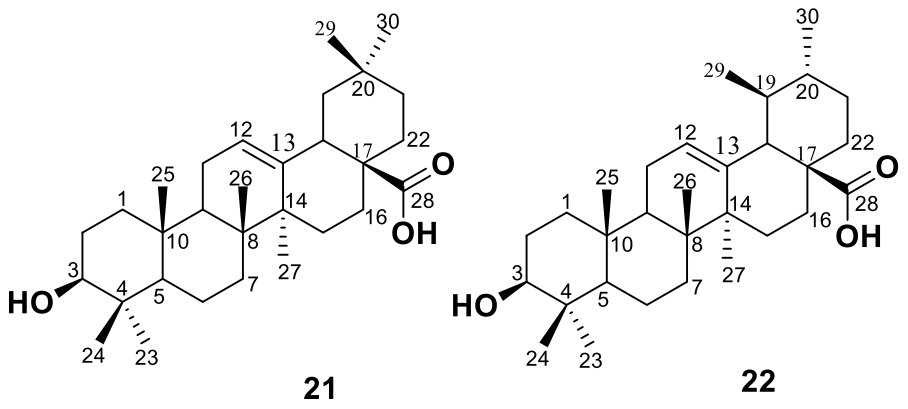

Fig. 5.22: Chemical structure of compounds **21** and **22**

Compounds **21** and **22** (Fig. 5.22) were isolated as an inseparable mixture (white solid) after successful purification of the combined fractions 10-12 (196 mg) of the main column on flash silica gel column chromatography, eluting with Hex–EtOAc (100 :0→50: 50) stepwise gradient. Inspection of the ^{1}H (Plate 21A in the appendix) and ^{13}C (Plate 21C in the appendix) NMR spectra revealed them to be a mixture of two pentacyclic triterpenoids-oleanolic (**21**) and ursolic acid (**22**); which were identified by comparison of their NMR with available literature data (Seebacher et al., 2003). The difference between these isomers is the position of one methyl group on the E ring (as shown above), thus their proton and carbon signals appeared almost identical proving challenging to assign unambiguously.

The ^{1}H NMR spectrum showed characteristic peaks such as the broad doublet at δ_H 5.48 (2H, *brd*, *J* = 2.7 Hz, H-12), and a multiplet at 3.44 (2H, *m*, H-3) all of which integrated for two protons (one for each compound). In addition, a strong doublet appeared at δ_H 2.62 (1H, *d*, *J* =11.3 Hz) and was assignable to H-18 in compound **22** because of the position of the methyl at C-19. Whereas in compound **21** this signal appeared as a doublet of doublets at δ_H 3.29 (1H, *d*, *J* = 3.9, 13.7 Hz, H-18). This evidence allowed the unambiguous assignment of the signals of 21 and 22 (Table 5.11). The biggest challenge was assigning the methylene and methyl protons due to the extensive *signal overlap in the* olefinic region (Seebacher et al., 2003). Nonetheless, these resonances δ_H appeared in the range 2.40 – 0.75 and were assigned through a combination of HSQC (Plate 21F in the appendix), and HMBC (Plate 21E in the appendix,

Fig. 5.23) experiments and direct comparison with literature data (Seebacher et al., 2003). Furthermore, the methyl group at δ_H 0.99 (3H, *brd*, *J* = 5.3 Hz, Me-29) appeared as a broad doublet due to its interaction with the signal at δ_H 1.47 (1H, *m*, H-19), and this could only be assigned to Me-29 in compound **22**. This assignment was corroborated by a three-bond cross peak on HMBC between the signal at δ_H 0.99 with the carbon signal at δ_C 53.3 (C-18). COSY experiments exhibited important correlations which permitted the differentiation of the signals of 21 and 22 (Fig. 5.22). The ^{13}C and DEPT-135 (Plate 21D in the appendix) NMR spectra of 21 and 22 displayed 60 signals (representing 30 carbon resonances for each compound), some of which were overlapping. The chemical shifts of C-30 (methine), C-29 (methyl carbon), C-22 (methylene carbon), C-20 (methine carbon), C-19 (methine carbon), C-18 (methine carbon), C-13 (quaternary carbon), and C-12 (methine carbon) appeared at δ_C 21.1, 17.2[a], 37.2, 39.1, 39.2, 53.3, 139.0, and 125.4, respectively, in compound **22** and could be easily distinguished from those of 21 (Table 5.11). While the carbonyl signal (of compound **22**) was assigned based on the HMBC correlation between the resonance at δ_H 2.62 (H-18) with δ_C 179.6 (C-28). The NMR of compounds **21** and **22** were found to be consistent with the literature data (Seebacher et al., 2003), therefore, based on the evidence that is provided here they were subsequently identified. Table 5.11 shows a summary of their NMR data. To the best of our knowledge, this is the first account of their isolation in *H. splendidum*.

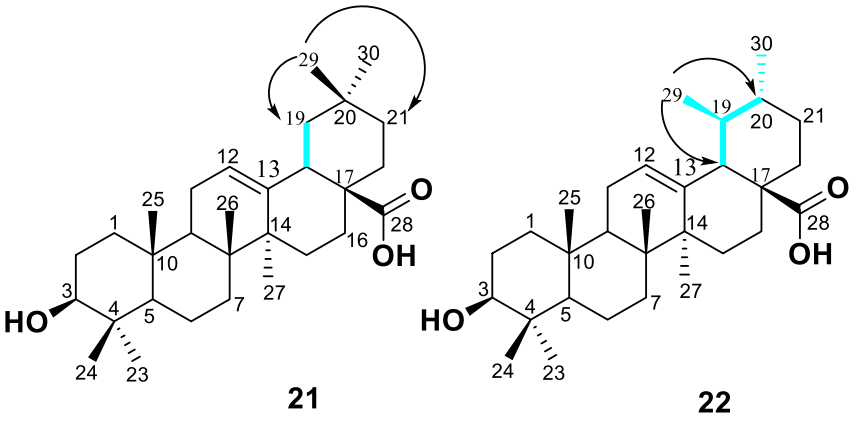

Fig. 5.23: Selected HMBC (black) and COSY (blue) correlations of compounds **21** and **22**

Table 5.11: ^{1}H and ^{13}C-NMR spectroscopic data (pyridine-d_5, 400 MHz) for compounds **21** and **22**

	Compound 21 (Oleanolic acid)					Compound 22 (Ursolic acid)			
#	δ_C[↓], type		δ_H[↓] (*J* in Hz)		HMBC	δ_C[↓], type		δ_H[↓] (*J* in Hz)	
1	38.7, CH_2	39.0[↓], CH_2	1.55 and 0.98, *m*	1.57[↓] and 1.02[↓]		38.8, CH_2	39.2[↓], CH_2	1.53 and 0.93, *m*	1.58[↓] and 1.00[↓]
2	27.8[a], CH_2	28.1[↓], CH_2	1.82[a], *m*	1.82[↓]		27.8[a], CH_2	28.2[↓], CH_2	1.82[a], *m*	1.81[↓]
3	77.8, CH	78.2[↓], CH	3.44[a], *m*	3.44[↓], *dd*	C-4[b/c], C-23[b/c], C-24[b/c]	77.9, CH	78.2[↓], CH	3.44[a], *m*	3.44[↓], *dd*
4	39.1[a], C	39.4[↓], C	-	-	-	39.1[a], C	39.6[↓], C	-	-
5	55.6[a], CH	55.9[↓], CH	0.85[a], *m*	0.88[↓], *d*	C-4[b/c], C-10[b/c]	55.6[a], CH	55.9[↓], CH	0.85[a], *m*	0.88[↓], *d*
6	18.5[a], CH_2	18.8[↓], CH_2	1.55[a] and 1.37[a], *m*	1.58[↓] and 1.39[↓]		18.5[a], CH_2	18.8[↓], CH_2	1.55[a] and 1.37[a], *m*	1.58[↓] and 1.39[↓]
7	33.0[a], CH_2	33.4[↓], CH_2	1.52 and 1.37	1.53[↓] and 1.36[↓]		33.3, CH_2	33.7[↓], CH_2	1.55 and 1.34, *m*	1.59[↓] and 1.39[↓]
8	39.5, C	39.8[↓], C	-	-	-	39.7, C	40.1[↓], C	-	-
9	47.9, CH	48.2[↓], CH	1.68, *m*	1.71[↓]	C-5[b/c], C-14[b/c], C-10[b/c], C-11[b/c], C-26[b/c], C-25[b/c]	47.8[a], CH	48.1[↓], CH	1.62, *m*	1.62[↓]
10	37.1, C	37.4[↓], C	-	-	-	37.0, C	37.5[↓], C	-	-
11	23.5, CH_2	23.8[↓], CH_2	1.94[a], *m*	1.96[↓]		23.4[a], CH_2	23.7[↓], CH_2	1.94[a], *m*	1.96[↓]
12	122.3, CH	122.6[↓], CH	5.48[a], *brd* (2.7)	5.49[↓], *s*	C-9[b/c], C-14[b/c], C-11[b/c]	125.4, CH	125.7[↓], CH	5.48[a], *brd* (2.7)	5.49[↓], *s*
13	144.6, C	144.8[↓], C	-	-	-	139.0, C	139.3[↓], C	-	-
14	41.9, C	42.2[↓], C	-	-	-	42.2, C	42.6[↓], C	-	-
15	28.0, CH_2	28.4[↓], CH_2	2.14[a] and 1.14, *m*	2.19[↓] and 1.22[↓]		28.4, CH_2	28.8[↓], CH_2	2.32 and 1.18, *m*	2.33[↓] and 1.22[↓]
16	23.4[a], CH_2	23.8[↓], CH_2	2.14[a] and 1.94, *m*	2.12[↓] and 1.96[↓]		24.6, CH_2	25.0[↓], CH_2	2.12 and 2.00, *m*	2.14[↓] and 2.01[↓]
17	46.4, C	46.7[↓], C	-	-	-	47.8[a], C	48.1[↓], C	-	-

18	41.7, CH	42.1[ǂ], CH	3.29, *dd* (3.9, 13.7)	3.30[ǂ]	C-16[b/c], C-17[b/c], C-12[b/c], C-13[b/c], C-14[b/c], C-28[c], C-19[b/c]	53.3, CH	53.6[ǂ], CH	2.62, *d* (11.3)	2.63[ǂ]
19	46.2, CH_2	46.6[ǂ], CH_2	1.80 and 1.29, *m*	1.83[ǂ] and 1.32[ǂ]	C-13[c], C-18[c], C-20[c]	39.2 CH	39.5[ǂ], CH	1.47, *m*	1.49[ǂ]
20	30.7, C	31.0[ǂ], C	-	-		39.1[a], CH	39.4[ǂ], CH	1.02, *m*	1.05[ǂ]
21	34.0, CH_2	34.3[ǂ], CH_2	1.44 and 1.20, *m*	1.46[ǂ] and 1.23[ǂ]		30.8, CH_2	31.1[ǂ], CH_2	1.45 and 1.40, *m*	1.49[ǂ] and 1.40[ǂ]
22	32.9, CH_2	33.2[ǂ], CH_2	2.03 and 1.83, *m*	2.04[ǂ] and 1.82[ǂ]		37.2, CH_2	37.4[ǂ], CH_2	1.96 and 1.33, *m*	1.97[ǂ]
23	28.5[a], CH_3	28.8[ǂ], CH_3	1.23[a], *s*	1.24[ǂ], *s*	C-3[b/c], C-5[b/c], C-4[b/c], C-24[b/c]	28.5[a], CH_3	28.8[ǂ], CH_3	1.23[a], *s*	1.24[ǂ], *s*
24	16.3[a], CH_3	16.5[ǂ], CH_3	1.01[a], *s*	1.02[ǂ], *s*	C-3[b/c], C-5[b/c], C-4[b/c], C-23[b/c]	16.3[a], CH_3	16.5[ǂ], CH_3	1.01[a], *s*	1.02[ǂ], *s*
25	15.3, CH_3	15.6[ǂ], CH_3	0.88[a], *s*	0.93[ǂ], *s*	C-10[b/c], C-1[b/c], C-9[b/c], C-5[b/c]	15.4, CH_3	15.7[ǂ], CH_3	0.88[a], *s*	0.92[ǂ], *s*
26	17.2[a], CH_3	17.5[ǂ], CH_3	1.04, *s*	1.04[ǂ], *s*	C-9[b], C-14[b/c], C-7[b/c]	17.3, CH_3	17.5[ǂ], CH_3	1.00[a], *s*	1.06[ǂ], *s*
27	25.9, CH_3	26.2[ǂ], CH_3	1.27, *s*	1.30[ǂ], *s*	C-13[b/c], C-14[b/c], C-8[b], C-15[b/c]	23.7, CH_3	24.0[ǂ], CH_3	1.22, *s*	1.24[ǂ], *s*
28	179.9, C	180.0[ǂ], C	-	-	-	179.6, C	179.7[ǂ], C	-	-
29	33.0[a], CH_3	33.4[ǂ], CH_3	0.94, *s*	0.97[ǂ], *s*	C-30[b], C-20[b], C-21[b], C-19[b], C-18[c]	17.2[a], CH_3	17.5[ǂ], CH_3	0.99, *brd* (5.3)	1.02[ǂ], *s*
30	23.5, CH_3	23.8[ǂ], CH_3	1.00[a], *s*	1.02[ǂ], *s*	C-19[b/c], C-29[b], C-20[c]	21.1, CH_3	21.4[ǂ], CH_3	0.95, *d*	0.97[ǂ], *s*

[a] -Overlapping signals. [b] -HMBC correlations for oleanolic acid. [c] -HMBC correlations for ursolic acid. [ǂ] -Literature data (Seebacher et al., 2003; pyridine-d_5, 600 MHz).

Ursolic and oleanolic acid are frequent triterpenoids that have been reported from various plant sources: *Olea europaea* (Simonsen, 1947), *Helichrysum stoechas* (de Quesada, Rodriguez and Valverde, 1972), *Clerodendranthus spicatus* (Yoshimura et al., 2003), *Helichrysum picardii* (Santos Rosa et al., 2007), *Silphium trifoliatum* (Kowalski, 2007), *Prunus padus* (Magiera et al., 2019). Though in plants their primary function is to prevent water loss and fend off attacks from pathogens (Szakiel et al., 2003), they have been shown in *in vitro* and *in vivo* models to exert numerous biological properties, including antidiabetic activity via the inhibition of the α-glucosidase enzyme (Ding et al., 2018), and insulin utilization (Castellano et al., 2013), among others. Their synthetic pathway is believed to take place via the mevalonate pathway involving the cyclization of 2,3-oxidosqualene (by oxidosqualene cyclases β/α-amyrin synthase) to β-amyrin (for oleanolic acid) or α-amyrin (for ursolic acid) which is then oxidized in sequential three-step oxidation at the C-28 position by a single cytochrome P450 enzyme to yield oleanolic acid through erythrodiol or ursolic acid through uvaol (Huang et al., 2012; Thimmappa et al., 2014).

5.7.2. Biological Evaluation of the Isolated Compounds

i. α-Glucosidase and α-amylase assays

The α-glucosidase and α-amylase assays were carried out as outlined in chapter 2. From the results, it was found that only the aqueous extract including an inseparable mixture of compounds 21 and 22 showed inhibition activity of 35.2 and 27.7 %, respectively, that was comparable to acarbose (positive control) in the α-glucosidase assay (Table 5.12). This is the first report of the antidiabetic evaluation of *H. splendidum* and therefore, further studies are needed to validate its antidiabetic potential.

Table 5.12: α-Amylase and α-glucosidase enzymes inhibition of compounds and extracts from *H. splendidum*

	Percentage Inhibition (%) at 200 µg/mL	
	α-amylase	α-glucosidase
Compounds 21 & 22	27.4	27.7
Compound 20	13.6	*
Compounds 12 & 13	12.4	*
Compounds 14 & 15	*	*
Compound 17	*	*
Compound 16	*	*

Compound 19	*	21.7
Compound 18	*	11.4
Aqueous Extract	*	**35.2**
DCM Extract	*	*
EtOAc Extract	*	12.7
BuOH Extract	*	*
Acarbose**	**99.5**	**38,2**

*Not active. **Control.

ii. Cell viability assay (MTT) - MDA-MB-231 cells

Cell viability assay was carried out as outlined in chapter 2. This technique is a valuable method of monitoring not only the effects of compounds in cell function but also measuring receptor binding and a variety of signal transduction events that may involve the expression of genetic reporters associated with disease such as diabetes (Riss et al., 2016). Compounds were initially screened for activity prior to more in depth testing. To achieve this, cells were exposed to 0.1, 10, and 100 µg/mL of each compound over 24 hours, and the MTT assay performed (Fig. 5.24). Codes used to denote each compound, for the purpose of activity screening, are shown in Table 5.13.

Table 5.13: Isolated compounds (and their designated codes) used for activity screening

Designated code	Compound
B1	16
B2	12 and 13 (mixture)
B3	20
B4	17
B5	19
B6	18
B7	21 and 22 (mixture)
B8	14 and 15 (mixture)

Following 24 hours of exposure, the greatest reduction in MDA-MB-231 cell viability was observed at 100 µg/mL of five compounds, namely **16**, **17**, **19**, including the inseparable mixtures of **14** and **15**, as well as **21** and **22**. These compounds were subsequently selected for further testing.

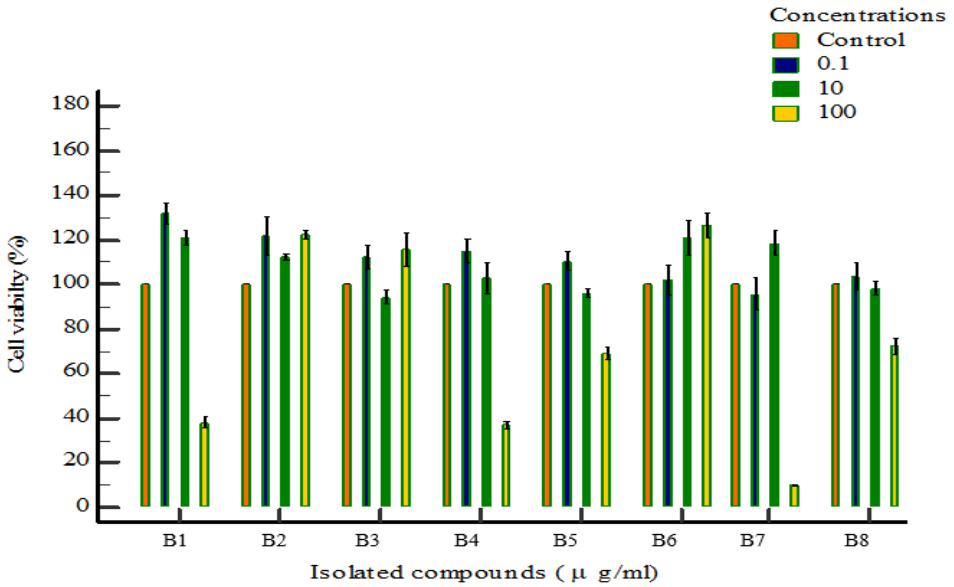

Fig. 5.24: Compound activity screening in MDA-MB-231 cells, as determined by the MTT assay over 24-hours of exposure to isolated compounds (B1-B-8)

Compounds 21 and 22 (mixture). Following 24-hours (Fig. 5.25) and 72-hours (Fig. 5.26) of exposure to the isolated compounds, the MTT assay was performed. Over 24-hours, the compound yielded significant ($P<0.0001$) reductions in cell viability at each respective concentration. Furthermore, the repeated-measured ANOVA yielded significant ($P<0.0001$) negative linear trend between control and 100 µg/mL, and one-way ANOVA revealed a similar significant ($P<0.001$) trend. Following 72-hours of exposure, the compound yielded further significant ($P<0.0001$) reductions in cell viability at 12.5, 25, 50, and 100 µg/mL, respectively. Repeated-measure ANOVA revealed a significant ($P<0.0001$) negative linear trend between the control and highest concentration. One-way ANOVA yielded a similar significant ($P<0.001$) trend between control and 100 µg/mL. The calculated IC_{50} values were recorded in Table 5.14.

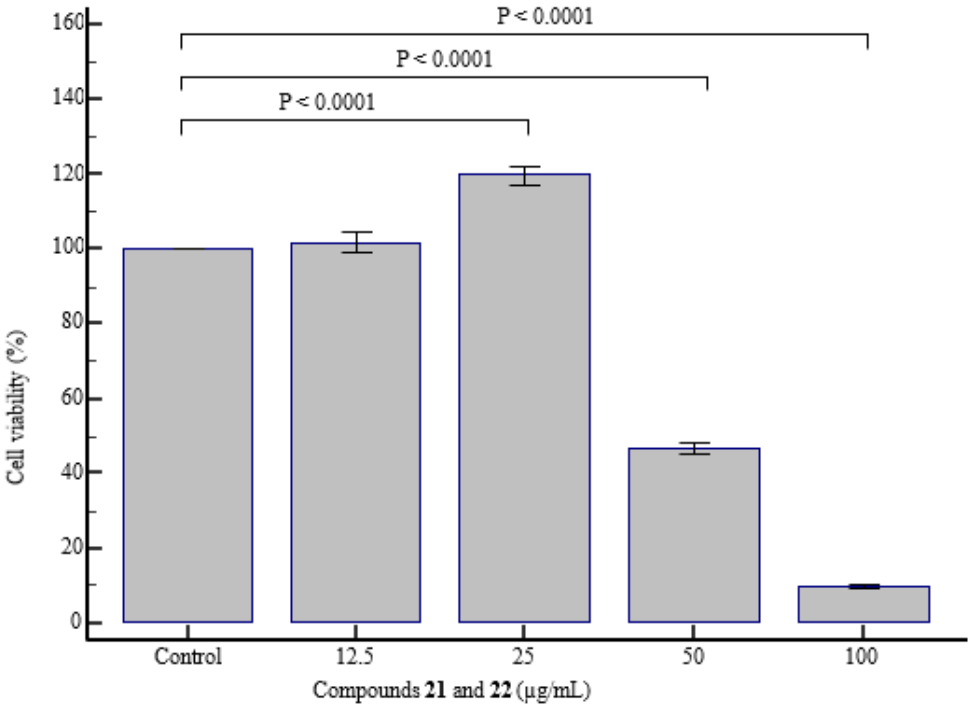

Fig. 5.25: MDA-MB-231 cell viability as determined by the MTT assay over 24-hours of exposure to the isolated compounds **21** and **22** (mixture)

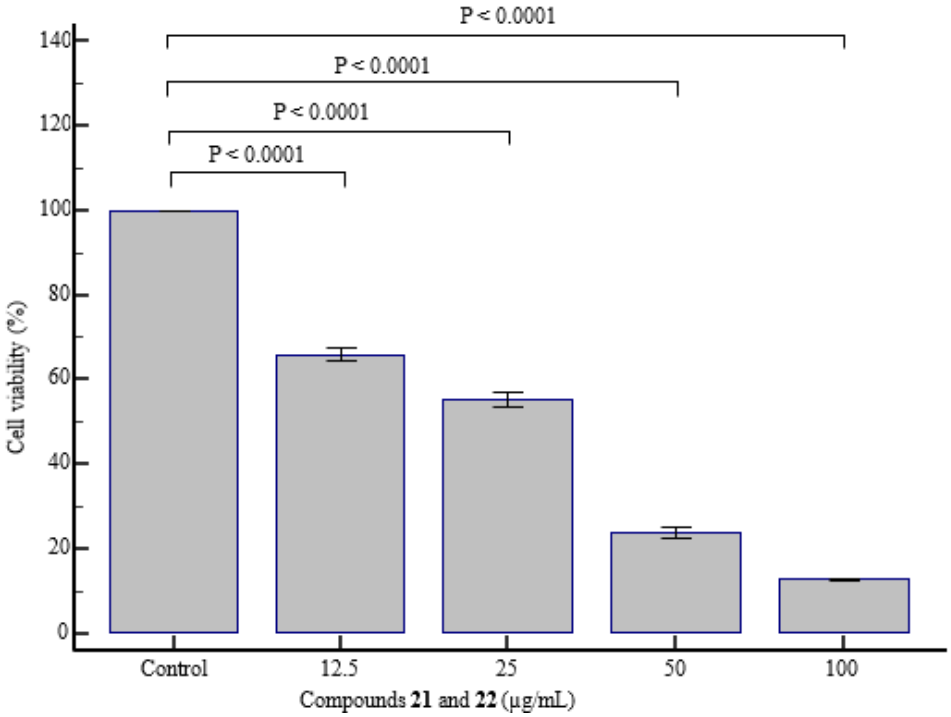

Fig. 5.26: MDA-MB-231 cell viability as determined by the MTT assay over 72-hours of exposure to the isolated compounds **21** and **22** (mixture)

Compound 17. Following 24-hours (Fig. 5.27) and 72-hours (Fig. 5.28) of exposure to the isolated compound **17**, the MTT assay was performed. Over 24-hours, the compound yielded significant reductions (P=0.0010) and (P<0.0001) in cell viability at 12.5 µg/mL and between 25–100 µg/mL, respectively. Moreover, the repeated-measures ANOVA yielded significant (P<0.0001) negative linear trend between control and 100 µg/mL. One-way ANOVA revealed a similar significant (P<0.001) trend. Following 72-hours of exposure, dose-dependent reductions in cell viability were observed at each concentration, being significant (P<0.0001) at 12.5, 25, 50, and 100 µg/mL, respectively. Repeated-measure ANOVA revealed a significant (P<0.0001) negative linear trend between the control and highest concentration. Similarly, one-way ANOVA yielded a significant (P<0.001) trend between control and 100 µg/mL. The calculated IC_{50} values were recorded in Table 5.14.

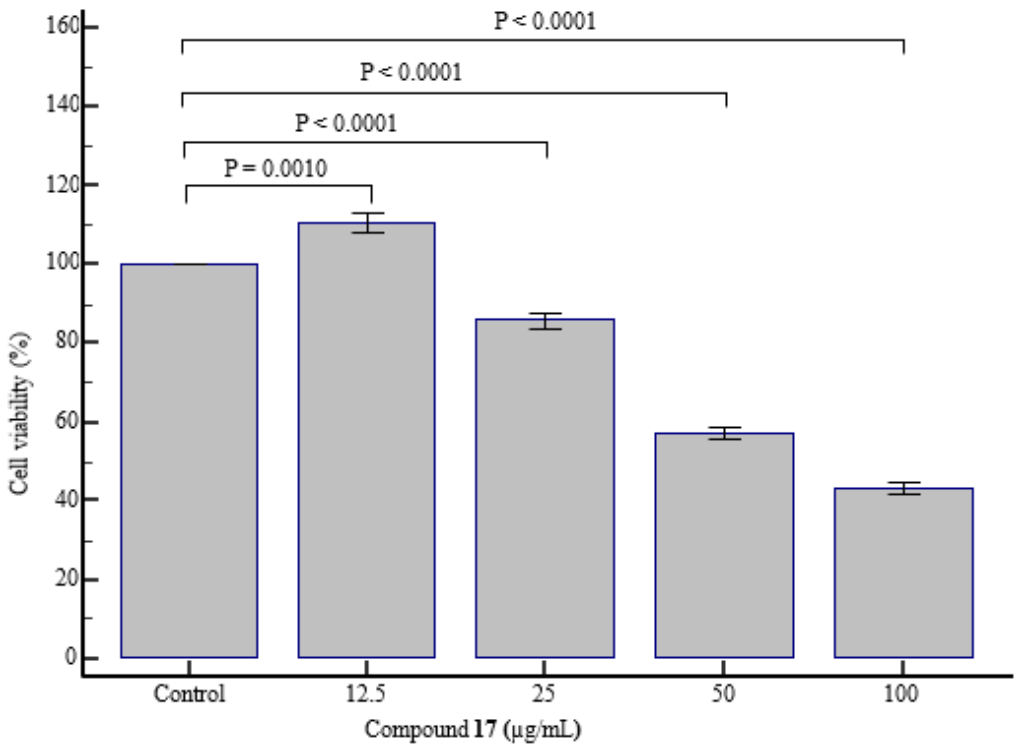

Fig. 5.27: MDA-MB-231 cell viability as determined by the MTT assay over 24-hours of exposure to the isolated compound **17**

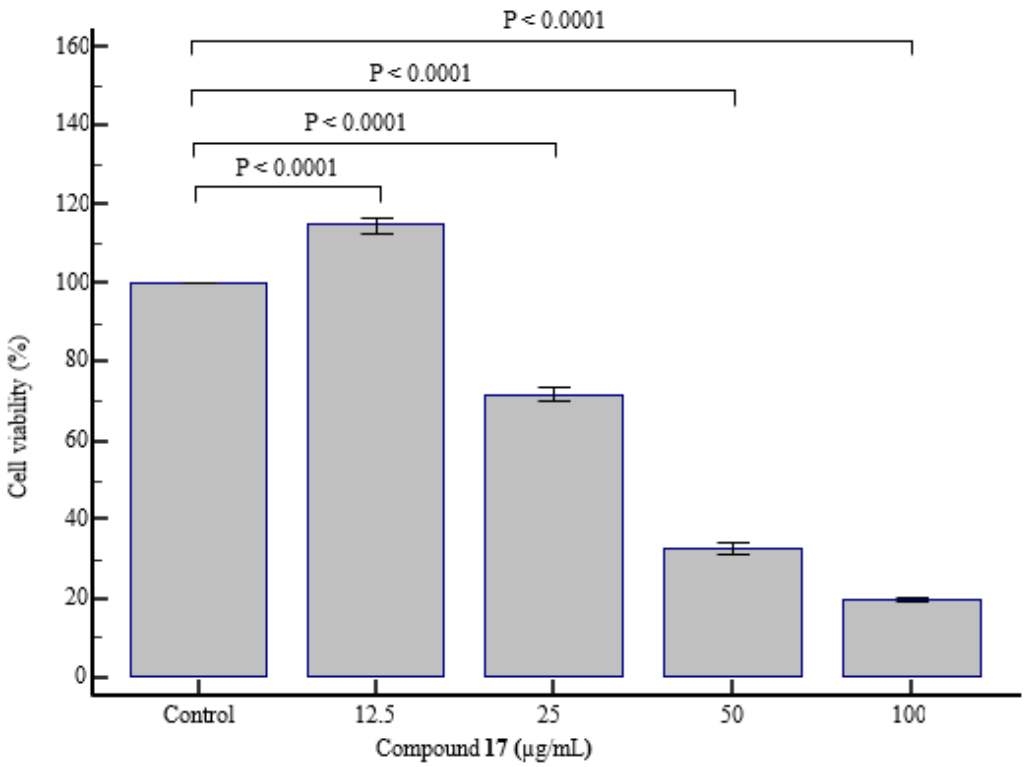

Fig. 5.28: MDA-MB-231 cell viability as determined by the MTT assay over 72-hours of exposure to the isolated compound **17**

Compound 16. Following 24-hours (Fig. 5.29) and 72-hours (Fig. 5.30) of exposure to the isolated compound **16**, the MTT assay was performed. Over 24-hours, the compound yielded significant (P=0.0002) reductions in cell viability between 12.5 and 100 µg/mL, respectively. Furthermore, the Friedman test yielded significant (P <0.00001) trend between control and 100 µg/mL, and the Kruskal-Wallis test revealed a similar significant (P=0.000001) trend. Following 72-hours of exposure, the compound revealed dose-dependent reductions in cell viability at each concentration used, being significant (P=0.0002) at 50 and 100 µg/mL. Repeated-measure ANOVA revealed a significant (P<0.0001) negative linear trend between the control and highest concentration. Similarly, one-way ANOVA yielded a significant (P<0.001) trend between control and 100 µg/mL. The calculated IC_{50} values were recorded in Table 5.14.

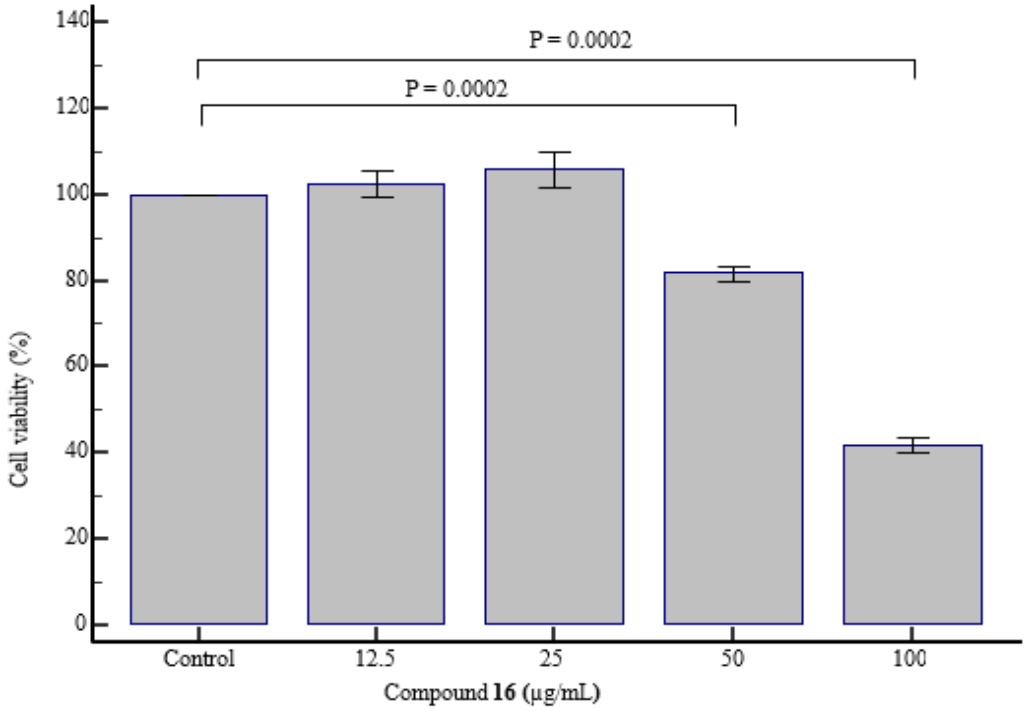

Fig. 5.29: MDA-MB-231 cell viability as determined by the MTT assay over 24-hours of exposure to the isolated compound **16**

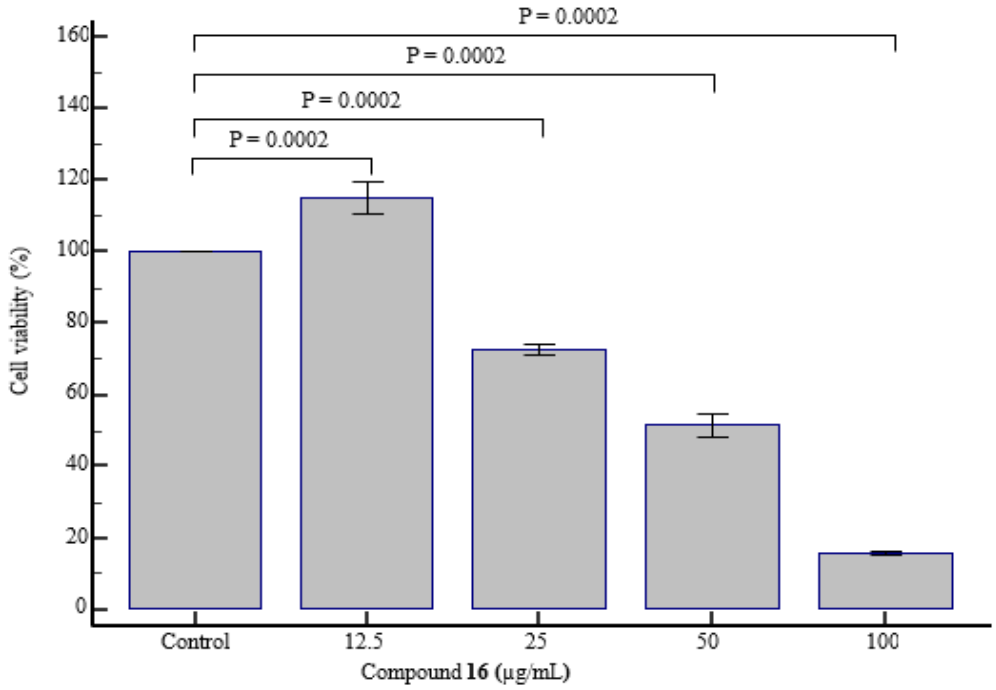

Fig. 5.30: MDA-MB-231 cell viability as determined by the MTT assay over 72-hours of exposure to the isolated compound **16**

Compound 19. Following 24-hours (Fig. 5.31) and 72-hours (Fig. 5.32) of exposure to the isolated compound **19**, the MTT assay was performed. Over 24-hours, significant (P<0.0001) reductions in cell viability were observed at 12.5, 25, 50 and 100 µg/mL, respectively. Further analysis using the repeated-measures ANOVA revealed a significant (P<0.0001) negative linear trend between control and 100 µg/mL. One-way ANOVA revealed a similar significant (P<0.001) trend. Following 72-hours of exposure, the compound revealed comparable reductions in cell viability at each concentration, exhibiting significant (P=0.0002) reductions in cell viability at 12.5, 25, 50 and 100 µg/mL, respectively. The Friedman test revealed a significant (P<0.00001) trend between the control and highest concentration, and similarly analysis using the Kruskal-Wallis test yielded a significant (P=0.000017) trend between control and 100 µg/mL. The calculated IC_{50} values were recorded in Table 5.14.

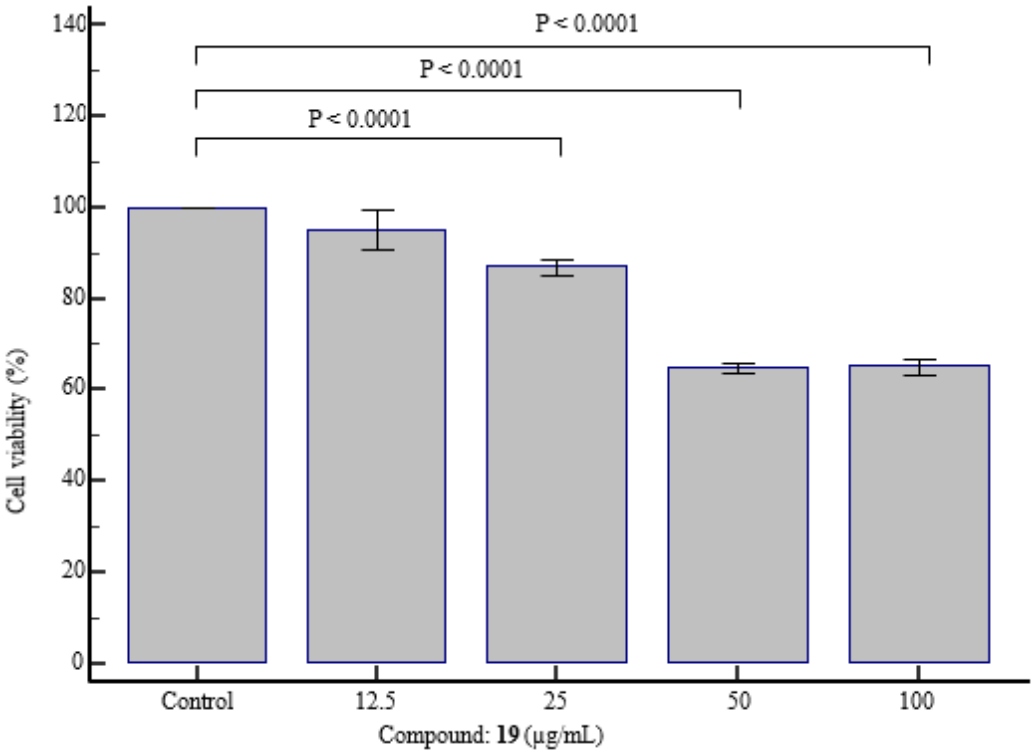

Fig. 5.31: MDA-MB-231 cell viability as determined by the MTT assay over 24-hours of exposure to the isolated compound **19**

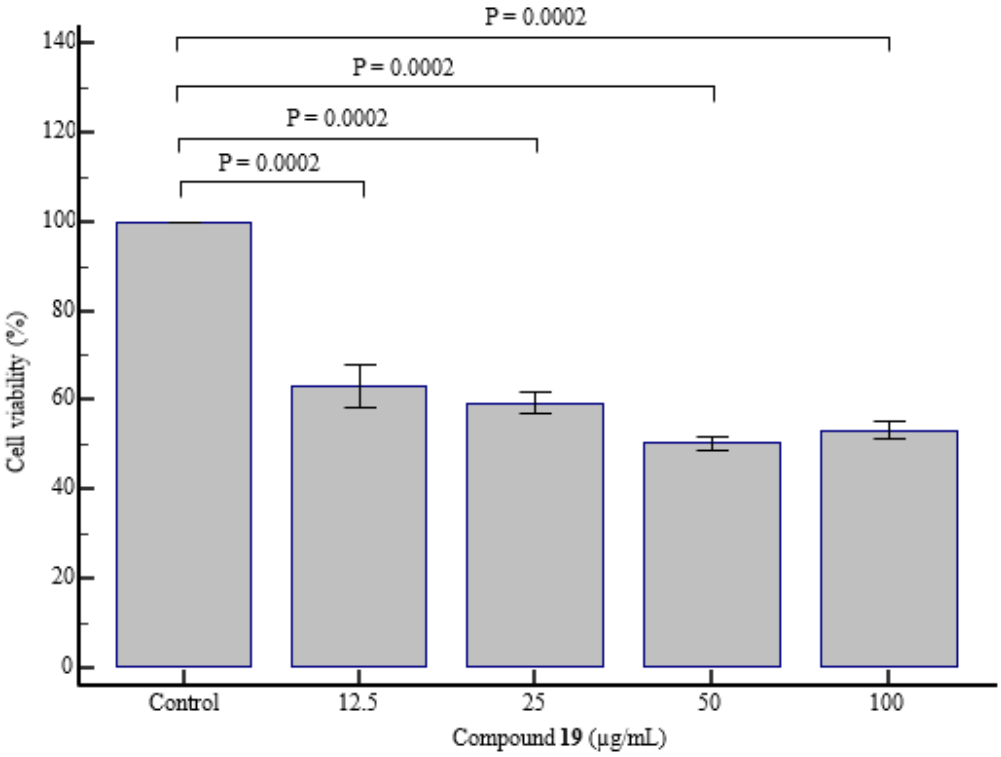

Fig. 5.32: MDA-MB-231 cell viability as determined by the MTT assay over 72-hours of exposure to the isolated compound **19**

Compounds 14 and 15 (mixture). Following 24-hours (Fig. 5.34) and 72-hours (Fig. 5.35) of exposure to the isolated compounds, the MTT assay was performed. Over 24-hours, the compound yielded significant (P=0.0002) reductions in cell viability at 12.5, 25, 50 and 100 µg/mL, respectively. Analysis using the Friedman test revealed a significant (P=0.00001) trend between control and 100 µg/mL, similarly the Kruskal-Wallis test yielded a similar significant (P=0.000069) trend. Following 72-hours of exposure significant (P<0.0001) reductions in cell viability were observed at 12.5, 25, 50, and 100 µg/mL, respectively. Repeated-measure ANOVA revealed a significant (P<0.0001) negative linear trend between the control and highest concentration. Similarly, one-way ANOVA yielded a significant (P<0.001) trend between control and 100 µg/mL. The calculated IC_{50} values were recorded in Table 5.14.

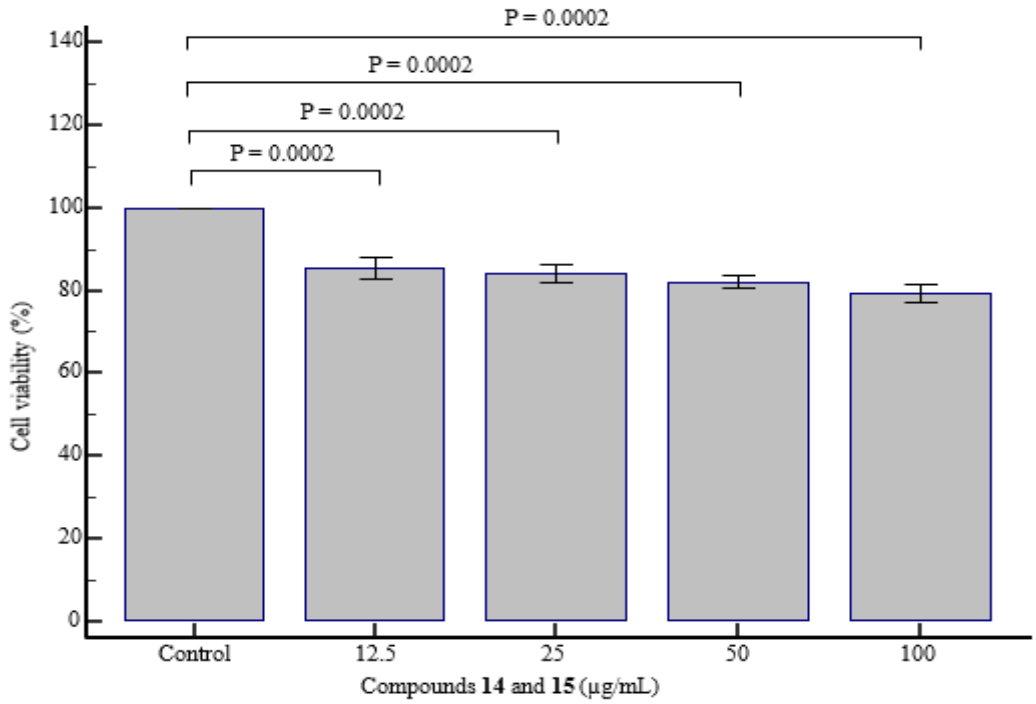

Fig. 5.34: MDA-MB-231 cell viability as determined by the MTT assay over 24-hours of exposure to the isolated compounds **14** and **15** (mixture)

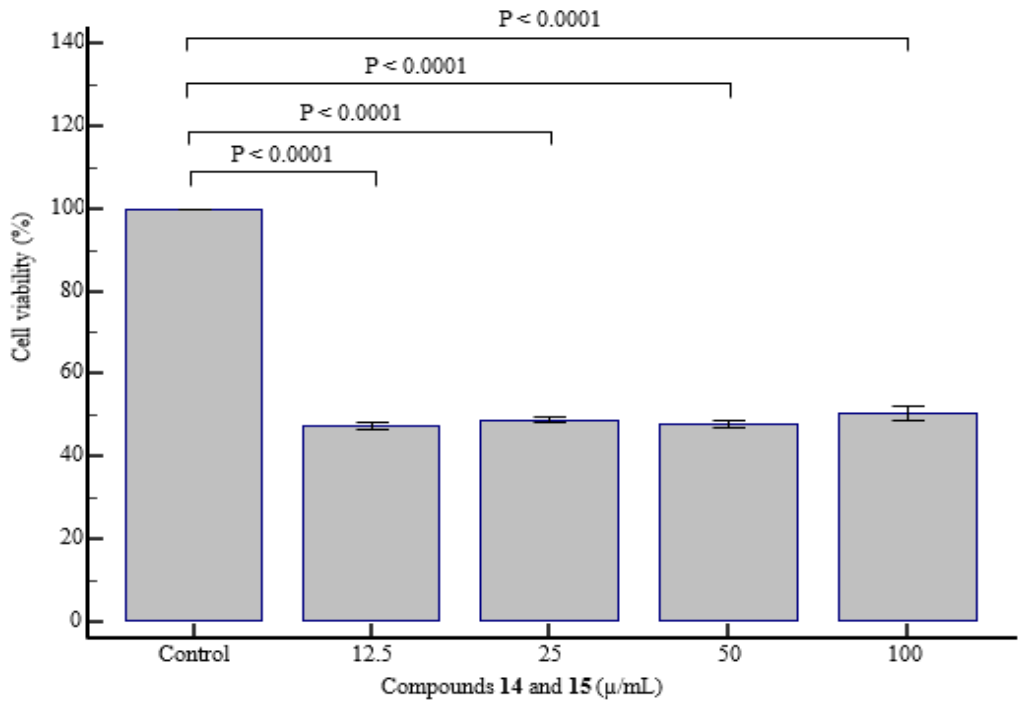

Fig. 5.35: MDA-MB-231 cell viability as determined by the MTT assay over 72-hours of exposure to the isolated compounds **14** and **15** (mixture)

Table 5.14: Calculated IC_{50} values over 24 and 72 hours for the isolated compounds

	IC_{50} (µg/mL)	
Compound(s)	**24-hours exposure**	**72-hours exposure**
14 and **15**	2439	38.04
16	88.44	48.79
17	74.00	40.27
19	160.3	67.83
21 and **22**	49.77	24.05

R-squared values:
-Compounds **14** and **15**, 0.7463 (24 hours exposure) and 0.6935 (72 hours exposure)
-Compounds **16**, 0.9209 (24 hours exposure) and 0.9223 (72 hours exposure)
-Compounds **17**, 0.8822 (24 hours exposure) and 0.9159 (72 hours exposure)
-Compound **19**, 0.8274 (24 hours exposure) and 0.8097 (72 hours exposure)
-Compounds **21** and **22**, 0.9414 (24 hours exposure) and 0.9799 (72 hours exposure)

5.7.3. Conclusion

This study successfully reported the isolation and characterization of 11 compounds from the leaves of *Helichrysum splendidum* (some of which were obtained as inseparable mixtures). Among the list, compounds **18**, **19**, **20**, **21**, and **22** are reported for the first time from the plant. In addition, compound **15** (given the trivial name iso-lemmonin C) was tentatively proposed as a new stereoisomer of lemmonin C based on 1D and 2D NMR experiments which showed distinguishable peaks (δ_C 84.0 assigned C-8 in compound 15, while this appeared 82.8 for lemmnonin C). Further purification, however, using HPLC, chemical reactions such as acetylation or methylation, including X-ray crystallography studies will need to be done to confirm the proposed structure. Similarly, chemical derivatization (acetylation or methylation) followed by purification (open column silica gel chromatography) of compound **18**, which we have proposed as a biflavonoid, needs to be explored to unambiguously confirm its structure. Furthermore, this study has also provided for the first time the ^{13}C NMR for compounds **12** and **13** isomers. The antidiabetic activity of the isolated compounds and extracts was explored to establish their mechanism of action towards diabetes. However, none of them showed any significant inhibition activity in α-glucosidase and α-amylase enzyme assays. More studies would need to be done, particularly for the aqueous extract since it displayed comparable results (35.2 %) to acarbose (38,2 %), control, at the screening concentration (200 µg/mL). On the other hand, upon evaluating the cytotoxicity effects of the isolated compounds

from this plant against MDA-MB-231 cells, it was established that only **16**, **17**, **19**, including the inseparable mixtures of **14** and **15**, as well as **21** and **22**, showed significant activity. In fact, compounds **21** and **22** (identified to be a mixture of ursolic and oleanolic acid) displayed a significant ($P<0.001$) trend between control and 100 µg/mL, followed, respectively, by compounds **17**, and **16**. The IC_{50} values of the compounds (**21** and **22**, **16**, **17**, **19**, as well as **14** and **15**), respectively, were found to be 24.05, 38.04, 40.27, 48.79, and 67.83 µg/mL. We recommend further studies using more cell lines to determine the primary mechanism of cytotoxicity of the compounds.

References

Abraham, R.J., Byrne, J.J., Griffiths, L. and Koniotou, R., 2005. ^{1}H chemical shifts in NMR: Part 22—Prediction of the ^{1}H chemical shifts of alcohols, diols and inositols in solution, a conformational and solvation investigation. *Magnetic Resonance in Chemistry*, *43*(8), pp.611-624.

Ahmed, A.A., Mohamed, A.Y., Spring, O., Bierner, M.W. and Mabry, T.J., 2002. Sesquiterpene lactones and flavonoids from *Hymenoxys jamesii* (Asteraceae) and their systematic significance. *Biochemical systematics and ecology*, *5*(30), pp.487-491.

Akimanya, A., Midiwo, J.O., Matasyoh, J., Okanga, F., Masila, V.M., Walker, L., Tekwani, B.L., Muhammad, I. and Omosa, L.K., 2015. Two polymethoxylated flavonoids with antioxidant activities and a rearranged clerodane diterpenoid from the leaf exudates of *Microglossa pyrifolia*. *Phytochemistry Letters*, *11*, pp.183-187.

Al-Ja'fari, A.H., Vila, R., Freixa, B., Tomi, F., Casanova, J., Costa, J. and Cañigueral, S., 2011. Composition and antifungal activity of the essential oil from the rhizome and roots of *Ferula hermonis*. *Phytochemistry*, *72*(11-12), pp.1406-1413.

Angyal, S.J. and Odier, L., 1983. Selective deuteration. The rate of protium-deuterium exchange in inositols with Raney-nickel catalyst, and the effect thereon of O-methylation. *Carbohydrate research*, *123*(1), pp.13-22.

Bailey, K. and Butterfield, A.G., 1981. Structure of condensation products between isonicotinylhydrazine and reducing sugars by ^{13}C NMR spectroscopy. *Canadian Journal of Chemistry*, *59*(3), pp.641-646.

Blay, G., Bargues, V., Cardona, L., Collado, A.M., García, B., Muñoz, M.C. and Pedro, J.R., 2000. Stereoselective synthesis of 4α-Hydroxy-8, 12-guaianolides from santonin. *The Journal of organic chemistry*, *65*(7), pp.2138-2144.

Bohlmann, F., Zdero, C. and Ahmed, M., 1982. New sesquiterpene lactones, geranyllinalol derivatives and other constituents from *Geigeria* species. *Phytochemistry*, *21*(7), pp.1679-1691.

Bohlmann, **F. and Suwita, A., 1979**. Ein neues Guajanolid und ein Secoguajanolid aus *Helichrysum splendidum*. *Phytochemistry*.

Bubb, W.A., 2003. NMR spectroscopy in the study of carbohydrates: Characterizing the structural complexity. *Concepts in Magnetic Resonance Part A: An Educational Journal*, *19*(1), pp.1-19.

Casiglia, S., Bruno, M., Bramucci, M., Quassinti, L., Lupidi, G., Fiorini, D. and Maggi, F., 2017. Kundmannia sicula (L.) DC: a rich source of germacrene D. *Journal of Essential Oil Research*, *29*(6), pp.437-442.

Castellano, J.M., Guinda, A., Delgado, T., Rada, M. and Cayuela, J.A., 2013. Biochemical basis of the antidiabetic activity of oleanolic acid and related pentacyclic triterpenes. *Diabetes*, *62*(6), pp.1791-1799.

Chagonda, L.S., Makanda, C. and Chalchat, J.C., 1999. Essential Oils of Four Wild and Semi-Wild Plants from Zimbabwe: *Colospermum mopane* (Kirk ex Benth.) Kirk ex Leonard, *Helichrysum splendidum* (Thunb.) Less, *Myrothamnus flabellifolia* (Welw.) and *Tagetes minuta* L. *Journal of Essential Oil Research*, *11*(5), pp.573-578.

Chang, H.T., Cheng, Y.H., Wu, C.L., Chang, S.T., Chang, T.T. and Su, Y.C., 2008. Antifungal activity of essential oil and its constituents from *Calocedrus macrolepis* var. formosana Florin leaf against plant pathogenic fungi. *Bioresource technology*, *99*(14), pp.6266-6270.

Cheng, X., Zeng, Q., Ren, J., Qin, J., Zhang, S., Shen, Y., Zhu, J., Zhang, F., Chang, R., Zhu, Y. and Zhang, W., 2011. Sesquiterpene lactones from *Inula falconeri*, a plant endemic to the Himalayas, as potential anti-inflammatory agents. *European journal of medicinal chemistry*, *46*(11), pp.5408-5415.

Cheng, X.R., Li, W.W., Ren, J., Zeng, Q., Zhang, S.D., Shen, Y.H., Yan, S.K., Ye, J., Jin, H.Z. and Zhang, W.D., 2012. Sesquiterpene lactones from *Inula hookeri*. *Planta medica*, *78*(05), pp.465-471.

Cheng, X.R., Ye, J., Ren, J., Zeng, Q., Zhang, F., Qin, J.J., Shen, Y.H., Zhang, W.D. and Jin, H.Z., 2012. Terpenoids from *Inula sericophylla* Franch. and their chemotaxonomic significance. *Biochemical systematics and ecology*, *42*, pp.75-78.

Conforti, F., Statti, G., Loizzo, M.R., Sacchetti, G., Poli, F. and Menichini, F., 2005. In vitro antioxidant effect and inhibition of α-amylase of two varieties of *Amaranthus caudatus* seeds. *Biological and pharmaceutical bulletin*, *28*(6), pp.1098-1102.

do Nascimento, K.F., Moreira, F.M.F., Santos, J.A., Kassuya, C.A.L., Croda, J.H.R., Cardoso, C.A.L., do Carmo Vieira, M., Ruiz, A.L.T.G., Foglio, M.A., de Carvalho, J.E. and Formagio, A.S.N., 2018. Antioxidant, anti-inflammatory, antiproliferative and antimycobacterial activities of the essential oil of *Psidium guineense* Sw. and spathulenol. *Journal of ethnopharmacology*, *210*, pp.351-358.

De Almeida, M.V., Couri, M.R.C., De Assis, J.V., Anconi, C.P., Dos Santos, H.F. and De Almeida, W.B., 2012. ^{1}H NMR analysis of O-methyl-inositol isomers: a joint experimental and theoretical study. *Magnetic Resonance in Chemistry*, *50*(9), pp.608-614.

De Olinda, T.M., Lemos, T.L.G., Machado, L.L., Rao, V.S. and Santos, F.A., 2008. Quebrachitol-induced gastroprotection against acute gastric lesions: Role of prostaglandins, nitric oxide and K+ ATP channels. *Phytomedicine*, *15*(5), pp.327-333.

de Quesada, T.G., Rodriguez, B. and Valverde, S., 1972. The constituents of *Helichrysum stoechas*. *Phytochemistry*, *11*(1), pp.446-449.

Díaz, M., González, A., Castro-Gamboa, I., Gonzalez, D. and Rossini, C., 2008. First record of L-quebrachitol in *Allophylus edulis* (Sapindaceae). *Carbohydrate research*, *343*(15), pp.2699-2700.

Ding, H., Hu, X., Xu, X., Zhang, G. and Gong, D., 2018. Inhibitory mechanism of two allosteric inhibitors, oleanolic acid and ursolic acid on α-glucosidase. *International journal of biological macromolecules*, *107*, pp.1844-1855.

Fokialakis, N., Cantrell, C.L., Duke, S.O., Skaltsounis, A.L. and Wedge, D.E., 2006. Antifungal activity of thiophenes from *Echinops ritro*. *Journal of agricultural and food chemistry*, *54*(5), pp.1651-1655.

Gao, F., Wang, H. and Mabry, T.J., 1990. Sesquiterpene lactone aglycones and glycosides from *Hymenoxys lemmonii*. *Phytochemistry*, *29*(5), pp.1601-1607.

Govindarajan, M. and Benelli, G., 2016. Eco-friendly larvicides from Indian plants: effectiveness of lavandulyl acetate and bicyclogermacrene on malaria, dengue, and Japanese encephalitis mosquito vectors. *Ecotoxicology and Environmental Safety*, *133*, pp.395-402.

Guerrini, A., Sacchetti, G., Grandini, A., Spagnoletti, A., Asanza, M. and Scalvenzi, L., 2016. Cytotoxic effect and TLC bioautography-guided approach to detect health properties of amazonian *Hedyosmum sprucei* essential oil. *Evidence-Based Complementary and Alternative Medicine*, *2016*.

Hada, T., Shiraishi, A., Furuse, S., Inoue, Y., Hamashima, H., Matsumoto, Y., Masuda, K., Shiojima, K. and Shimada, J., 2003. Inhibitory effects of terpenes on the growth of *Staphylococcus aureus*. *Natural medicines 57*(2), pp.64-67.

Hilliard, O.M., 1983. Asteraceae. In: Leistner, O.A. (Ed.), Flora of Southern Africa, vol.33, part 7 (Inuleae). Botanical Research Institute of South Africa, Pretoria, pp.7,2:61–7,2:317.

Ho, C.L., Liao, P.C., Wang, E.I.C. and Su, Y.C., 2011. Composition and antifungal activities of the leaf essential oil of *Neolitsea parvigemma* from Taiwan. *Natural product communications*, *6*(9), p.1934578X1100600935.

Huang, H.Q., Yan, M.N., Piao, X.L. And Cui, J., 2011. Chemical constituents from *Inula helianthus-aquatica*. *Chinese Journal of Experimental Traditional Medical Formulae*, *14*.

Huang, L., Li, J., Ye, H., Li, C., Wang, H., Liu, B. and Zhang, Y., 2012. Molecular characterization of the pentacyclic triterpenoid biosynthetic pathway in *Catharanthus roseus*. *Planta*, *236*(5), pp.1571-1581.

Hudson, J.B., Graham, E.A., Rossi, R.E.N.Z.O., Carpita, A.D.R.I.A.N.O., Neri, D. and Towers, G.H.N., 1993. Biological activities of terthiophenes and polyynes from the Asteraceae. *Planta medica*, *59*(05), pp.447-450.

Hui, L.M., Zhao, G.D. and Zhao, J.J., 2015. *δ*-Cadinene inhibits the growth of ovarian cancer cells via caspase-dependent apoptosis and cell cycle arrest. *International journal of clinical and experimental pathology*, *8*(6), p.6046.

Jakupovic, J., Schuster, A., Bohlmann, F., King, R.M. and Lander, N.S., 1988. Sesquiterpene lactones from *Gnephosis* species. *Phytochemistry*, *27*(10), pp.3181-3185.

Jakupovic, J., Zdero, C., Grenz, M., Tsichritzis, F., Lehmann, L., Hashemi-Nejad, S.M. and Bohlmann, F., 1989. Twenty-one acylphloroglucinol derivatives and further constituents from South African *Helichrysum* species. *Phytochemistry*, *28*(4), pp.1119-1131.

Junior, H.N., Cunha, G.M.A., Moraes, M.O., Luciana, M.F.D., Oliveira, R.A., Maia, F.D., Nogueira, M.A.S., Lemos, T.L.G. and Rao, V.S., 2006. Quebrachitol (2-O-methyl-L-inositol) attenuates 6-hydroxydopamine-induced cytotoxicity in rat fetal mesencephalic cell cultures. *Food and chemical toxicology*, *44*(9), pp.1544-1551.

Kallio, H., Lassila, M., Järvenpää, E., Haraldsson, G.G., Jonsdottir, S. and Yang, B., 2009. Inositols and methylinositols in sea buckthorn (*Hippophae rhamnoides*) berries. *Journal of Chromatography B*, *877*(14-15), pp.1426-1432.

Kim, J., Durai, P., Jeon, D., Jung, I.D., Lee, S.J., Park, Y.M. and Kim, Y., 2018. Phloretin as a potent natural TLR2/1 inhibitor suppresses TLR2-induced inflammation. *Nutrients*, *10*(7), p.868.

Kowalski, R., 2007. Studies of selected plant raw materials as alternative sources of triterpenes of oleanolic and ursolic acid types. *Journal of Agricultural and Food chemistry*, *55*(3), pp.656-662.

Kubo, I. and Morimitsu, Y., 1995. Cytotoxicity of green tea flavor compounds against two solid tumor cells. *Journal of Agricultural and Food Chemistry*, *43*(6), pp.1626-1628.

Lanzetta, R., Lama, G., Mauriello, G., Parrilli, M., Racioppi, R. and Sodano, G., 1991. Ichthyotoxic sesquiterpenes and xanthanolides from *Dittrichia graveolens*. *Phytochemistry*, *30*(4), pp.1121-1124.

Lee, J.Y., Jeong, K.W., Shin, S., Lee, J.U. and Kim, Y., 2009. Antimicrobial natural products as β-ketoacyl-acyl carrier protein synthase III inhibitors. *Bioorganic & medicinal chemistry*, *17*(15), pp.5408-5413.

Lemos, T.L., Machado, L.L., Souza, J.S., Fonseca, A.M., Maia, J.L. and Pessoa, O.D., 2006. Antioxidant, icthyotoxicity and brine shrimp lethality tests of *Magonia glabrata*. *Fitoterapia*, *77*(6), pp.443-445.

Lourens, A.C., 2008. Structural and synthetic studies of sesquiterpenoids and flavonoids isolated from *Helichrysum species* (Doctoral dissertation, University of KwaZulu-Natal, Pietermaritzburg).

Lourens, A.C.U., Van Vuuren, S.F., Viljoen, A.M., Davids, H. and Van Heerden, F.R., 2011. Antimicrobial activity and *in vitro* cytotoxicity of selected South African *Helichrysum* species. *South African journal of botany*, *77*(1), pp.229-235.

Lourens, A.C.U., Viljoen, A.M. and Van Heerden, F.R., 2008. South African *Helichrysum* species: a review of the traditional uses, biological activity and phytochemistry. *Journal of Ethnopharmacology*, *119*(3), pp.630-652.

Magiera, A., Marchelak, A., Michel, P., Owczarek, A. and Olszewska, M.A., 2019. Lipophilic extracts from leaves, inflorescences, and fruits of *Prunus padus* L. as potential sources of corosolic, ursolic and oleanolic acids with anti-inflammatory activity. *Natural product research*, pp.1-6.

Mao, Y.W., Tseng, H.W., Liang, W.L., Chen, I.S., Chen, S.T. and Lee, M.H., 2011. Anti-inflammatory and free radial scavenging activities of the constituents isolated from *Machilus zuihoensis*. *Molecules*, *16*(11), pp.9451-9466.

Marcinek-Hüpen-Bestendonk, C., Willuhn, G., Steigel, A., Wendisch, D., Middelhauve, B., Wiebcke, M. and Mootz, D., 1990. Germacranolide, Guaianolide und Xanthanolide aus Blüten von *Arnica mollis* und Röntgenstrukturanalyse von Baileyinacetat1. *Planta medica*, *56*(01), pp.104-110.

Marco, J.A., Barberá, O., Rodríguez, S., Domingo, C. and Adell, J., 1988. Flavonoids and other phenolics from *Artemisia hispanica*. *Phytochemistry*, *27*(10), pp.3155-3159.

Ostlund, R.E., McGill, J.B., Herskowitz, I., Kipnis, D.M., Santiago, J.V. and Sherman, W.R., 1993. D-chiro-inositol metabolism in diabetes mellitus. *Proceedings of the National Academy of Sciences*, *90*(21), pp.9988-9992.

Marques, A.M., Peixoto, A.C.C., de Paula, R.C., Nascimento, M.F.A., Soares, L.F., Velozo, L.S., Guimarães, E.F. and Kaplan, M.A.C., 2015. Phytochemical investigation of anti-plasmodial metabolites from Brazilian native *Piper* species. *Journal of Essential Oil-Bearing Plants*, *18*(1), pp.74-81.

Mashigo, M., Combrinck, S., Regnier, T., Du Plooy, W., Augustyn, W. and Mokgalaka, N., 2015. Chemical variations, trichome structure and antifungal activities of essential oils of *Helichrysum splendidum* from South Africa. *South African Journal of Botany*, *96*, pp.78-84.

Matboli, M., Saad, M., Hasanin, A.H., Saleh, L.A., Baher, W., Bekhet, M.M. and Eissa, S., 2021. New insight into the role of isorhamnetin as a regulator of insulin signalling pathway in type 2 diabetes mellitus rat model: Molecular and computational approach. *Biomedicine & Pharmacotherapy*, *135*, p.111176.

Milella, L., Milazzo, S., De Leo, M., Vera Saltos, M.B., Faraone, I., Tuccinardi, T., Lapillo, M., De Tommasi, N. and Braca, A., 2016. α-Glucosidase and α-amylase inhibitors from *Arcytophyllum thymifolium*. *Journal of natural products*, *79*(8), pp.2104-2112.

Murata, S., Shiragami, R., Kosugi, C., Tezuka, T., Yamazaki, M., Hirano, A., Yoshimura, Y., Suzuki, M., Shuto, K., Ohkohchi, N. and Koda, K., 2013. Antitumor effect of 1, 8-cineole against colon cancer. *Oncology reports*, *30*(6), pp.2647-2652.

Passreiter, C.M., Merfort, I., Bestendonk, C., Willuhn, G. and Steigel, A., 1996. 11α, 13- and 11β, 13-Dihydro-4H-xanthalongin 4-O-β-Glucopyranosides: New Sesquiterpene Lactone Glycosides from Flowers of *Arnica amplexicaulis* and *A. mollis*. *Planta Medica*, *62*(01), pp.39-41.

Phoopha, S., Wattanapiromsakul, C., Pitakbut, T. and Dej-Adisai, S., 2020. A new stilbene derivative and isolated compounds from *Bauhinia pottsii* var. *pottsii* with their anti-alpha-glucosidase activity. *Pharmacognosy Magazine*, *16*(68), p.161.

Pérez-López, A., Cirio, A.T., Rivas-Galindo, V.M., Aranda, R.S. and de Torres, N.W., 2011. Activity against Streptococcus pneumoniae of the essential oil and *δ*-cadinene isolated from *Schinus molle* fruit. *Journal of Essential Oil Research*, *23*(5), pp.25-28.

Pooley, E., 2003. A Field Guide to Wild-Flowers KwaZulu-Natal and the Eastern Region. Natal Flora Publications Trust, Durban.

Pontin, M., Bottini, R., Burba, J.L. and Piccoli, P., 2015. *Allium sativum* produces terpenes with fungistatic properties in response to infection with Sclerotium cepivorum. *Phytochemistry*, *115*, pp.152-160.

Qin, J.J., Zhu, J.X., Zeng, Q., Cheng, X.R., Zhang, S.D., Jin, H.Z. and Zhang, W.D., 2012. Sesquiterpene lactones from *Inula hupehensis* inhibit nitric oxide production in RAW264. 7 macrophages. *Planta medica*, *78*(10), pp.1002-1009.

Rezk, B.M., Haenen, G.R., van der Vijgh, W.J. and Bast, A., 2002. The antioxidant activity of phloretin: the disclosure of a new antioxidant pharmacophore in flavonoids. *Biochemical and biophysical research communications*, *295*(1), pp.9-13.

Riss, T.L., Moravec, R.A., Niles, A.L., Duellman, S., Benink, H.A., Worzella, T.J. and Minor, L., 2016. Cell viability assays. *Assay Guidance Manual [Internet]*.

Rustaiyan, A., Jakupovic, J., Chau-Thi, T.V., Bohlmann, F. and Sadjadi, A., 1987. Further sesquiterpene lactones from the genus Dittrichia. *Phytochemistry*, *26*(9), pp.2603-2606.

Santos Rosa, C., Gimenez, G., Saenz Rodriguez, M.T. and De la Puerta Vazquez, R., 2007. Antihistaminic and antieicosanoid effects of oleanolic and ursolic acid fraction from *Helichrysum picardii*. *Die Pharmazie-An International Journal of Pharmaceutical Sciences*, *62*(6), pp.459-462.

Santos, F.A. and Rao, V.S.N., 2000. Antiinflammatory and antinociceptive effects of 1, 8-cineole a terpenoid oxide present in many plants' essential oils. *Phytotherapy Research: An International Journal Devoted to Pharmacological and Toxicological Evaluation of Natural Product Derivatives*, *14*(4), pp.240-244.

Schilling, N., Dittrich, P. and Kandler, O., 1972. Formation of L-quebrachitol from D-bornesitol in leaves of Acer pseudoplatanus. *Phytochemistry*, *11*(4), pp.1401-1404.

Seebacher, W., Simic, N., Weis, R., Saf, R. and Kunert, O., 2003. Complete assignments of ^{1}H and ^{13}C NMR resonances of oleanolic acid, 18-α-oleanolic acid, ursolic acid and their 11-oxo derivatives. *Magnetic Resonance in Chemistry*, *41*(8), pp.636-638.

Simonsen, J.L., 1947. *The terpenes* (Vol. 2). University Press.

Sharopov, F.S., Wink, M. and Setzer, W.N., 2015. Radical scavenging and antioxidant activities of essential oil components–An experimental and computational investigation. *Natural product communications*, *10*(1), p.1934578X1501000135.

Silva, A.C.R.D., Lopes, P.M., Azevedo, M.M.B.D., Costa, D.C.M., Alviano, C.S. and Alviano, D.S., 2012. Biological activities of a-pinene and β-pinene enantiomers. *Molecules*, *17*(6), pp.6305-6316.

Smith, T.J., 2000. Squalene: potential chemopreventive agent. *Expert Opinion on Investigational Drugs*, *9*(8), pp.1841-1848.

Su, Y.C., Hsu, K.P., Wang, E.I.C. and Ho, C.L., 2013. Composition and *in vitro* anticancer activities of the leaf essential oil of *Neolitsea variabillima* from Taiwan. *Natural product communications*, *8*(4), p.1934578X1300800432.

Su, Y.C., Hsu, K.P., Wang, E.I.C. and Ho, C.L., 2015. Composition, *in vitro* cytotoxic, and antimicrobial activities of the flower essential oil of *Diospyros discolor* from Taiwan. *Natural product communications*, *10*(7), p.1934578X1501000744.

Su, Y.C., Hsu, K.P. and Ho, C.L., 2018. Composition, *in vitro* anti-mildew fungal activities of the heartwood essential oil of *Chamaecyparis formosensis* from Taiwan. *Natural Product Communications*, *13*(10), p.1934578X1801301032.

Szakiel, A., Grzelak, A., Dudek, P. and Janiszowska, W., 2003. Biosynthesis of oleanolic acid and its glycosides in *Calendula officinalis* suspension culture. *Plant Physiology and Biochemistry*, *41*(3), pp.271-275.

Tampieri, M.P., Galuppi, R., Macchioni, F., Carelle, M.S., Falcioni, L., Cioni, P.L. and Morelli, I., 2005. The inhibition of Candida albicans by selected essential oils and their major components. *Mycopathologia*, *159*(3), pp.339-345.

Tanret, C., 1889. The Icevo-and racemic forms of inositol. *Compt. rend*, *109*, p.908.

Thimmappa, R., Geisler, K., Louveau, T., O'Maille, P. and Osbourn, A., 2014. Triterpene biosynthesis in plants. *Annual review of plant biology*, *65*, pp.225-257.

Valant-Vetschera, K.M. and Wollenweber, E., 1995. Flavonoid aglycones from the leaf surfaces of some *Artemisia* spp. (Compositae-Anthemideae). *Zeitschrift für Naturforschung C*, *50*(5-6), pp.353-357.

Valant-Vetschera, K.M. and Wollenweber, E., 1996. Comparative analysis of leaf exudate flavonoids in *Achillea subsect*. Filipendulinae. *Biochemical systematics and ecology*, *24*(5), pp.435-446.

Van Wyk, B.E. and Gericke, N., 2000. *People's plants: A guide to useful plants of Southern Africa*. Briza publications.

Vinholes, J., Gonçalves, P., Martel, F., Coimbra, M.A. and Rocha, S.M., 2014. Assessment of the antioxidant and antiproliferative effects of sesquiterpenic compounds in *in vitro* Caco-2 cell models. *Food chemistry*, *156*, pp.204-211.

Vuuren, S.V. and Viljoen, A.M., 2007. Antimicrobial activity of limonene enantiomers and 1, 8-cineole alone and in combination. *Flavour and fragrance journal*, *22*(6), pp.540-544.

Wang, Q., Mei, W.L., Dai, H.F., Zhang, J.M. and Huang, S.Z., 2020. Sesquiterpene glycoside diversities with anti-nematodal activities from *Pulicaria insignis*. *Phytochemistry Letters*, *38*, pp.161-165.

Wu, Z.C., Zhang, J.Q., Zhao, J.T., Li, J.G., Huang, X.M. and Wang, H.C., 2018. Biosynthesis of quebrachitol, a transportable photosynthate, in Litchi chinensis. *Journal of experimental botany*, *69*(7), pp.1649-1661.

Yang, Z., Wu, N., Zu, Y. and Fu, Y., 2011. Comparative anti-infectious bronchitis virus (IBV) activity of (-)-pinene: effect on nucleocapsid (N) protein. *Molecules*, *16*(2), pp.1044-1054.

Yang, C., Wang, C.M. and Jia, Z.J., 2003. Sesquiterpenes and other constituents from the aerial parts of *Inula japonica*. *Planta medica*, *69*(07), pp.662-666.

Yoshimura, H., Sugawara, K., Saito, M., Saito, S., Murakami, S., Miyata, N., Kawashima, A., Morimoto, S., Gao, N., Zhang, X. and Yang, J., 2003. In vitro TGF-β1 antagonistic activity of ursolic and oleanolic acids isolated from *Clerodendranthus spicatus*. *Planta medica*, *69*(07), pp.673-675.

Zhao, B., Huo, J., Liu, N., Zhang, J. and Dong, J., 2018. Transketolase is identified as a target of herbicidal substance α-terthienyl by proteomics. *Toxins*, *10*(1), p.41.

Chapter 6

Literature Review of the *Bulbine* Genus.

6.1.Introduction

This chapter aims to summarize the existing literature (using SciFinder, Google Scholar, PubMed, and Scopus search engines) regarding South African indigenous *Bulbine* species used traditionally to manage diabetes. The chemistry and known biological activity (of extracts or pure isolates) as applicable to this study are also described.

6.1.1. *Bulbine* Genus

The *Bulbine* genus belongs to the Asphodelaceae family (*syn*. = Xanthorrhoeaceae), and it constitutes about 84 species of flowering plants which are spread mainly throughout Southern Africa and Australia (Van Jaarsveld and Forster, 2020). Although several species are acaulescent, *Bulbine* species vary in size: from bushy caulescent to dwarf groups (Hall, 1984). The leaves also show considerable diversity, varying from grass-like to almost globose and highly succulent (Williamson, 2016). The roots are bulb-shaped and tuberous (Mocktar, 2000). Several species of this genus are traditionally used as medicinal plants and are valued in many South African cultures (for treating skin ailments, burns, diarrhea, sexually transmitted diseases, diabetes, etc.). However, for this study particular attention is only given to those that are used traditionally to manage diabetes.

6.1.2. Ethnopharmacology and Biological Activity: *on diabetes mellitus*

According to a literature search (using keywords such as "*Bulbine* species and diabetes", "South African *Bulbine* species", and "*Bulbine* species used in traditional medicine"), only four species of this genus have reported usage in South African traditional medicine for the management of diabetes mellitus (Table 6.1): *Bulbine abyssinica* (Kibiti and Afolayan, 2015), *Bulbine natalensis* (= *B. latifolia*) (Erasto et al., 2005), *Bulbine frutesscens* (Erasto et al., 2005), and *Bulbine narcissifolia* (Balogun, Tshabalala and Ashafa, 2016). Despite this, not all have been evaluated to support their ethnopharmacological use in diabetes. Nevertheless, the antidiabetic effects of *B. abyssinica* were reported by Kibiti and Afolayan (2015). While that of *B. frutescens* (this species is investigated and discussed in detail in chapter 7) was shown by van Huyssteen et al. (2011).

Table 6.1: South African *Bulbine* species (Asphodelaceae) used in traditional medicine for treating diabetes, with information on the plant parts used, methods of preparation/route of administration, and type of antidiabetic study

Scientific name [Local names]	Plant part used	Preparation and mode of administration	Type of anti-diabetic study (*in vitro/in vivo*)	References
❖ *Bulbine abyssinica* A. Rich. [Uyakayakana, utswelana, intelezi, (isiXh.*); moetsa-mollo (S.S*)]	❖ Whole plant.	❖ Decoction (two teaspoonfuls, orally).	❖ Aqueous (IC_{50} = 3.28 µg/mL) and acetone extracts IC_{50} = 4.27 µg/mL) *in vitro* on α-amylase and α-glucosidase, respectively.	❖ Kibiti and Afolayan (2015)
❖ *Bulbine natalensis* (= *B. latifolia* (L.f.) Spreng.) Mill. [Ibuchu (isiXh.*/isiZu.*); ingcelwane (isiXh.*); rooiwortel (Afri.*)]	❖ Roots.	❖ Decoction (fresh roots are boiled and two teaspoonfuls taken orally).	❖ Not available.	❖ Erasto et al. (2005)
❖ *Bulbine narcissifolia* Salm-Dyck [Lintblaar bulbine, geelslangkop, wildekopieva	❖ Not specified.	❖ Not specified.	❖ Not available.	❖ Balogun, Tshabalala and Ashafa (2016)

(Afr.*); khomo-ea-balisa, serelelile (S. S*)]				
❖ ***Bulbine frutesscens* L.** [Ibuchu (isiXh.*/isiZu.*); ingcelwane (isiXh.*); balsem kopieva, geelkatstert (Afri.*)]	❖ Roots, whole plant.	❖ Decoction (fresh roots are boiled and taken orally).	❖ Glucose utilization using the whole plant aqueous and ethanol extracts against Chang liver cells	❖ Erasto et al. (2005) ❖ van Huyssteen et al. (2011)#

* -Afr. = Afrikaans. S. S = South Sotho. IsiXh. = isiXhosa. IsiZu. = IsiZulu. # -Author showing the antidiabetic activity. ***Bulbine frutesscens* L.** is investigated in this study and its literature is discussed in detail in chapter 7.

6.1.3. Phytochemistry

Recently, a comprehensive review covering the phytochemistry of this genus (including its pharmacology and ethnobotany) was reported (Bodede and Prinsloo, 2020). Despite this, the chemistry of most species is unknown. Chrysophanol, an anthraquinone that is chemotaxonomically significant to this genus (Van Wyk, Yenesew and Dagne, 1995), has been reported from the aerial parts of *Bulbine abyssinica* (Wanjohi et al., 2005) and roots of *B. narcissifolia* (Van Wyk, Yenesew and Dagne, 1995). Flavonoid glycosides having various structural backbones: flavonol (quercetin 3-O-(6″-malonyl-glucoside) 7-O-glucoside, rutin, variabiloside A, and kaempferol-3-O-rutinoside), flavanone (astilbin), and anthocyanidin (petunidin-3-O-rutinoside, cyanidin-3-O-rutinoside) have only been identified from *Bulbine abyssinica* (leaves) using liquid chromatography and mass spectroscopy (Odeyemi and Afolayan, 2018). Interestingly, this was the only reported study that evaluated the South African *B. abyssinica* population. On the other hand, considering the rich literature on the phytochemistry of *B. natalensis*; van Staden and Drewes (1994), as well as Van Wyk, Yenesew and Dagne (1995), are the only authors who evaluated the chemistry of the South African population. No phytochemical studies have been reported from the South African indigenous *B. narcissifolia* species. It is thus surprising that the phytochemistry of the South African indigenous *Bulbine* species has remained neglected though species of this genus are mainly concentrated in Southern Africa.

Nevertheless, as shown in below Table 6.2, this study will only highlight the compounds that were isolated from the species used traditionally in South African to manage diabetes (see above in Table 6.1) with reported antidiabetic studies (whether reported from this genus or species from other genera).

Table 6.2: Secondary metabolites isolated from South African indigenous *Bulbine* species (used to manage diabetes mellitus) with reported anti-diabetic activities

Species	Structure and name of the compound (class)	Anti-diabetic activity /mechanism of action	Study type (*in vitro**/*in vivo***)	References
❖ *Bulbine abyssinica* A. Rich.	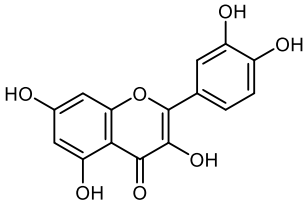 Quercetin (flavanol)	❖ Glucose uptake assay against L6 myotubes, the compound enhanced 2-NBDG uptake via AMPK and p38 MAPK.	❖ *In vitro*.*	❖ Dhanya et al. (2017) ❖ Odeyemi and Afolayan (2018)
	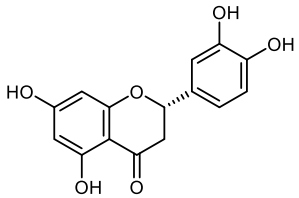 Eriodictyol (flavanone)	❖ Insulin secretion via cAMP/PKA pathway against isolated mice islets and MIN6 cells (with maximum effect at 200 µM).* ❖ 10-20 mg/kg eriodictyol treatment decreased the blood glucose levels in diabetic rats and enhanced plasma insulin.**	❖ *In vitro*.* ❖ *In vivo*.**	❖ Hameed et al. (2018) ❖ Odeyemi and Afolayan (2018)

	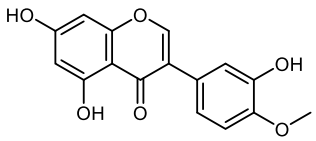 Pratensein (isoflavone)	❖ Glucose uptake assay against HepG2 cells (concentration-dependent manner).*	❖ *In vitro*.*	❖ Chen et al. (2010) ❖ Odeyemi and Afolayan (2018)
	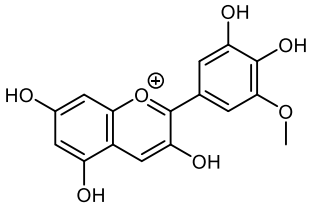 Petunidin (anthocyanidin)	❖ α-Glucosidase assay, (IC_{50} = 30.78±1.17 μM at the tested concentration).*	❖ *In vitro*.*	❖ Odeyemi and Afolayan (2018) ❖ Promyos, Temviriyanukul and Suttisansanee (2020)
	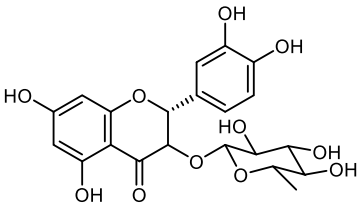 Astilbin (flavanone glycoside)	❖ Diabetic nephropathy model against HK-2 cells, the results (10 and 20 μM) showed strong inhibition of the progression of diabetic nephropathy via the PI3K/Akt pathway.*	❖ *In vitro*.*	❖ Chen et al. (2018) ❖ Odeyemi and Afolayan (2018)

	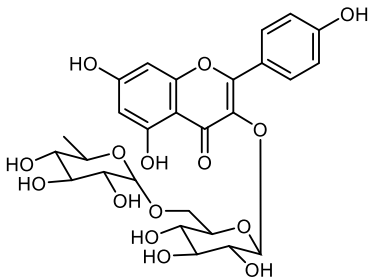 Kaempferol-3-O-rutinoside (flavonol glycoside)	❖ α-Glucosidase assay, (IC_{50} = 214.5 ± 0.0 µM at the tested concentrations).*	❖ *In vitro*.*	❖ Odeyemi and Afolayan (2018) ❖ Parveen, Farooq and Kyunn (2020)
	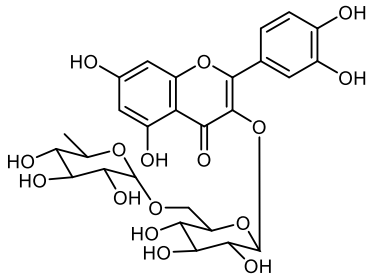 Rutin (flavonoid glycoside)	❖ Using glucose transport inhibition and glucose uptake assays against STZ-nicotinamide induced diabetic rats, the compound exhibited 41.3% inhibition after 30 minutes, and demonstrated 27.2% uptake.*	❖ *In vitro*.*	❖ Jadhav and Puchchakayala (2012) ❖ Odeyemi and Afolayan (2018)

	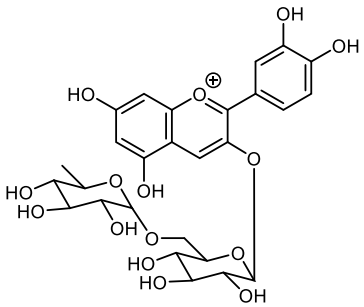 Cyanidin-3-O-rutinoside (anthocyanidin glycoside)	❖ α-Amylase assay, ($IC_{50} = 24.4 \pm 0.1$ μM at the tested concentrations).*	❖ *In vitro*.*	❖ Akkarachiyasit et al. (2011) ❖ Odeyemi and Afolayan (2018)
	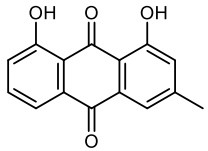 Chrysophanol (anthraquinone)	❖ Diabetic nephropathy model against STZ-induced mice.** ❖ Anti-diabetic activity (glucose transport assay against L6 rat myotube).*	❖ *In vitro*.* ❖ *In vivo*.**	❖ Guo et al. (2020) ❖ Lee and Sohn (2008) ❖ Wanjohi et al. (2005)
	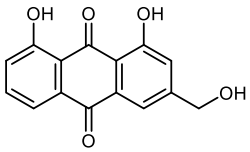 Aloe-emodin (anthraquinone)	❖ Using oral glucose tolerance test against male Wistar albino rats at doses of 3 mg/g body weight, ($p < 0.05$).**	❖ *In vivo*.**	❖ Arvindekar et al. (2015) ❖ Dagne and Yenesew (1994)

	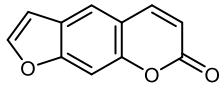 Psoralen (furanocoumarin)	❖ Diabetic nephropathy assay against HK-2 cells, via upregulation of miR-874.*	❖ *In vitro*.*	❖ Lin et al. (2020) ❖ Odeyemi and Afolayan (2018)
❖ *Bulbine narcissifolia* Salm-Dyck	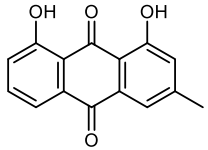 Chrysophanol (anthraquinone)	❖ Diabetic nephropathy model against STZ-induced mice.** ❖ Anti-diabetic activity (glucose transport assay against L6 rat myotube).*	❖ *In vitro*.* ❖ *In vivo*.**	❖ Guo et al. (2020) ❖ Lee and Sohn (2008) ❖ Van Wyk, Yenesew and Dagne (1995)
	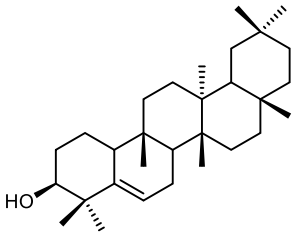 Glutinol (triterpenoid)	❖ Insulin secretory assay against isolated mice islets and MIN-6 pancreatic β-cells (137.25 ± 7.63 %).*	❖ *In vitro*.*	❖ Bodede (2020) ❖ Sharma et al. (2015)

	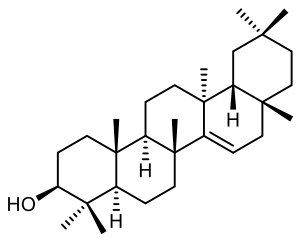 Taraxerol (triterpenoid)	❖ Diabetic nephropathy assay against STZ-induced diabetic mice (35 mg/kg body weight). The compound (20 mg/kg, body weight) stimulates glucose metabolism in skeletal muscle, and regulates blood glycaemic status.	❖ *In vivo*.*	❖ Bodede (2020) ❖ Khanra et al. (2017)
	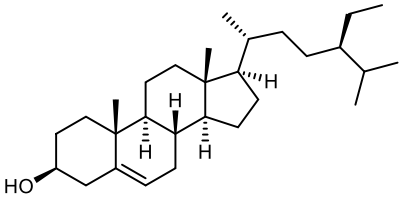 β-sitosterol (triterpenoid)	❖ α-Amylase inhibition assay (25.5 ± 3.5% at 10 mg/mL).* ❖ Insulin sensitivity via PPARγ and GLUT4 protein expression against high fat diet and STZ-induced diabetic rats (35 mg/kg body weight).**	❖ *In vitro*.* ❖ *In vivo*.**	❖ Bae et al. (2019) ❖ Ramalingam et al. (2020) ❖ Saeidnia et al. (2016)

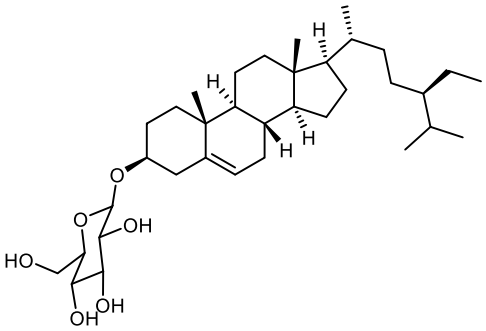 Daucosterol (triterpene glycoside)	❖ α-Amylase inhibition assay (57.5 % at 10 mg/mL).*	❖ *In vitro*.*	❖ Bae et al., (2019) ❖ Saeidnia et al. (2016)
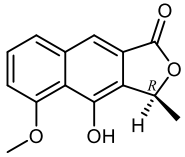 Eleutherol A (naphthoquinone)	❖ Maltase inhibition the compound demonstrated moderate activity with an IC_{50} >1.00 mM.*	❖ *In vitro*.*	❖ Bae et al. (2019) ❖ Ieyama, Gunawan-Puteri and Kawabata (2011)

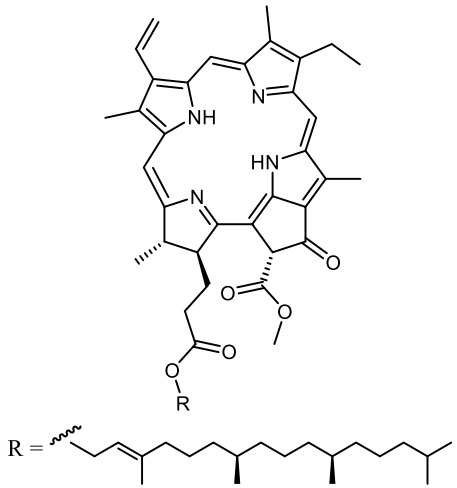 Pheophytin A (chlorins)	❖ Glucose uptake against L6 cells (EC_{50} = 5 ± 0.9 nM at the tested concentrations).*	❖ *In vitro*.*	❖ Bodede (2020) ❖ Semaan et al. (2018)
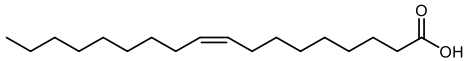 *cis*-Oleic acid (fatty acid)	❖ At 3.0 mmol/L it shows a dose-dependent increase in glucose (16.7 mmol/L)-stimulated insulin secretion against isolated mouse islets.*	❖ *In vitro*.*	❖ Bodede (2020) ❖ Kudahl et al. (1999)
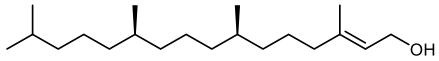 Trans-Phytol (fatty acid)	❖ Hepatic glucose uptake effects and glycaemic control through activation of RXR receptor against high fat diet diabetic/insulin-resistant rats.**	❖ *In vivo*.**	❖ Bodede (2020) ❖ Elmazar et al. (2013)

	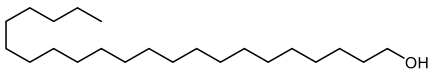 n-Docosanol (fatty acid)	❖ α-Glucosidase inhibition in Caco-2 cells had 15.5 ± 3.8 % lowering glucose concentration at 4 mg/kg body weight.*	❖ *In vitro*.*	❖ Bodede (2020) ❖ Riyaphan et al. (2018)
	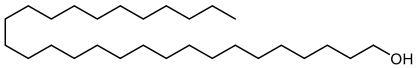 Octacosanol (fatty acid)	❖ 10 and 50 mg/kg body weight treatment with the compound improved hypertriglyceridemia in type 2 diabetic KKAy mice (2 g/kg body weight).**	❖ *In vivo*.**	❖ Bodede (2020) ❖ Ohashi, Ishikawa and Ohta (2011)
❖ ***Bulbine frutesscens* L.**	Discussed in detail in chapter 7.			

Abbreviation = half maximal effective concentration (EC_{50}), half maximal inhibitory concentration (IC_{50}), human colon adenocarcinoma (Caco-2), human liver cancer cell line (HepG2), human kidney *2* (HK-2), retinoid X receptor (RXR), peroxisome proliferator-activated receptors (PPARγ), glucose transporter type 4 (GLUT4), 2-(N-(7-Nitrobenz-2-oxa-1,3-diazol-4-yl) Amino)-2-Deoxyglucose (2-NBDG), phosphatidylinositol 3-kinase (PI3K), protein kinase B (Akt), micro-ribonucleic acid (miR-874), streptozotocin (STZ), p38 mitogen-activated protein kinase pathways (p38 MAPK), adenosine monophosphate kinase (AMPK), mouse insulinoma pancreatic β-cells (MIN6), cyclic adenosine monophosphate (cAMP), protein kinase A (PKA).

***Bulbine frutesscens* L.** is investigated in this study and its chemistry is discussed in detail in chapter 7.

References

Akkarachiyasit, S., Yibchok-Anun, S., Wacharasindhu, S. and Adisakwattana, S., 2011. *In vitro* inhibitory effects of cyandin-3-rutinoside on pancreatic α-amylase and its combined effect with acarbose. *Molecules*, *16*(3), pp.2075-2083.

Arvindekar, A., More, T., Payghan, P.V., Laddha, K., Ghoshal, N. and Arvindekar, A., 2015. Evaluation of anti-diabetic and alpha glucosidase inhibitory action of anthraquinones from *Rheum emodi*. *Food & function*, *6*(8), pp.2693-2700.

Bae, J.Y., Ali, Z., Wang, Y.H., Chittiboyina, A.G., Zaki, A.A., Viljoen, A.M. and Khan, I.A., 2019. Anthraquinone-based specialized metabolites from rhizomes of *Bulbine natalensis*. *Journal of natural products*, *82*(7), pp.1893-1901.

Balogun, F.O., Tshabalala, N.T. and Ashafa, A.O.T., 2016. Antidiabetic medicinal plants used by the Basotho tribe of Eastern Free State: a review. *Journal of Diabetes Research*, *2016*.

Bodede, O., 2020. Bioactive metabolites of *Bulbine natalensis* (Baker): Isolation, characterization, and antioxidant properties. *International Journal of Green Pharmacy (IJGP)*, *14*(1).

Bodede, O. and Prinsloo, G., 2020. Ethnobotany, phytochemistry and pharmacological significance of the genus *Bulbine* (Asphodelaceae). *Journal of Ethnopharmacology*, p.112986.

Chen, F., Sun, Z., Zhu, X. and Ma, Y., 2018. Astilbin inhibits high glucose-induced autophagy and apoptosis through the PI3K/Akt pathway in human proximal tubular epithelial cells. *Biomedicine & Pharmacotherapy*, *106*, pp.1175-1181.

Chen, Q.C., Zhang, W.Y., Jin, W., Lee, I.S., Min, B.S., Jung, H.J., Na, M., Lee, S. and Bae, K., 2010. Flavonoids and isoflavonoids from *Sophorae flos* improve glucose uptake *in vitro*. *Planta medica*, *76*(01), pp.79-81.

Dagne, E. and Yenesew, A., 1994. Anthraquinones and chemotaxonomy of the Asphodelaceae.

Dhanya, R., Arya, A.D., Nisha, P. and Jayamurthy, P., 2017. Quercetin, a lead compound against type 2 diabetes ameliorates glucose uptake via AMPK pathway in skeletal muscle cell line. *Frontiers in Pharmacology*, *8*, p.336.

Elmazar, M.M., El-Abhar, H.S., Schaalan, M.F. and Farag, N.A., 2013. Phytol/Phytanic acid and insulin resistance: potential role of phytanic acid proven by docking simulation and modulation of biochemical alterations. *PLoS One*, *8*(1), p.e45638.

Erasto, P., Adebola, P.O., Grierson, D.S. and Afolayan, A.J., 2005. An ethnobotanical study of plants used for the treatment of diabetes in the Eastern Cape Province, South Africa. *African Journal of Biotechnology*, *4*(12).

Guo, C., Wang, Y., Piao, Y., Rao, X. and Yin, D., 2020. Chrysophanol Inhibits the Progression of Diabetic Nephropathy via Inactivation of TGF-β Pathway. *Drug Design, Development and Therapy*, *14*, p.4951.

Hall, L.I., 1984. Three new species of *Bulbine* (Liliaceae) from the Vanrhynsdorp district, Cape Province. *South African Journal of Botany*, *3*(6), pp.356-358.

Hameed, A., Hafizur, R.M., Hussain, N., Raza, S.A., Rehman, M., Ashraf, S., Ul-Haq, Z., Khan, F., Abbas, G. and Choudhary, M.I., 2018. Eriodictyol stimulates insulin secretion through cAMP/PKA signalling pathway in mice islets. *European journal of pharmacology*, *820*, pp.245-255.

Ieyama, T., Gunawan-Puteri, M.D. and Kawabata, J., 2011. α-Glucosidase inhibitors from the bulb of *Eleutherine americana*. *Food Chemistry*, *128*(2), pp.308-311.

Jadhav, R. and Puchchakayala, G., 2012. Hypoglycemic and antidiabetic activity of flavonoids: boswellic acid, ellagic acid, quercetin, rutin on streptozotocin-nicotinamide induced type 2 diabetic rats. *Group*, *1*, p.100g.

Khanra, R., Bhattacharjee, N., Dua, T.K., Nandy, A., Saha, A., Kalita, J., Manna, P. and Dewanjee, S., 2017. Taraxerol, a pentacyclic triterpenoid, from *Abroma augusta* leaf attenuates diabetic nephropathy in type 2 diabetic rats. *Biomedicine & Pharmacotherapy*, *94*, pp.726-741.

Kibiti, C.M. and Afolayan, A.J., 2015. Preliminary phytochemical screening and biological activities of *Bulbine abyssinica* used in the folk medicine in the Eastern Cape Province, South Africa. *Evidence-Based Complementary and Alternative Medicine*, *2015*.

Kudahl, A.K., Søren, G., Majgaard, J.H., Laust, T.J. and Hermansen, K., 1999. Differential effects of cis and trans fatty acids on insulin release from isolated mouse islets. *Metabolism*, *48*(1), pp.22-29.

Lee, M.S. and Sohn, C.B., 2008. Anti-diabetic properties of chrysophanol and its glucoside from *Rhubarb* rhizome. *Biological and Pharmaceutical Bulletin*, *31*(11), pp.2154-2157.

Lin, Y., Zhong, L., Li, H., Xu, Y., Li, X. and Zheng, D., 2020. Psoralen alleviates high glucose-induced HK-2 cell injury by inhibition of Smad 2 signalling via upregulation of microRNA 874. *BMC Pharmacology and Toxicology*, *21*(1), pp.1-10.

Mocktar, C., 2000. *Antimicrobial and chemical analyses of selected Bulbine species* (Doctoral dissertation).

Odeyemi, S.W. and Afolayan, A.J., 2018. Identification of antidiabetic compounds from polyphenolic-rich fractions of *Bulbine abyssinica* A. rich leaves. *Pharmacognosy research*, *10*(1), p.72.

Ohashi, K., Ishikawa, H. and Ohta, Y., 2011. Octacosanol ameliorates hyperlipidemia and oxidative stress in KKAy mice with type 2 diabetes. *Journal of Analytical Bio-Science Vol*, *34*(3).

Parveen, A., Farooq, M.A. and Kyunn, W.W., 2020. A New Oleanane Type Saponin from the Aerial Parts of *Nigella sativa* with Anti-Oxidant and Anti-Diabetic Potential. *Molecules*, *25*(9), p.2171.

Promyos, N., Temviriyanukul, P. and Suttisansanee, U., 2020. Investigation of anthocyanidins and anthocyanins for targeting α-glucosidase in diabetes mellitus. *Preventive Nutrition and Food Science*, *25*(3), p.263.

Ramalingam, S., Packirisamy, M., Karuppiah, M., Vasu, G., Gopalakrishnan, R., Gothandam, K. and Thiruppathi, M., 2020. Effect of β-sitosterol on glucose homeostasis by sensitization of insulin resistance via enhanced protein expression of PPRγ and glucose transporter 4 in high fat diet and streptozotocin-induced diabetic rats. *Cytotechnology*, *72*(3), pp.357-366.

Riyaphan, J., Jhong, C.H., Lin, S.R., Chang, C.H., Tsai, M.J., Lee, D.N., Sung, P.J., Leong, M.K. and Weng, C.F., 2018. Hypoglycemic efficacy of docking selected natural compounds against α-glucosidase and α-amylase. *Molecules*, *23*(9), p.2260.

Saeidnia, S., Ara, L., Hajimehdipoor, H., Read, R.W., Arshadi, S. and Nikan, M., 2016. Chemical constituents of *Swertia longifolia* Boiss. with α-amylase inhibitory activity. *Research in pharmaceutical sciences*, *11*(1), p.23.

Semaan, D.G., Igoli, J.O., Young, L., Gray, A.I., Rowan, E.G. and Marrero, E., 2018. *In vitro* anti-diabetic effect of flavonoids and pheophytins from *Allophylus cominia* Sw. on the glucose uptake assays by HepG2, L6, 3T3-L1 and fat accumulation in 3T3-L1 adipocytes. *Journal of ethnopharmacology*, *216*, pp.8-17.

Sharma, K.R., Adhikari, A., Hafizur, R.M., Hameed, A., Raza, S.A., Kalauni, S.K., Miyazaki, J.I. and Choudhary, M.I., 2015. Potent insulin secretagogue from *Scoparia dulcis* Linn of Nepalese origin. *Phytotherapy Research*, *29*(10), pp.1672-1675.

Van Jaarsveld, E. and Forster, P.I., 2020. *Bulbine* ASPHODELACEAE. *Monocotyledons*, pp.713-739.

van Staden, L.F. and Drewes, S.E., 1994. Knipholone from *Bulbine latifolia* and *Bulbine frutescens*. *Phytochemistry*, *35*(3), pp.685-686.

Van Wyk, B.E., Yenesew, A. and Dagne, E., 1995. Chemotaxonomic significance of anthraquinones in the roots of Asphodeloideae (Asphodelaceae). *Biochemical Systematics and Ecology*, *23*(3), pp.277-281.

Wanjohi, J.M., Yenesew, A., Midiwo, J.O., Heydenreich, M., Peter, M.G., Dreyer, M., Reichert, M. and Bringmann, G., 2005. Three dimeric anthracene derivatives from the fruits of *Bulbine abyssinica*. *Tetrahedron*, *61*(10), pp.2667-2674.

Williamson, G., 2016. An account of the interesting biodiversity in a selected number of species in the genus *Bulbine* Wolf, Asphodelaceae. *Cactus and Succulent Journal*, *88*(1), pp.4-22.

Chapter 7

Phytochemistry of *Bulbine frutescens* (L.) Willd.

7.1. Introduction

This chapter focuses on the phytochemistry of *Bulbine frutescens* (L.) Willd., which is a plant that has been selected for investigation. Section A briefly discusses the literature of the plant, while section B are results and discussions.

7.2. General Experimental Procedures. See chapter 2.

7.3. Plant Material

The leaves of *B. frutescens* were collected in Kirstenbosch National Botanical Gardens, South Africa, Cape Town (-33° 59' 13.19" S, 18° 25' 29.39" E) on 17 December 2020, and the identity of the species was confirmed by the curator of the Compton Herbarium. The plant material was washed with distilled water and extracted immediately.

7.4. Extraction and Isolation

Fresh leaves (1.70 kg) of *B. frutescens* were homogenized into solution using an electrical blender, then centrifuged at 4200 rpm (Microfuge 16 Centrifuge, FX241.5P Rotor, 50/60 Hz and 220–240 V) for 20 minutes and extracted three times for 48 hours with 80% MeOH (3 x 3L. After each extraction, the supernatant was obtained by filtration using a Buchner funnel (Whatman 0.4-micron filter paper), combined, and concentrated (to remove the MeOH) under reduced pressure (at 45 °C) using a Büchi® Rotavapor® R-210 evaporator with jack and water bath, 29/32 joint, 240V. The remnant (brownish) was freeze-dried to obtain approximately 5.0 g of the total extract, which was suspended in water and extracted sequentially to furnish the crude extracts: hexane (5.00 mg), $CHCl_3$ (20.0 mg), EtOAc (500 mg), and BuOH (4.00 g). The BuOH extract was chromatographed on silica gel (gel 60, 70-230 mesh ASTM, Merck, dry packing), eluting with DCM:MeOH gradient for the target compounds. TLC (detection with vanillin sulfuric acid reagent and heating to 105 °C) employing various solvent systems was used to monitor the fractions. An application of fractions 99-146 (300 mg) to repeated column chromatography on silica gel (dry packing), eluting with $CHCl_3$:EtOAc (20:80 →0:100) gradient resulted in compounds **23** (4.40 mg) and **24** (6.60 mg). While an inseparable mixture containing compounds **25** (50.0 mg) and **26** (50.0 mg) was obtained as a brown solid upon

leaving fractions 176-203 of the main silica gel column to stand over five days. The amounts for the hexane, $CHCl_3$, and EtOAc extracts were too small to attempt isolation.

7.5. Biological Evaluation

i. α-Glucosidase and α-Amylase enzyme inhibition assays. See chapter 2.

ii. Cell viability assay (MTT). See chapter 2.

Scheme 7.1: A summary of the experimental procedure for the isolation of compounds from *B. frutescens*

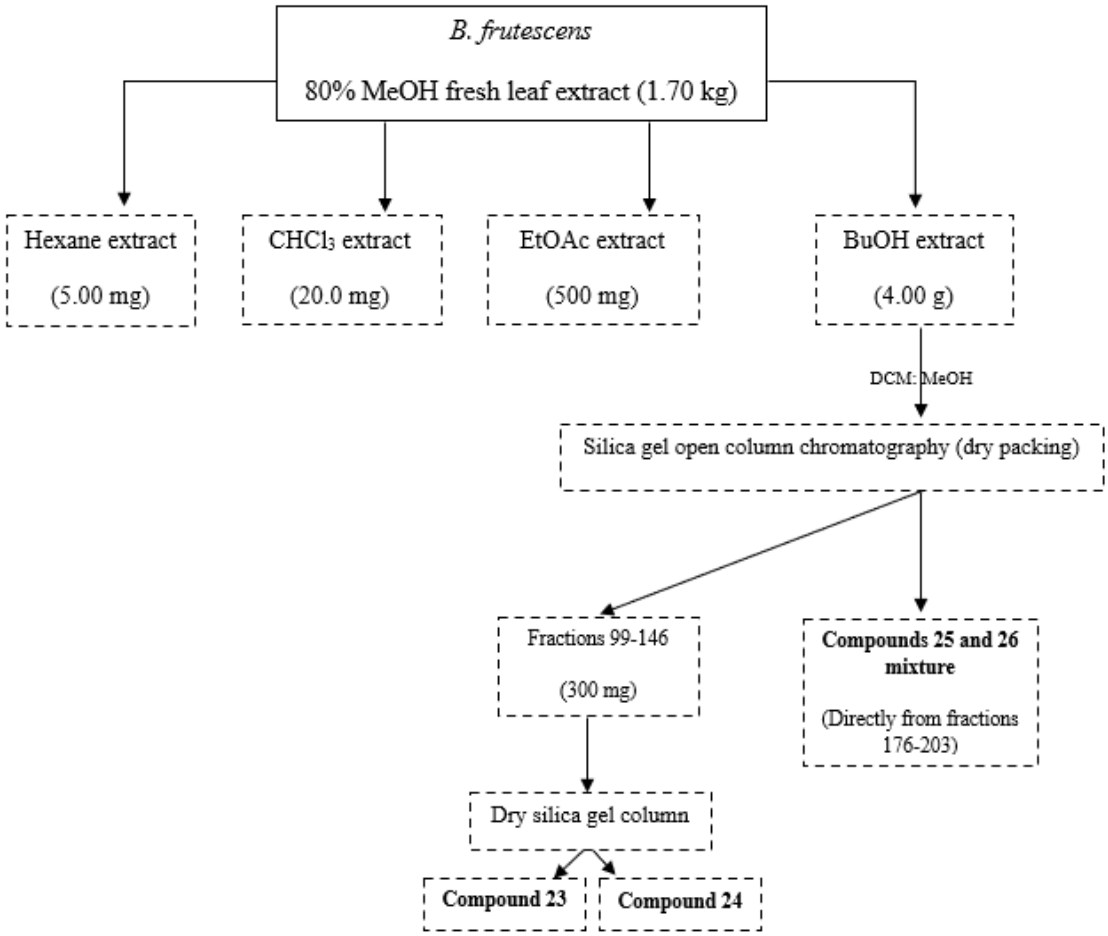

7.6. Section A

7.6.1. Taxonomy

Kingdom: Plantae

Division: Magnoliophyta

Class: Liliopsida

Order: Asparagales

Family: Asphodelaceae (= Xanthorrhoeaceae)

Genus: *Bulbine* Wolf

Species: *B. frutescens* (L.) Willd. (Pooley, 1998)

Fig. 7.1: Leaves and flowers of *B. frutescens* (source: http://pza.sanbi.org/bulbine-frutescens)

7.6.2. Background

Bulbine frutescens (L) Willd or locally known as "geelkatstert" in Afrikaans, "ibhucu" (isiZulu), "ingcelwane" (isiXhosa), and "khomo ya ntuka" (Southern Sotho) is a member of the Asphodelaceae family, which occurs widespread throughout parts of Northern, Western, and Eastern Cape in South Africa. (Van Wyk, Yenesew and Dagne, 1995). This indigenous plant, which can grow up to 15 cm tall, is highly characterized by its succulent, long-thin leaves, and brightly colored (orange-yellow) flowers as shown above in Fig. 7.1. Flowering occurs in spring (Van Jaarsveld and Forster, 2020). Although it is frequently cultivated as a groundcover there are reported uses in traditional medicine.

7.6.3. Ethnopharmacology

Bulbine frutescens is used in South Africa traditional medicine for treating skin related ailments (Van Wyk, Yenesew and Dagne, 1995), diarrhea, and blood disorders (Van Wyk, Oudtshoorn and Gericke, 1997; Felhaber, 1997), against colds, coughs, arthritis, urinary tract, and bladder infections, as well as some sexually transmissible diseases (Colson, 2013). Furthermore, a decoction made from fresh roots is reported to be used in the management of diabetes (Erasto et al., 2005).

7.6.4. Biological Activity: *diabetes mellitus*

i. In vitro

Enzyme

No data was available in the literature.

Cell-lines

The whole plant aqueous and ethanol extracts were evaluated against Chang liver cells in a glucose utilization assay (van Huyssteen et al., 2011). At 0.5 µg/mL concentration the aqueous extract showed 143.5% glucose utilization in a concentration-independent manner.

ii. In vivo (*mice*).

No data was available in the literature.

7.6.5. Other Bioactivities

The wound-healing effect of this plant was shown using the aqueous leaf extract in the *in vitro* and *in vivo* models (Pather, Viljoen and Kramer, 2011). In addition, skin-related products such as BotanicaTIMOLA® and BotanicaTIMOLA® Nat have been obtained from the leaves of this plant and are used in cosmetic formulations by a South African company called Botanica Natural Products. Other activities such as antimicrobial (Mocktar, 2000), antioxidant (Shikalepo et al., 2018), anti-inflammatory (Ghuman et al., 2019), anticancer (Kushwaha et al., 2019), and antiviral activity (Shikalepo et al., 2018) have also been reported.

7.6.6. Previous Work: *phytochemistry*

The chemistry of this plant has been previously studied (van Staden and Drewes, 1994; Van Wyk, Yenesew and Dagne, 1995; Abegaz et al., 2002; Mutanyatta et al., 2005; Bringmann et al., 2008; Abdissa et al., 2014). All the authors independently identified various knipholone-type phenylanthraquinones (monomeric/dimeric), mainly from the roots, deferring in the

substitution pattern at the hydroxyl groups of the acetylphloroglucinol moiety and/or the oxidation state of the anthraquinone moiety. Phenylanthraquinones (and their derivatives) generally exist as scalemic mixtures (*M* or *P*–enantiomer) and have been shown to possess unique bioactivities (Kuroda et al., 2003). Bringmann et al. (2008) found two dimeric knipholone derivatives: joziknipholone A and B in the roots (from a population collected in Kenya). While Mutanyatta et al. (2005) isolated *O*-sulfated phenylanthraquinones from the dried powdered roots of the Botswana population. Furthermore, anthraquinones such as chrysophanol and 3,8-dihydroxy-1-methylanthraquinone-2-carboxylic acid (obtained from the roots), in which the octaketide chain is folded in a usual way (Abdissa et al., 2014), have also been identified by the authors. Interestingly, only two studies have examined the chemistry of the South African population: knipholone was isolated from the bulbs (van Staden and Drewes, 1994) and roots (Van Wyk, Yenesew and Dagne, 1995) of the plant, while chrysophanol, as well as isoknipholone, were both obtained from the roots (Van Wyk, Yenesew and Dagne, 1995). As such, this prompted us to re-investigate this species (discussed later in the chapter, section B) as sources of novel compounds, especially with respect to the leaves since they are linked with ethnopharmacological uses in the management of diabetes but have not received much attention from a phytochemical point of view. Nonetheless, Table 7.1 summarizes the secondary metabolites obtained from *B. frutescens* along with some reported biological activities.

Table 7.1: Secondary metabolites isolated from *Bulbine frutescens* (including plant part from which it was isolated) and their known biological activities

Structure/name (class)	Part of the plant	Biological Activity	Study type (*in vitro**/*in vivo***)	References
❖ **3,8-Dihydroxy-1-methylanthraquinone-2-carboxylic acid (anthraquinone)** 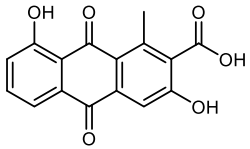	❖ Roots.	❖ Antiproliferative activity (IC_{50} =13.0, 10.4, and 36.3 µM, respectively, against glioma cell lines: U251, U87MG, and SHG44).* ❖ Protection of gastro-intestinal (enhanced mucosal damage in sepsis via junction proteins in intestinal microvascular endothelial cells).*	❖ *In vitro*.*	❖ Abdissa et al. (2014) ❖ Chen et al. (2018) ❖ Wang et al. (2017)
❖ **Islandicin (anthraquinone)** 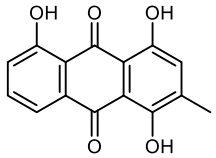	❖ Roots.	❖ Cytotoxicity activity (using LDR assay against a panel of non-small cell lung cancer cell lines. No activity was shown).* ❖ Anti-diabetic activity (had poor activity in α-glucosidase enzyme).*	❖ *In vitro*.*	❖ Dagne and Yenesew (1994) ❖ Hu, Martinez and MacMillan (2012) ❖ Jibril, Sirat and Basar (2017)

❖ **Chrysophanol (anthraquinone)** 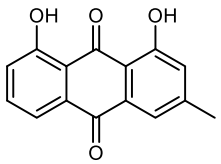	❖ Roots.	❖ Anti-inflammatory activity (suppression of NF-κB/Caspase-1 activation against mouse peritoneal macrophages).* ❖ Anti-diabetic activity (glucose transport assay against L6 rat myotube).* ❖ Antiproliferative activity (showed IC_{50} = 5.62 ± 1.58 μM in human breast cancer cells).*	❖ *In vitro*.*	❖ Kim et al (2010) ❖ Lee and Sohn (2008) ❖ Van Wyk, Oudtshoorn and Gericke (1995) ❖ Zhang et al. (2012)
❖ **Aloe-emodin (anthraquinone)** 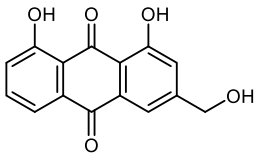	❖ Roots.	❖ Antifungal activity (had strong MIC = 25 μg/mL against *Trichophyton mentagrophytes* fungi).* ❖ Antiglycation activity (had strong effects towards glycated albumin at 25 μM concentration).* ❖ Anti-inflammatory (inhibited iNOS mRNA expression and NO production at 5–40 μM in RAW 264.7 macrophages).*	❖ *In vitro*.*	❖ Agarwal et al. (2000) ❖ Dagne and Yenesew (1994) ❖ Froldi et al. (2019) ❖ Park, Kwon and Sung (2009)

❖ **Knipholone (phenyl anthraquinone)** 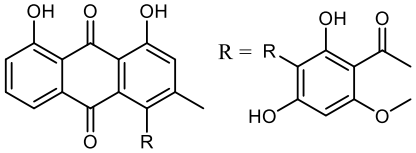	❖ Bulbs.	❖ Cytotoxicity activity (showed IC_{50} = 0.43 mM in human cervix carcinoma KB-3-1 cell line).* ❖ Anti-plasmodial activity (showed IC_{50} = 0.67–9.3 µg/mL in *Plasmodium falciparum* (strain K1 and NF54), *Trypanosoma cruzi*, and *Trypanosoma brucei rhodesiense*).* ❖ Antibacterial activity (100 µM concentrations showed a 30% growth inhibition in *Aliivibrio fischeri* DSM507 and *Mycobacterium tuberculosis* strains).* ❖ Antioxidant activity (showed IC_{50} = 22 ± 1.5 µM).*	❖ *In vitro*.*	❖ Abegaz et al. (2002) ❖ Abdissa et al. (2014) ❖ Feilcke et al. (2019) ❖ Habtemariam (2007) ❖ van Staden and Drewes (1994)
❖ **Isoknipholone (phenyl anthraquinone)** 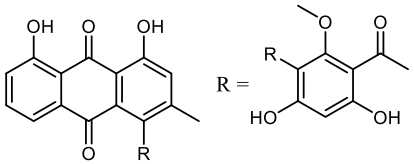	❖ Roots.	❖ Anti-plasmodial activity (showed IC_{50} = 0.12 µg/mL against the chloroquine resistant strain K1 of *Plasmodium falciparum*).*	❖ *In vitro*.*	❖ Mutanyatta et al. (2005) ❖ Van Wyk, Oudtshoorn and Gericke (1995)

❖ **Gaboroquinone A (phenylanthraquinones)** 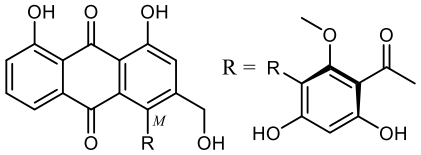	❖ Roots.	❖ Anti-plasmodial activity (showed IC_{50} = 4.8-4.2, in *Plasmodium falciparum*, 33.1 in *Trypanosoma cruzi*, and 5.1 µg/mL in *Trypanosoma brucei rhodesiense*).*	❖ *In vitro*.*	❖ Abegaz et al. (2002)
❖ **Gaboroquinone B (phenylanthraquinones)** 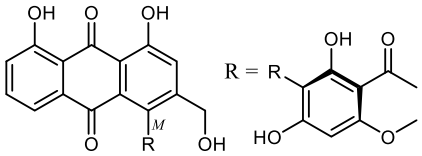	❖ Roots.	❖ Anti-plasmodial activity (showed IC_{50} = 5.0, in *Plasmodium falciparum*, 90.0 in *Trypanosoma cruzi*, and 45.5 µg/mL in *Trypanosoma brucei rhodesiense*).*	❖ *In vitro*.*	❖ Abegaz et al. (2002)
❖ **6',8-*O*-Dimethylknipholone (phenylanthraquinone)** 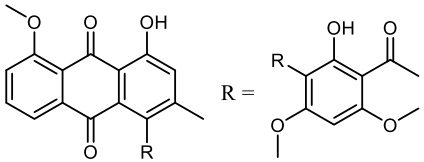	❖ Roots.	❖ Cytotoxicity activity (had poor activity in human cervix carcinoma KB-3-1 cell line).*	❖ *In vitro.**	❖ Abdissa et al. (2014)

❖ **4`-*O*-demethylknipholone (phenylanthraquinone)** 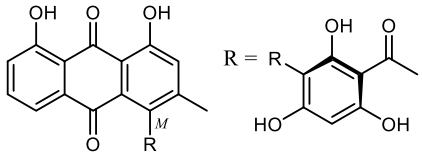	❖ Roots.	❖ Antiplasmodial Activity (showed IC_{50} = 1.80 in K 1 and 1.55 µM in NF 54 *Plasmodium falciparum* strains).*	❖ *In vitro*.*	❖ Abegaz et al. (2002) ❖ Bringmann et al. (1999)
❖ **4`-*O*-Demethylknipholone-4`-*O*-β-D-glucoside (phenylanthraquinone glucoside)** 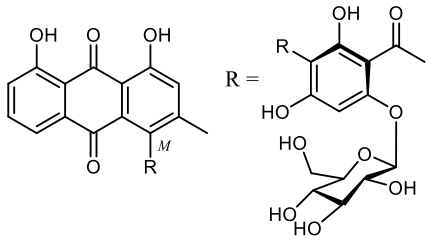	❖ Roots.	❖ Anti-plasmodial activity (showed IC_{50} = 0.41–0.7 µg/mL against *Plasmodium falciparum* (strain K1 and NF54), *Trypanosoma cruzi*, and *Trypanosoma brucei rhodesiense*).*	❖ *In vitro*.*	❖ Abegaz et al. (2002)

❖ **Sodium *ent*-knipholone-6`-*O*-sulfate (*O*-sulfated phenylanthraquinone)** 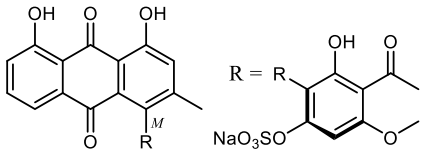	❖ Roots.	❖ Anti-plasmodial activity (had poor activity against the chloroquine-resistant strain K1 of *Plasmodium falciparum*).*	❖ *In vitro.**	❖ Mutanyatta et al. (2005)
❖ **Sodium isoknipholone-6`-*O*-sulfate (*O*-sulfated phenylanthraquinone)** 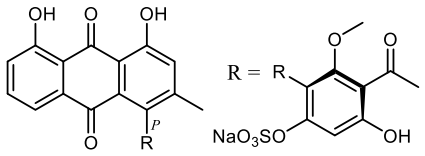	❖ Roots.	❖ Anti-plasmodial activity (had poor activity against the chloroquine-resistant strain K1 of *Plasmodium falciparum*).*	❖ *In vitro.**	❖ Mutanyatta et al. (2005)
❖ **Sodium 4`-*O*-Demethylknipholone-6`-*O*-sulfate (*O*-sulfated phenylanthraquinone)** 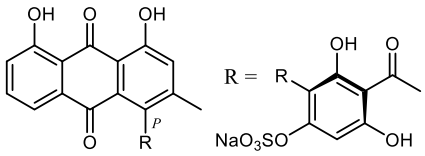	❖ Roots.	❖ Anti-plasmodial activity (had poor activity against the chloroquine-resistant strain K1 of *Plasmodium falciparum*).*	❖ *In vitro.**	❖ Mutanyatta et al. (2005)

❖ **Sodium 4`-*O*-demethylknipholone-4`-*O*-β-D-glupyranoside-6`-*O*-sulfate (*O*-sulfated phenylanthraquinone glucoside)** 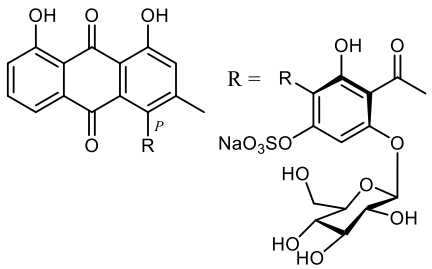	❖ Roots.	❖ Anti-plasmodial activity (had poor activity against the chloroquine-resistant strain K1 of *Plasmodium falciparum*).*	❖ *In vitro*.*	❖ Mutanyatta et al. (2005)
❖ **Knipholone anthrone (phenylanthraquinone)** 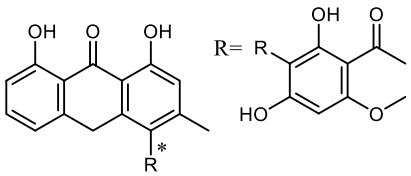	❖ Roots.	❖ Antioxidant activity (had an IC_{50} = 22 ± 1.5 μM in DPPH radicals scavenging assay).* ❖ Anti-plasmodial activity (showed IC_{50} = 0.38 in K1 and 0.42 μM in NF 54 *Plasmodium falciparum* strains).* ❖ Cytotoxicity activity (induced a rapid onset of cytotoxicity with IC_{50} = 0.5–3.3 μM range in RAW 264.7, THP-1, and B16 cell lines).*	❖ *In vitro*.*	❖ Bringmann et al. (1999) ❖ Dagne and Yenesew (1994) ❖ Habtemariam (2007) ❖ Habtemariam (2010)

❖ **8-Hydroxy-6-methylxanthone-1-carboxylic acid (xanthone)** 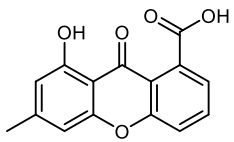	❖ Roots.	❖ Cytotoxicity activity (at 10 µM had significant activity against human prostatic cancer cell lines: 82.1% in C4-2B and 77.7% in 22RV1).*	❖ *In vitro*.*	❖ Abdissa et al. (2014) ❖ Wang et al. 2020)
❖ **Joziknipholone A (dimeric phenylanthraquinones)** 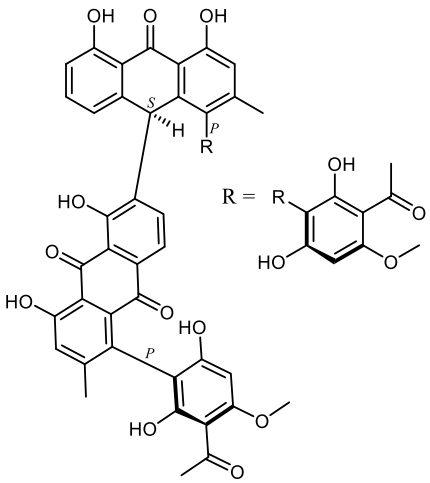	❖ Roots.	❖ Anti-plasmodial activity (showed IC_{50} = 0.14 µg/mL against *Plasmodium falciparum*).* ❖ Cytotoxicity (showed IC_{50} = 16.3 µg/mL against rat skeletal myoblast L6 cells).* ❖ Antitumoral activity (showed IC_{50} = 10 µg/mL against murine leukemic lymphoma L5178y cells).*	❖ *In vitro*.*	❖ Bringmann et al. (2008)

❖ **5,8-Dihydroxy-1-methylnaphtho[2,3-c]furan-4,9-dione (isofuranonaphthoquinone)** 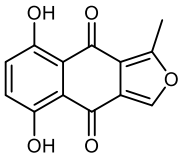	❖ Roots.	❖ Anti-plasmodial activity (showed IC_{50} = 70 µmol/L against two strains of *Plasmodium falciparum* 3D7 and K1).*	❖ *In vitro*.*	❖ Bringmann et al. (2008) ❖ Bezabih et al. (2001)
❖ **Joziknipholone B (dimeric phenylanthraquinones)** 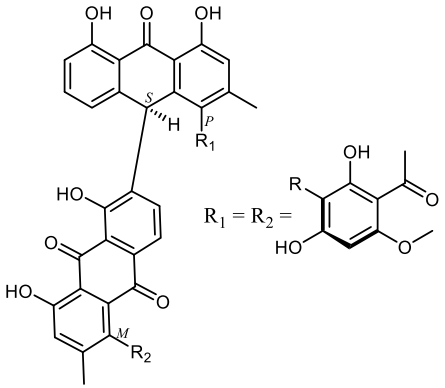	❖ Roots.	❖ Anti-plasmodial activity (showed IC_{50} = 0.23 µg/mL in *Plasmodium falciparum*).* ❖ Cytotoxicity (showed IC_{50} = 17.4 µg/mL against rat skeletal myoblast L6 cells).* ❖ Antitumoral activity (showed IC_{50} = 8.7 µg/mL against murine leukemic lymphoma L5178y cells).*	❖ *In vitro*.*	❖ Bringmann et al. (2008)

❖ **5,8-Dihydroxy-1-hydroxymethylnaphtho[2,3-c]furan-4,9-dione (isofuranonaphthoquinone)** 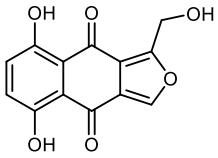	❖ Roots.	❖ Antiproliferative Activity (displayed 75% cell viability at 37.5 μg/mL against Jurkat T Cells).*	❖ *In vitro*.*	❖ Bringmann et al. (2008) ❖ Tambama, Abegaz and Mukanganyama (2014)
❖ **4-*O*-Methyleleutherol (monomethyl ether derivative)** 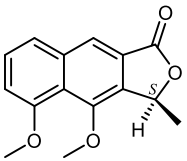	❖ Roots.	❖ Anti-diabetic activity (α-glucosidase assay but showed no activity).*	❖ *In vitro*.*	❖ Bringmann et al. (2008) ❖ Liao et al. (2019)

❖ **Vanillic acid (phenolic acids)**	❖ Roots.	❖ Antidiabetic activity (50 mg kg/body reduced fasting plasma glucose, insulin, and blood pressure in male Wistar rats).* ❖ Anti-inflammatory activity (in murine macrophage via cytokine production).* ❖ Antioxidant activity (had 85.8 and 63.1 % free radicals scavenging in superoxide and hydroxyl radical scavenging assay, respectively).* ❖ Antibacterial activity (had MIC = 0.8 mg/mL in *Enterobacter hormaechei*).*	❖ *In vitro.**	❖ Bringmann et al. (2008) ❖ Calixto-Campos et al. (2015) ❖ Prince, Rajakumar and Dhanasekar (2011) ❖ Qian et al. (2020) ❖ Vinothiya and Ashokkumar (2017)
❖ ***p*-Coumaric acid (phenolic acids)**	❖ Roots.	❖ Anti-diabetic activity (oral administration of the compound increased the expression of GLUT-2 mRNA in the pancreatic tissue of STZ-induced rats).**	❖ *In vitro.** ❖ *In vivo.***	❖ Amalan et al. (2016) ❖ Bringmann et al. (2008) ❖ Kiliç and Yeşiloğlu (2013) ❖ Lou et al. (2012)

		❖ Antioxidant activity (showed a 71.2% inhibition at 45l µg/mL concentration).* ❖ Antibacterial activity (showed an MIC = 10 µg/mL against *Shigella dysenteriae*).*		
❖ **Dihydro-*p*-coumaric acid (phenolic acids)** 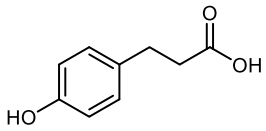	❖ Roots.	❖ Antioxidant activity (had 79.8% inhibition at 100 µM in PC-12 cells).* ❖ Tyrosinase inhibitory activity (had weak inhibition at the tested concentration).*	❖ *In vitro.**	❖ Bringmann et al. (2008) ❖ Choi et al. 2015) ❖ Takahash and Miyazawa (2010)

Abbreviation = inducible nitric oxide synthase (iNOS), nitric oxide (NO), streptozotocin (STZ), glucose transporter 2 (GLUT2), ligation detection reaction (LDR), 2,2-diphenyl-1-picrylhydrazyl (DPPH), minimum inhibitory concentrations (MIC), half-maximal inhibitory concentration (IC_{50}) messenger RNA (mRNA), deoxyribonucleic acid (DNA), pheochromocytoma (PC 12)

7.7. Section B

7.7.1 Results and Discussion

The treatment and extraction of the plant material (*Bulbine frutescens*) was carried out as outlined below in the experimental subsection. Phytochemical study of the leaf extracts from *B. frutescens* resulted in isolation and identification of four compounds, all of which are reported for the first time from this plant. The characterization is of each compound is discussed.

Compound 23: 4-*O*-β-D-glucopyranosyl-2-hydroxy-6-methoxyacetophenone

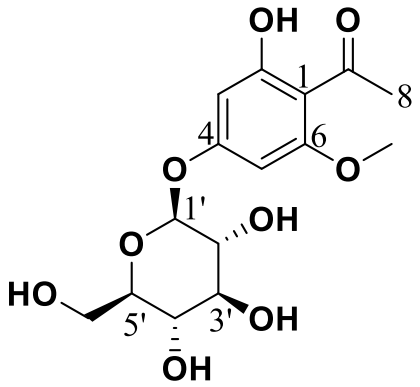

Fig. 7.2: Structure of compound **23**

Compound **23** (Fig. 7.2) was obtained as a colourless solid after subjecting fractions 99 – 146 (300 mg) of the main column to repeated chromatography on silica gel, eluting with $CHCl_3$:EtOAc (20:80 →0:100) stepwise gradient. The structural characterization of this compound was determined by employing spectroscopic techniques (one- and two-dimensional experiments) and comparison with available literature (Aljubiri et al., 2021).

The proton nuclear magnetic resonance spectrum, ^{1}H NMR, (Plate 22A in the appendix) displayed two de-shielded doublet resonances at δ_H 6.15 (1H, *d*, *J* = 2.2 Hz) and 6.22 (1H, *d*, *J* = 2.1 Hz) that were attributed to the meta-coupled protons of H-3 and H-5, respectively (Aljubiri et al., 2021). In addition, a strong singlet chemical shift appeared downfield at δ_H 13.53, which could be attributed to an OH group that is close to a carbonyl. Two characteristic signals (each integrating for three protons) were also visible at δ_H 3.87 (3H, *s*) and 2.56 (3H, *s*) and could be attributed to a methyl ether (OCH_3) as well as an aromatic bounded acetyl group

($OCCH_3$), respectively. Other signals, which were characteristic of the sugar moiety, appeared between δ_H 3.35–3.88 and the anomeric proton at δ_H 4.99 (1H, *d*, *J* = 7.5 Hz, H-1`). Therefore, this suggested a tetrasubstituted phenyl ring system (Singh et al., 1997). Nonetheless, it has been shown in the literature (Roslund et al., 2008) that the coupling constant *J* is unique for the orientation of the anomeric proton (~ 2.7 for α-orientation and ~ 7.2 Hz for β-orientation). As such, compound **23** was assigned a β-orientation (*J* = 7.5) and agreed with previous data (Aljubiri et al., 2021). On the other hand, 15 carbon signals δ_C were observed and identified using carbon thirteen, ^{13}C, (Plate 22C in the appendix) and distortionless enhancement by polarization transfer, DEPT-135 NMR (Plate 22D in the appendix) experiments: 203.4 (C-7), 165.8 (C-2), 164.1 (C-4), 163.1 (C-6), 106.7 (C-1), 100.0 (C-1`), 96.6 (C-3), 92.4 (C-5), 77.7 (C-3`), 77.0 (C-5`), 73.5 (C-2`), 70.1 (C-4`), 61.1 (C-6`), 56.5 (OCH_3), and 33.2 ($OCCH_3$). The chemical shifts were assigned according to (^1H) – (^{13}C) heteronuclear single quantum correlation, HSQC, (Plate 22E in the appendix) and heteronuclear multiple bond correlation, HMBC, (Plate 22F in the appendix) experiments. In the HMBC (Fig. 7.3), important correlations were observed between the $OCCH_3$ group protons with C-7 and C-1, as well as OCH_3 group protons with C-6 which allowed for their differentiation. Whereas H-3 and H-5 showed correlations with C-2 and C-6, respectively. Furthermore, the OH-group also showed important correlations with C-2, C-1, C-3; whereas the sugar moiety was placed at C-4 to unambiguously confirm the existence of a phloroglucinol type of substitution pattern (Singh et al., 1997). Therefore, based on the spectroscopic evidence and corroboration with the available literature compound **23** was identified as 4-*O*-β-D-glucopyranosyl-2-hydroxy-6-methoxyacetophenone (rodiolinozide or annphenone). Table 7.2 shows a summary of the NMR data of compound **23**. To the best of our knowledge, this is the first isolation of this compound from *B. frutescens* and family Asphodelaceae.

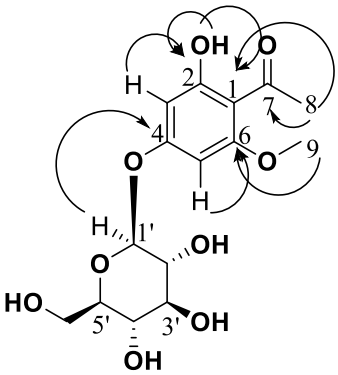

Fig. 7.3: Selected HMBC correlations of compound **23**

Table 7.2: ^{1}H and ^{13}C NMR spectral (DMSO-d6, 400MHz) data for compound **23**

#	**δ_C[ǂ], type**		**δ_H[ǂ] (*J* in Hz)**		**HMBC**
1	106.7, C	106.4[ǂ], C	-	-	-
2	165.8, C	166.3[ǂ], C	-	-	-
3	96.6, CH	96.4[ǂ], CH	6.15, *d* (2.2)	6.22[ǂ], *d* (2.6)	C-1, C-5, C-2, C-4
4	164.1, C	164.1[ǂ], C	-	-	-
5	92.4, CH	91.4[ǂ], CH	6.22, *d* (2.1)	6.29[ǂ], *d* (2.6)	C-1, C-3, C-4, C-6
6	163.1, C	163.3[ǂ], C	-	-	-
7	203.4, C	203.5[ǂ], C	-	-	-
8	33.2, CH_3	31.8[ǂ], CH	2.56, *s*	2.61[ǂ], *s*	C-7, C-1
OCH_3	56.5	54.3[ǂ]	3.87, *s*	3.90[ǂ], *s*	C-6
2-OH	-	-	13.53, *s*		C-2, C-3, C-1
Sugar moiety					
1`	100.0, CH	99.9[ǂ], CH	4.99, *d* (7.5)	5.00[ǂ], *d* (9.4)	C-4
2`	73.5, CH	74.3[ǂ], CH	3.24, *m*	3.42[ǂ], *m*	
3`	77.7, CH	77.1[ǂ], CH	3.40, *m*	3.48[ǂ], *m*	
4`	70.1, CH	69.9[ǂ], CH	3.14, *m*	3.35[ǂ], *m*	
5`	77.0, CH	76.5[ǂ], CH	3.29, *m*	3.45[ǂ], *m*	
6`	61.1, CH_2	61.1[ǂ], CH_2	3.87, *m*	3.88[ǂ], *m*	
			2.56, *m*	3.68[ǂ], *m*	

[ǂ] -Literature data (Aljubiri et al., 2021; 850 MHz, CD_3OD).

Apart from *B. frutescens*, rodiolinozide has been previously identified from several other plants including the aerial parts of *Artemisia sacrorum* (Konda et al., 1991), *Celosia argentea* (Shen et al., 2010), *Euphorbia balsamifera* (Aljubiri et al., 2021), *Ikonnikovia kaufmanniana* (Baiseitova et al., 2021), and leaves of *Monochaetum multiflorum* (Isaza, Ito and Yoshida, 2001). The antioxidant effects of this compound were evaluated using DPPH scavenging assay and IC_{50} value of 23.23 ± 1.8 (µg/mL) was shown (Wang et al., 2018).

Compound 24: Methyl-α-D-arabinofuranoside

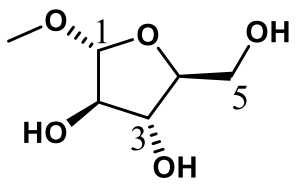

Fig. 7.4: Structure of compound **24**

Compound **24** (Fig. 7.4) was obtained as a white solid after subjecting fractions 99-146 (300 mg) of the main column to repeated chromatography on silica gel, eluting with $CHCl_3$:EtOAc (20:80 →0:100) stepwise gradient. The structural characterization of this compound was determined by employing spectroscopic techniques (^{1}H, ^{13}C, HSQC, DEPT-135, and HMBC) and comparison with available literature (Gorin and Mazurek, 1976; Wu et al., 1983).

The ^{1}H NMR spectrum (Plate 23A in the appendix) displayed chemical shifts δ_H that were characteristic of a sugar unit corresponding to a furanoside backbone: 4.94 (1H, *d*, *J* = 1.4 Hz, H-1), 4.07 (1H, *m*, H-2), 4.05 (1H, *m*, H-4), 3.96 (1H, *m*, H-3), 3.83 (1H, *m*, H-5a), 3.72 (1H, *m*, H-5b), and 3.43 (3H, *s*, Me). This was confirmed by the presence of five carbon signals δ_C in the ^{13}C (Plate 23C) and DEPT-135 NMR (Plate 23D in the appendix) spectra: 108.2 (C-1), 83.8 (C-4), 80.6 (C-2), 76.2 (C-3), and 61.1 (C-5). While another chemical shift appeared up-field at δ_C 54.8 and could be assigned to the methoxy carbon. The assignment of the resonances was achieved through HSQC (Plate 23E in the appendix) and confirmed by COSY (Plate 23B in the appendix), and HMBC correlations (Plate 23F in the appendix). Important HMBC correlations (Fig. 7.5) were observable between the Me-group protons with C-1, H-5a/b with C-4, as well as H-1 with C-4. These assignments were corroborated by COSY experiments which displayed correlations between H-1 and H-2, as well as H-5 and H-4 (Fig. 7.5). Therefore, based on these results, the assignments of the remaining signals (proton/carbon) were achieved (Table 7.3). After careful consideration of NMR data of compound **24** and comparison with known methyl pentofuranoside isomers (Tables 7.4 and 7.5), including inspection of its coupling constant *J* 1.4 (Cicero et al., 1991), it was tentatively assigned as methyl-α-D-arabinofuranoside. Though there is a possibility that it could also be methyl-β-L-arabinofuranoside its mirror image, which we will explore in future studies. To the best of our

knowledge, this is the first isolation of this compound from *B. frutescens* and family Asphodelaceae.

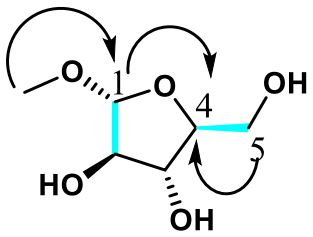

Fig. 7.5: Selected HMBC (black arrows) and COSY (blue) correlations of compound **24**

Table 7.3: ^{1}H and ^{13}C NMR spectral data (CD_3OD, 400 MHz) of compound **24**

#	δ_C, type	δ_H (*J* in Hz)	HMBC	COSY
1	108.2, CH	4.94, *d* (1.4)	C-4, C-3, OCH_3	H-2
2	80.6, CH	4.07, *m*	C-3,	H-1, H-3
3	76.2, CH	3.96, *dd* (3.3, 5.8)	C-2, C-5	H-4, H-2
4	83.8, CH	4.05, *m*		H-3, H-5
5	61.1, CH_2	3.72, *brdd* (5.7, 12.3)	C-3, C-4	H-4
		3.83, brdd (3.3, 12.2)		
6	54.8, OCH_3	3.43, *s*	C-1	-

Table 7.4: ^{13}C NMR spectral data of reported methyl pentofuranoside isomers (D_2O) and compound **24** (D_2O, 100 MHz)

	δC, type								
#	**Compound 25**	**A**	**B**	**C**	**D**	**E**	**F**	**G**	**H**
1	109.2, CH	109.3, CH	103.2, CH	109.1, CH	103.2, CH	103.0, CH	109.6, CH	104.2, CH	109.0, CH
2	81.5, CH	81.9, CH	77.5, CH	77.0, CH	72.9, CH	77.7, CH	80.9, CH	72.1, CH	75.3, CH
3	77.2, CH	77.5, CH	75.7, CH	72.0, CH	70.7, CH	76.0, CH	76.0, CH	70.8, CH	71.9, CH
4	84.7, CH	84.9, CH	83.1, CH	81.3, CH	81.9, CH	79.3, CH	83.5, CH	85.5, CH	83.9, CH
5	62.0, CH_2	62.4, CH_2	64.2, CH	61.2, CH	62.4, CH	61.5, CH	62.1, CH	62.6, CH	63.9, CH
6	55.8, OCH_3	56.1, OCH_3	56.3, OCH_3	56.9, OCH_3	56.5, OCH_3	56.6, OCH_3	56.2, OCH_3	56.5, OCH_3	56.3, OCH_3

A = methyl-α-D-arabinofuranoside. B = methyl-β-D-arabinofuranoside. C = methyl-α-D-lyxofuranoside. D = methyl-β-D-lyxofuranoside. E = methyl-α-D-xylofuranoside. F = methyl-β-D-xylofuranoside. G =methyl-α-D-ribofuranoside. H = methyl-β-D-ribofuranoside. (Gorin and Mazurek, 1976).

Table 7.5: ^{1}H NMR spectral data of reported methyl pentofuranoside isomers (D_2O) and compound **24** (D_2O, 400 MHz)

	δH (*J* in Hz)								
#	**Compound 25**	**A**	**B**	**C**	**D**	**E**	**F**	**G**	**H**
1	4.94, *d* (1.4)	4.91	4.89	4.95	4.91	4.99	4.89	4.99	4.88
2	4.07, *m*	4.04	4.13	4.11	4.19	4.14	4.12	4.11	4.02
3	3.96, *dd* (3.3, 5.8)	3.93	4.00	4.32	4.24	4.29	4.21	4.03	4.14
4	4.05, *m*	4.02	3.88	4.24	4.15	4.23	4.35	4.09	4.00
5	3.72, *brdd* (5.7, 12.3)	3.69	3.61	3.73	3.72	3.69	3.73	3.66	3.59
	3.83, *brdd* (3.3, 12.2)	3.80	3.76	3.81	3.83	3.76	3.83	3.73	3.78
6	3.43, *s*	3.40	3.41	3.44	3.40	3.44	3.39	3.43	3.38

A = methyl-α-D-arabinofuranoside. B = methyl-β-D-arabinofuranoside. C = methyl-α-D-lyxofuranoside. D = methyl-β-D-lyxofuranoside. E = methyl-α-D-xylofuranoside. F = methyl-β-D-xylofuranoside. G = methyl-α-D-ribofuranoside. H = methyl-β-D-ribofuranoside. (Wu et al., 1983).

Compounds 25 and 26: α-and-β-D-Glucopyranose (mixture)

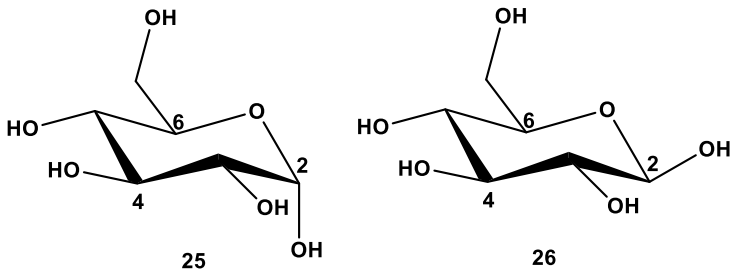

Fig. 7.6: Structures of compounds **25** and **26**

Compounds **25** and **26** were obtained as a mixture (brown solid) directly from fractions 176 – 203 of the main silica gel column using DCM:MeOH eluant in a stepwise gradient (100 :0→50: 50). Following structure characterization, they were readily deduced as a mixture of α-and-β-glucopyranose (Fig. 7.6) based on their NMR data and comparison with the literature (Pomin, 2012). The nature of these compounds has been extensively studied in carbohydrate chemistry (Casu et al., 1965; Dorman and Roberts, 1970; Pomin, 2012); thus, they do not warrant any further discussion.

Nonetheless, the ^{1}H NMR spectrum (Fig. 7.7) displayed chemical shifts δ_H that were characteristic of two sugar units with a pyranose backbone between 3.23-3.92. The anomeric signals appeared at δ_H 5.24 (1H, *d*, *J* = Hz) and 4.65 (1H, *d*, *J* = Hz) for the α-and β-units, respectively. The ^{13}C (Fig. 7.8) NMR spectrum confirmed the presence of twelve carbon signals δ_C, some of which were overlapping. Table 7.6 shows a summary of the NMR of α-and β-D-glucopyranose and those reported in the literature (Pomin, 2012). To the best of our knowledge, this is the first report of this compound in the *B. frutescens*.

Table 7.6: ^{1}H and ^{13}C-NMR spectroscopic data (D_2O, 400 MHz) of compounds **25** and **26**

	δ_C ǂ, type				**δ_H ǂ (*J* in Hz)**			
#	α		β		α		β	
1	92.0, CH	91.4ǂ, CH	95.8, CH	95.9ǂ, CH	5.24, *d* (3.7)	5.32ǂ	4.65, *d* (7.9)	4.74ǂ
2	71.4[a], CH	71.8ǂ, CH	75.7, CH	74.1ǂ, CH	3.23-3.92	3.63ǂ	3.25, *t* (7.9)	3.37ǂ
3	72.7, CH	72.4ǂ, CH	75.9, CH	75.8ǂ, CH	3.23-3.92	3.83ǂ	3.23-3.92	3.60ǂ
4	71.4[a], CH	71.2ǂ, CH	74.1, CH	71.2ǂ, CH	3.23-3.92	3.92ǂ	3.23-3.92	3.92ǂ
5	69.6, CH	69.8ǂ, CH	69.5, CH	69.8ǂ, CH	3.23-3.92	3.50ǂ	3.23-3.92	3.50ǂ
6	60.5, CH_2	60.3ǂ, CH_2	60.7, CH_2	60.3ǂ, CH_2	3.23-3.92	3.82ǂ	3.23-3.92	3.82ǂ
						3.91ǂ		3.91ǂ

ǂ -Literature data (Pomin, 2012; 400 MHz; D_2O). [a] -Overlapping signals.

Fig. 7.7: ^{1}H NMR spectrum (D_2O, 400 MHz) of compounds **25** and **26**

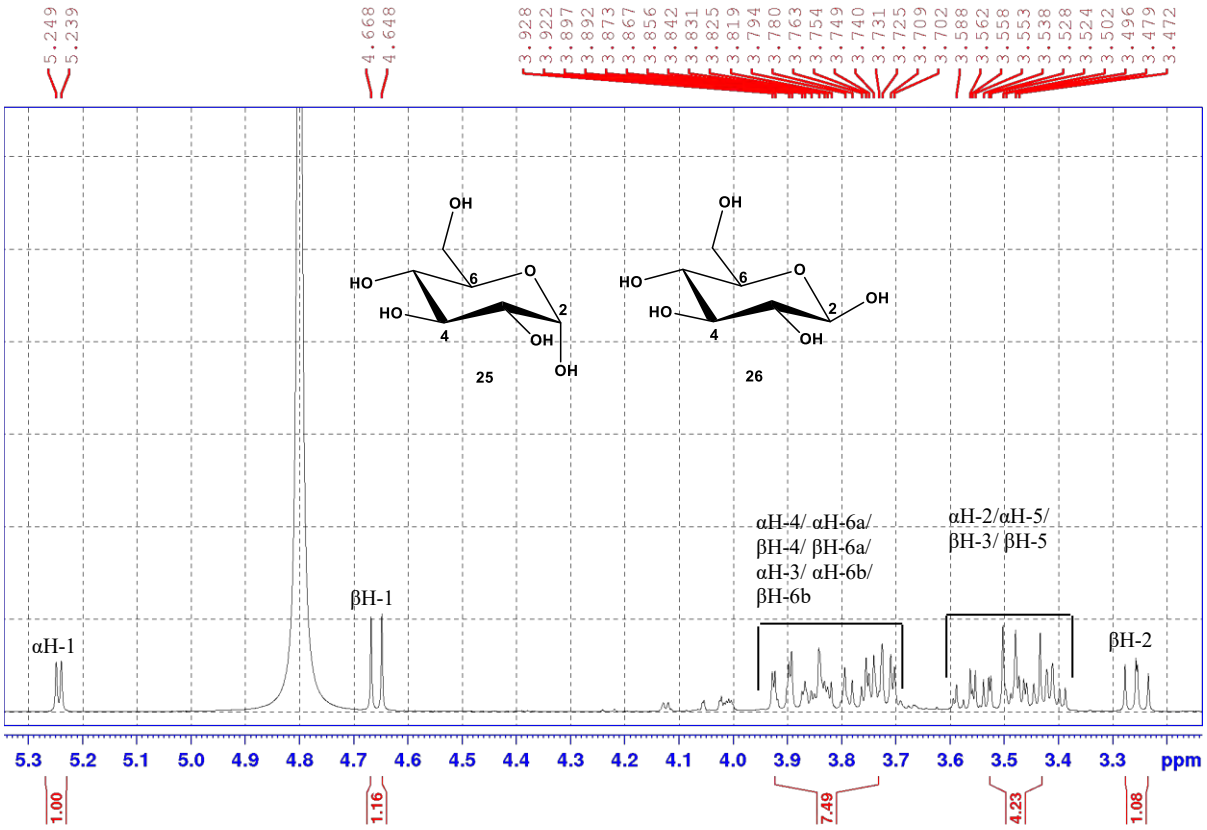

Fig. 7.8: ^{13}C NMR spectrum (D_2O, 100 MHz) of compounds **25** and **26**

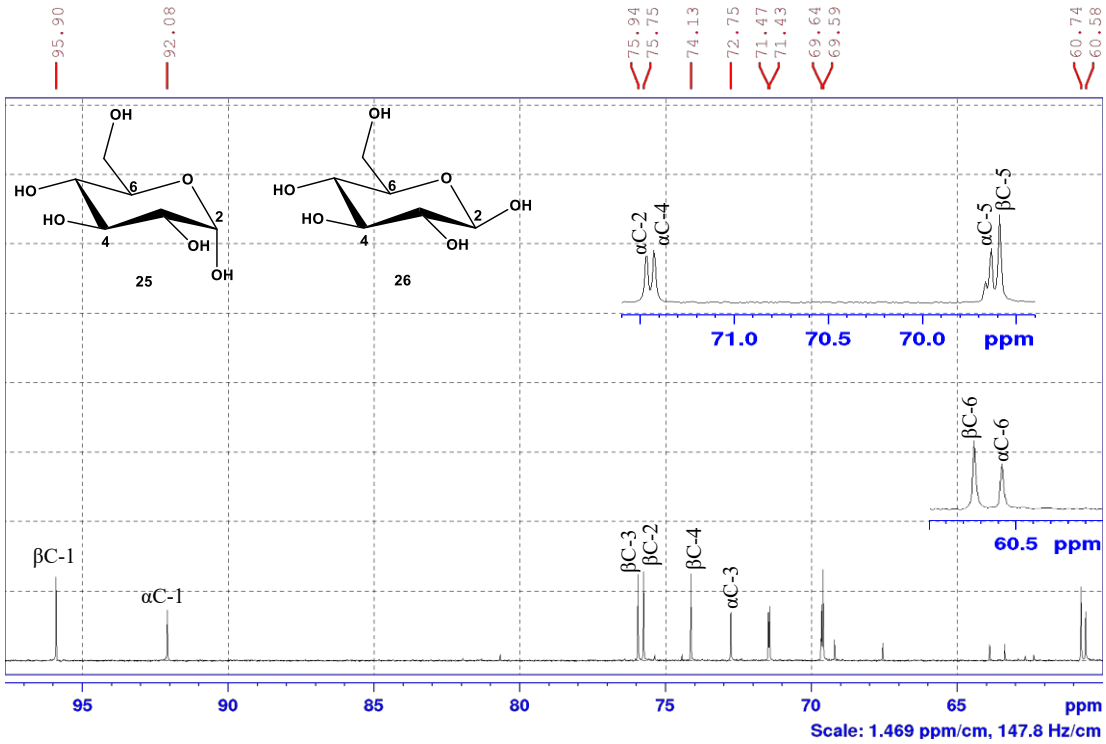

7.7.2. Biological Activity

i. α-Glucosidase and α-amylase inhibition assays

The α-glucosidase and α-amylase assays were carried out as outlined in chapter 2. All extracts and compounds did not show any activity at the tested concentration. Previously, the antidiabetic activity of the whole plant aqueous extract was shown by van Huyssteen et al. (2011). This is the first report of the antidiabetic evaluation of the leaves of this plant and therefore, further studies are needed to explore its antidiabetic potential/or mechanism.

ii. Cell viability assay (MTT) - MDA-MB-231 cell

Cell viability assay was carried out as outlined in chapter 2. To achieve this, cells were exposed to 0.1, 10, and 100 µg/mL of each compound over 24 hours, and the MTT assay was performed (Fig. 7.9). However, all the compounds exhibited cytotoxicity effects toward MDA-MB-231 cells at the initial screening stage with compound **23** being the most toxic overall. Therefore, no further studies were done. We recommend exploring these compounds further to determine their mechanism of action.

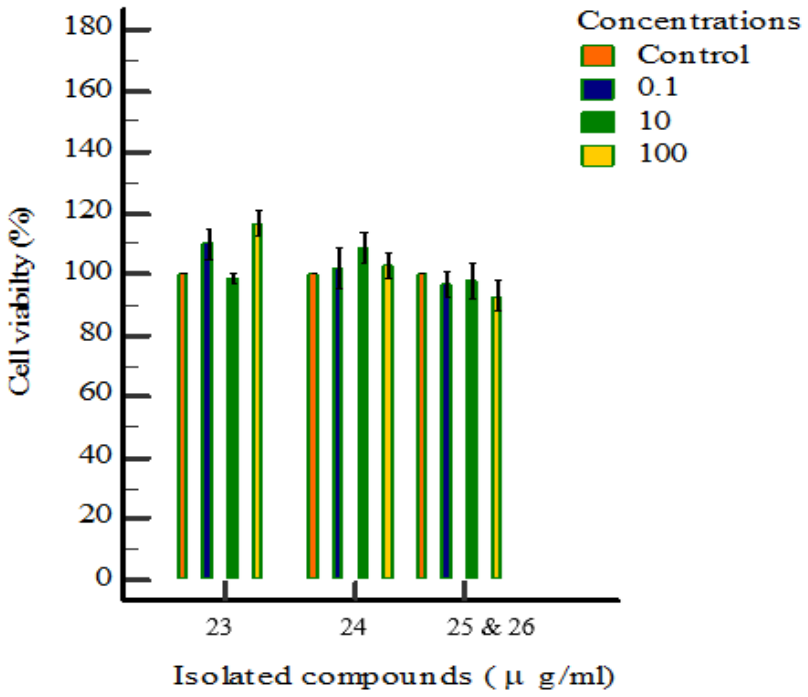

Fig.7.9: Compound activity screening in MDA-MB-231 cells, as determined by the MTT assay over 24-hours of exposure to isolated compounds **23-26**

7.7.3. Conclusion

Phytochemical study of the butanol leaf extract from *B. frutescens* resulted in the isolation and identification of four compounds for the first time from the plant, namely **23**, **24**, **25**, and **26**. Compound **23** (phenyl glycoside) is the only phenolic compound that was identified from this study. The quantities of other compounds and extracts were too small to characterize, thus the chemistry of the leaves will be subject to further investigations. In addition, any of the isolated compounds will also be tested against α-glucosidase and α-amylase assays (including other antidiabetic assays) to determine their mechanism of action towards diabetes. Furthermore, all compounds were found to be toxic towards MDA-MB-231 cells and their mechanism of cytotoxicity will be explored in future studies.

References

Abdissa, N., Heydenreich, M., Midiwo, J.O., Ndakala, A., Majer, Z., Neumann, B., StammLer, H.G., Sewald, N. and Yenesew, A., 2014. A xanthone and a phenylanthraquinone from the roots of *Bulbine frutescens*, and the revision of six seco-anthraquinones into xanthones. *Phytochemistry Letters*, *9*, pp.67-73.

Abegaz, B.M., Bezabih, M., Msuta, T., Brun, R., Menche, D., Mühlbacher, J. and Bringmann, G., 2002. Gaboroquinones A and B and 4 '-O-Demethylknipholone-4 '-O-β-d-glucopyranoside, Phenylanthraquinones from the Roots of *Bulbine frutescens*. *Journal of natural products*, *65*(8), pp.1117-1121.

Agarwal, S.K., Singh, S.S., Verma, S. and Kumar, S., 2000. Antifungal activity of anthraquinone derivatives from *Rheum emodi*. *Journal of ethnopharmacology*, *72*(1-2), pp.43-46.

Aljubiri, S.M., Mahgoub, S.A., Almansour, A.I., Shaaban, M. and Shaker, K.H., 2021. Isolation of diverse bioactive compounds from *Euphorbia balsamifera*: Cytotoxicity and antibacterial activity studies. *Saudi journal of biological sciences*, *28*(1), pp.417-426.

Amalan, V., Vijayakumar, N., Indumathi, D. and Ramakrishnan, A., 2016. Antidiabetic and antihyperlipidemic activity of p-coumaric acid in diabetic rats, role of pancreatic GLUT 2: *In vivo* approach. *Biomedicine & Pharmacotherapy*, *84*, pp.230-236.

Baiseitova, A., Jenis, J., Kim, J.Y., Li, Z.P. and Park, K.H., 2021. Phytochemical analysis of aerial part of *Ikonnikovia kaufmanniana* and their protection of DNA damage. *Natural product research*, *35*(5), pp.880-883.

Bezabih, M., Abegaz, B.M., Dufall, K., Croft, K., Skinner-Adams, T. and Davis, T.M., 2001. Antiplasmodial and antioxidant isofuranonaphthoquinones from the roots of *Bulbine capitata*. *Planta medica*, *67*(04), pp.340-344.

Bringmann, G., Menche, D., Bezabih, M., Abegaz, B.M. and Kaminsky, R., 1999. Antiplasmodial activity of knipholone and related natural phenylanthraquinones. *Planta medica*, *65*(08), pp.757-758.

Bringmann, G., Mutanyatta-Comar, J., Maksimenka, K., Wanjohi, J.M., Heydenreich, M., Brun, R., Müller, W.E., Peter, M.G., Midiwo, J.O. and Yenesew, A., 2008. Joziknipholones A and B: the first dimeric phenylanthraquinones, from the roots of *Bulbine frutescens*. *Chemistry–A European Journal*, *14*(5), pp.1420-1429.

Calixto-Campos, C., Carvalho, T.T., Hohmann, M.S., Pinho-Ribeiro, F.A., Fattori, V., Manchope, M.F., Zarpelon, A.C., Baracat, M.M., Georgetti, S.R., Casagrande, R. and Verri Jr, W.A., 2015. Vanillic acid inhibits inflammatory pain by inhibiting neutrophil recruitment, oxidative stress, cytokine production, and NFκB activation in mice. *Journal of natural products*, *78*(8), pp.1799-1808.

Casu, B., Reggiani, M., Gallo, G.G. and Vigevani, A., 1965. NMR spectra and conformation of glucose and some related carbohydrates in dimethylsulphoxide solution. *Tetrahedron letters*, *6*(27), pp.2253-2259.

Chen, M., Chai, W., Song, T., Ma, M., Lian, X.Y. and Zhang, Z., 2018. Anti-glioma natural products downregulating tumor glycolytic enzymes from marine actinomycete *Streptomyces* sp. ZZ406. *Scientific reports*, *8*(1), pp.1-10.

Choi, J., An, X., Lee, B.H., Lee, J.S., Heo, H.J., Kim, T., Ahn, J.W. and Kim, D.O., 2015. Protective effects of bioactive phenolics from jujube (*Ziziphus jujuba*) seeds against H 2 O 2–induced oxidative stress in neuronal PC-12 cells. *Food science and biotechnology*, *24*(6), pp.2219-2227.

Cicero, D., Marino, C. and Varela, O., 1991. Conformational analysis of methyl tetrofuranosides and pentofuranosides from ^{1}H, ^{1}H coupling constants.

Colson, M., Cremer Oleo GmbH and Co KG, 2013. *Bulbine frutescens* extract. U.S. Patent 8,486,459.

Dagne, E. and Yenesew, A., 1994. Anthraquinones and chemotaxonomy of the Asphodelaceae.

Dorman, D.E. and Roberts, J.D., 1970. Nuclear magnetic resonance spectroscopy. Carbon-13 spectra of some pentose and hexose aldopyranoses. *Journal of the American Chemical Society*, *92*(5), pp.1355-1361.

Erasto, P., Adebola, P.O., Grierson, D.S. and Afolayan, A.J., 2005. An ethnobotanical study of plants used for the treatment of diabetes in the Eastern Cape Province, South Africa. *African Journal of Biotechnology*, *4*(12).

Feilcke, R., Arnouk, G., Raphane, B., Richard, K., Tietjen, I., Andrae-Marobela, K., Erdmann, F., Schipper, S., Becker, K., Arnold, N. and Frolov, A., 2019. Biological activity and stability analyses of knipholone anthrone, a phenyl anthraquinone derivative isolated from *Kniphofia foliosa* Hochst. *Journal of pharmaceutical and biomedical analysis*, *174*, pp.277-285.

Felhaber, T. ed., 1997. *South African traditional healers' primary health care handbook*. Kagiso Publishers.

Habtemariam, S., 2007. Antioxidant activity of Knipholone anthrone. *Food chemistry*, *102*(4), pp.1042-1047.

Froldi, G., Baronchelli, F., Marin, E. and Grison, M., 2019. Antiglycation activity and HT-29 cellular uptake of aloe-emodin, aloin, and aloe arborescens leaf extracts. *Molecules*, *24*(11), p.2128.

Ghuman, S., Ncube, B., Finnie, J.F., McGaw, L.J., Njoya, E.M., Coopoosamy, R.M. and Van Staden, J., 2019. Antioxidant, anti-inflammatory and wound healing properties of medicinal plant extracts used to treat wounds and dermatological disorders. *South African Journal of Botany*, *126*, pp.232-240.

Gorin, P.A. and Mazurek, M., 1976. Carbon-13 and proton nuclear magnetic resonance studies on methyl aldofuranosides and their O-alkyl derivatives. *Carbohydrate research*, *48*(2), pp.171-186.

Habtemariam, S., 2010. Knipholone anthrone from *Kniphofia foliosa* induces a rapid onset of necrotic cell death in cancer cells. *Fitoterapia*, *81*(8), pp.1013-1019.

Hu, Y., Martinez, E.D. and MacMillan, J.B., 2012. Anthraquinones from a marine-derived *Streptomyces spinoverrucosus*. *Journal of natural products*, *75*(10), pp.1759-1764.

Isaza, J.H., Ito, H. and Yoshida, T., 2001. A flavonol glycoside-lignan ester and accompanying acylated glucosides from *Monochaetum multiflorum*. *Phytochemistry*, *58*(2), pp.321-327.

Jibril, S., Sirat, H.M. and Basar, N., 2017. Bioassay-guided isolation of antioxidants and α-glucosidase inhibitors from the root of *Cassia sieberiana* DC (Fabaceae). *Rec. Nat. Prod*, *11*, pp.406-410.

Kiliç, I. and Yeşiloğlu, Y., 2013. Spectroscopic studies on the antioxidant activity of p-coumaric acid. *Spectrochimica Acta Part A: Molecular and Biomolecular Spectroscopy*, *115*, pp.719-724.

Kim, S.J., Kim, M.C., Lee, B.J., Park, D.H., Hong, S.H. and Um, J.Y., 2010. Anti-Inflammatory activity of chrysophanol through the suppression of NF-kB/caspase-1 activation *in vitro* and in vivo. *Molecules*, *15*(9), pp.6436-6451.

Konda, Y., Funato, N., Harigaya, Y., Li, X., Zhang, D. and Onda, M., 1991. A phenolic glycoside from *Artemisia sacrorum*. *Journal of heterocyclic chemistry*, *28*(8), pp.1949-1951.

Kuroda, M., Mimaki, Y., Sakagami, H. and Sashida, Y., 2003. Bulbinelonesides A− E, Phenylanthraquinone Glycosides from the Roots of *Bulbinella floribunda*. *Journal of natural products*, *66*(6), pp.894-897.

Kushwaha, P.P., Kumar, A., Maurya, S., Singh, A.K., Sharma, A.K. and Kumar, S., 2019. *Bulbine frutescens* phytochemicals as a promising anti-cancer drug discovery source: A computational study. In *Phytochemistry: An in-silico and in-vitro Update* (pp. 491-510). Springer, Singapore.

Lee, M.S. and Sohn, C.B., 2008. Anti-diabetic properties of chrysophanol and its glucoside from *Rhubarb* rhizome. *Biological and Pharmaceutical Bulletin*, *31*(11), pp.2154-2157.

Liao, H.X., Shao, T.M., Mei, R.Q., Huang, G.L., Zhou, X.M., Zheng, C.J. and Wang, C.Y., 2019. Bioactive secondary metabolites from the culture of the mangrove-derived fungus *Daldinia eschscholtzii* HJ004. *Marine drugs*, *17*(12), p.710.

Lou, Z., Wang, H., Rao, S., Sun, J., Ma, C. and Li, J., 2012. p-Coumaric acid kills bacteria through dual damage mechanisms. *Food control*, *25*(2), pp.550-554.

Mocktar, C., 2000. *Antimicrobial and chemical analyses of selected bulbine species* (Doctoral dissertation).

Mutanyatta, J., Bezabih, M., Abegaz, B.M., Dreyer, M., Brun, R., Kocher, N. and Bringmann, G., 2005. The first 6′-O-sulfated phenylanthraquinones: isolation from *Bulbine frutescens*, structural elucidation, enantiomeric purity, and partial synthesis. *Tetrahedron*, *61*(35), pp.8475-8484.

Park, M.Y., Kwon, H.J. and Sung, M.K., 2009. Evaluation of aloin and aloe-emodin as anti-inflammatory agents in aloe by using murine macrophages. *Bioscience, Biotechnology, and Biochemistry*, *73*(4), pp.828-832.

Pather, N., Viljoen, A.M. and Kramer, B., 2011. A biochemical comparison of the in vivo effects of *Bulbine frutescens* and *Bulbine natalensis* on cutaneous wound healing. *Journal of ethnopharmacology*, *133*(2), pp.364-370.

Pooley, E., 1998. *A field guide to wildflowers: KwaZulu-Natal and the eastern region*. Natal Flora Publ. Trust.

Pomin, V.H., 2012. Unravelling glycobiology by NMR spectroscopy. In *Glycosylation* pp. 63-98. London: IntechOpen.

Prince, P.S.M., Rajakumar, S. and Dhanasekar, K., 2011. Protective effects of vanillic acid on electrocardiogram, lipid peroxidation, antioxidants, proinflammatory markers and histopathology in isoproterenol induced cardiotoxic rats. *European journal of pharmacology*, *668*(1-2), pp.233-240.

Qian, W., Yang, M., Wang, T., Sun, Z., Liu, M., Zhang, J., Zeng, Q., Cai, C. and Li, Y., 2020. Antibacterial mechanism of vanillic acid on physiological, morphological, and biofilm properties of carbapenem-resistant enterobacter hormaechei. *Journal of food protection*, *83*(4), pp.576-583.

Roslund, M.U., Tähtinen, P., Niemitz, M. and Sjöholm, R., 2008. Complete assignments of the ^{1}H and ^{13}C chemical shifts and *J* H, H coupling constants in NMR spectra of D-glucopyranose and all D-glucopyranosyl-D-glucopyranosides. *Carbohydrate research*, *343*(1), pp.101-112.

Shen, S., Ding, X., Ouyang, M.A., Wu, Z.J. and Xie, L.H., 2010. A new phenolic glycoside and cytotoxic constituents from *Celosia argentea*. *Journal of Asian natural products research*, *12*(9), pp.821-827.

Shikalepo, R., Mukakalisa, C., Kandawa-Schulz, M., Chingwaru, W. and Kapewangolo, P., 2018. In vitro anti-HIV and antioxidant potential of *Bulbine frutescens* (Asphodelaceae). *Journal of Herbal Medicine*, *12*, pp.73-78.

Tambama, P., Abegaz, B. and Mukanganyama, S., 2014. Antiproliferative activity of the isofuranonaphthoquinone isolated from *Bulbine frutescens* against jurkat T cells. *BioMed research international*, *2014*.

van Huyssteen, M., Milne, P.J., Campbell, E.E. and van de Venter, M., 2011. Antidiabetic and cytotoxicity screening of five medicinal plants used by traditional African health practitioners in the Nelson Mandela Metropole, South Africa. *African Journal of Traditional, Complementary and Alternative Medicines*, *8*(2).

Van Jaarsveld, E. and Forster, P.I., 2020. *Bulbine* ASPHODELACEAE. *Monocotyledons*, pp.713-739.

van Staden, L.F. and Drewes, S.E., 1994. Knipholone from *Bulbine latifolia* and *Bulbine frutescens*. *Phytochemistry*, *35*(3), pp.685-686.

Van Wyk, B.E., Yenesew, A. and Dagne, E., 1995. Chemotaxonomic significance of anthraquinones in the roots of Asphodeloideae (Asphodelaceae). *Biochemical Systematics and Ecology*, *23*(3), pp.277-281.

Van Wyk, B.E., Oudtshoorn, B.V. and Gericke, N., 1997. *Medicinal Plants of South Africa*. Briza.

Vinothiya, K. and Ashokkumar, N., 2017. Modulatory effect of vanillic acid on antioxidant status in high fat diet-induced changes in diabetic hypertensive rats. *Biomedicine & Pharmacotherapy*, *87*, pp.640-652.

Wang, L., Cui, Y.L., Zhang, Z., Lin, Z.F. and Chen, D.C., 2017. *Rhubarb* monomers protect intestinal mucosal barrier in sepsis via junction proteins. *Chinese medical journal*, *130*(10), p.1218.

Wang, C.N., Lu, H.M., Gao, C.H., Guo, L., Zhan, Z.Y., Wang, J.J., Liu, Y.H., Xiang, S.T., Wang, J. and Luo, X.W., 2020. Cytotoxic benzopyranone and xanthone derivatives from a coral symbiotic fungus *Cladosporium halotolerans* GXIMD 02502. *Natural Product Research*, pp.1-8.

Wang, A., Gao, X., Huo, X., Huang, S., Feng, L., Sun, C., Zhang, B., Ma, X., Jia, J. and Wang, C., 2018. Antioxidant acetophenone glycosides from the roots of *Euphorbia ebracteolata* Hayata. *Natural product research*, *32*(18), pp.2187-2192.

Wu, G.D., Serianni, A.S. and Barker, R., 1983. Stereoselective deuterium exchange of methylene protons in methyl tetrofuranosides: hydroxymethyl group conformations in methyl pentofuranosides. *The Journal of Organic Chemistry*, *48*(10), pp.1750-1757.

Zhang, H., Guo, Z., Wu, N., Xu, W., Han, L., Li, N. and Han, Y., 2012. Two novel naphthalene glucosides and an anthraquinone isolated from *Rumex dentatus* and their antiproliferation activities in four cell lines. *Molecules*, *17*(1), pp.843-850.

Chapter 8

Conclusions and Future Recommendations.

Ethnopharmacological studies of medicinal plants are an invaluable way of targeting (new) compounds which may have useful applications against various diseases like diabetes. As a result, documentation of these medicinal plants is imperative. Three South African indigenous medicinal plants (*Helichrysum petiolare*, *H. splendidum*, and *Bulbine frutescens*) with a documented use traditionally in the management of diabetes mellitus were selected to carry out a comprehensive phytochemical investigation of the extracts (hexane, DCM, EtOAc, and BuOH). Initially, extraction of the plant materials was achieved by 80% methanol which was followed by partitioning sequentially (hexane, DCM, EtOAc, and BuOH). Structural characterization was of the isolated compounds was achieved by means of spectroscopic techniques (1D and 2N NMR, HRESIMS, and UV-vis). Furthermore, the extracts, including isolated compounds were screened for their ability to inhibit α-glucosidase and α-amylase enzymes to support the ethnopharmacological claims. Cytotoxicity effects using MTT assay of the isolated compounds were also evaluated against MDA-MB-231 cells.

Phytochemical study of the leaves of *Helichrysum petiolare* resulted in the isolation and identification of eleven compounds, two of which are new and were named petiolactone A (**1**) and B (**2**). Compounds **3**–**11** are reported for the first time from this plant. This study has also provided for the first time the ^{13}C NMR data of compound **5**. Biological screening (at 200 µg/mL) of the extracts and isolated compounds in the α-glucosidase and α-amylase assays did not show any significant activity in both assays. It was suggested that either the active metabolites towards diabetes have not been isolated or are not present in appreciable amounts in the leaves or there's a synergistic effect that occurs when the whole plant and/or extract is used. This will be explored in greater detail in future studies. In the MTT assay, compound **1** (petiolactone A) was found to be the most active (IC_{50} = 107.8 and 43.65 µg/mL, respectively, after 24- and 72-hours exposure) showing a clear dose-depended reduction in cell viability at 100 µg/mL ($P<0.001$). Interestingly, the derivative of this compound (petiolactone B) was more toxic to the cell, which may speak heavily about their differences in chemistry. Compounds **5** and **3**, respectively, had IC_{50} values at 40.03 and 41.32 µg/mL after 72 hours of exposure (at the same concentration). Further studies involving other types of cell lines still need to be done to establish the mechanism of cytotoxicity of the compounds and extracts.

Phytochemical study of the leaves of *Helichrysum splendidum* resulted in the isolation and identification of eleven compounds (some of which were obtained as inseparable mixtures **12** and **13**, **14** and **15**, as well as **21** and **22**). Among the list, compounds **18**, **19**, **20**, **21**, and **22** were reported for the first time from this plant. In addition, compound **15** (given the trivial name iso-lemmonin C) was tentatively proposed as a new stereoisomer of lemmonin C (compound **14**) based on 1D and 2D NMR experiments which showed distinguishable peaks (δ_C 84.0 assigned C-8 in compound 15, while this appeared 82.8 for lemmnonin C). Further purification, however, using HPLC, chemical reactions such as acetylation or methylation, including X-ray crystallography studies will need to be done to confirm the proposed structure. Similarly, chemical derivatization (acetylation or methylation) followed by purification (open column silica gel chromatography) of compound **18**, which we have proposed as a biflavonoid, needs to be explored to unambiguously confirm its structure. Furthermore, this study has also provided for the first time the ^{13}C NMR for compounds **12** and **13** isomers. The antidiabetic activity of the isolated compounds and extracts was explored to establish their potential in inhibiting α-glucosidase and α-amylase enzymes. However, none of them showed any significant inhibition activity in α-glucosidase and α-amylase enzyme assays. More studies would need to be done, particularly for the aqueous extract since it displayed comparable results (35.2 %) to acarbose (38.2 %), control, at the screening concentration (200 µg/mL). On the other hand, upon evaluating the cytotoxicity effects of the isolated compounds from this plant against MDA-MB-231 cells, it was established that only **16**, **17**, **19**, including the inseparable mixtures of **14** and **15**, as well as **21** and **22**, showed significant activity. In fact, compounds **21** and **22** (identified to be a mixture of ursolic and oleanolic acid) displayed a significant ($P<0.001$) trend between control and 100 µg/mL, followed, respectively, by compounds **17**, and **16**. The IC_{50} values of the compounds (**21** and **22**, **16**, **17**, **19**, as well as **14** and **15**), respectively, were found to be 24.05, 38.04, 40.27, 48.79, and 67.83 µg/mL. We recommend further studies using more cell lines to determine the primary mechanism of cytotoxicity of the compounds.

The phytochemical study of the leaf extracts from *Bulbine frutescens* was only limited to the butanol extract since the quantities of other extracts were too small. Nonetheless, four known compounds (**23**, **24**, **25**, and **26**) were characterized for the first time from this plant. Compound **23** (phenyl glycoside) is the only phenolic compound that was identified from this study. All compounds and extracts did not display any inhibition activity in the α-glucosidase and α-amylase assays. In addition, all compounds were found to be toxic towards MDA-MB-

231 cells. In future studies, reasonable amounts of plant material must be used to obtain sufficient yields of chemical compounds in the plant. In turn, this will allow a comprehensive evaluation of the antidiabetic and cytotoxicity mechanism of the isolates/extracts.

In general, the extraction approach (sequential extraction with solvents of different polarity) that was used in this study proved to be an effective way to target compounds rather than isolating directly from the total extract (80% methanolic extract), where there may be a huge risk of missing or overlooking some chemical compounds. Furthermore, there is a clear gap that exists between the claimed ethnopharmacological use of these medicinal plants in the management of diabetes and identifying the responsible metabolites. Therefore, we recommend that more studies should be aimed at identifying the active compounds and validating their mechanism of action towards diabetes. This will be explored in future studies.

Appendix A

Spectroscopic data of the isolated compounds from *Helichrysum petiolare*

Plate 3A: ^{1}H-NMR spectrum (DMSO-d_6, 400 MHz) of compound **3**

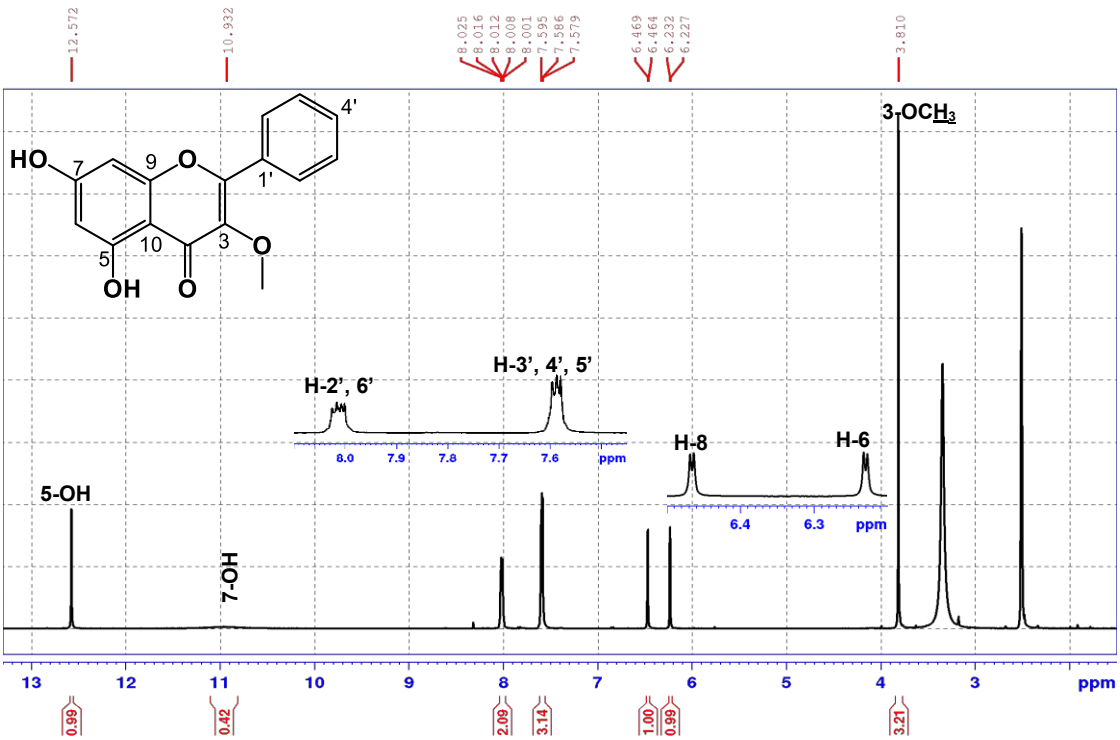

Plate 3B: COSY spectrum (DMSO-d_6) compound **3**

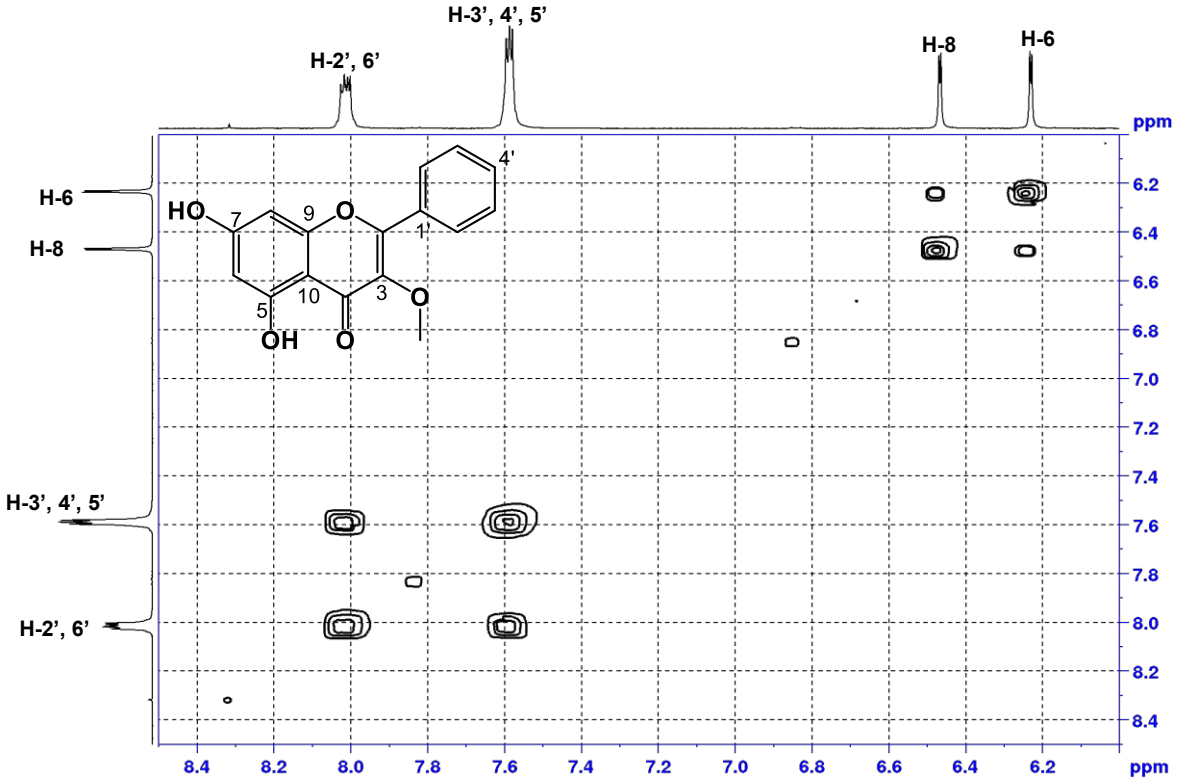

Plate 3C: ^{13}C-NMR spectrum (DMSO-d_6, 100 MHz) of compound **3**

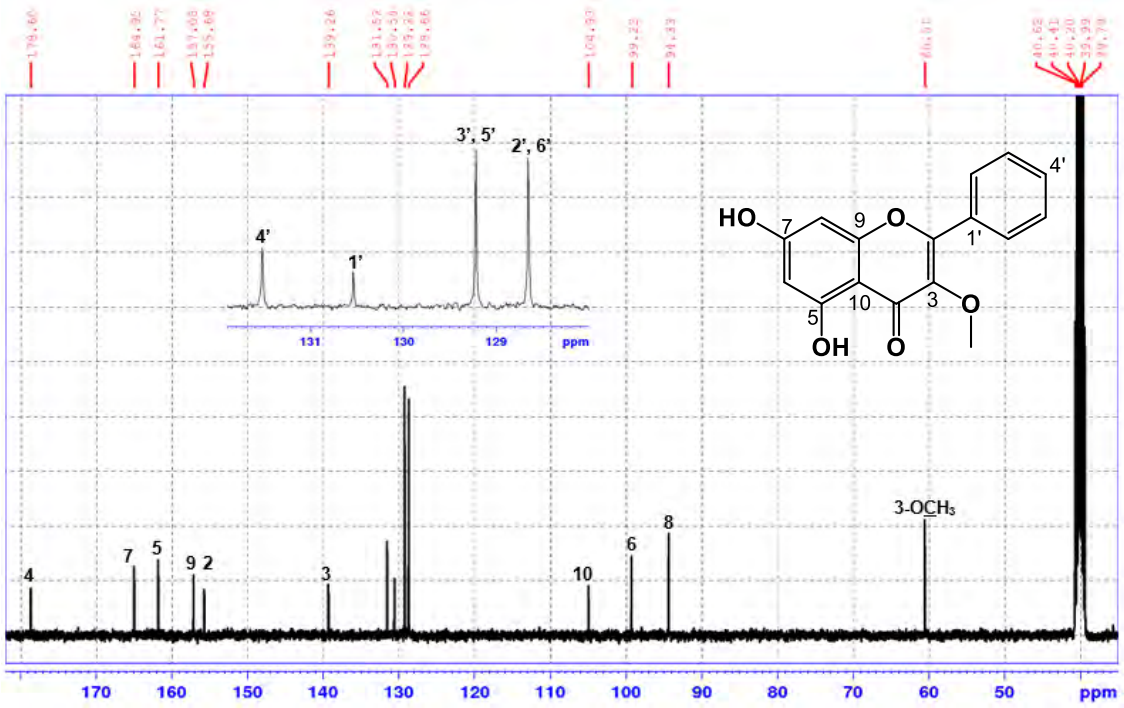

Plate 3D: DEPT-135 spectrum (DMSO-d_6) of compound **3**

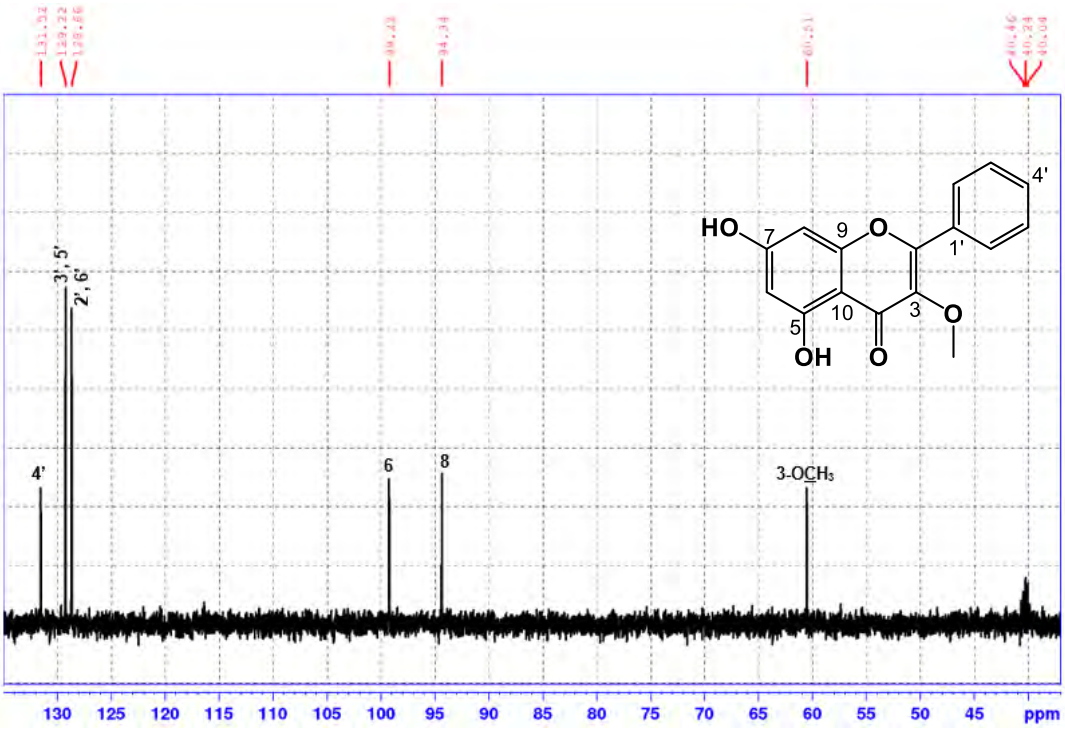

Plate 3E: HSQC spectrum (DMSO-d_6) of compound **3**

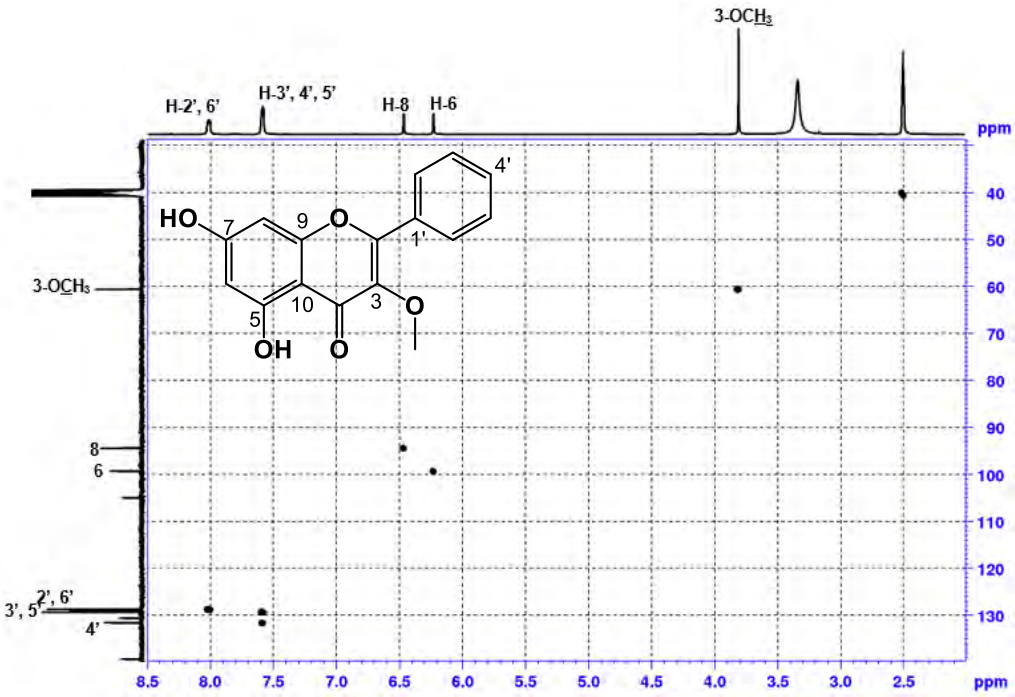

Plate 3F: HMBC spectrum (DMSO-d_6) of compound **3**

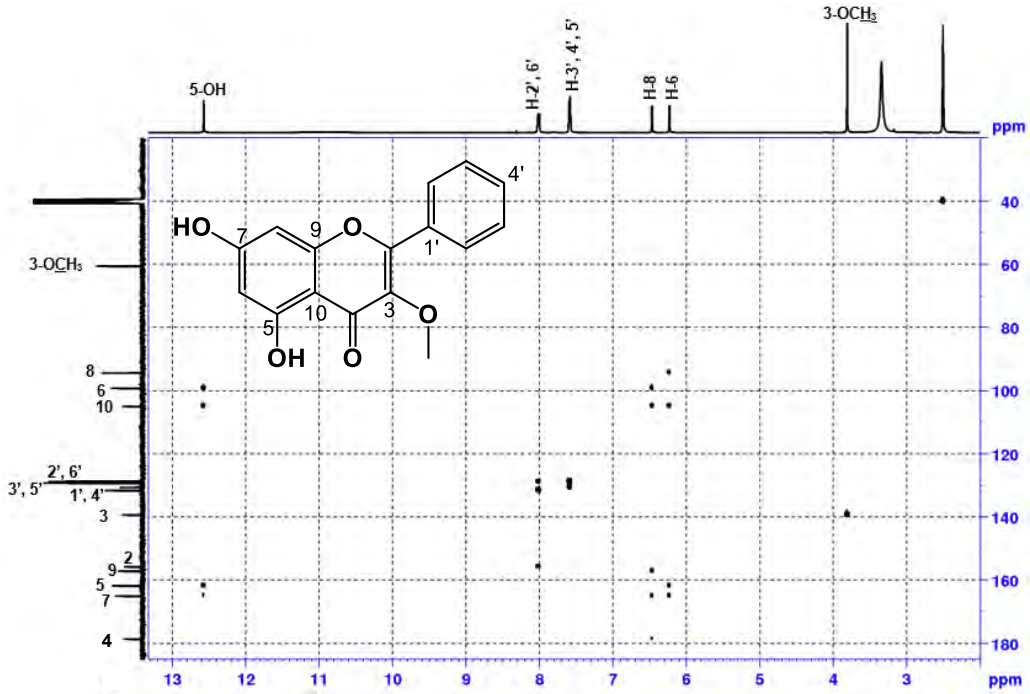

Plate 4A: ^{1}H-NMR spectrum ($CDCl_3$, 400 MHz) of compound **4**

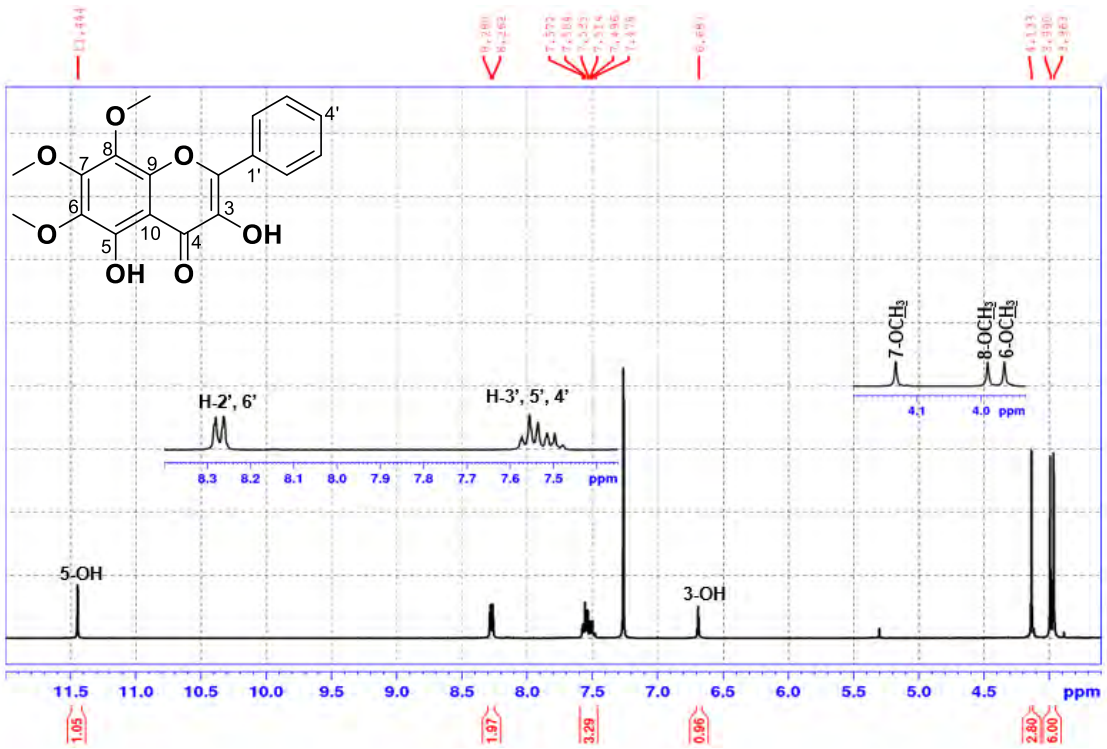

Plate 4B: COSY spectrum ($CDCl_3$) of compound **4**

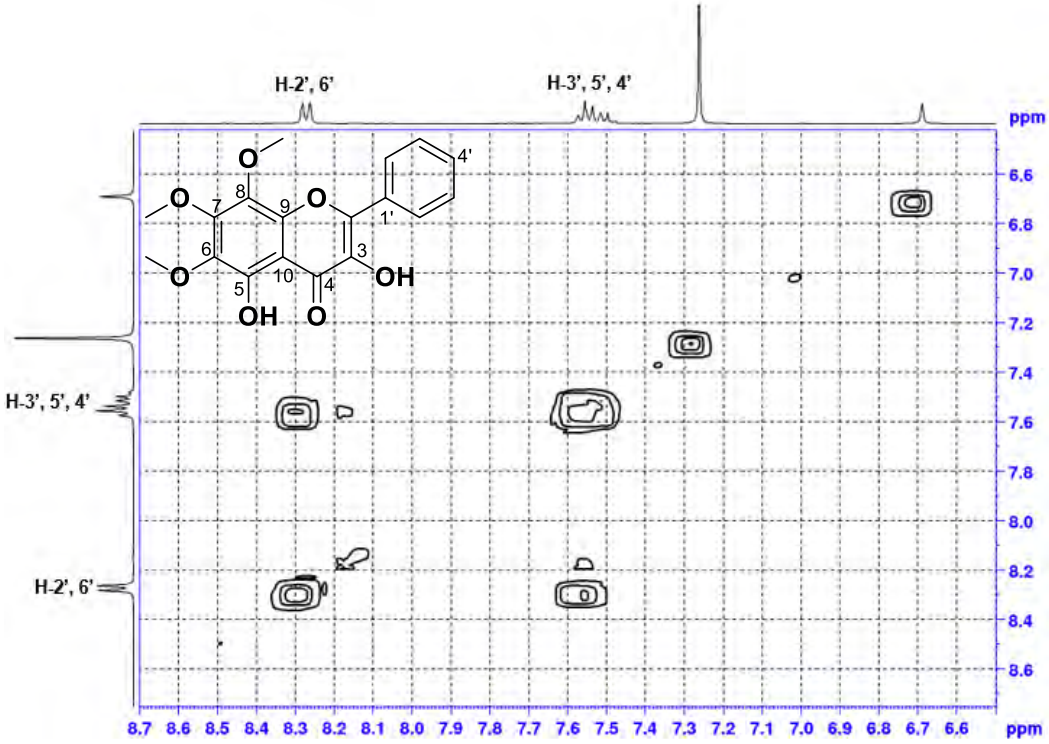

Plate 4C: ^{13}C-NMR spectrum ($CDCl_3$, 100 MHz) of compound **4**

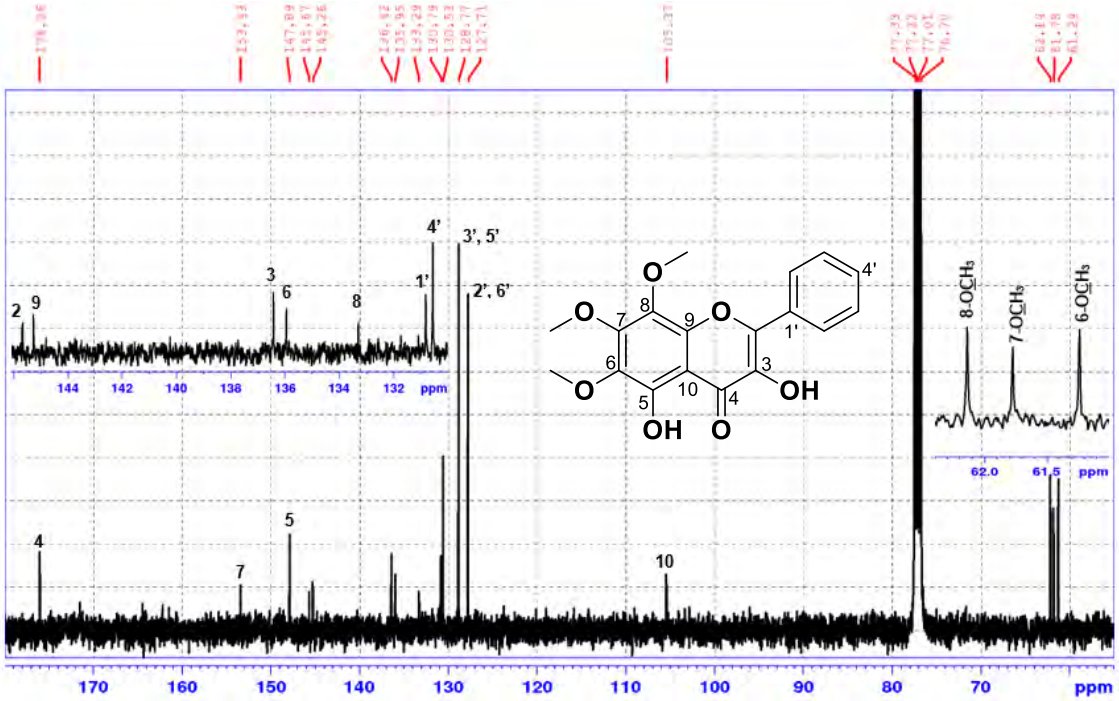

Plate 4D: DEPT-135 spectrum ($CDCl_3$) of compound **4**

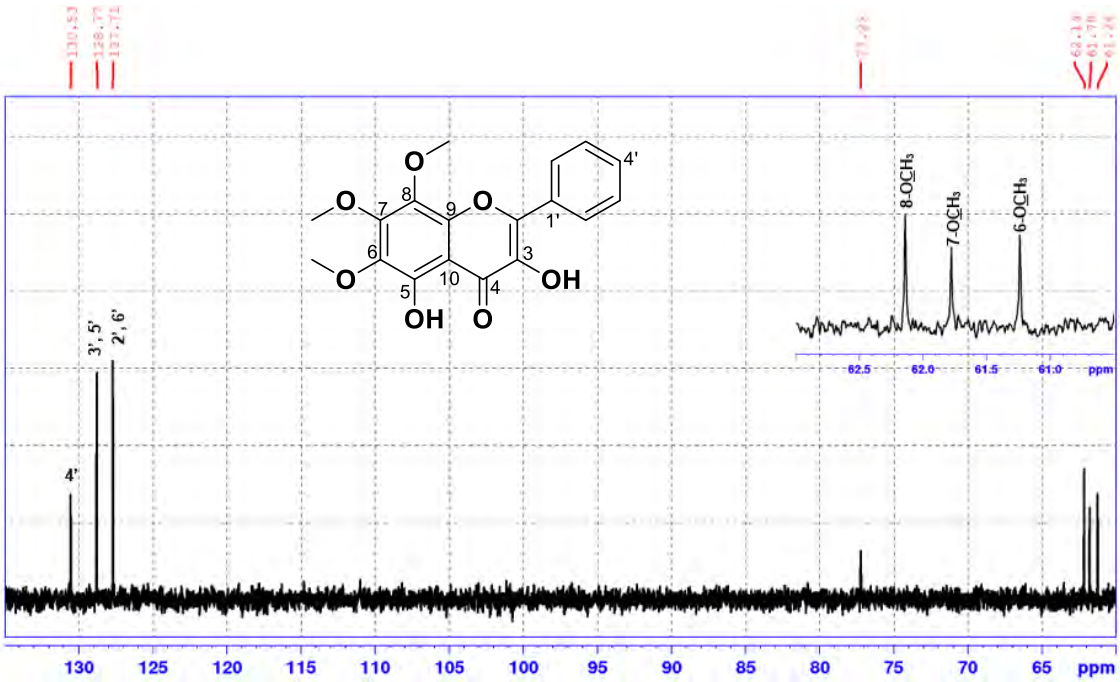

Plate 4E: HSQC spectrum ($CDCl_3$) of compound **4**

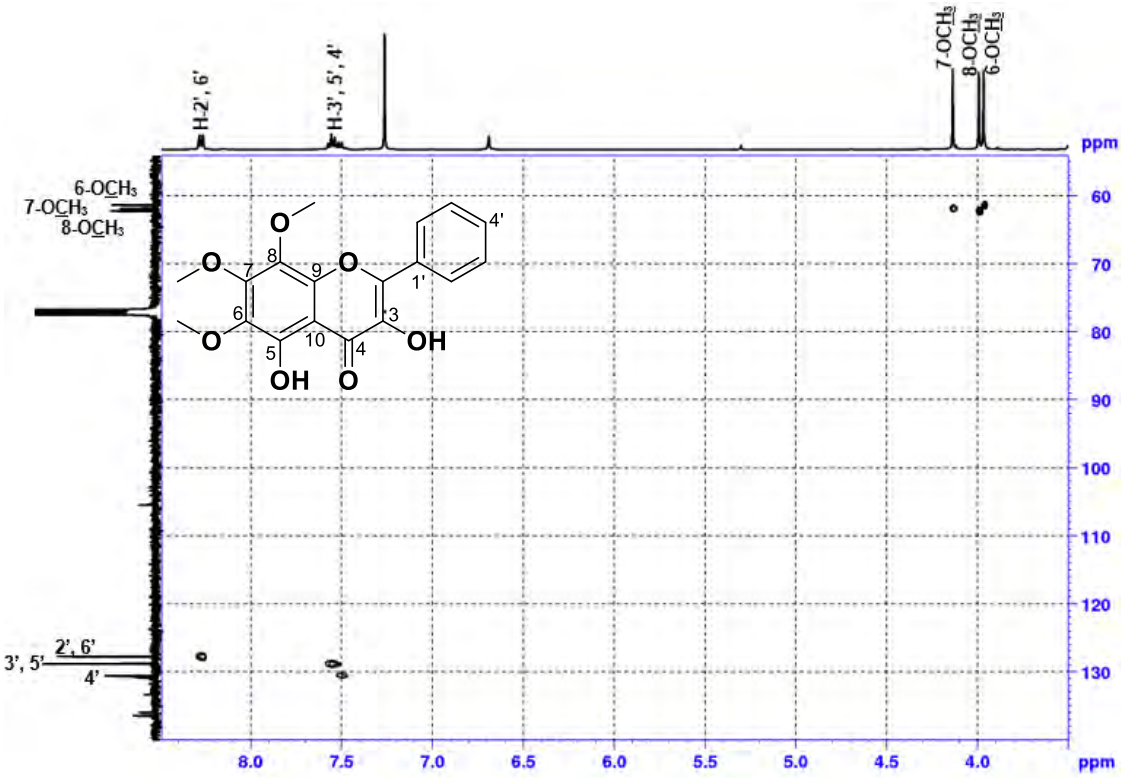

Plate 4F: HMBC spectrum ($CDCl_3$) of compound **4**

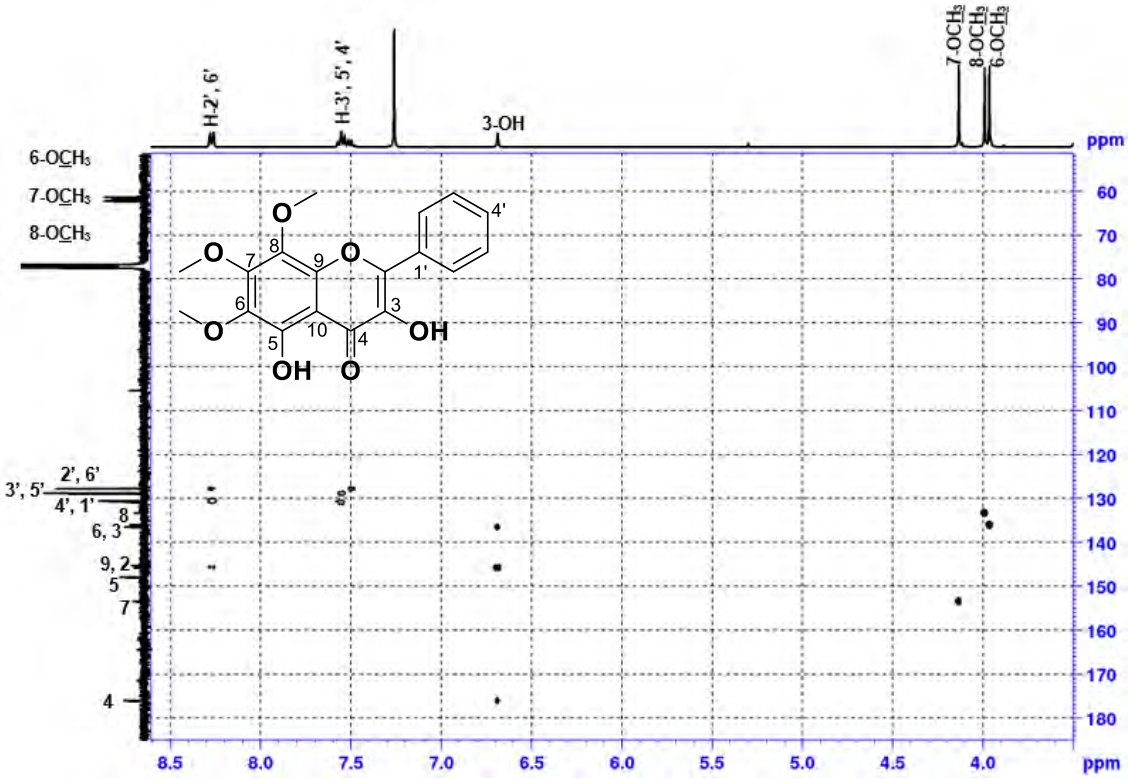

Plate 4G: HR-ESI-MS spectrum of compound **4**

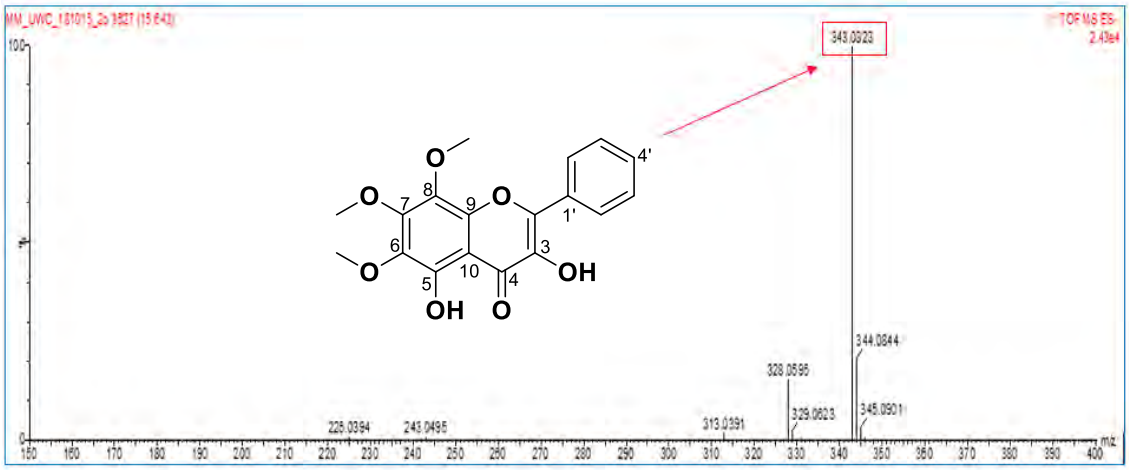

Plate 5A: ^{1}H-NMR spectrum ($CDCl_3$, 400 MHz) of compound **5**

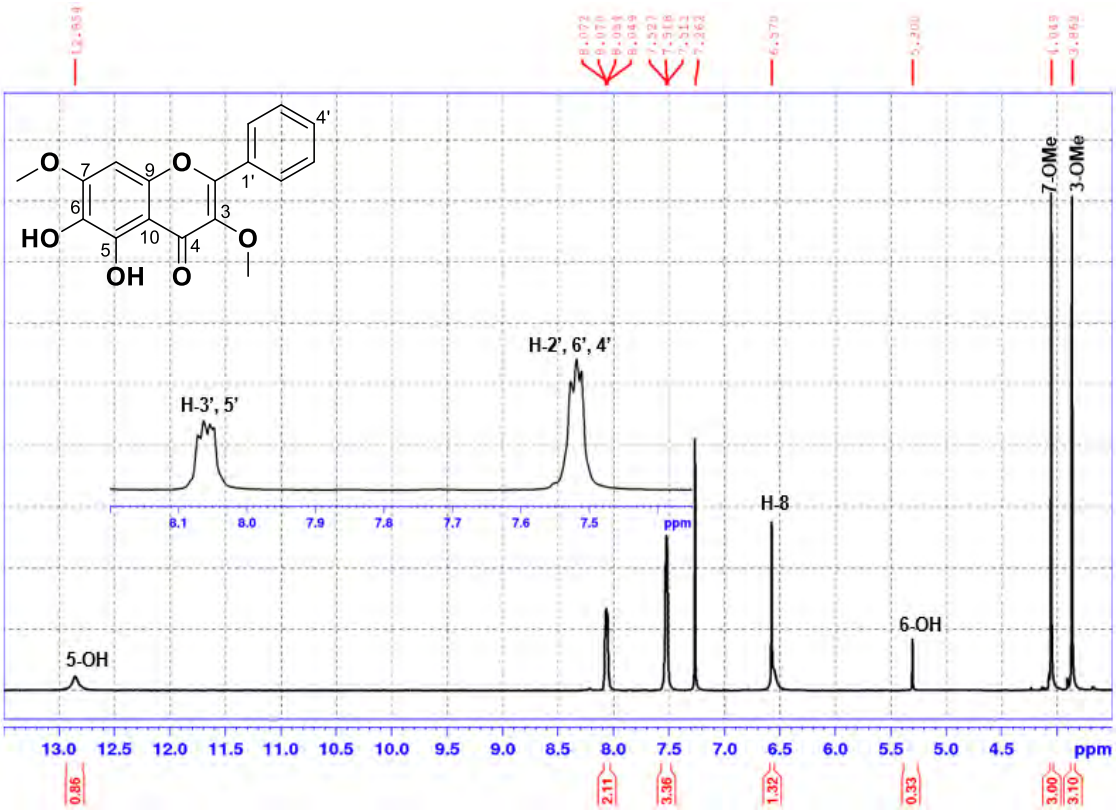

Plate 5B: COSY spectrum ($CDCl_3$) of compound **5**

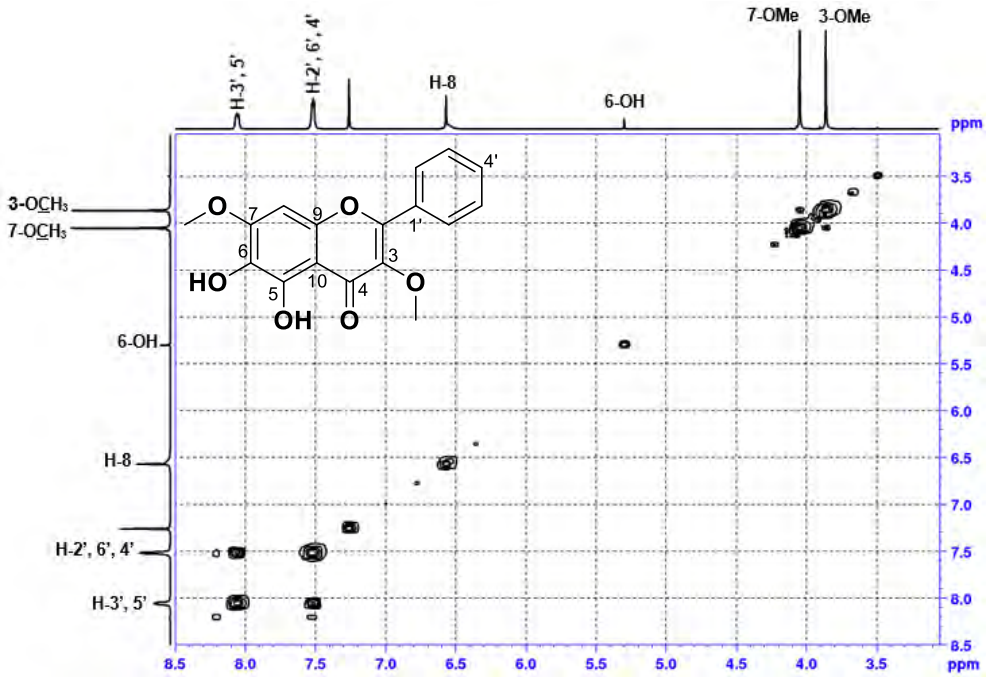

Plate 5C: ^{13}C-NMR spectrum ($CDCl_3$, 100 MHz) of compound **5**

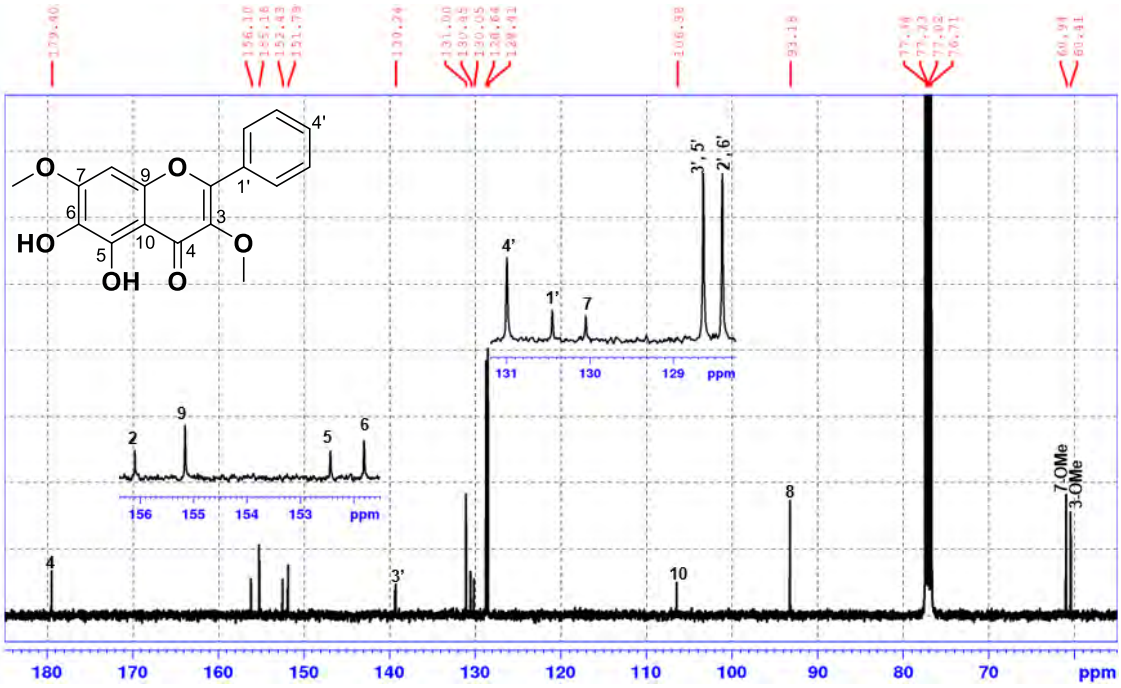

Plate 5D: DEPT-135 spectrum ($CDCl_3$) of compound **5**

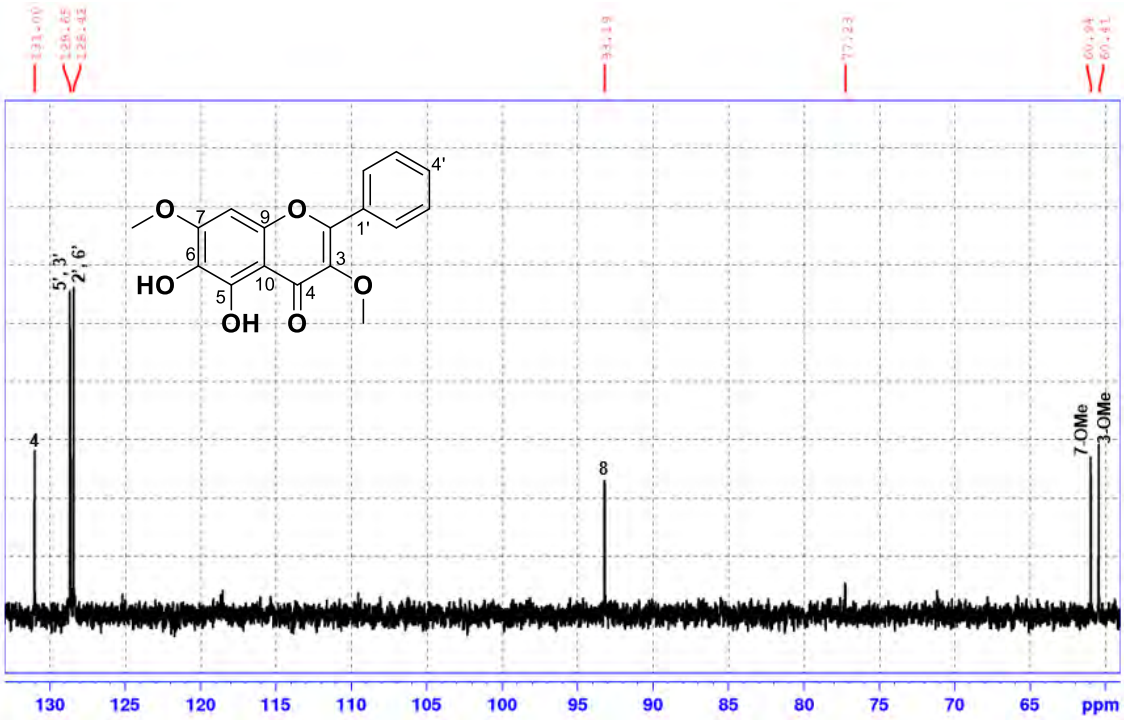

Plate 5E: HSQC spectrum ($CDCl_3$) of compound **5**

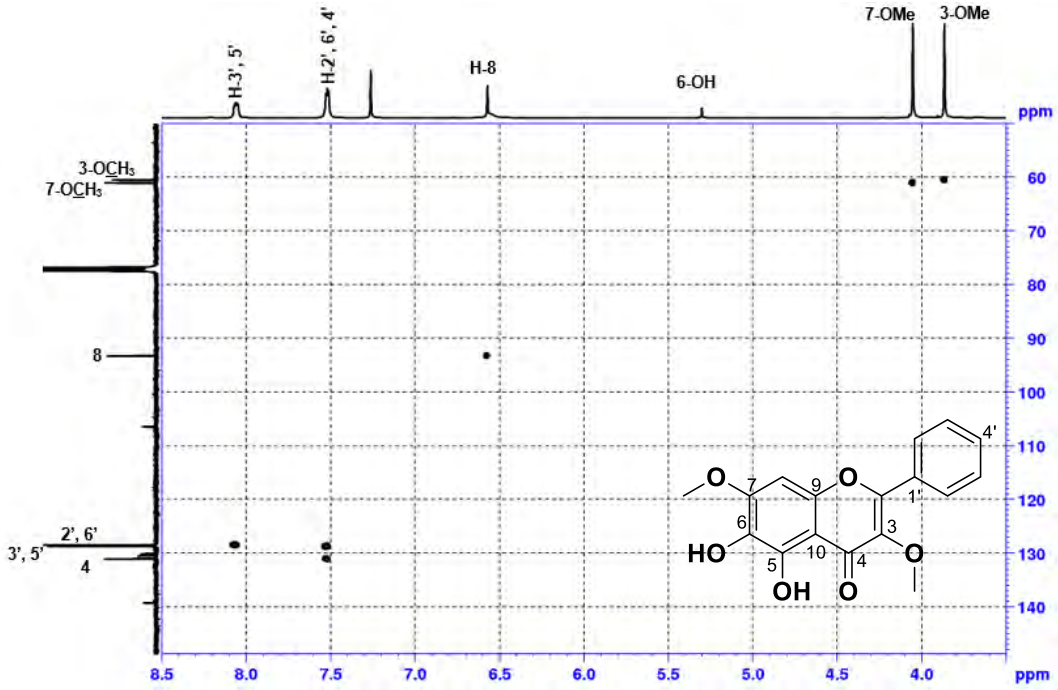

Plate 5F: HMBC spectrum ($CDCl_3$) of compound **5**

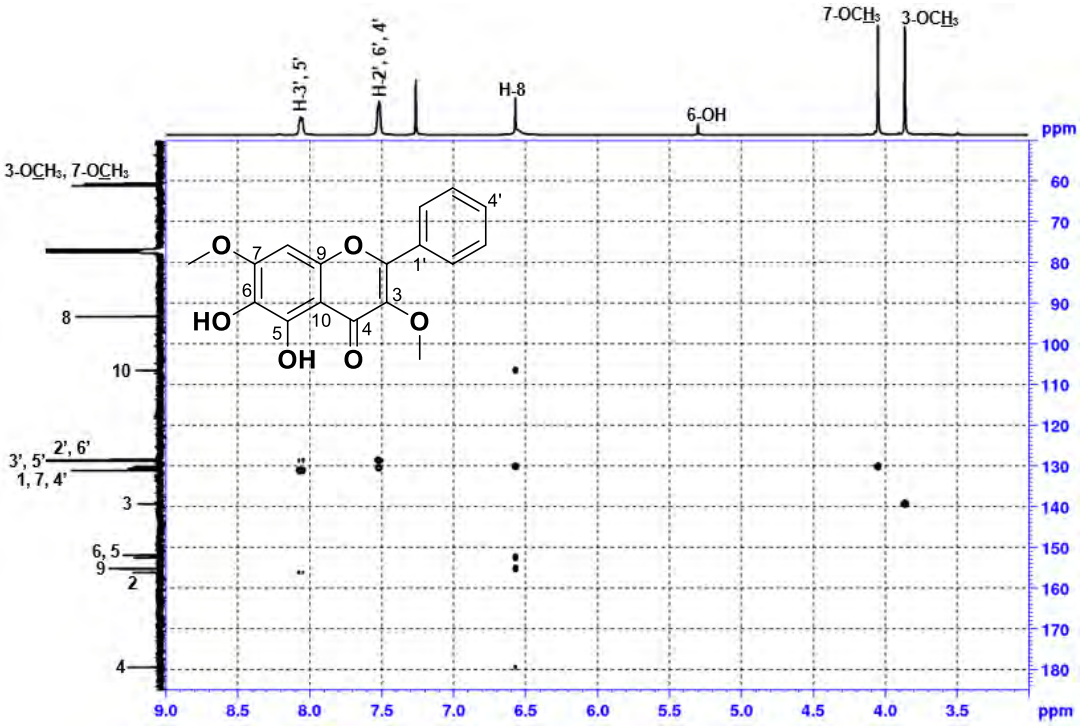

Plate 5G: HR-ESI-MS spectrum of compound **5**

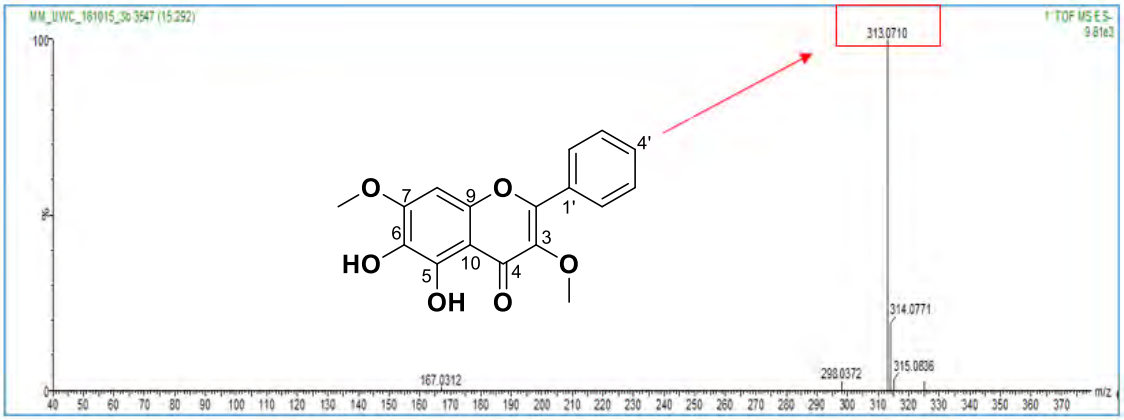

Plate 6A: ^{1}H-NMR spectrum ($CDCl_3$, 400 MHz) of compound **6**

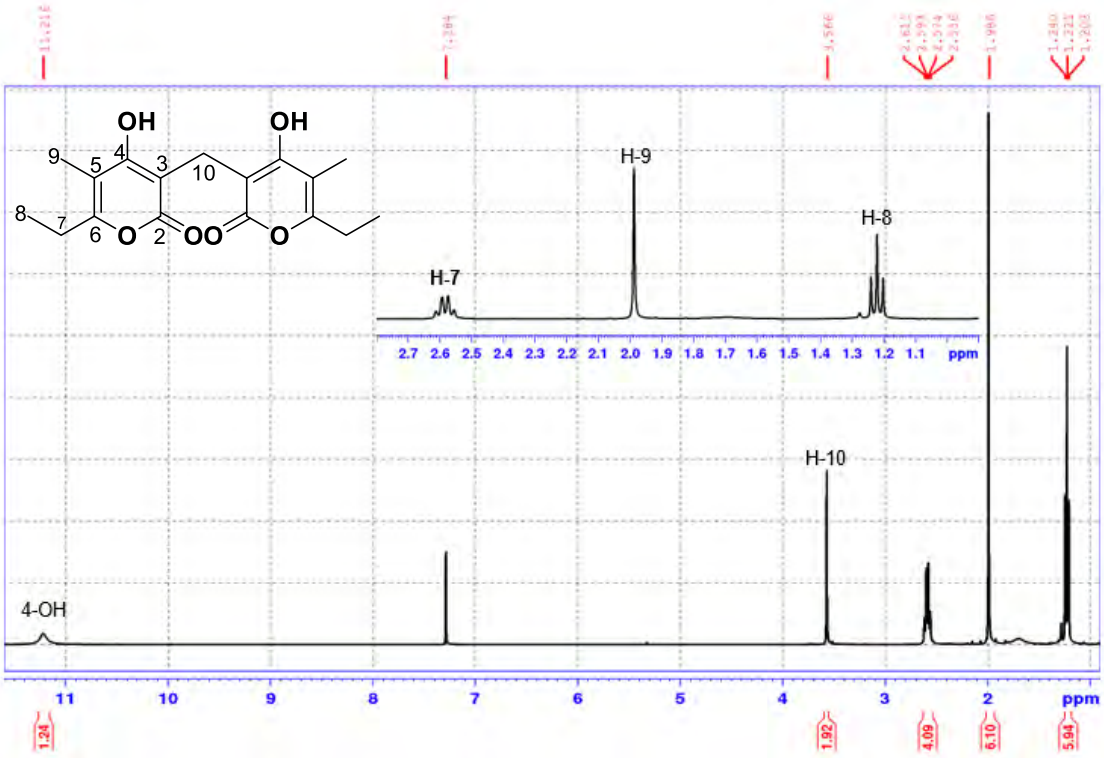

Plate 6B: COSY spectrum ($CDCl_3$) of compound **6**

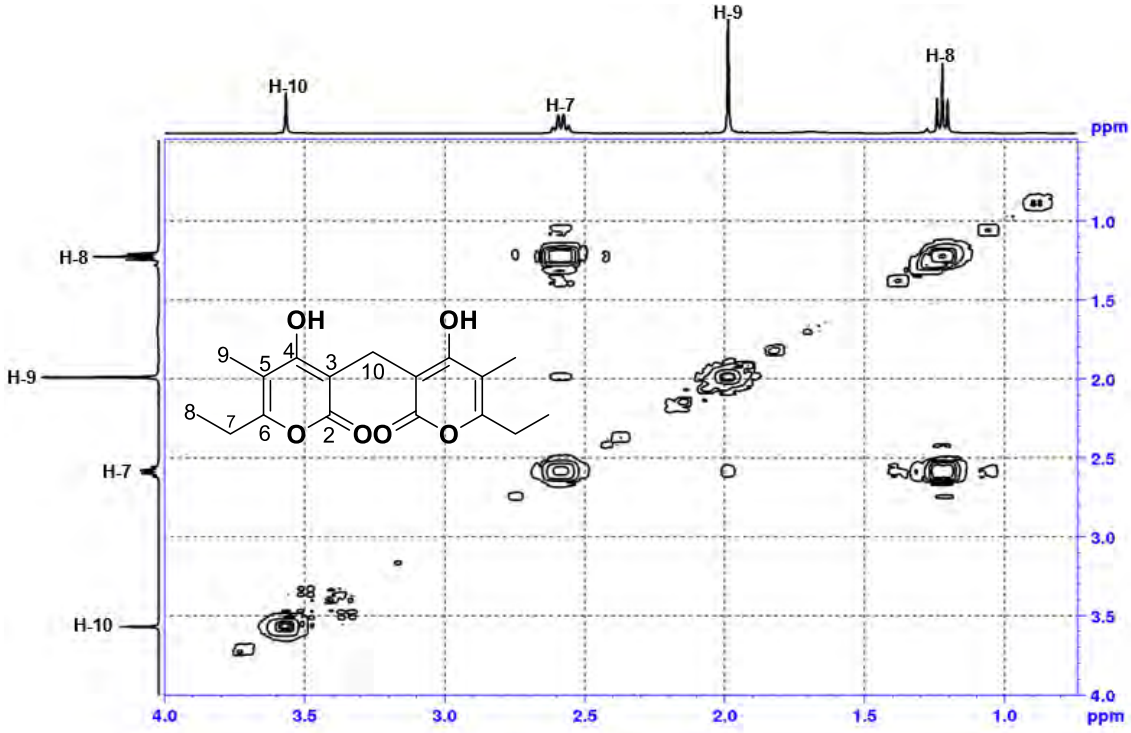

Plate 6C: 13C-NMR spectrum ($CDCl_3$, 100 MHz) of compound **6**

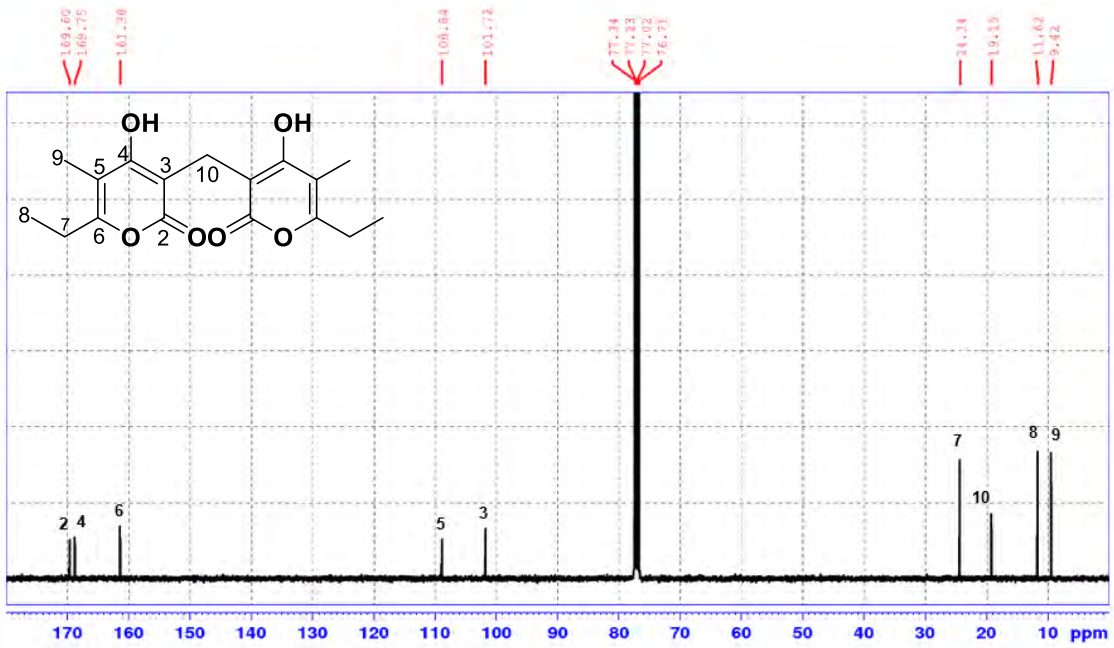

Plate 6D: DEPT-135 spectrum ($CDCl_3$) of compound **6**

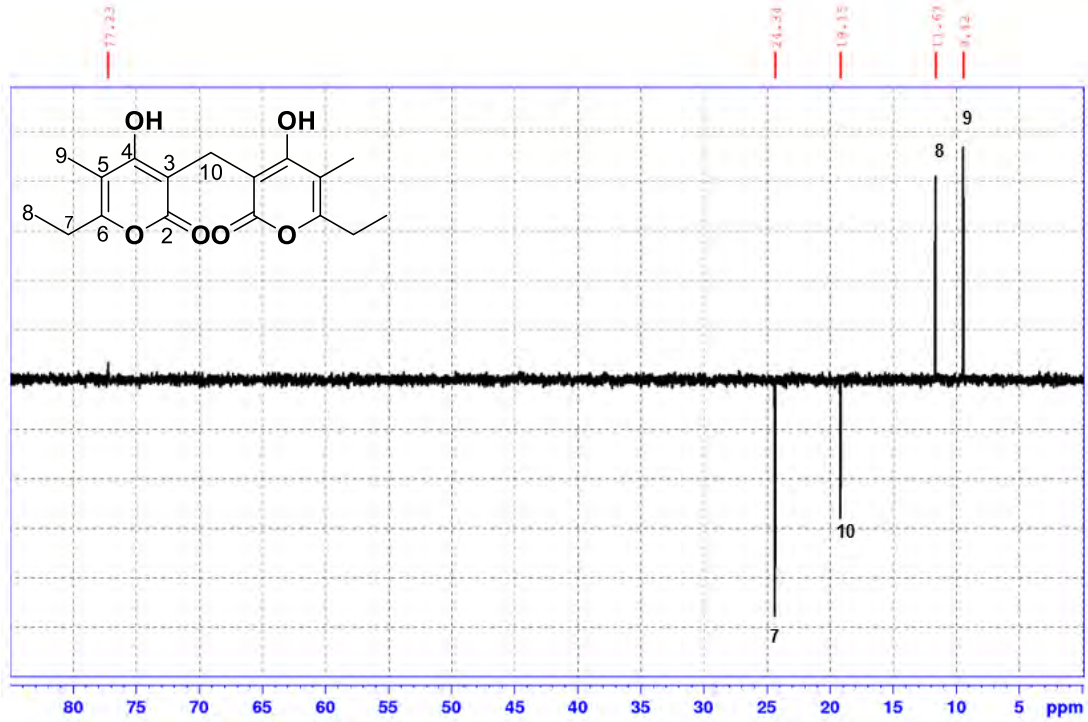

Plate 6E: HSQC spectrum ($CDCl_3$) of compound **6**

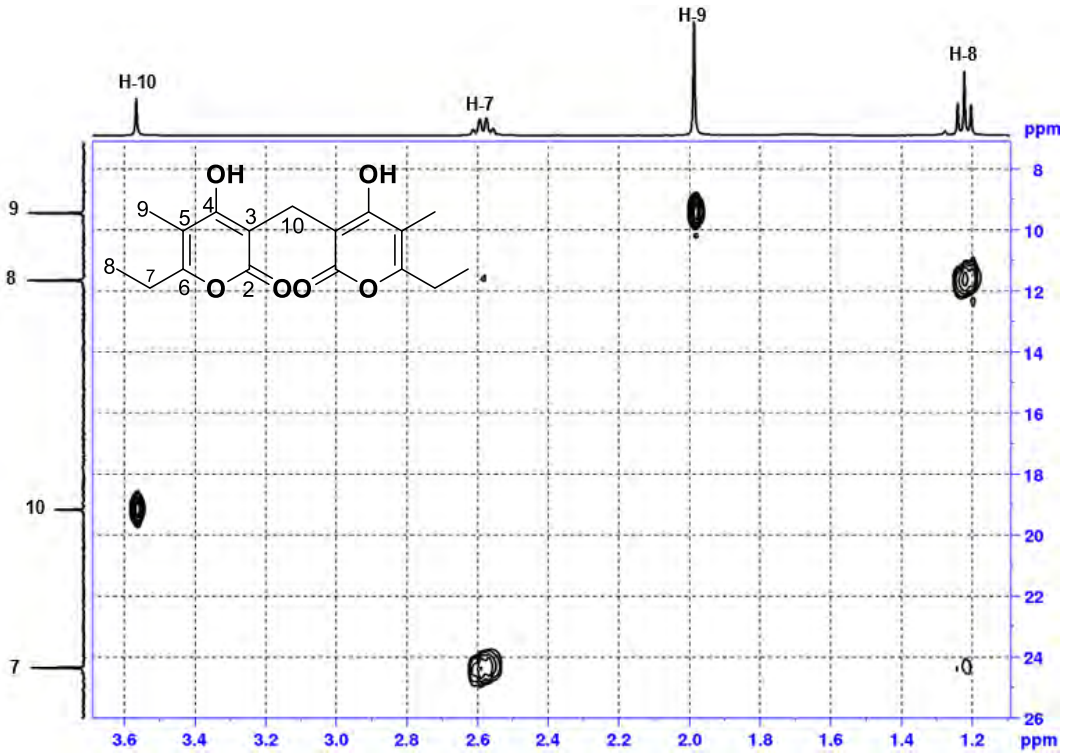

Plate 6F: HMBC spectrum ($CDCl_3$) of compound **6**

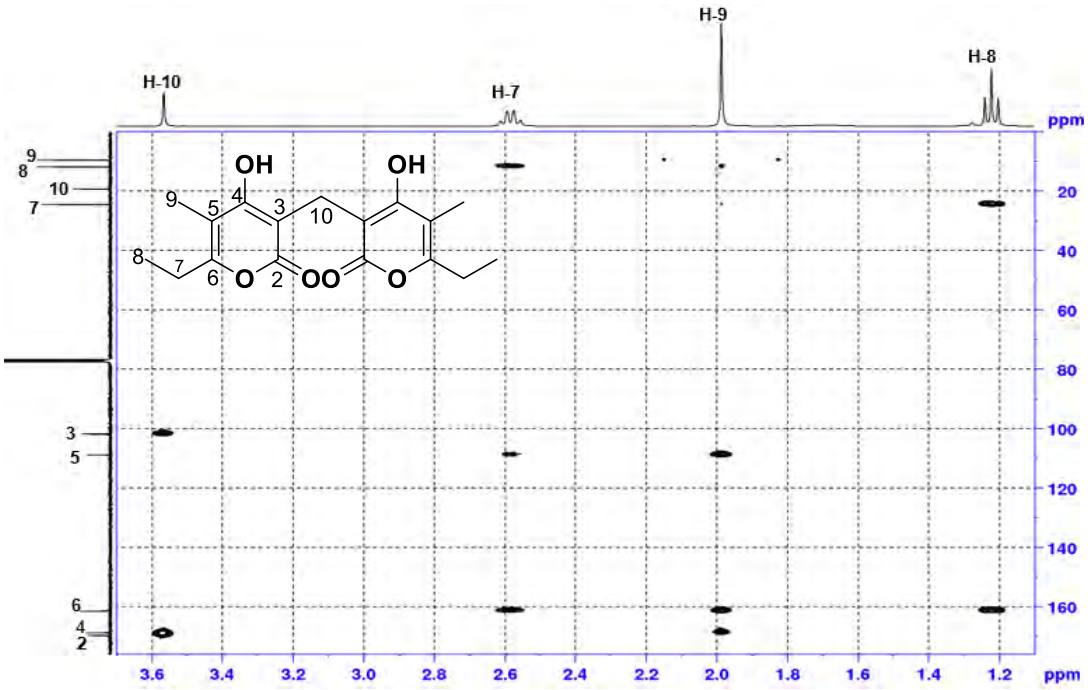

Plate 6G: HR-ESI-MS spectrum of compound **6**

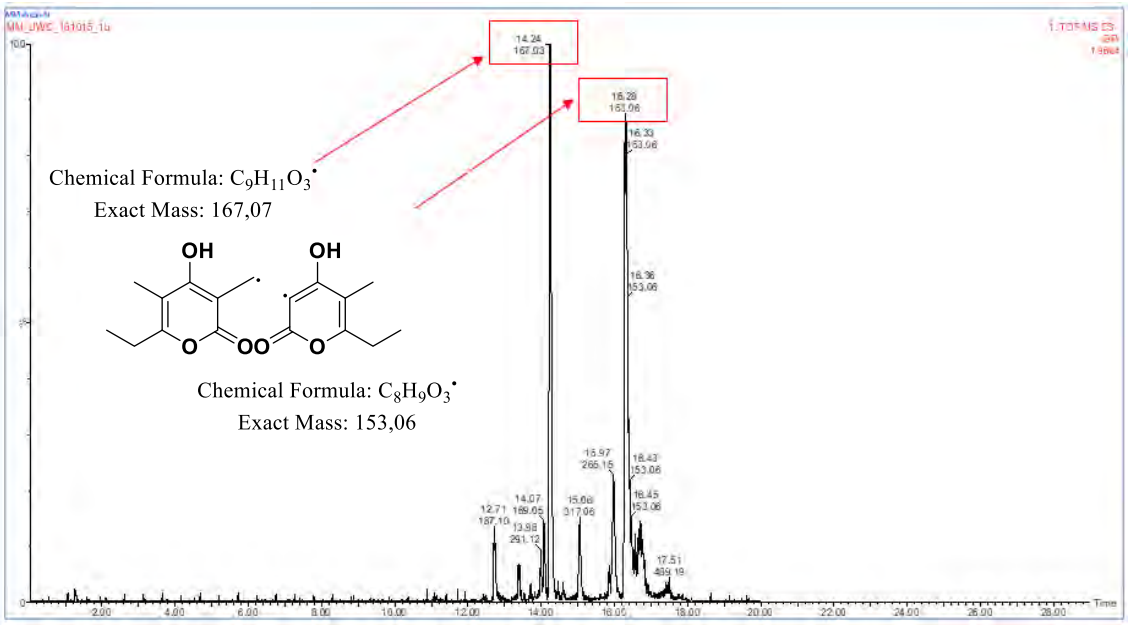

Plate 7A: ^{1}H-NMR spectrum (DMSO-d_6, 400 MHz) of compound **7**

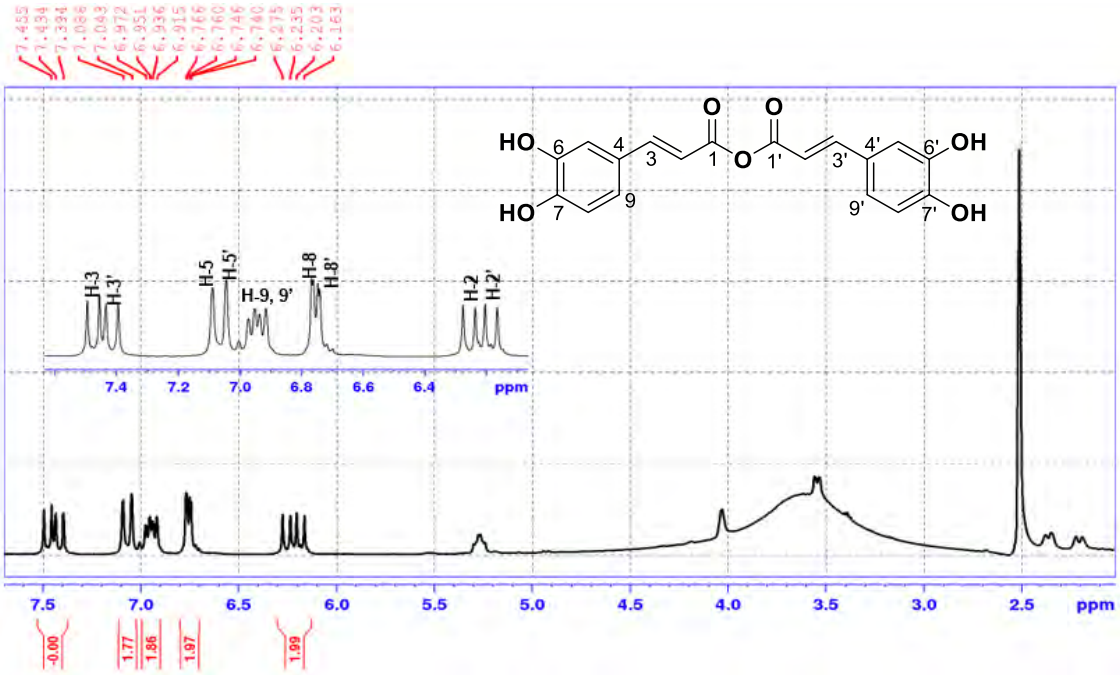

Plate 7B: COSY (DMSO-d_6) spectrum of compound **7**

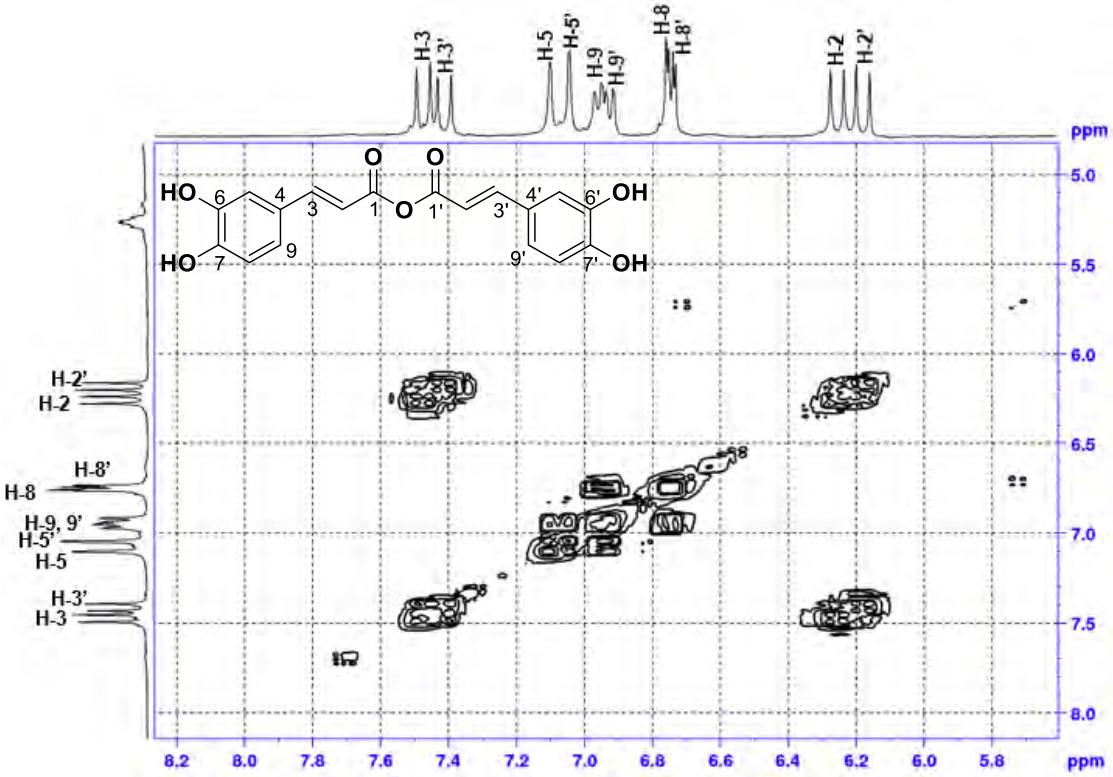

Plate 7C: ^{13}C-NMR spectrum (DMSO-d_6, 100 MHz) of compound **7**

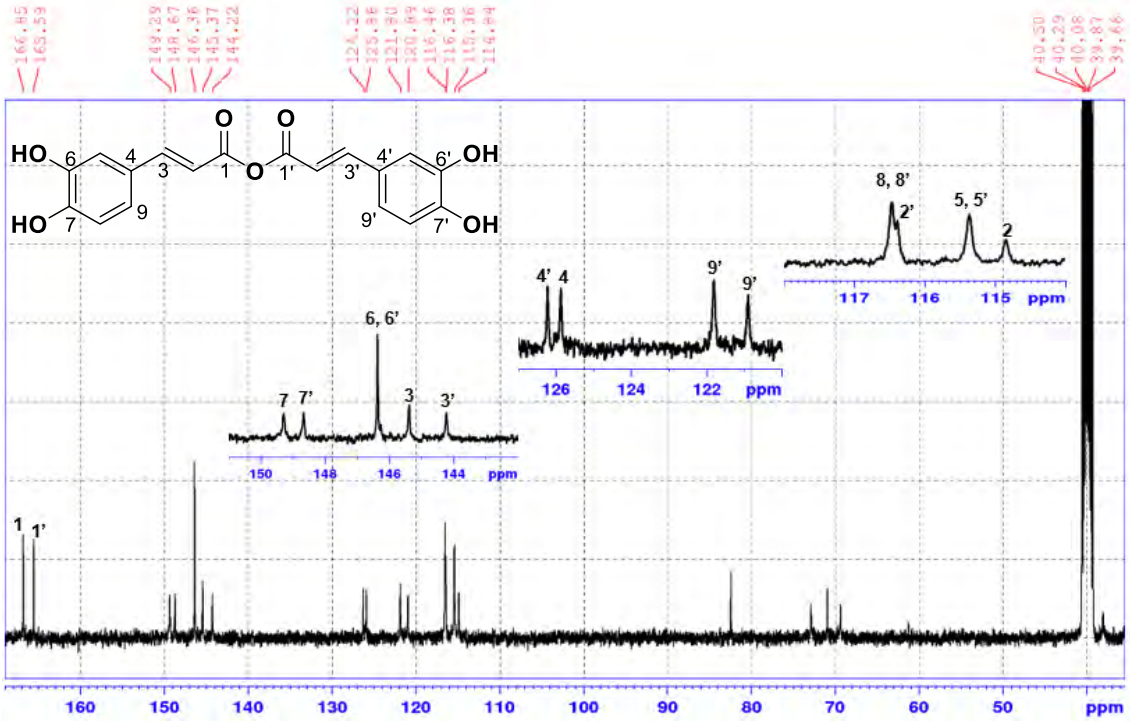

Plate 7D: DEPT-135 spectrum (DMSO-d_6) of compound **7**

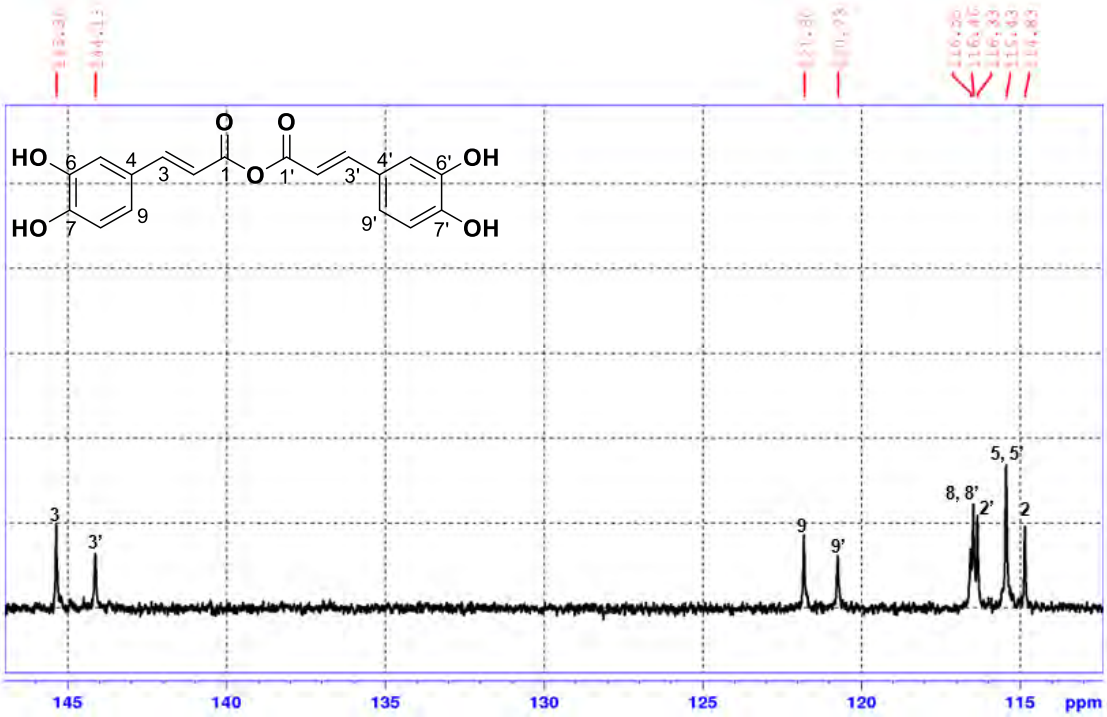

Plate 7E: HSQC spectrum (DMSO-d_6) of compound **7**

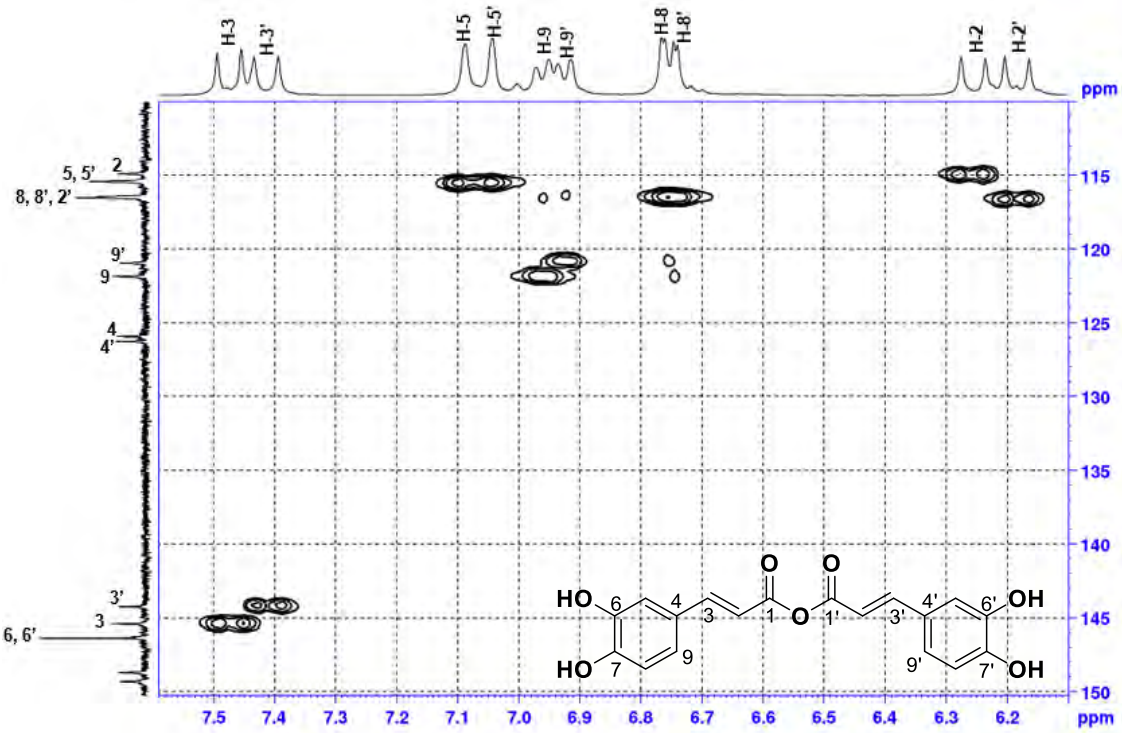

Plate 7F: HMBC spectrum (DMSO-d_6) of compound **7**

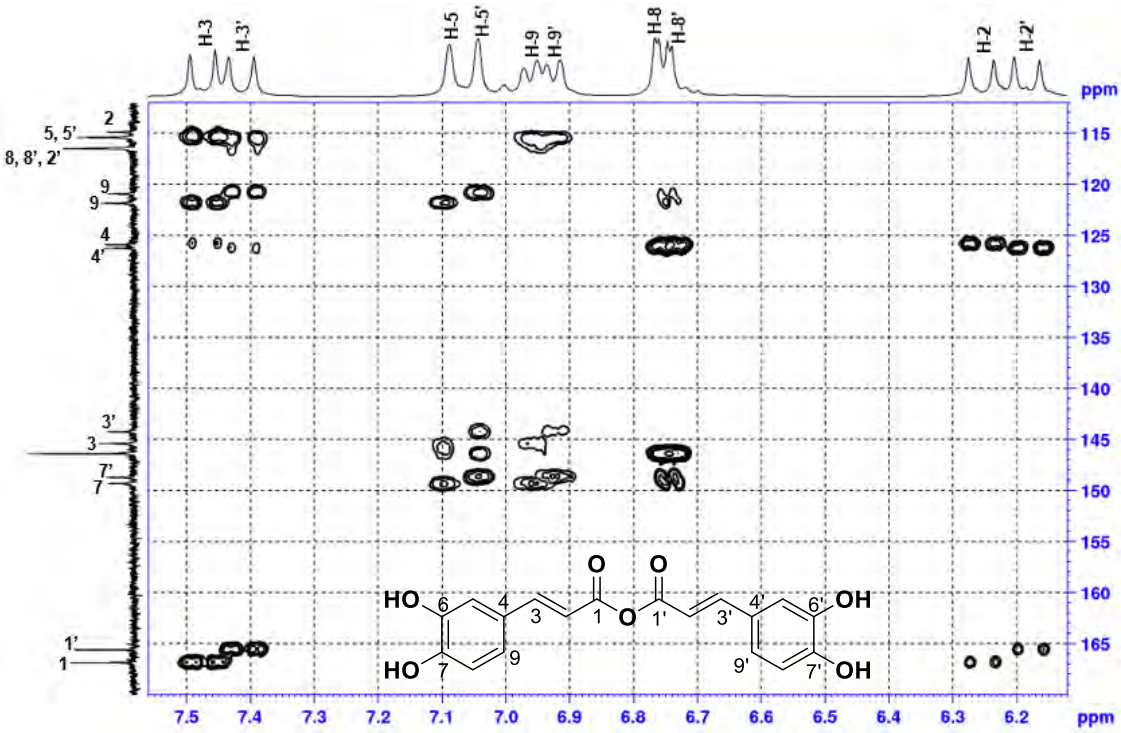

Plate 8A: ^{1}H-NMR spectrum (CD_3OD, 400 MHz) of compound **8**

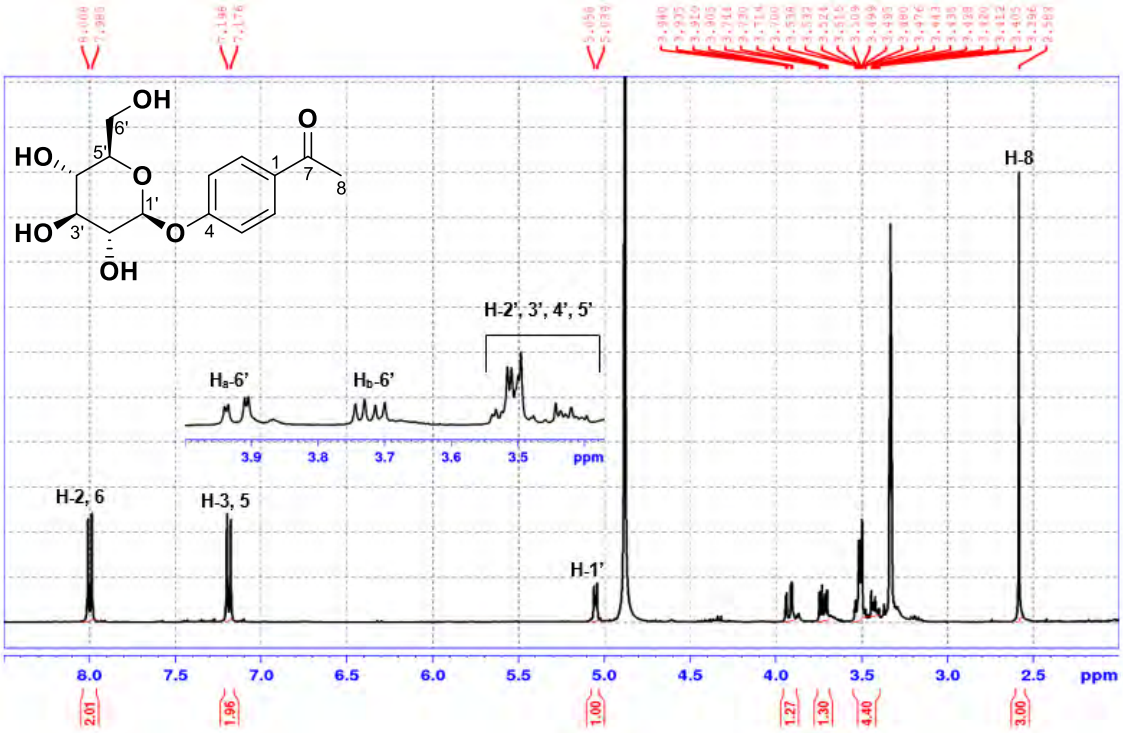

Plate 8B: COSY spectrum (CD_3OD) of compound **8**

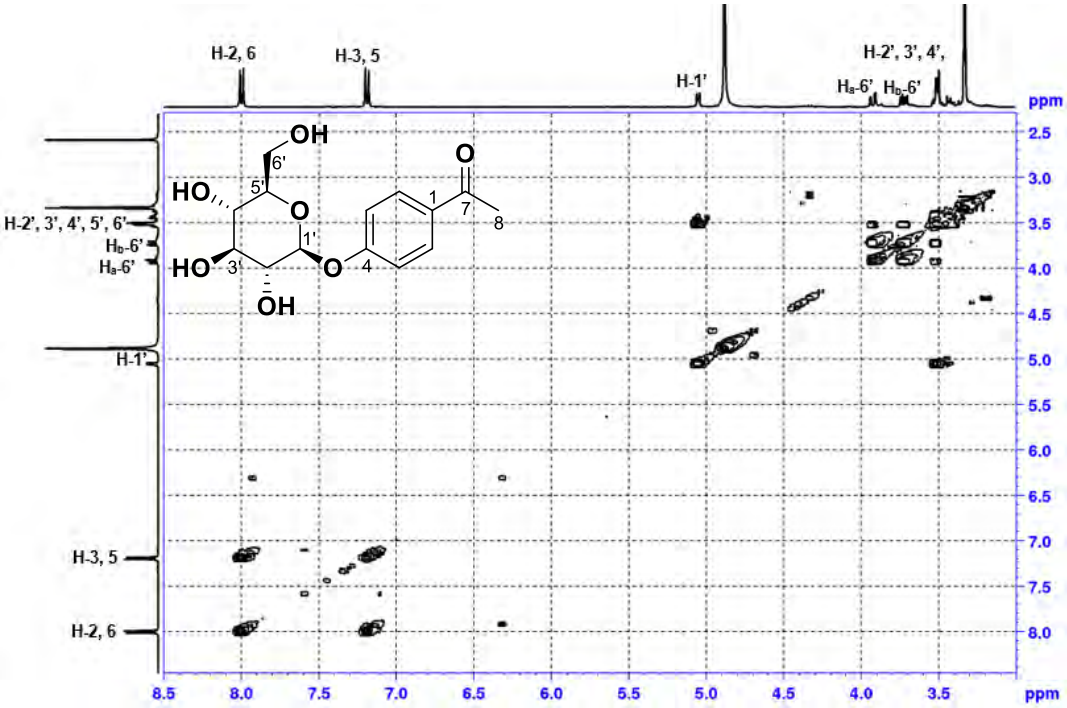

Plate 8C: ^{13}C-NMR spectrum (CD_3OD, 100 MHz) of compound **8**

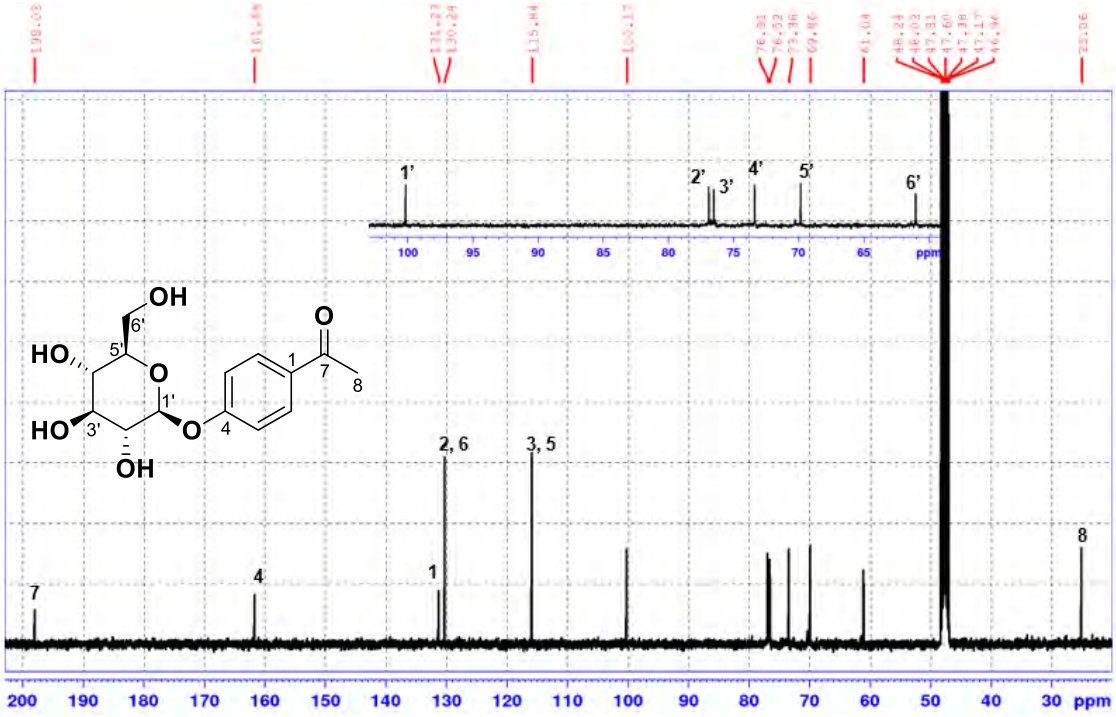

Plate 8D: DEPT-135 spectrum (CD_3OD) of compound **8**

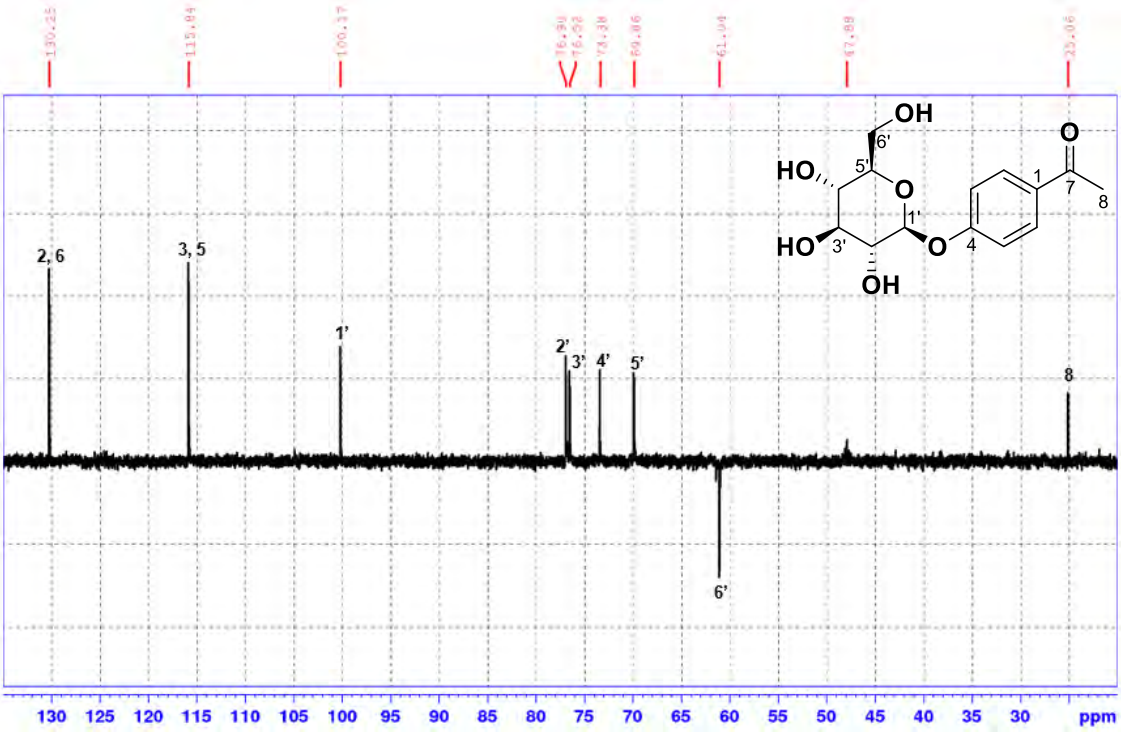

Plate 8E: HSQC spectrum (CD_3OD) of compound **8**

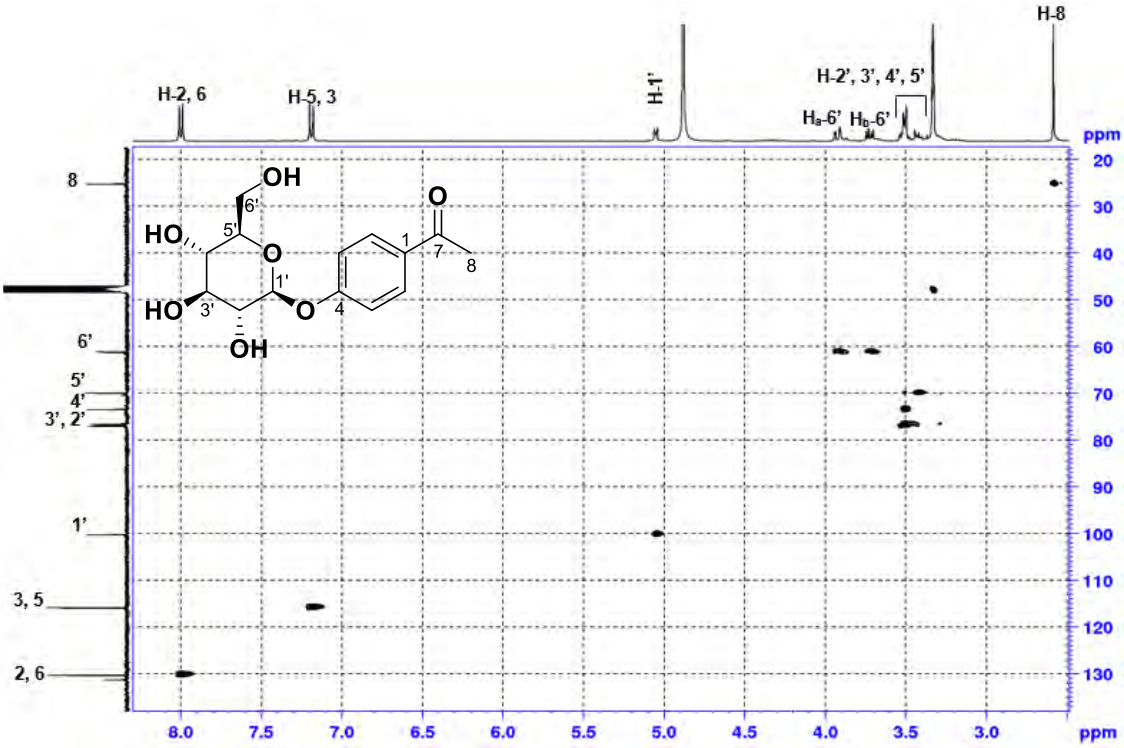

Plate 8F: HMBC spectrum (CD_3OD) of compound **8**

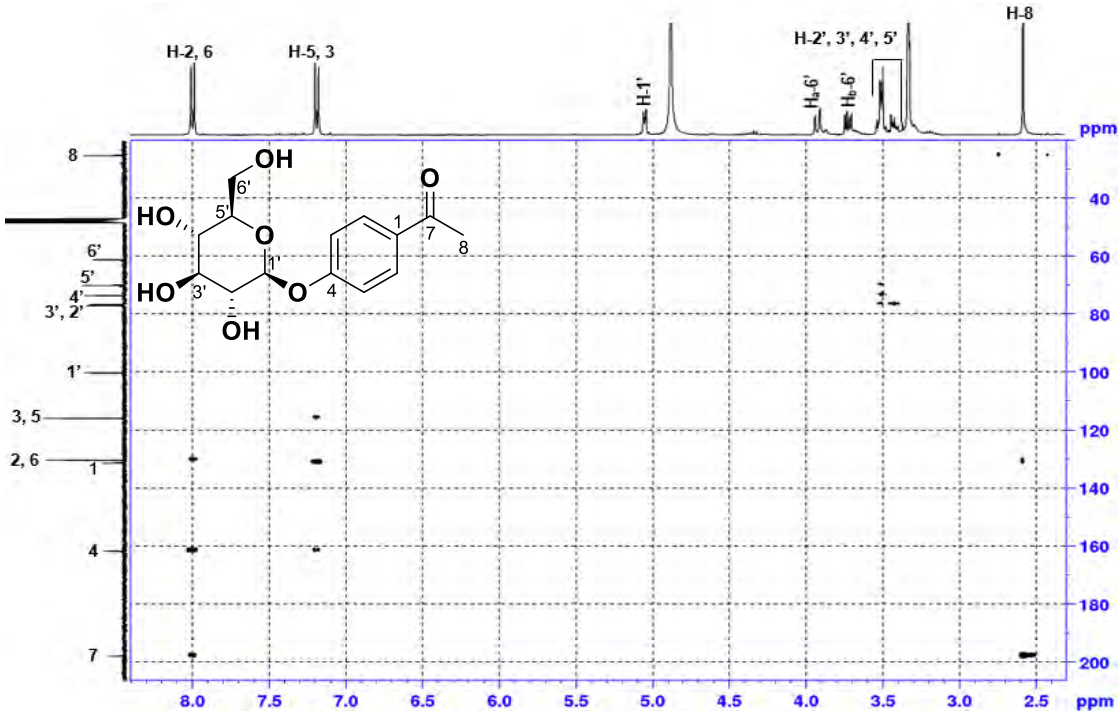

Plate 9A: ^{1}H-NMR spectrum (CD_3OD, 400 MHz) of compound **9**

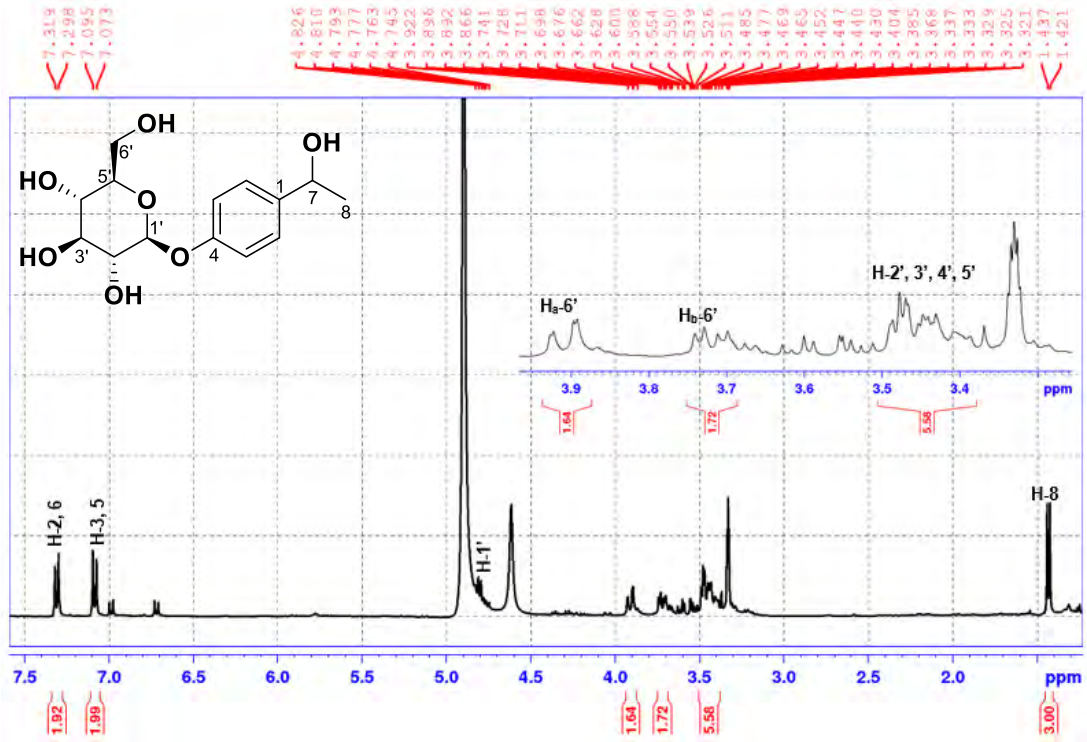

Plate 9B: COSY spectrum (CD_3OD) of compound **9**

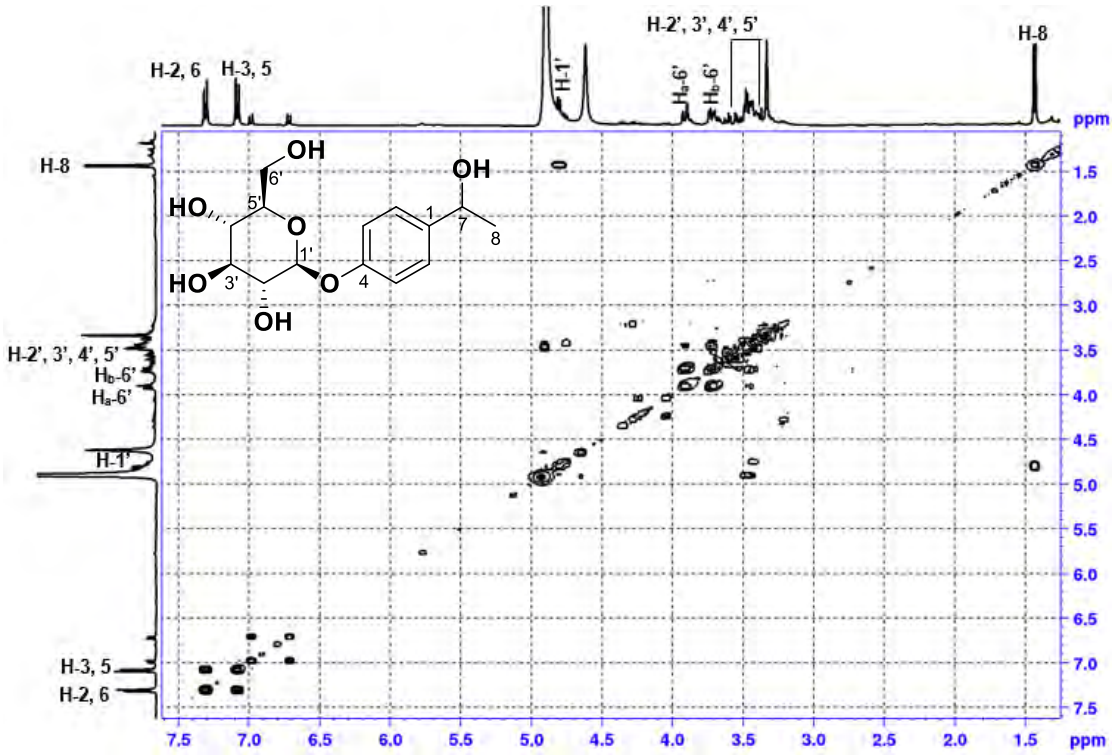

Plate 9C: ^{13}C NMR spectrum (CD_3OD, 100 MHz) of compound **9**

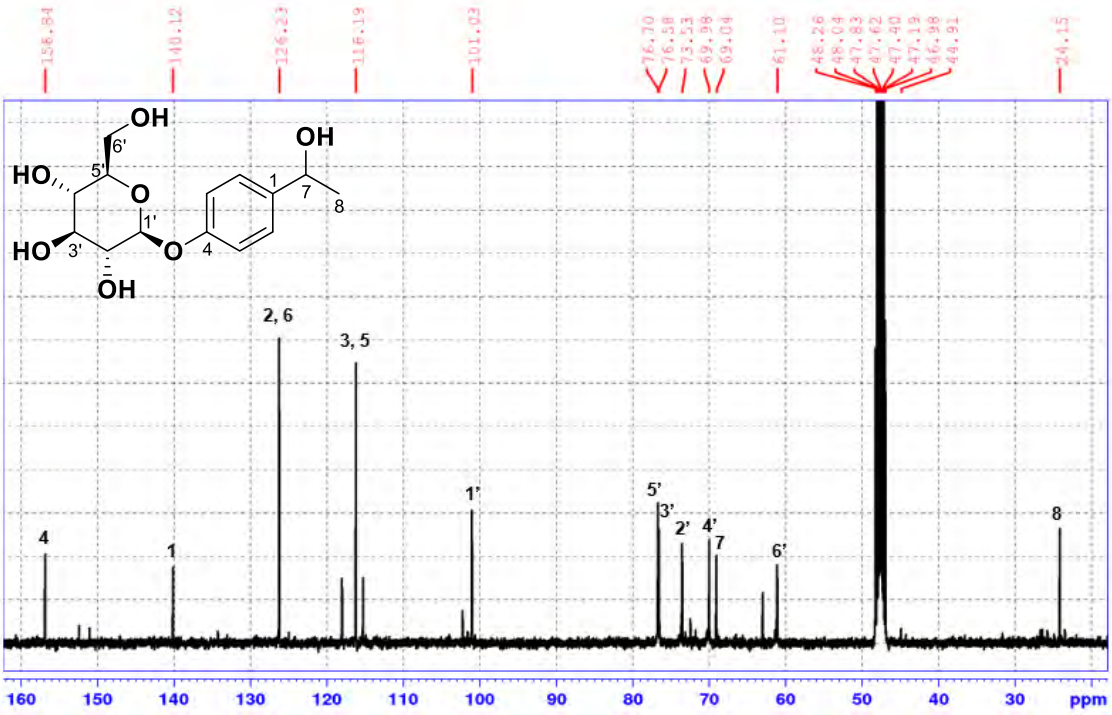

Plate 9D: DEPT-135 spectrum (CD_3OD) of compound **9**

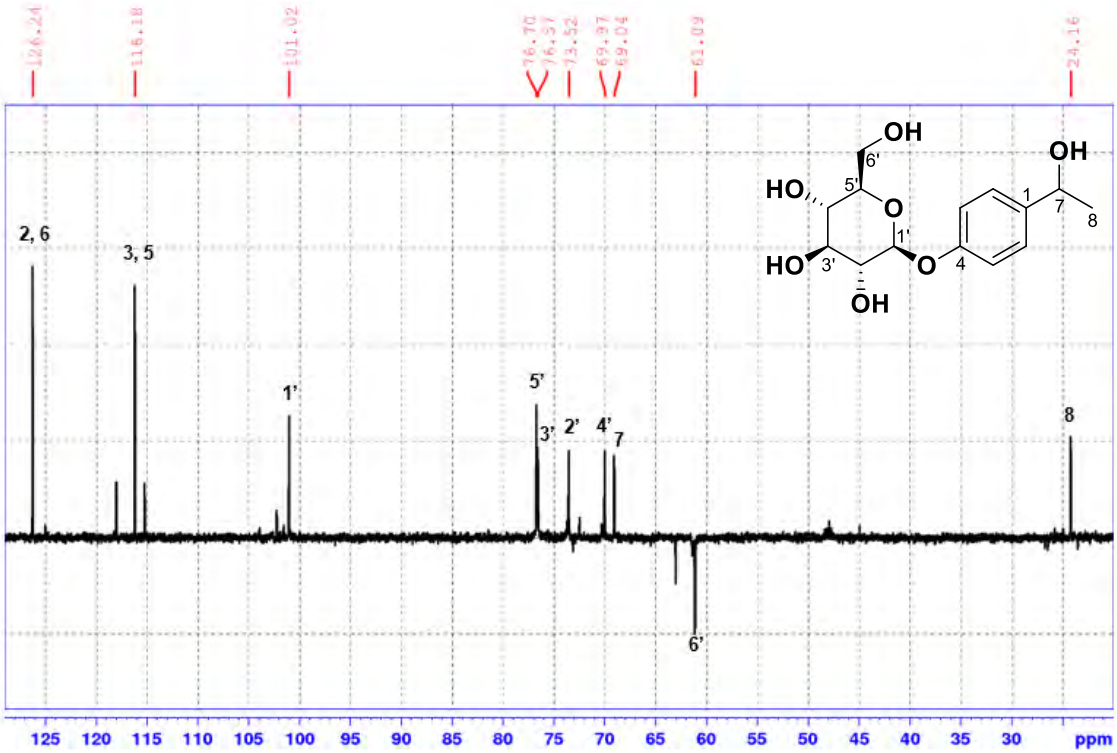

Plate 9E: HSQC spectrum (CD_3OD) of compound **9**

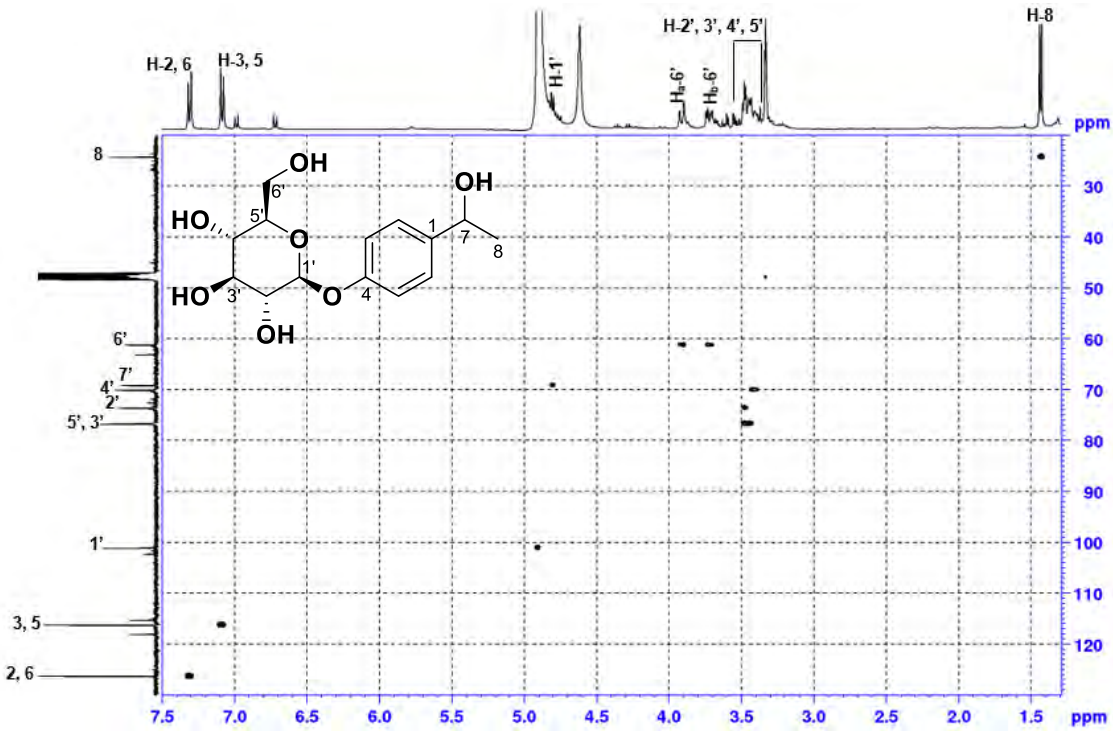

Plate 9F: HMBC spectrum (CD_3OD) of compound **9**

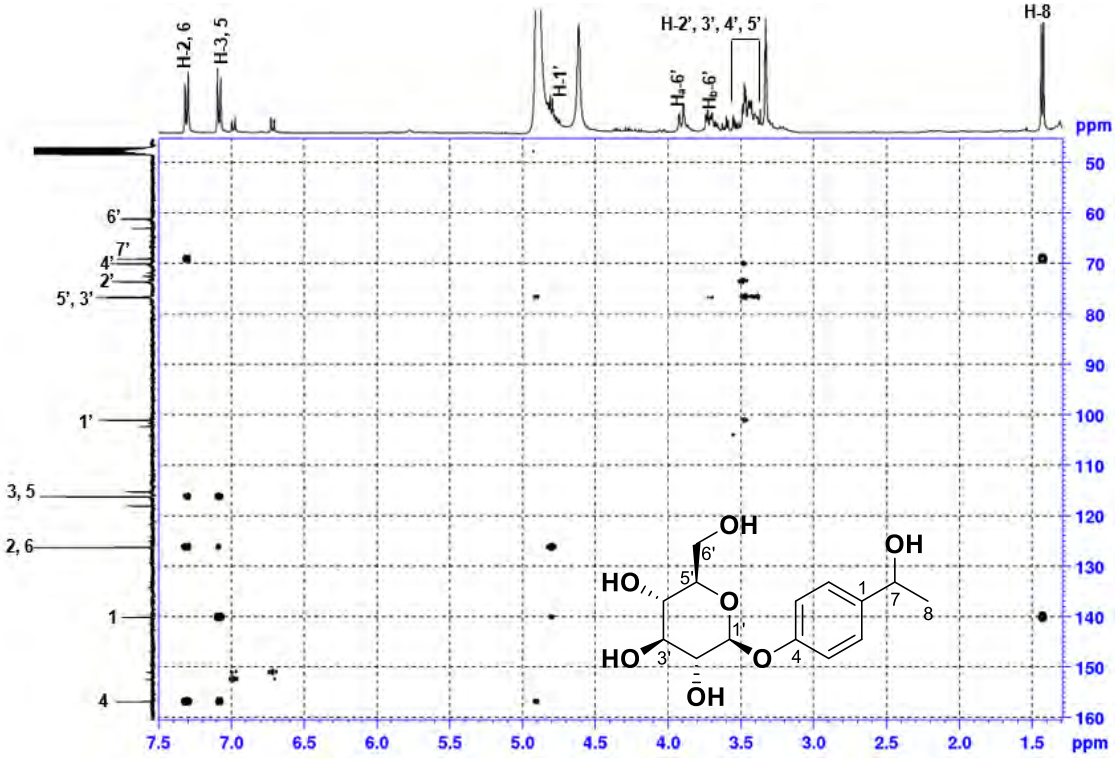

Plate 10A: ^{1}H NMR spectrum (DMSO-d_6, 400 MHz) of compound **10**

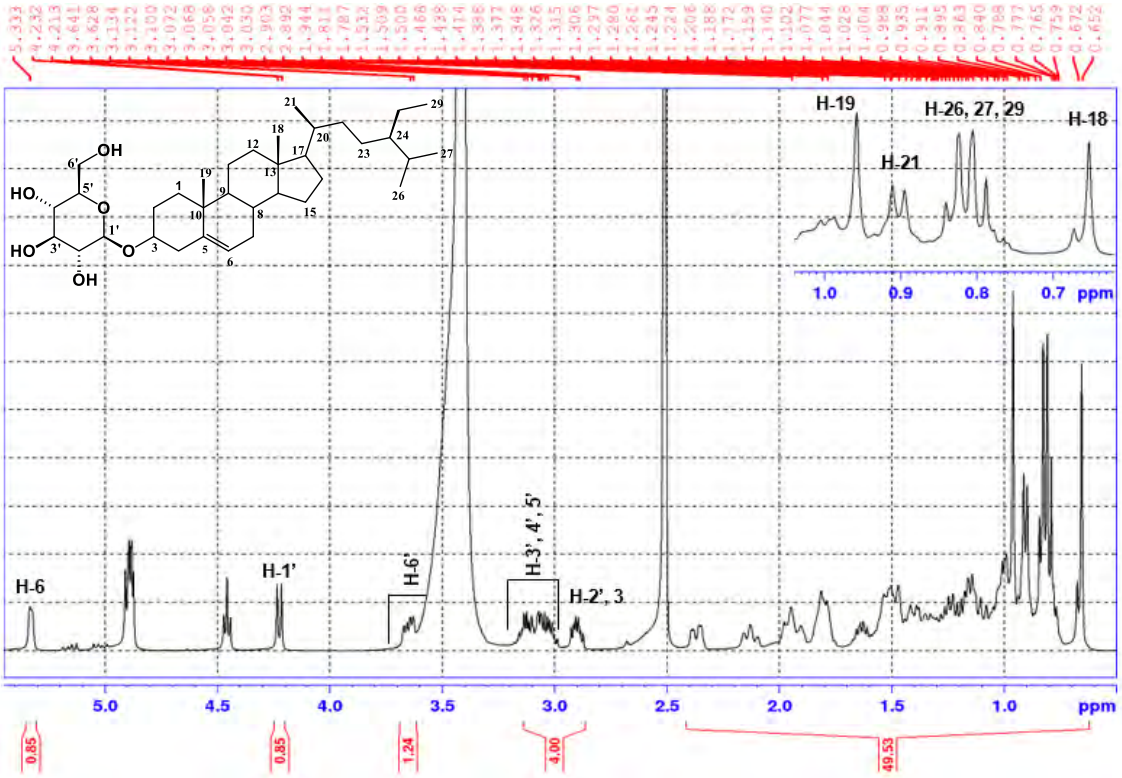

Plate 10B: COSY NMR spectrum (DMSO-d_6) of compound **10**

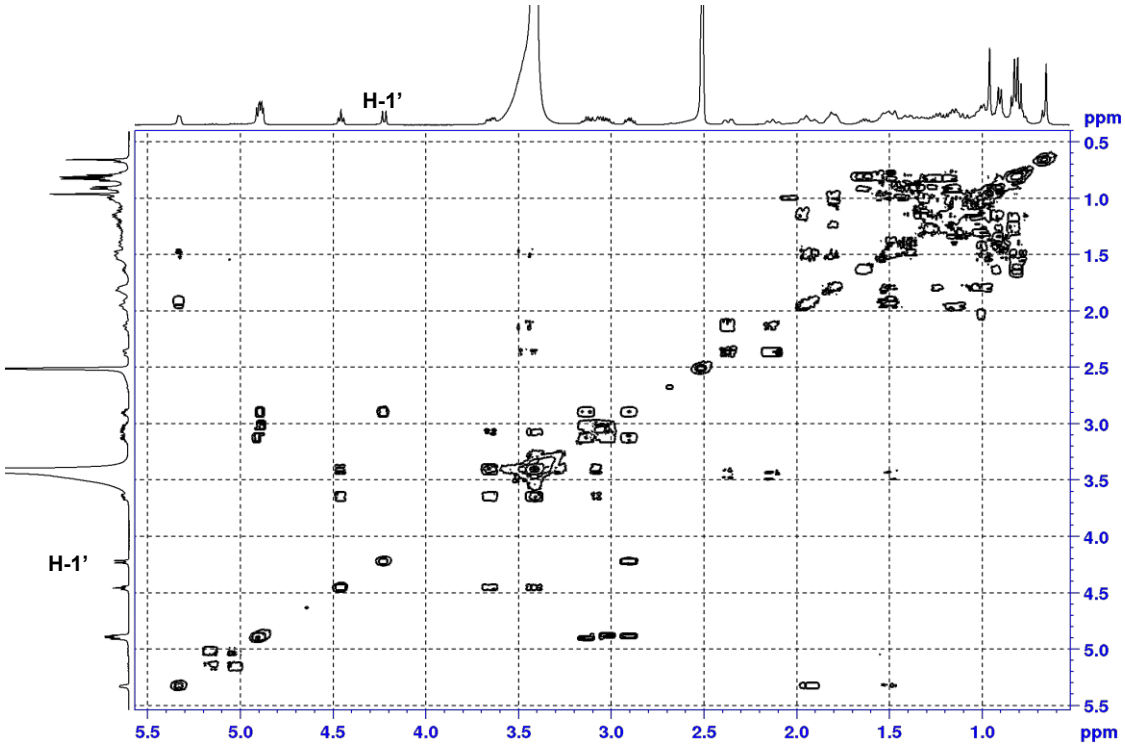

Plate 10C: ^{13}C NMR spectrum (DMSO-d_6, 100 MHz) of compound **10**

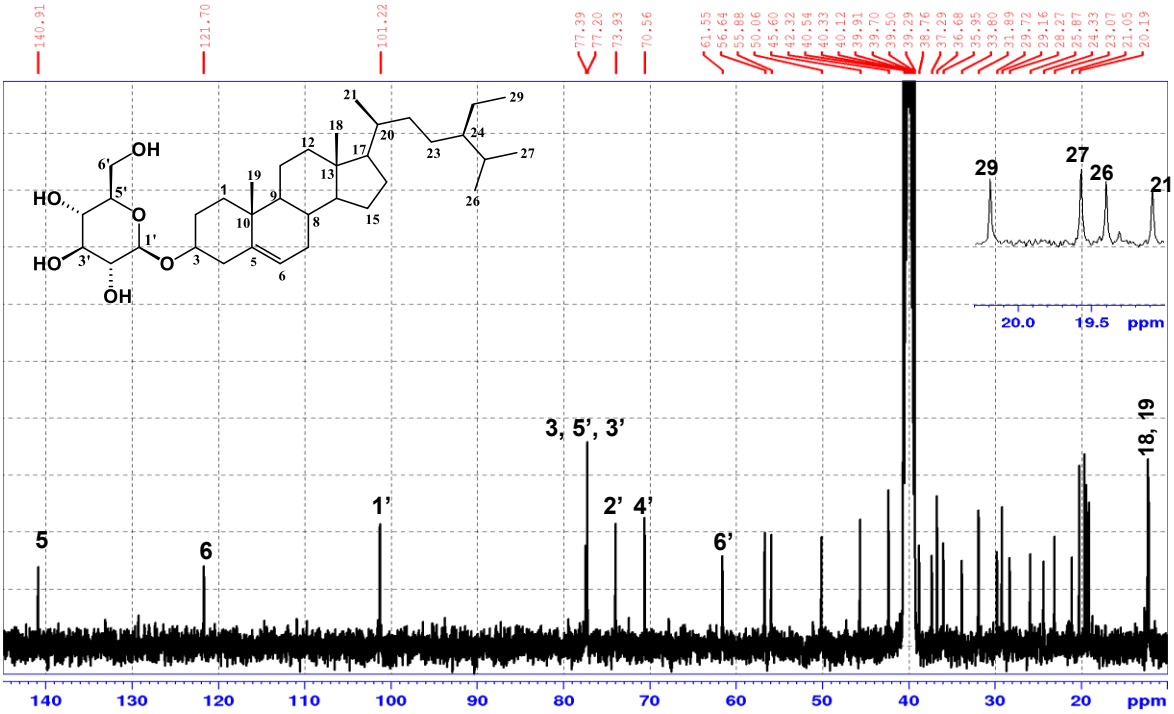

Plate 10D: DEPT-135 spectrum (DMSO-d_6) of compound **10**

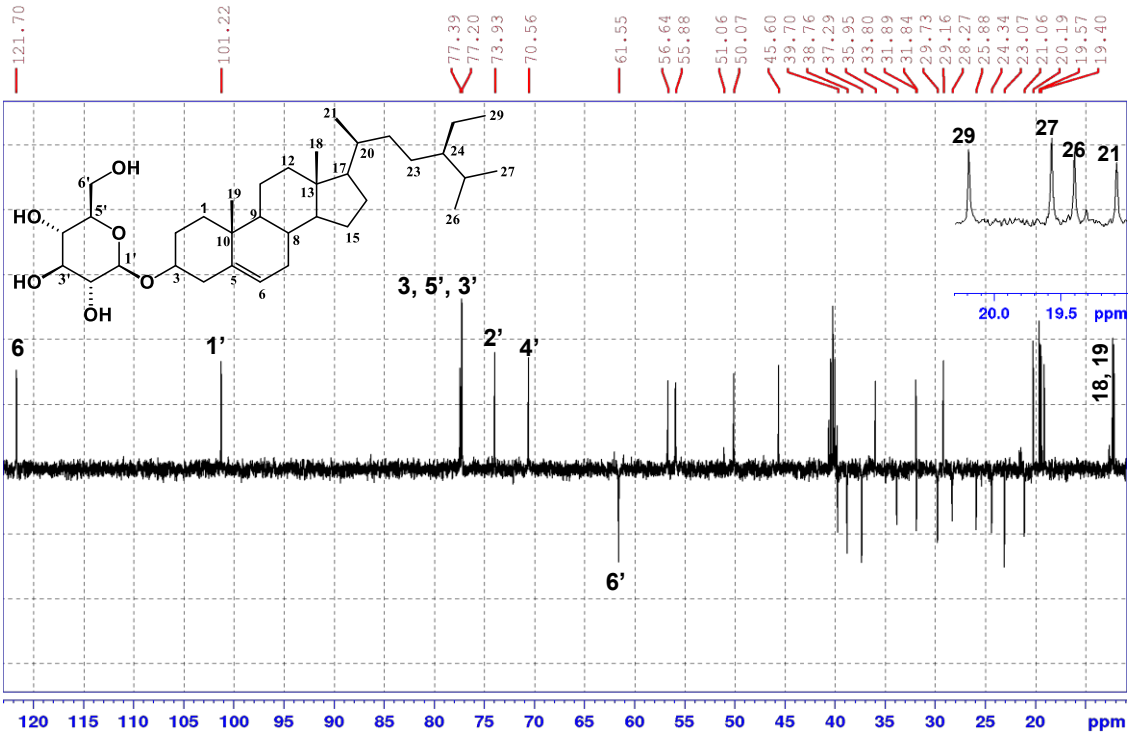

Plate 10E: HSQC spectrum (DMSO-d_6) of compound **10**

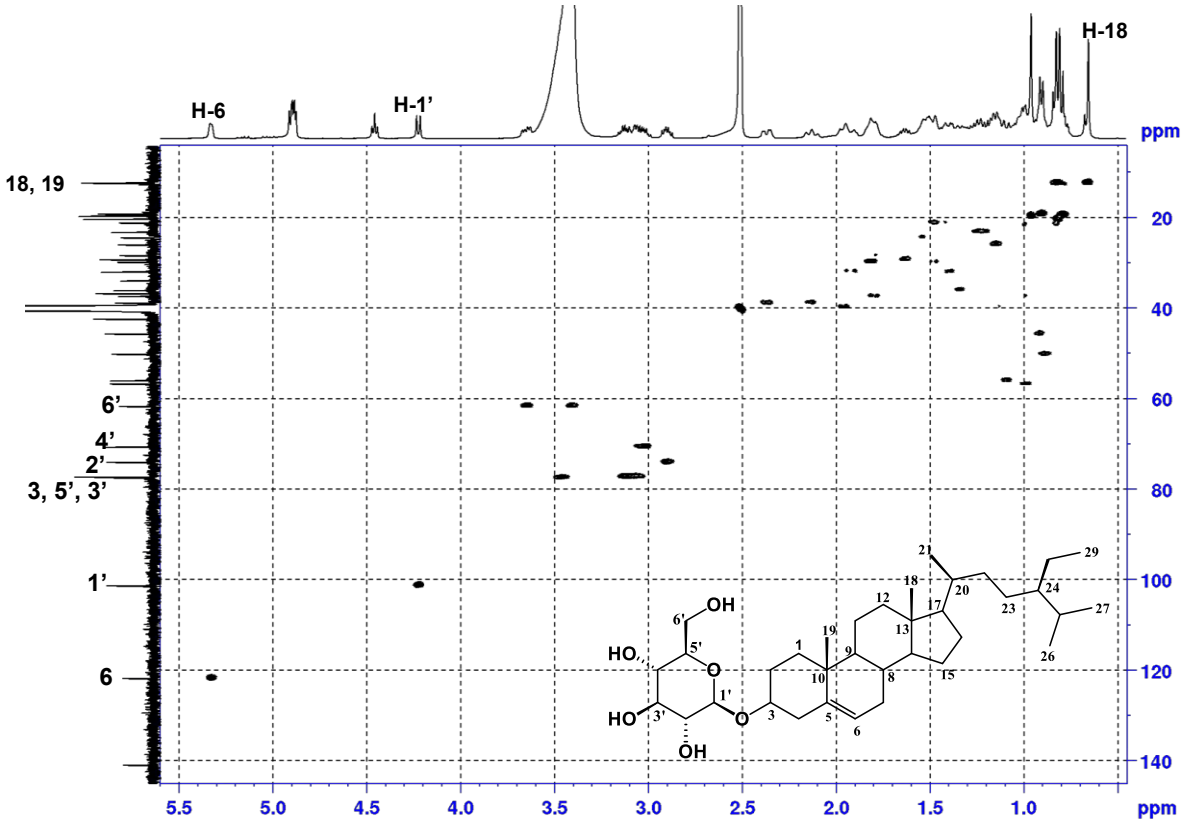

Plate 10F: HMBC spectrum (DMSO-d_6) of compound **10**

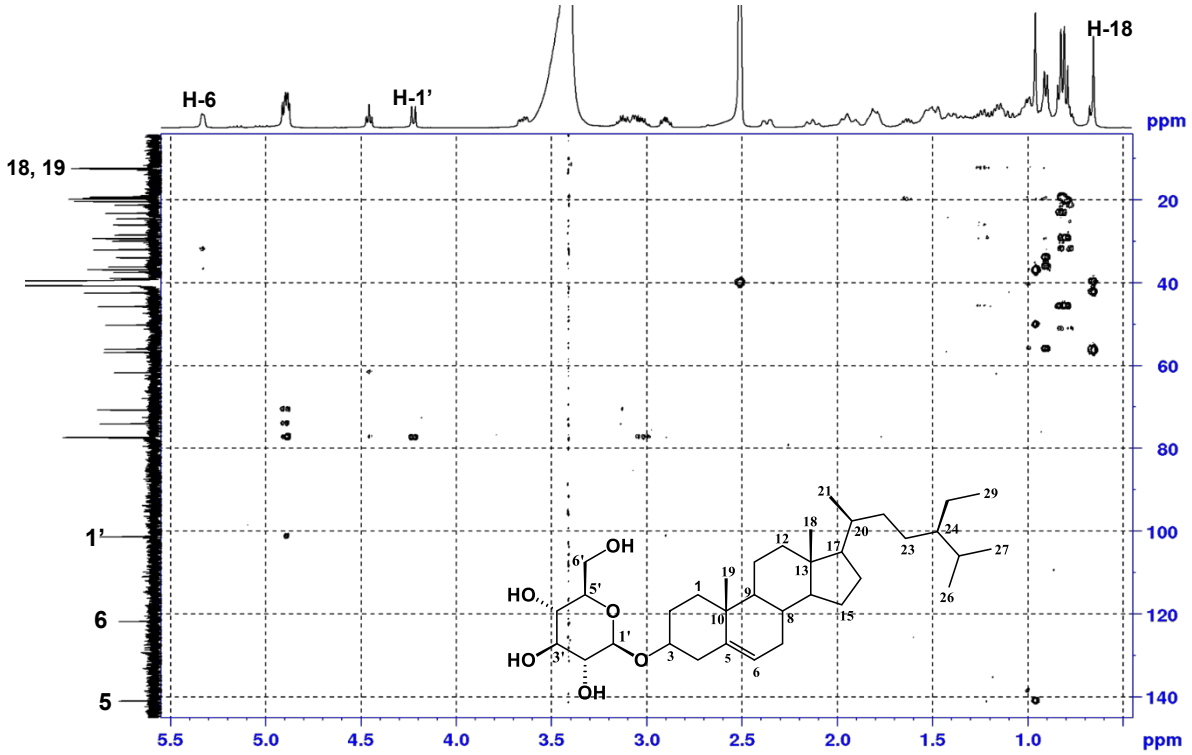

Plate 11A: ^{1}H NMR spectrum ($CDCl_3$, 400 MHz) of compound **11** (mixture)

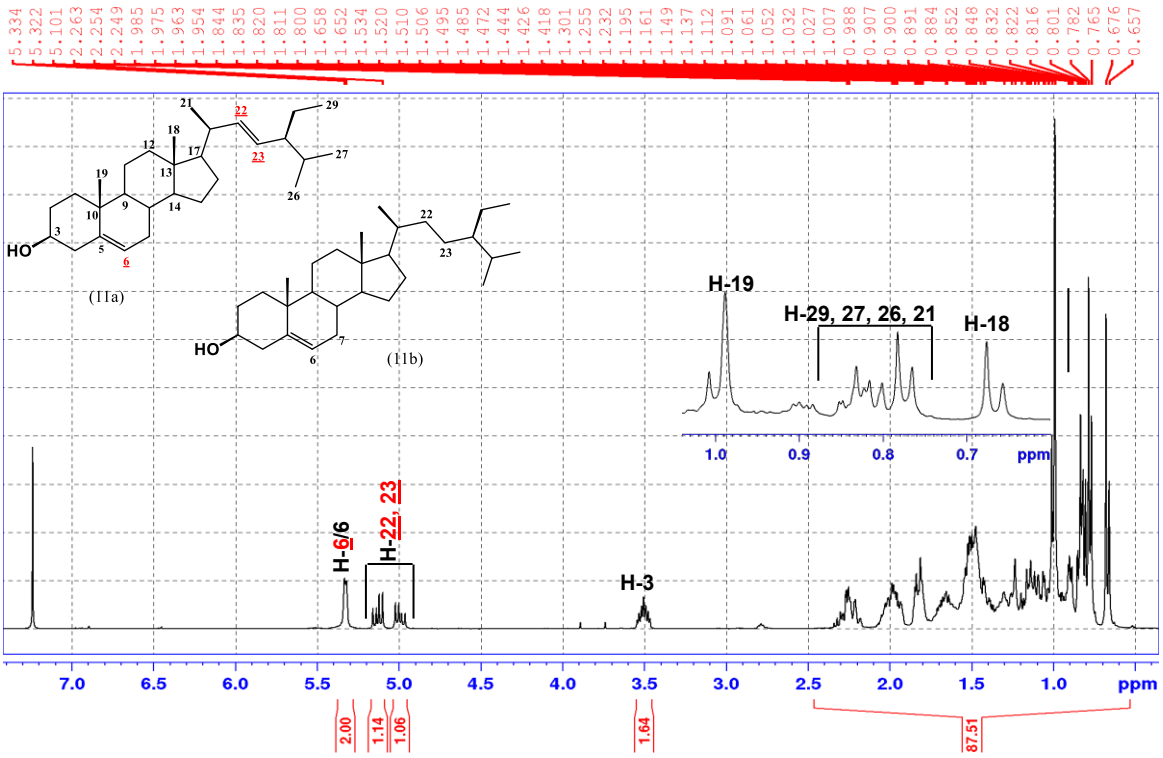

Plate 11B: ^{13}C NMR spectrum ($CDCl_3$, 400 MHz) of mixture compound **11** (mixture)

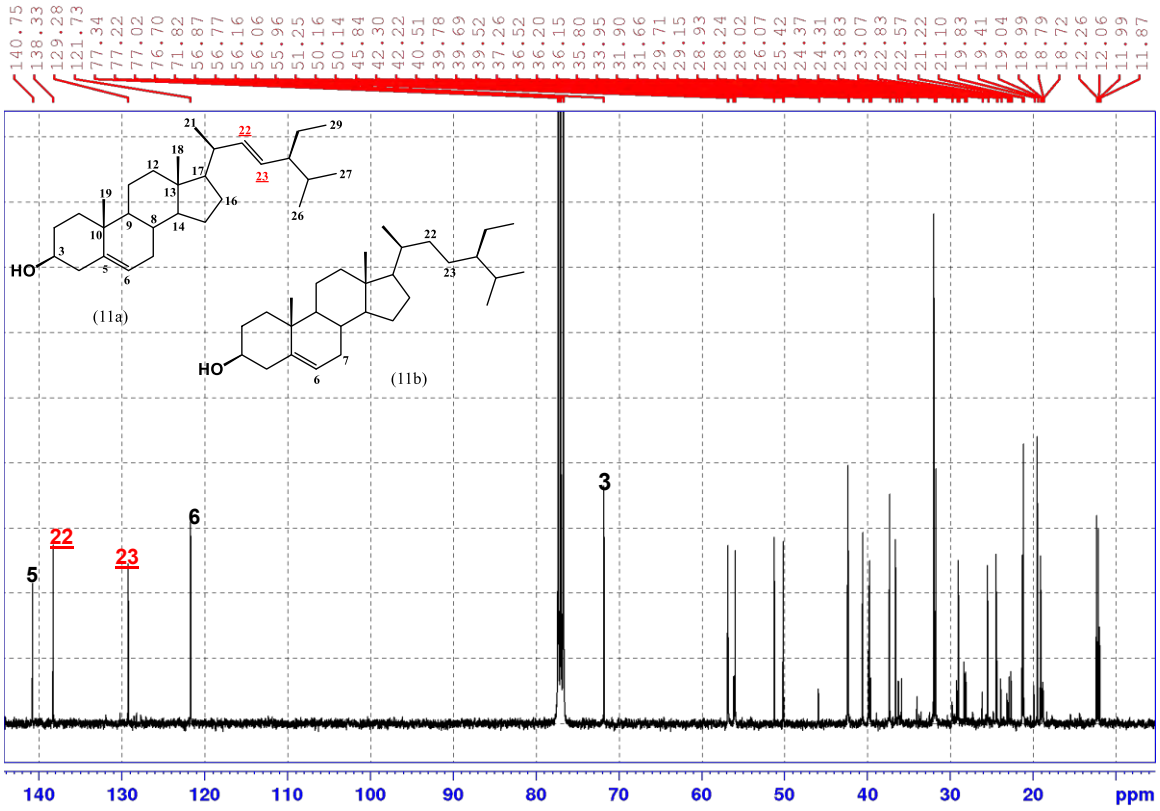

Plate 11C: GCMS data of mixture of compound **11** (mixture)

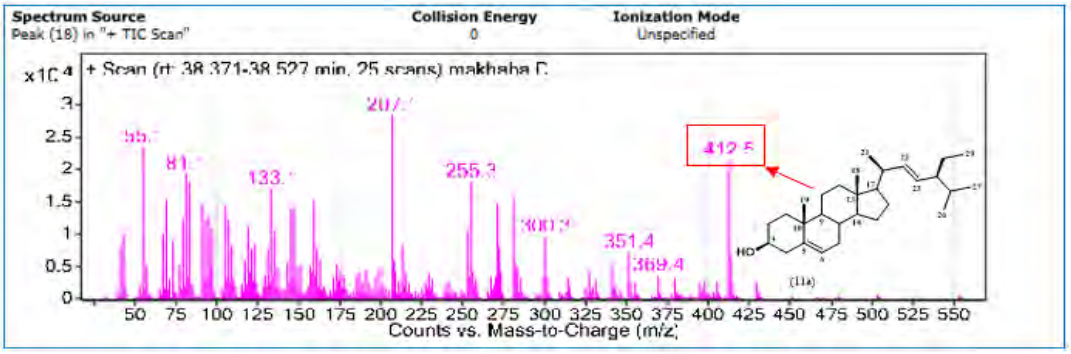

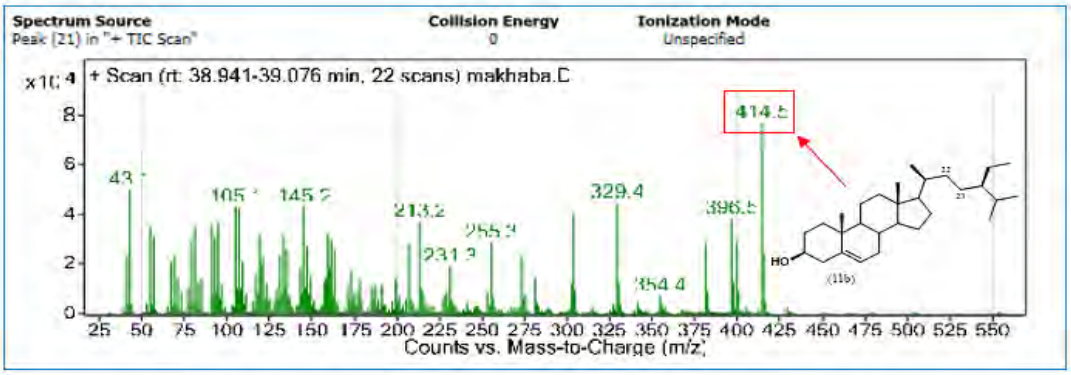

Plate 12A: ^{1}H NMR spectrum (400 MHz, $CDCl_3$) of the acetylated derivative of compound **1**

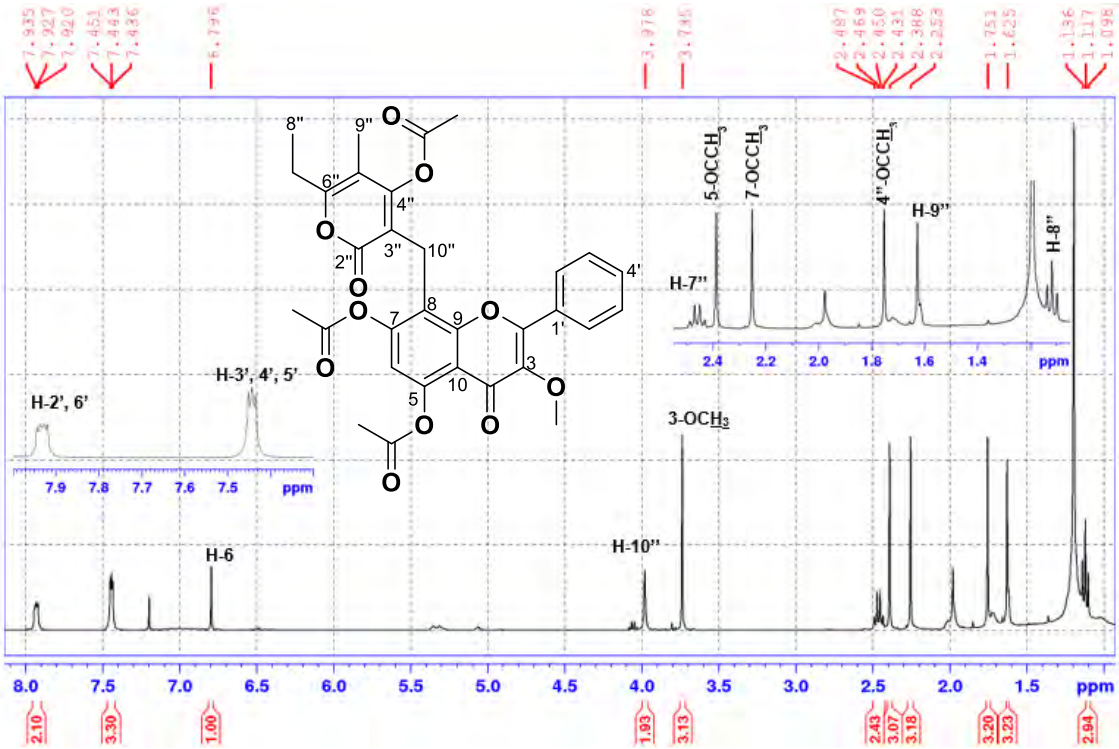

Table 4.8: NMR spectroscopic data (400 MHz, $CDCl_3$) for compound (1) and its acetylated derivative [[a] -overlapping (^1H and/or ^{13}C) signals. [b] -signals may be exchangeable. [*] -long range HMBC correlation]

	^{13}C NMR			^1H NMR	
#	Petiolactone A (1)	Acyl-Petiolactone A	HMBC	Petiolactone A (1)	Acyl-Petiolactone A
2	155.8 (C)	154.8, C		-	-
3	138.7 (C)	141.7, C		-	-
4	178.8 (C)	173.4, C		-	-
5	159.4 (C)	148.2, C		-	-
6	98.8 (CH)	114.2, CH	C-10, C-5, C-4[*], C-7, C-8	6.22, *s*	6.79, *s*
7	163.0 (C)	152.4, C		-	-
8	105.1 (C)	118.3, C		-	-
9	154.6 (C)	154.6, C		-	-
10	104.6 (C)	115.2, C		-	-
1'	130.8 (C)	130.2, C		-	-
2'/6'	128.9[a] (CH)	128.3[a], CH	C-4', C-3', 5', C-2	8.10[a], *m*	7.92[a], *m*
3'/5'	129.1[a] (CH)	128.7[a], CH	C-2', 6', C-1'	7.57[a], *t* (3.2)	7.43[a], *s*
4'	131.3 (CH)	131.0, CH	C-2',6', C-3', 5'	7.57[a], *t* (3.2)	7.43[a], *s*
2''	164.3 (C)	164.0, C		-	-
3''	100.3(C)	113.6, C		-	-
4''	166.2 (C)	160.2, C		-	-
5''	106.6 (C)	107.7, C		-	-
6''	159.6 (C)	161.4, C		-	-
7''	24.1 (CH_2)	24.5, CH_2	C-8'', C-5'', C-6''	2.43, *q* (7.5)	2.46, *q* (7.5)
8''	11.9 (CH_3)	11.5, CH_3	C-6'', C-7''	1.05, *t* (7.5)	1.11, *t* (7.5)
9''	10.2 (CH_3)	9.9, CH_3	C-5'', C-6'', C-4''	1.86, *s*	1.62, *s*
10''	17.8 (CH_2)	19.8, CH_2	C-3'', C-2'', C-4'', C-7, C-8, C-9	3.80[a], *s*	3.97, *s*
3-O<u>Me</u>	60.0, CH_3	60.2, CH_3		3.80[a], *s*	3.73, *s*
5-OH/OCCH$_3$	-	21.1[b], CH_3 169.4, C		12.65, *s*	2.38, *s*
7-OH/OCCH$_3$	-	20.9[b], CH_3 168.0, C			2.25, *s*
4''-OH/OCCH$_3$	-	19.6, CH_3 166.5, C			1.75, *s*

Plate 13A: ^{1}H NMR spectrum (400 MHz, $CDCl_3$) of the acetylated derivative of compound **2**

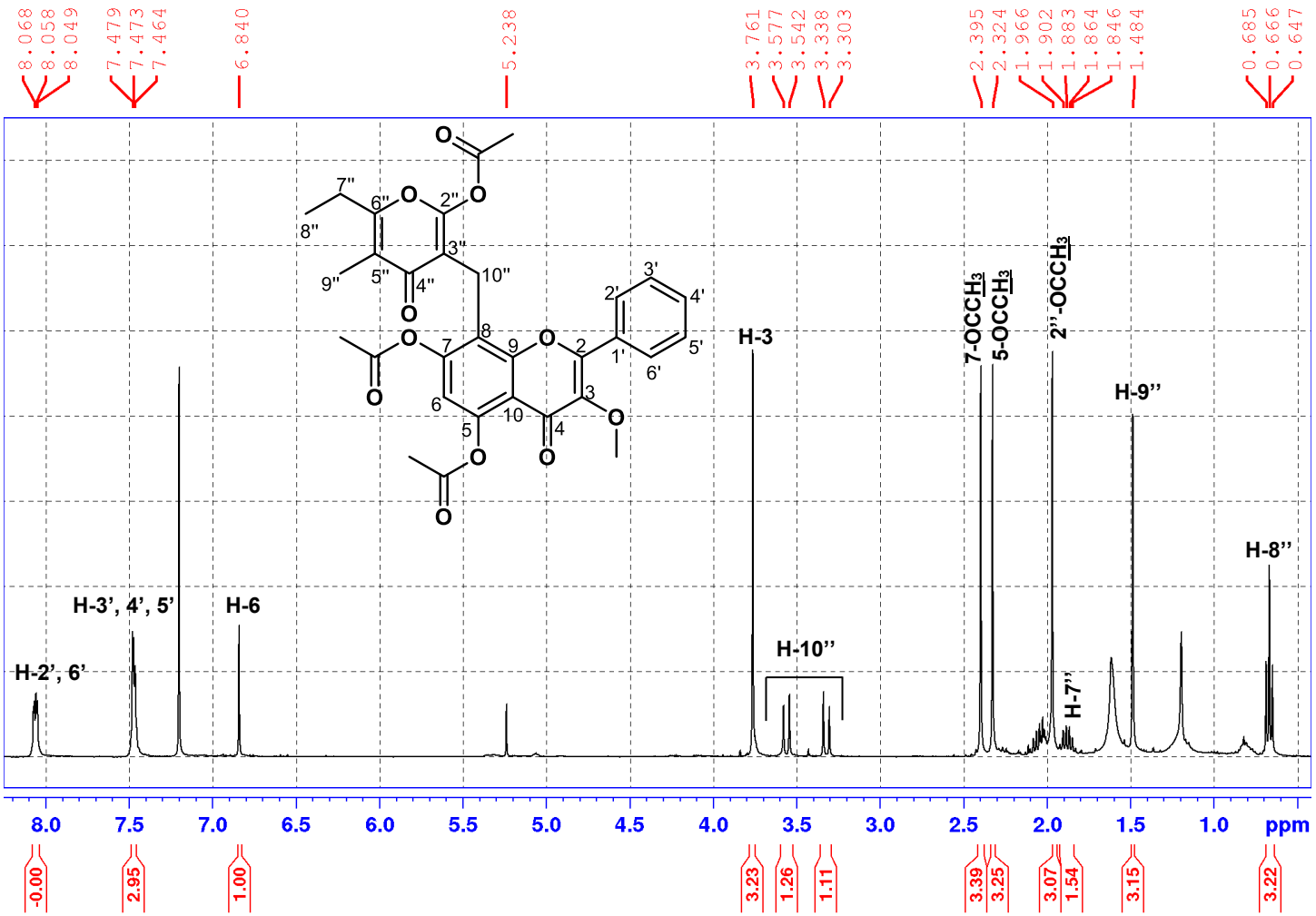

Table 4.9: NMR spectroscopic data (400 MHz, $CDCl_3$) for compound 2 and its acetylated derivative [[a] –overlapping (^1H and/or ^{13}C) signals. [b] –signals may be exchangeable. * –long range HMBC correlation]

	^{13}C NMR			^1H NMR	
#	Petiolactone B (2)	Acyl-Petiolactone B	HMBC	Petiolactone B (2)	Acyl-Petiolactone B
2	155. 3 (C)	154. 4, C		–	–
3	138.9 (C)	141.7, C		–	–
4	178.6 (C)	173.3, C		–	–
5	160.0 (C)	148.9, C		–	–
6	98.4 (CH)	113.9, CH	C-10, C-5, C-4*, C-7, C-8	6.24, *s*	6.84, *s*
7	163.6 (C)	153.0, C		–	–
8	100.3 (C)	112.7, C		–	–
9	155.4 (C)	155.6, C		–	–
10	104.7 (C)	115.1, C		–	–
1'	130.7 (C)	130.4, C		–	–
2'/6'	128.8[a] (CH_2)	128.4[a], CH	C-4', C-3', 5', C-2	8.21[a], *m*	8.06[a], *m*
3'/5'	129.1[a] (CH_2)	128.7[a], CH	C-2', 6', C-1'	7.56a, *brt* (3.3)	7.47[a], *t* (3.1)
4'	131.5 (CH)	131.0, CH	C-2',6', C-3', 5'	7.56[a], *brt* (3.3)	7.46[a], *t* (3.1)
2''	104.0[a] (C)	100.1[a], C		–	–
3''	104.0[a] (C)	100.1[a], C		–	–
4''	201.6 (C)	199.5, C		–	–
5''	107.1 (C)	109.8, C		–	–
6''	186.4 (C)	185.4, C		–	–
7''	21.7 (CH_2)	21.4, CH_2	C-8'', C-5'', C-6''	2.22, *q* (7.7)	1.86, *q* (7.7)
8''	9.9 (CH_3)	9.4, CH_3	C-6'', C-7''	0.75, *t* (7.6)	0.66, *t* (7.6)
9''	5.6 (CH_3)	5.3, CH_3	C-5'', C-6'', C-4''	1.41, *s*	1.48, *s*
10''	29.7 (CH_2)	29.4, CH_2	C-3'', C-2'', C-4'', C-7, C-8, C-9	3.18, *m*	3.56 and 3.32, *m*
3-O<u>Me</u>	60.4, CH_3	60.2, CH_3		3.81, *s*	3.76, *s*
5-OH/OCCH$_3$	–	21.1[b], CH_3 167.9, C		12.47, *s*	2.32, *s*
7-OH/OCCH$_3$	–	21.1[b], CH_3 169.4, C			2.39, *s*
2"-OH/OCCH$_3$	–	20.5, CH_3 167.3, C			1.96, *s*

Appendix

Spectroscopic data of the isolated compound from *Helichrysum splendidum*

Plate 14A: ^{1}H-NMR spectrum ($CDCl_3$, 400 MHz) of compounds **12** and **13**(#)

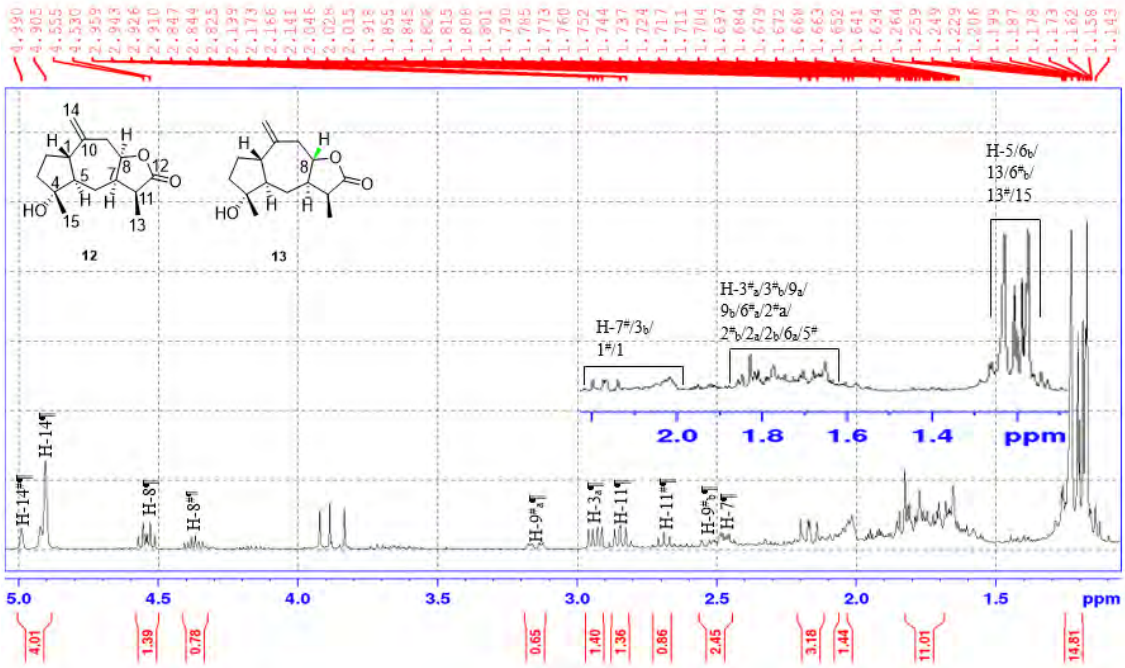

Plate 14B: COSY spectrum ($CDCl_3$) of compounds **12** and **13**(#)

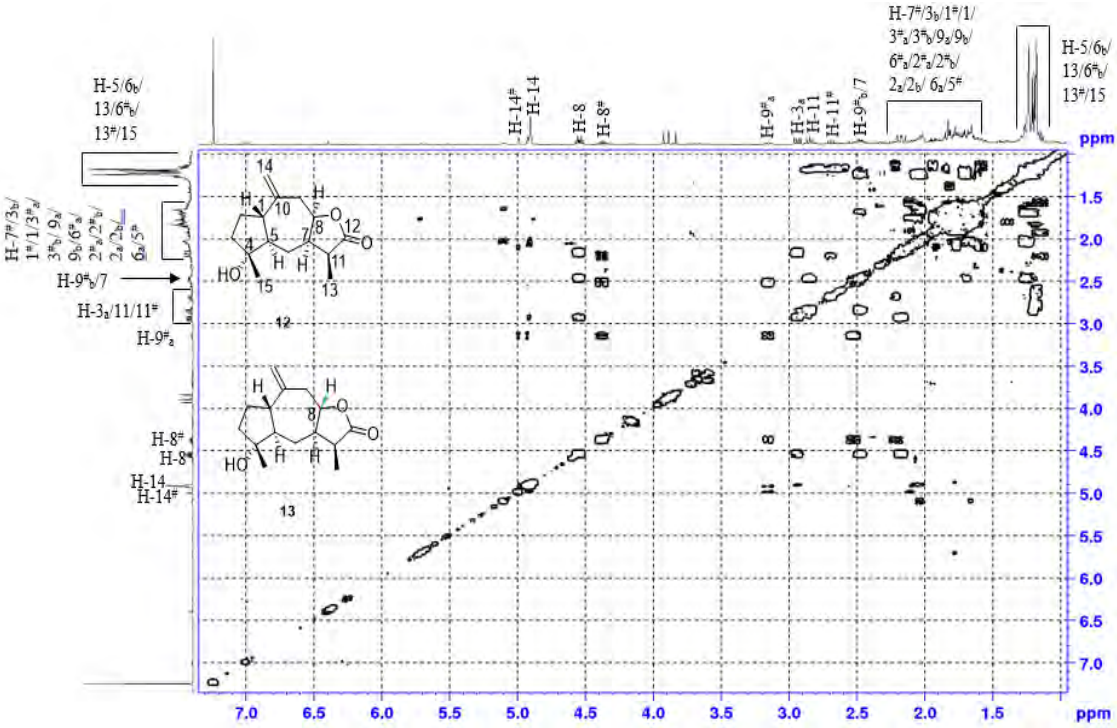

Plate 14C: NOESY spectrum ($CDCl_3$) of compounds **12** and **13**(#)

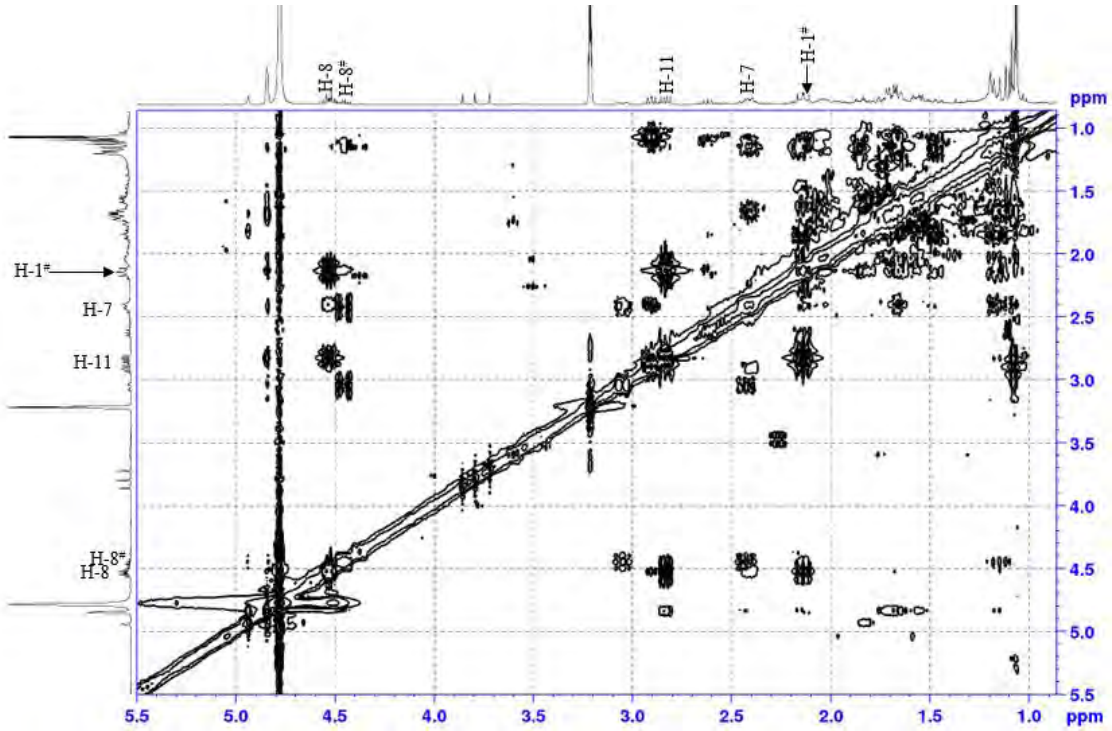

Plate 14D: ^{13}C-NMR spectrum ($CDCl_3$, 100 MHz) of compounds **12** and **13**(#)

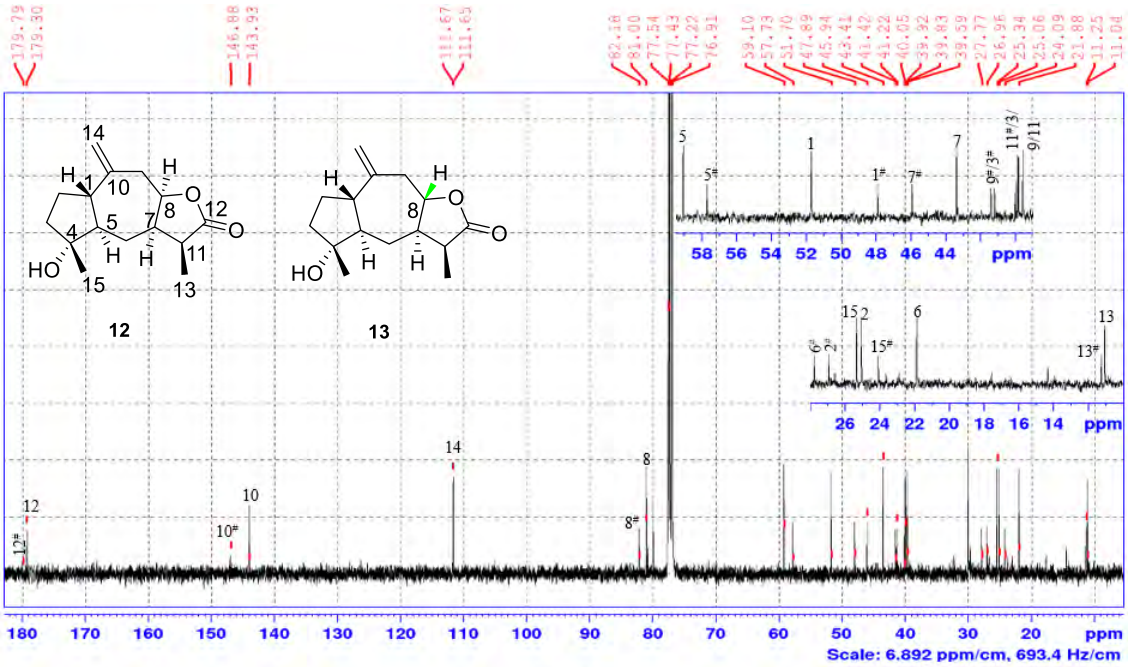

Plate 14E: DEPT-135 spectrum ($CDCl_3$) of compounds **12** and **13**(#)

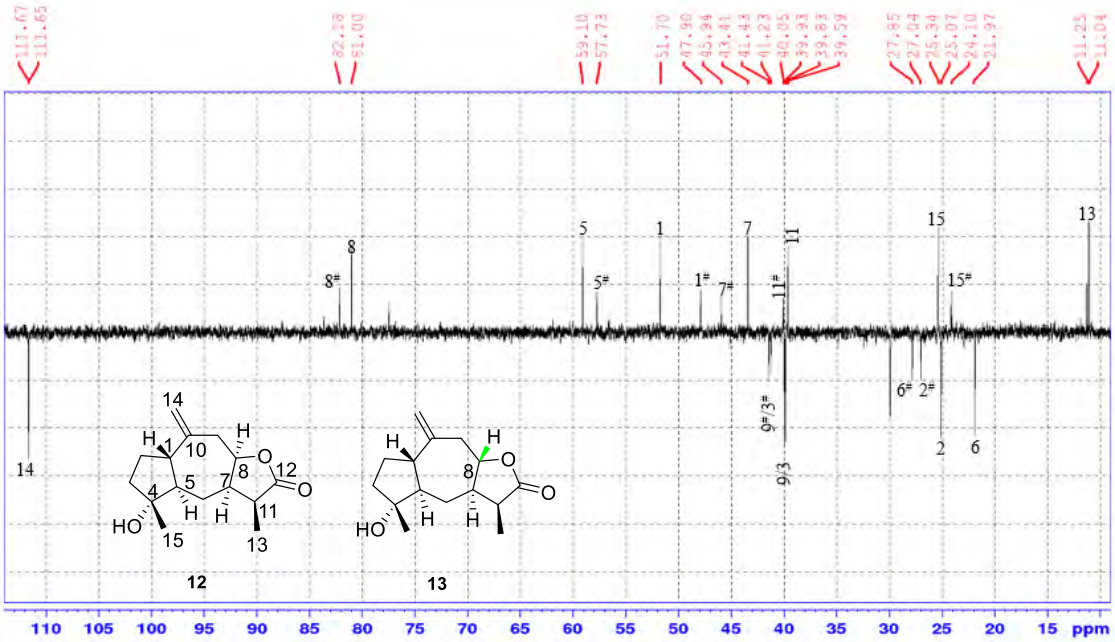

Plate 14F: HSQC spectrum ($CDCl_3$) of compounds **12** and **13**(#)

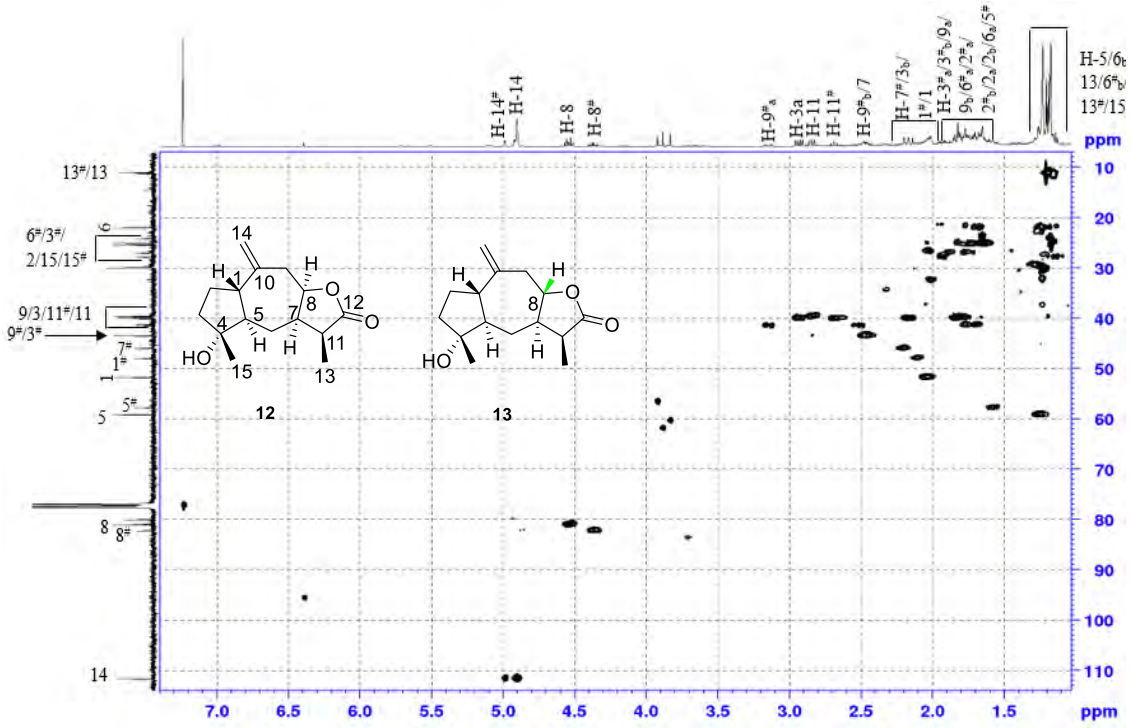

Plate 14G: HMBC spectrum ($CDCl_3$) of compounds **12** and **13**(#)

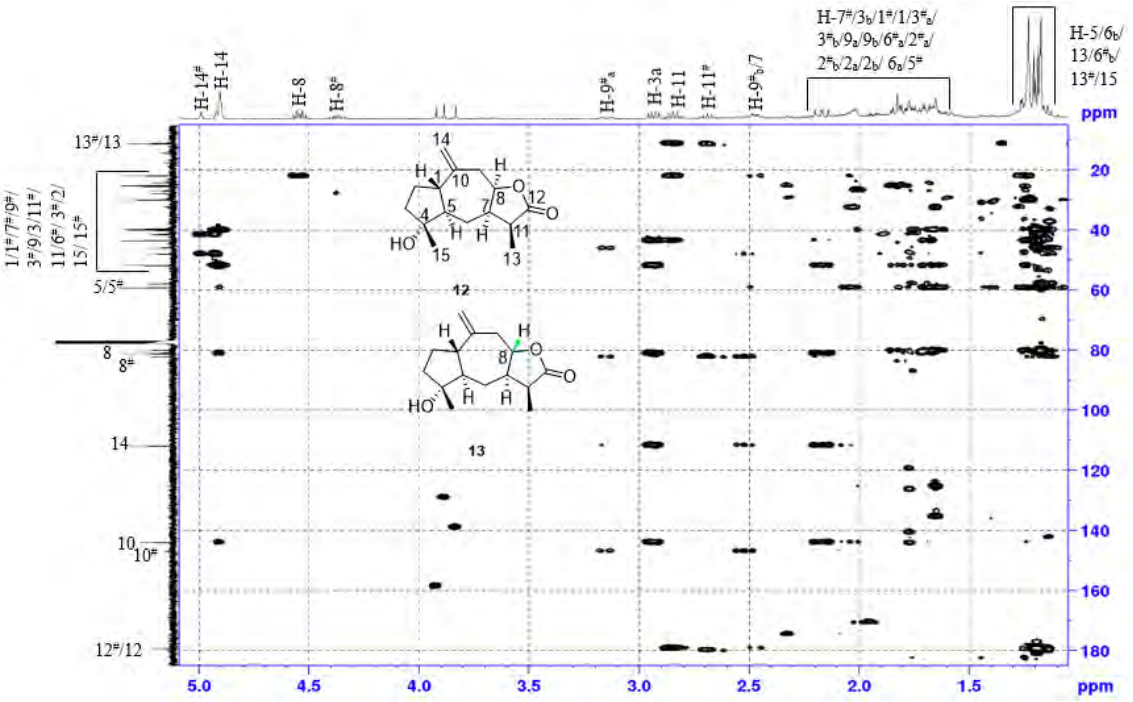

Plate 15A: COSY spectrum (CD_3OD) of compounds **14** and **15**(#)

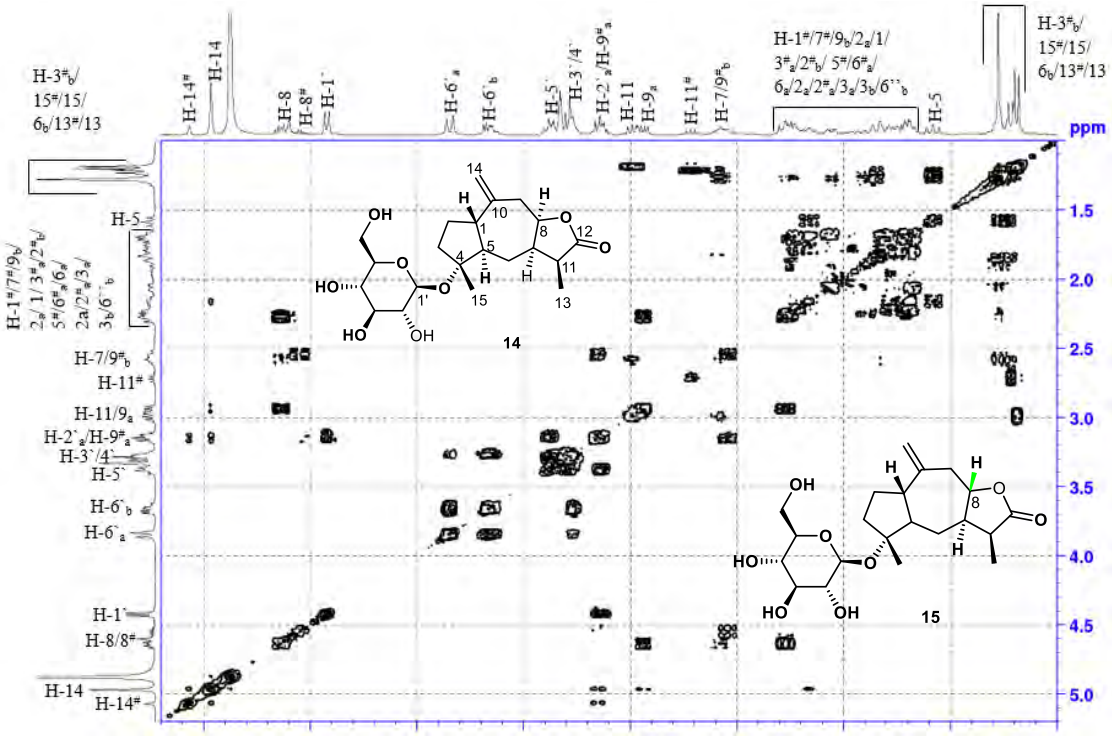

Plate 15B: DEPT-135 spectrum (CD_3OD) of compounds **14** and **15**(#)

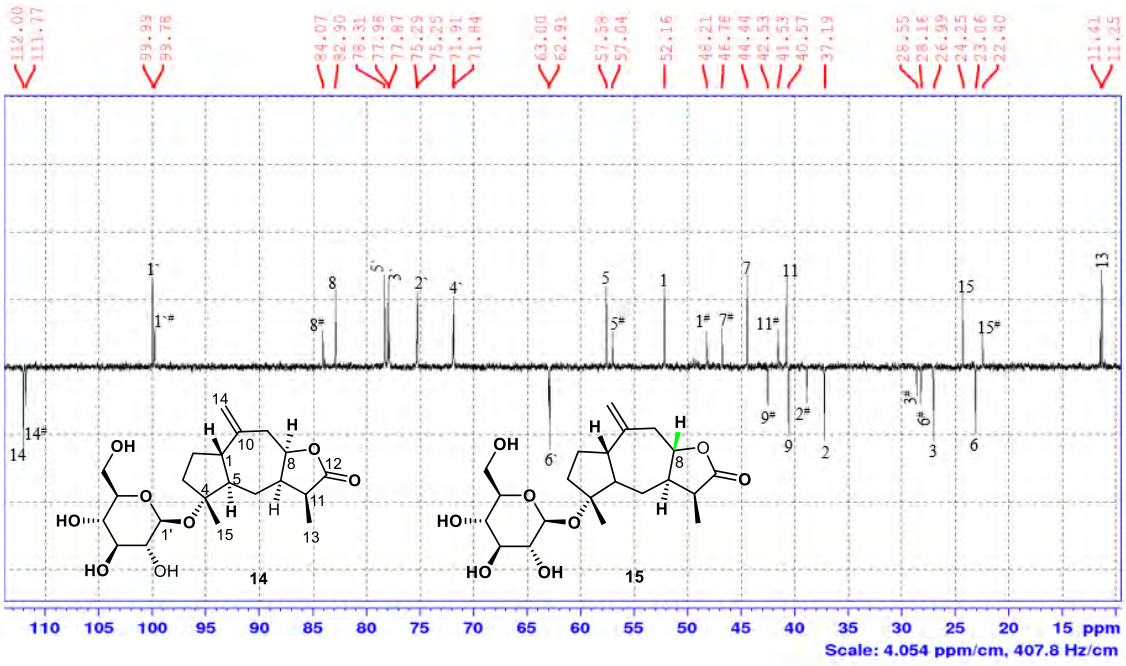

Plate 15C: HSQC spectrum (CD_3OD) of compounds **14** and **15**(#)

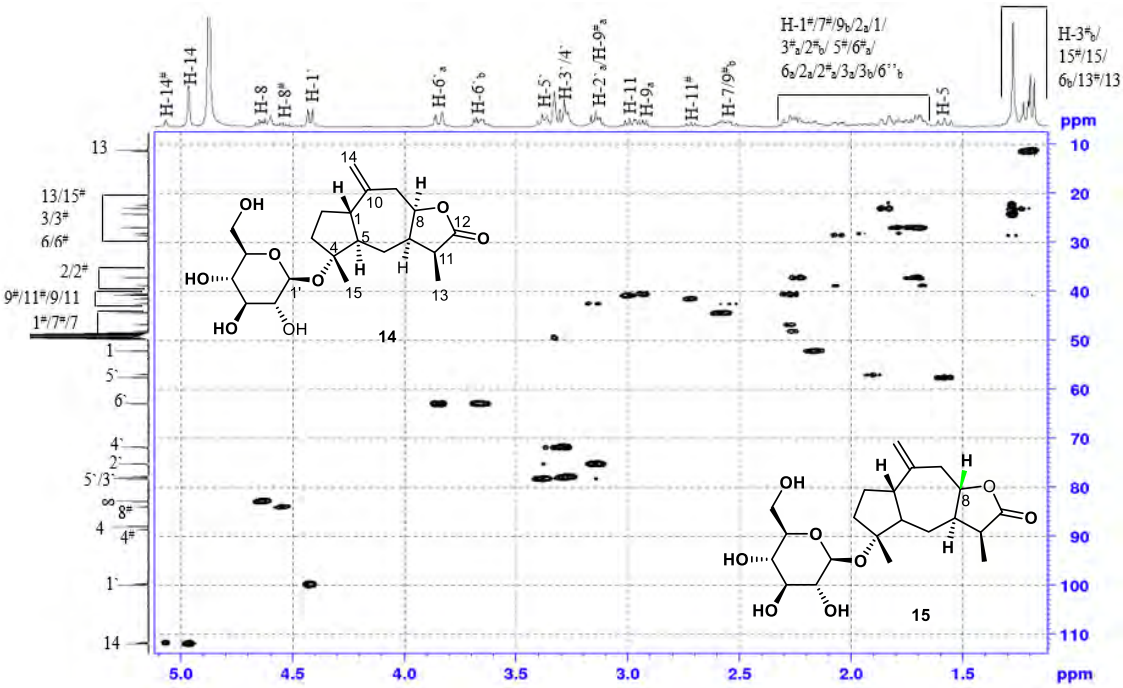

Plate 15D: HMBC spectrum (CD_3OD) of compounds **14** and **15**(#)

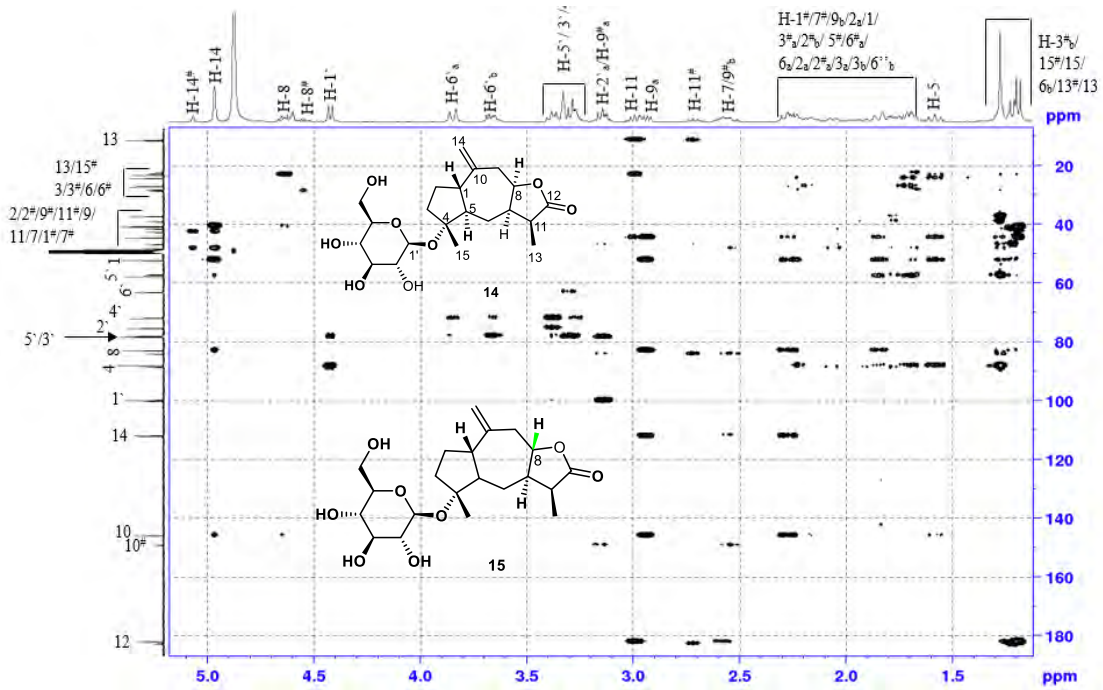

Plate 16A: ^{1}H-NMR spectrum ($CDCl_3$, 400 MHz) of compound **16**

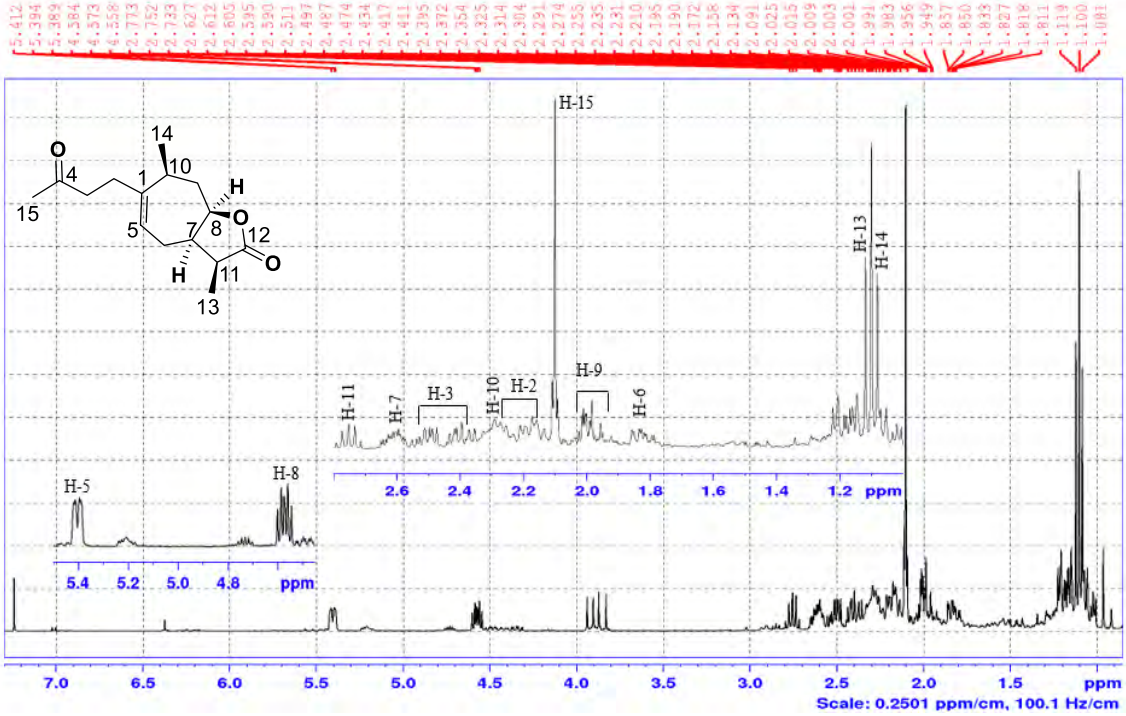

Plate 16B: COSY spectrum ($CDCl_3$) of compound **16**

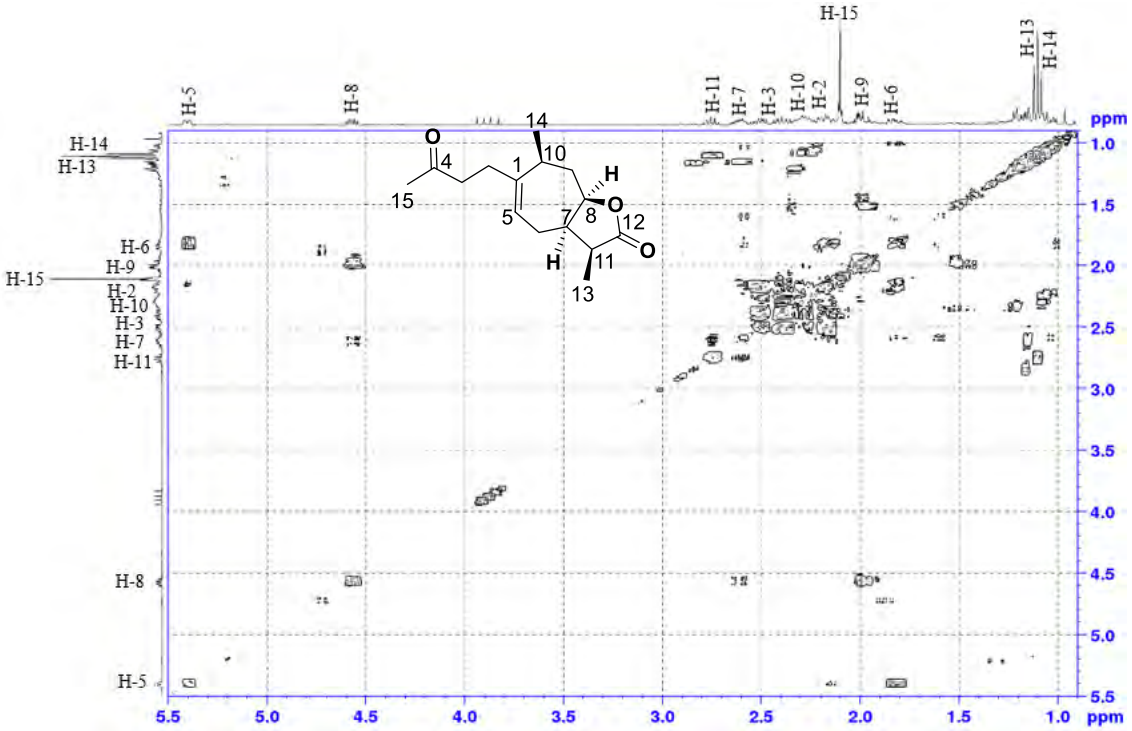

Plate 16C: Selected 1D NOE NMR spectrum ($CDCl_3$) of compound **16**

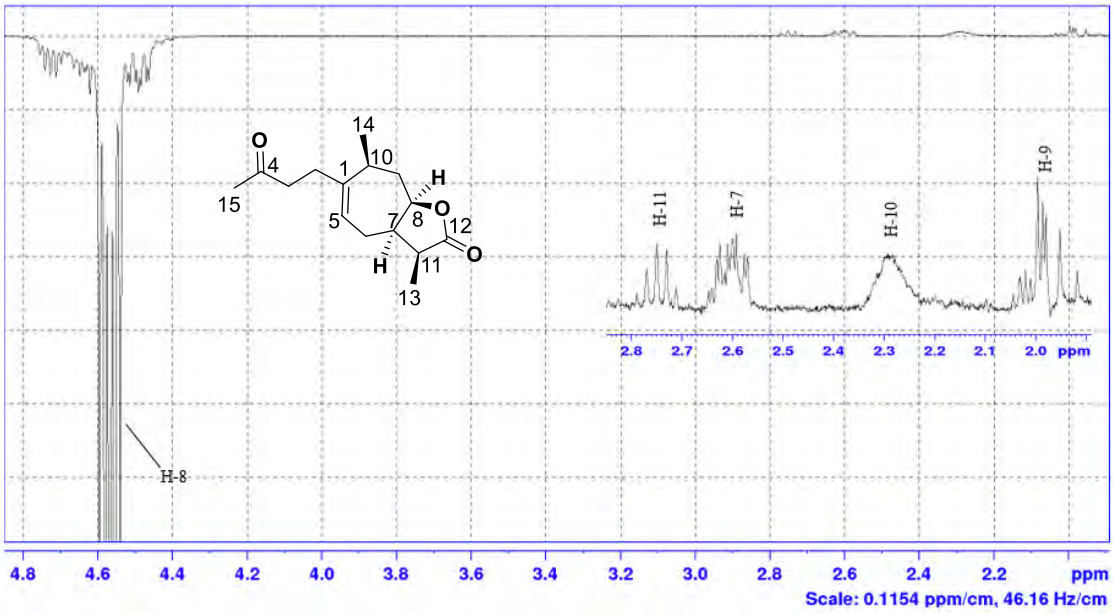

Plate 16D: ^{13}C-NMR spectrum ($CDCl_3$, 100 MHz) of compound **16**

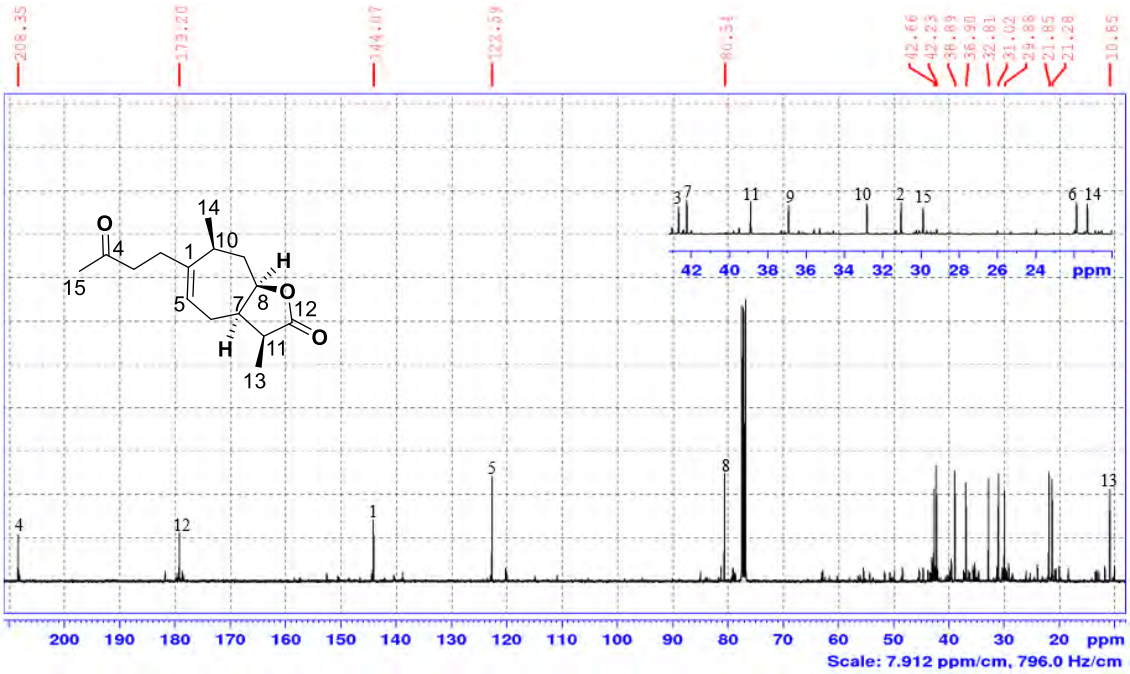

Plate 16E: DEPT-135 spectrum ($CDCl_3$) of compound **16**

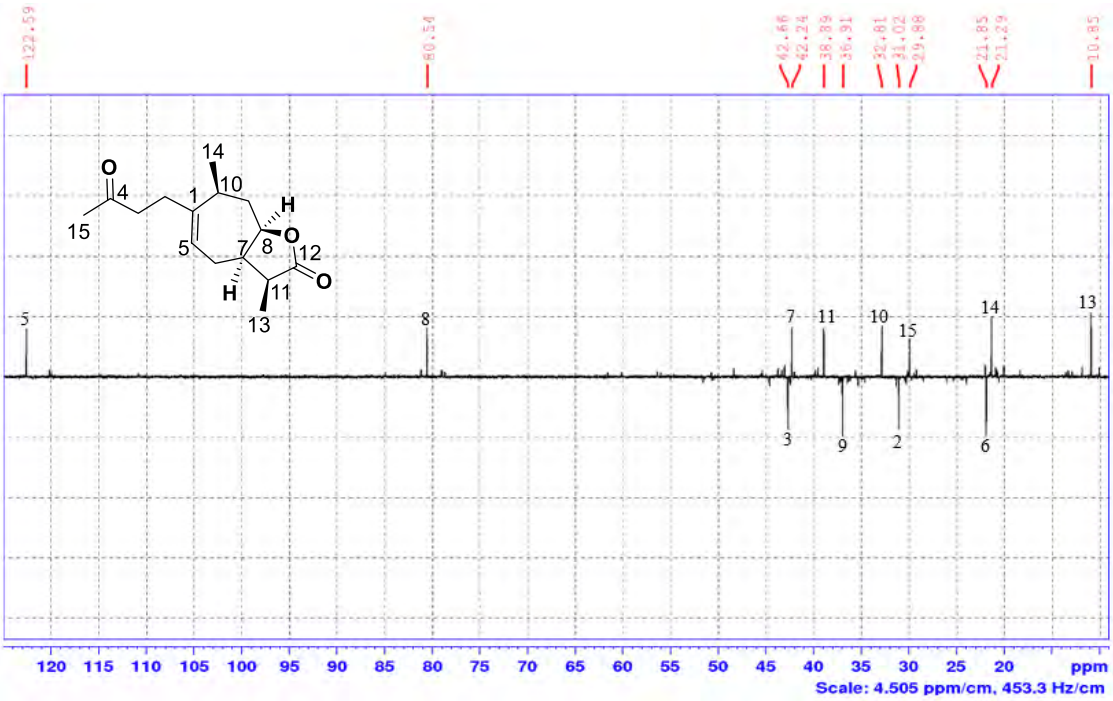

Plate 16F: HSQC spectrum ($CDCl_3$) of compound **16**

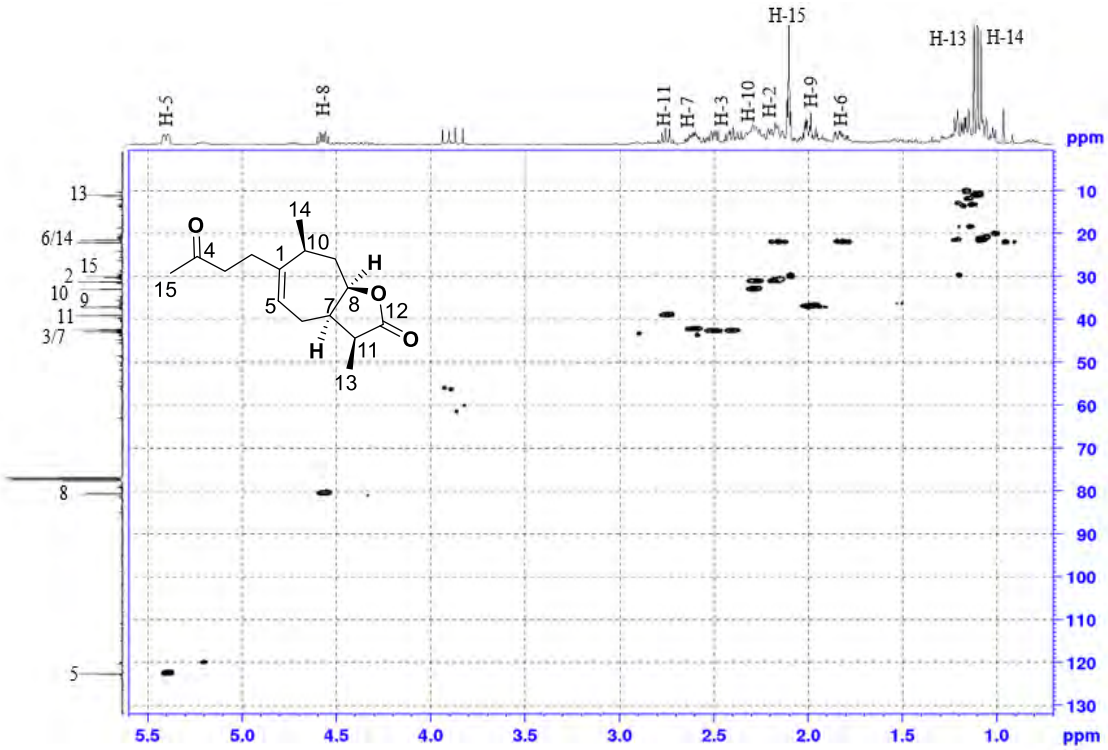

Plate 16G: HMBC spectrum ($CDCl_3$) of compound **16**

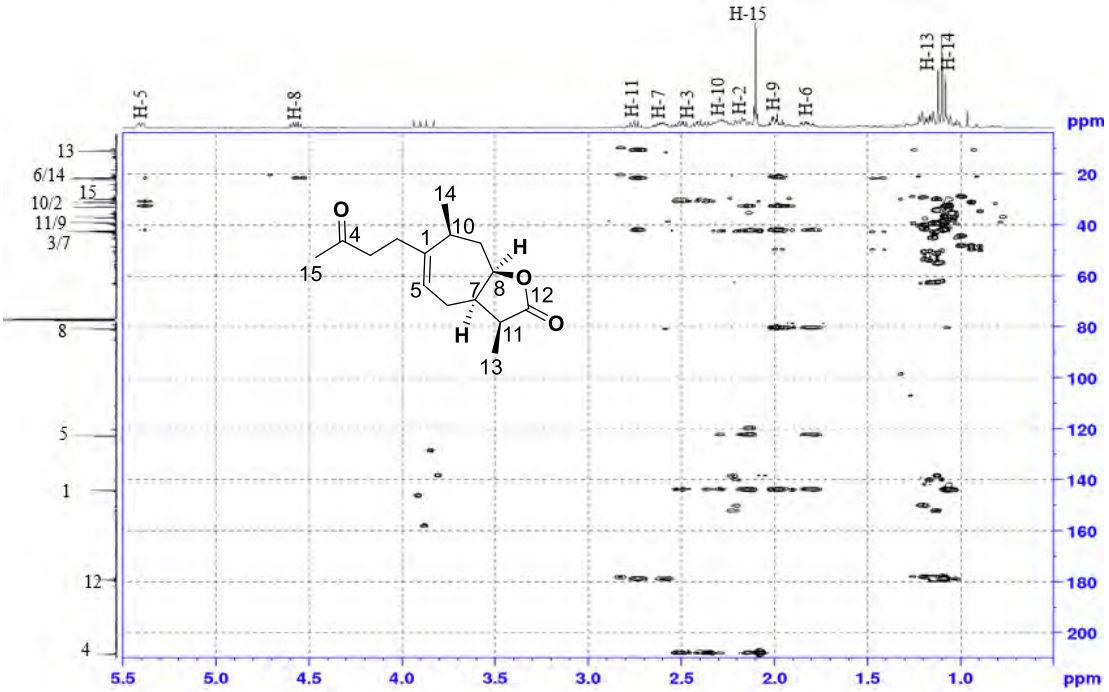

Plate 17A: ^{1}H-NMR spectrum ($CDCl_3$, 400 MHz) of compound **17**

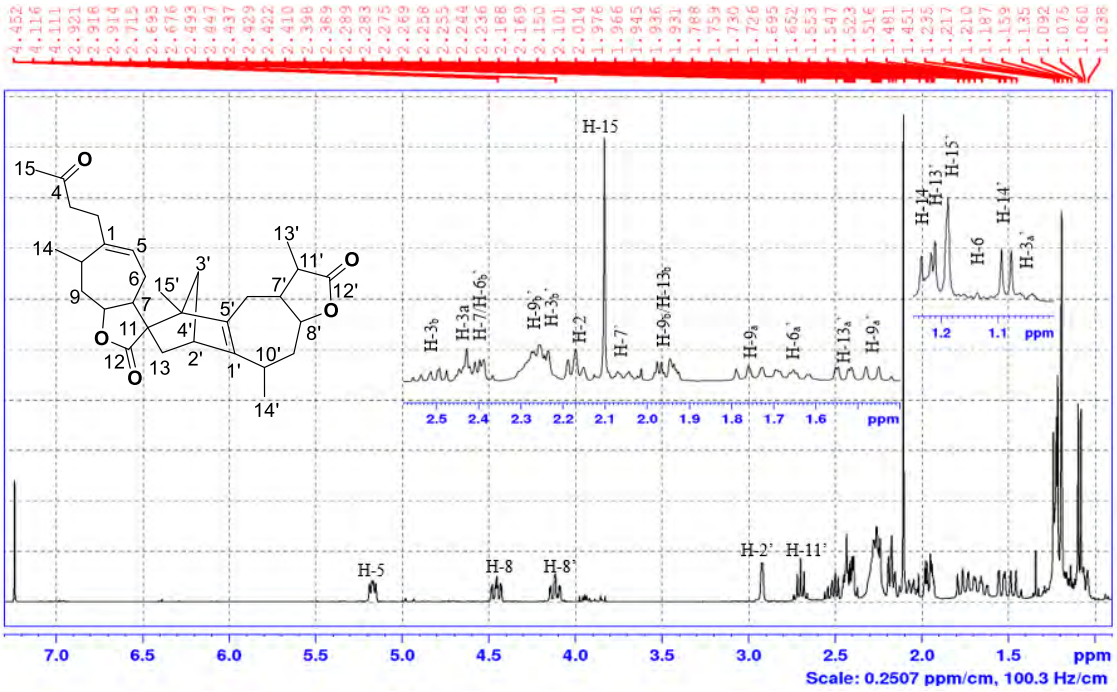

Plate 17B: COSY spectrum ($CDCl_3$) of compound **17**

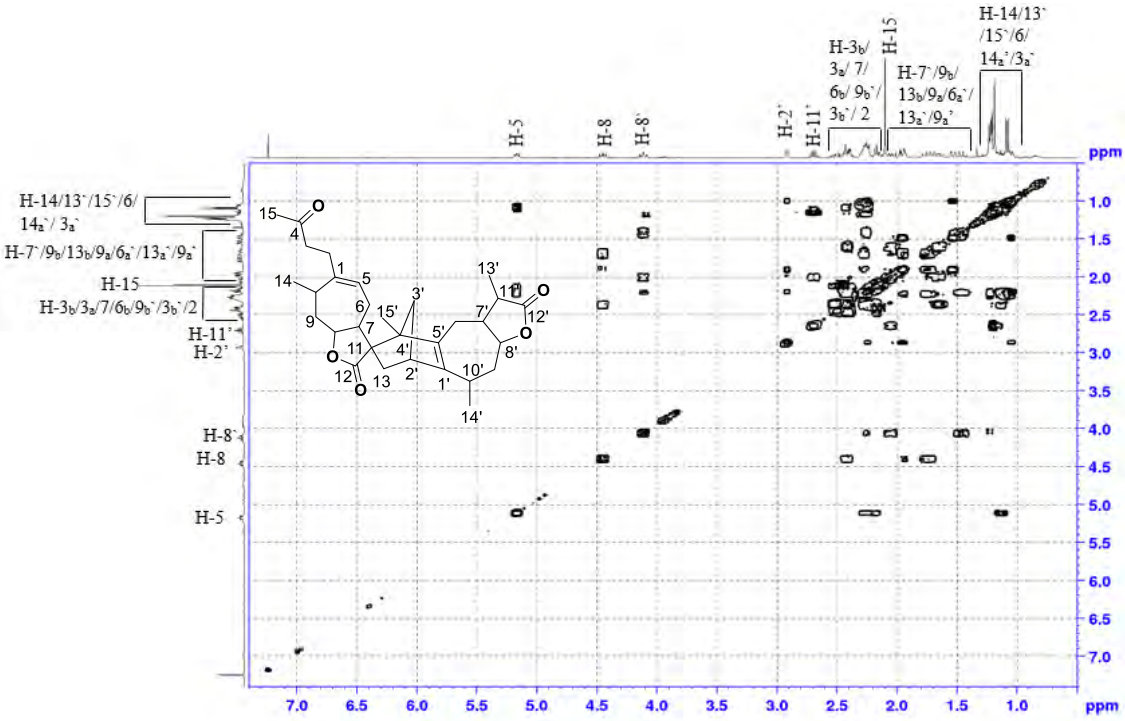

Plate 17C: ^{13}C-NMR spectrum ($CDCl_3$, 100 MHz) of compound **17**

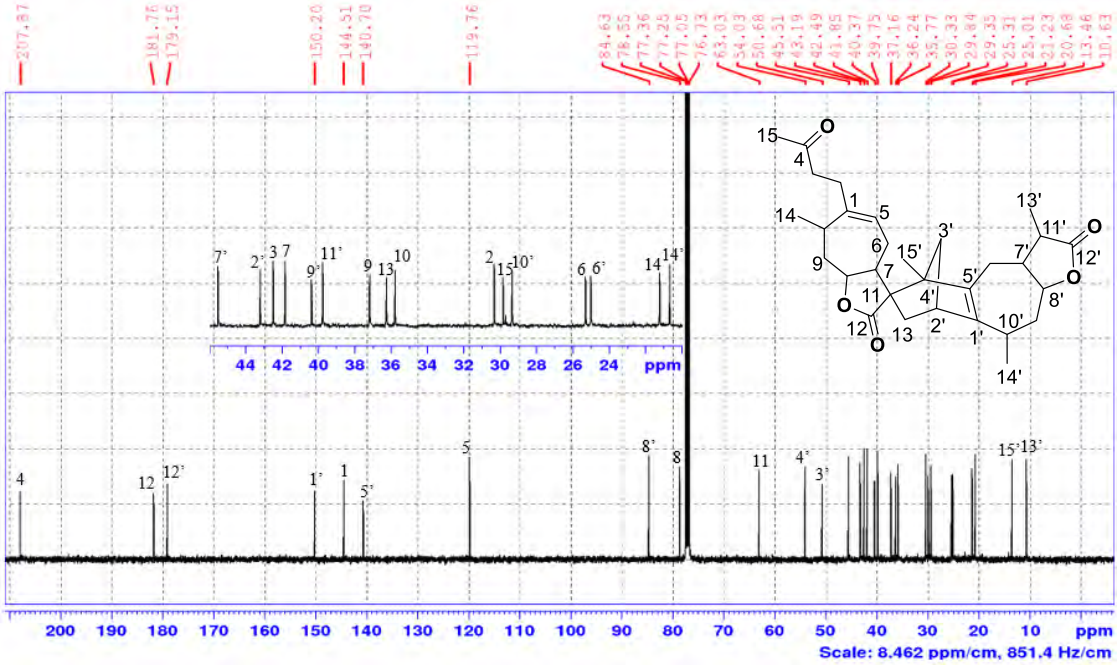

Plate 17D: DEPT-135 spectrum ($CDCl_3$) of compound **17**

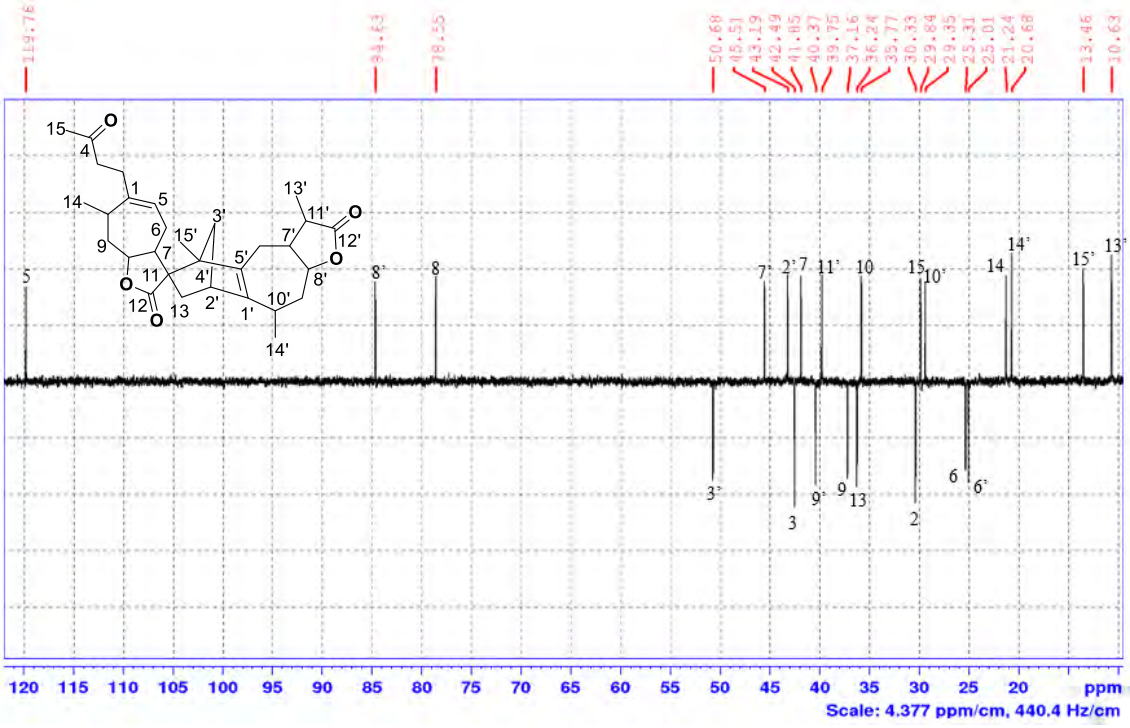

Plate 17F: HSQC spectrum ($CDCl_3$) of compound **17**

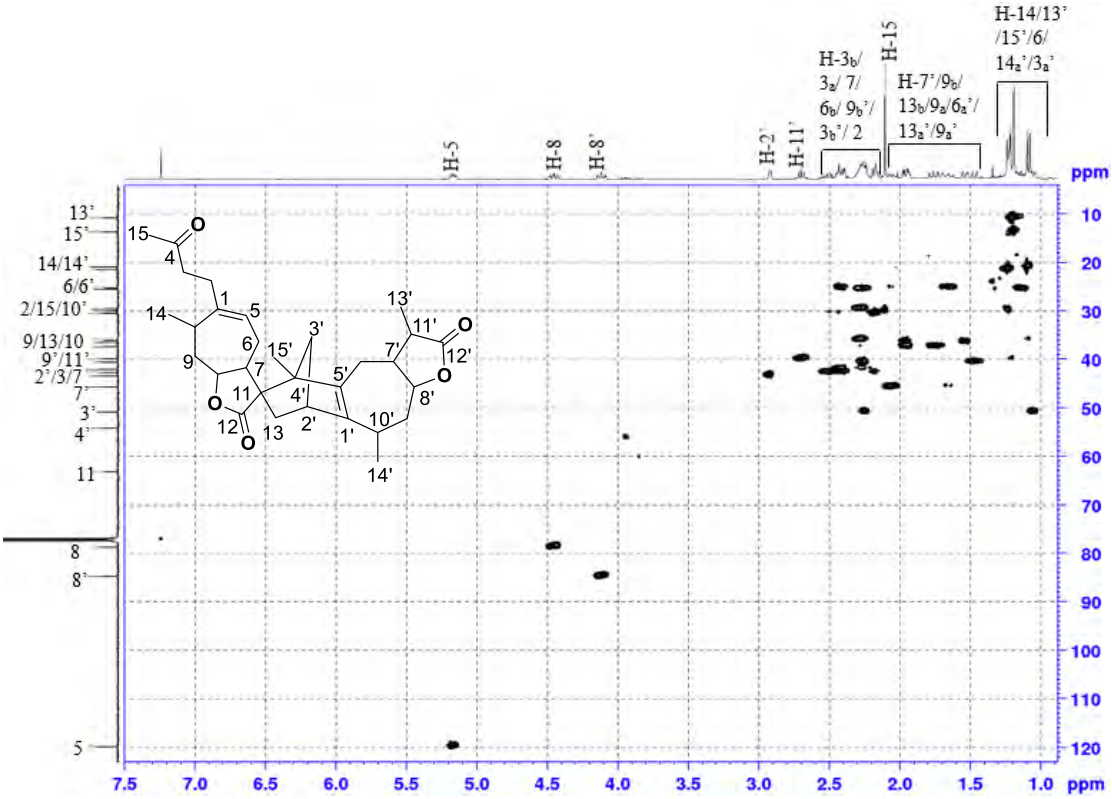

Plate 17F: HMBC spectrum ($CDCl_3$) of compound **17**

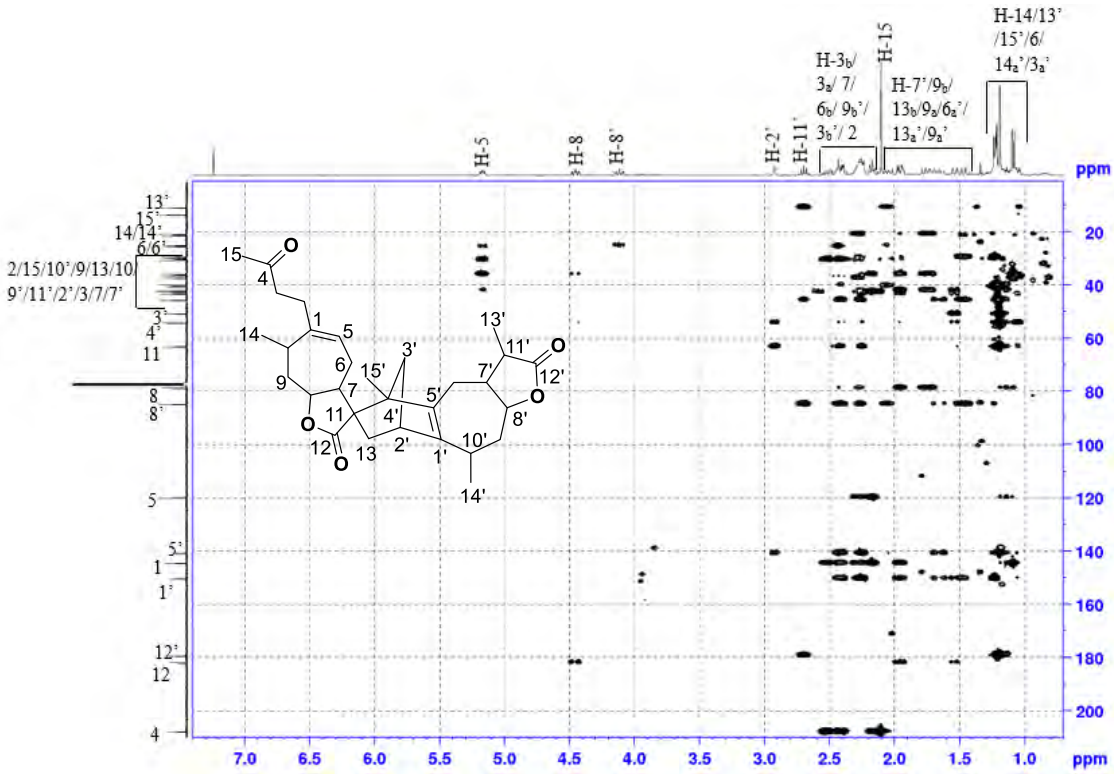

Plate 18A: ^{1}H-NMR spectrum (CD_3OD, 400 MHz) of compound **18**

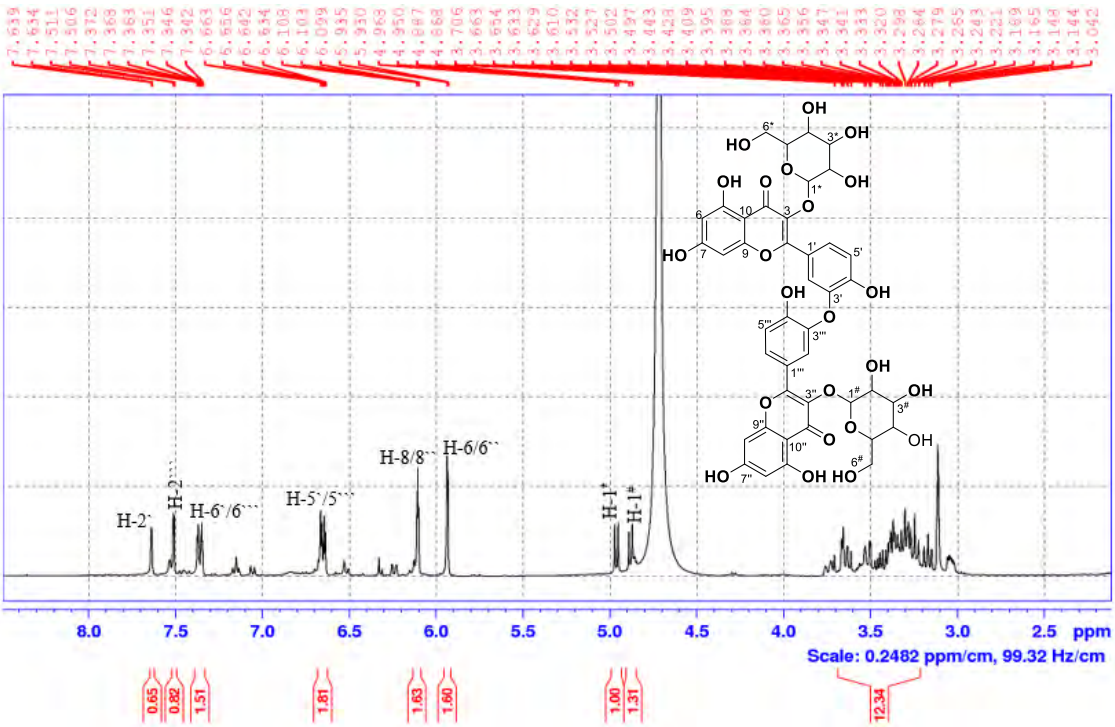

Plate 18B: COSY spectrum (CD_3OD) of compound **18**

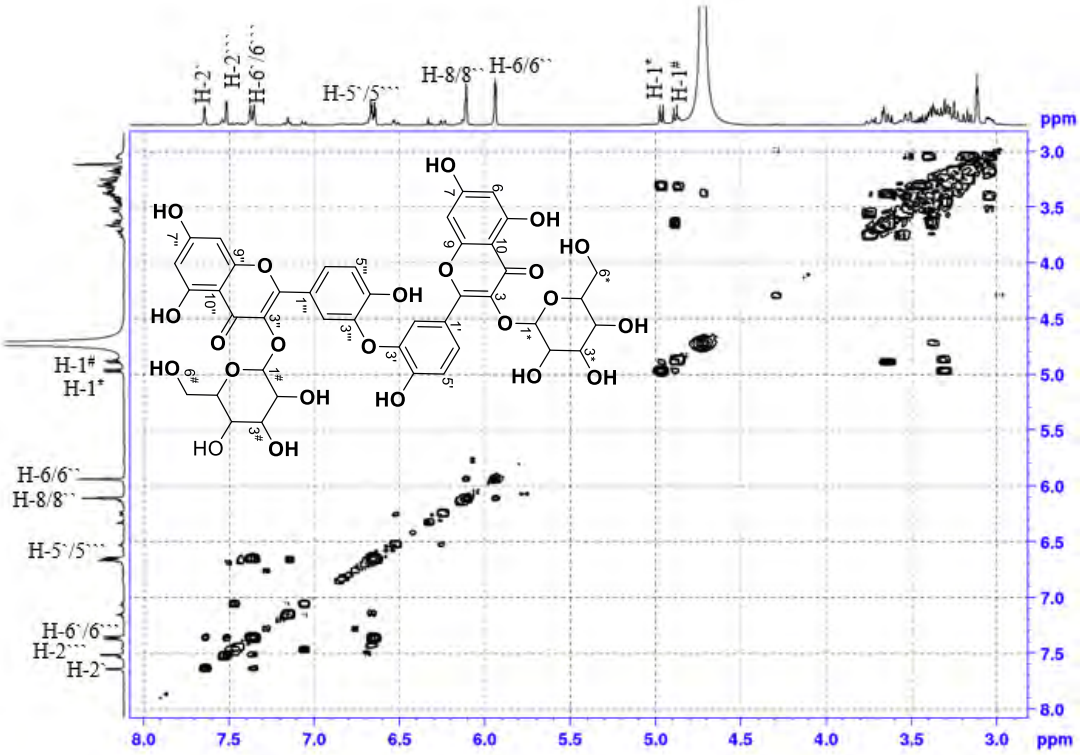

Plate 18C: NOE spectrum (CD_3OD) of compound **18**

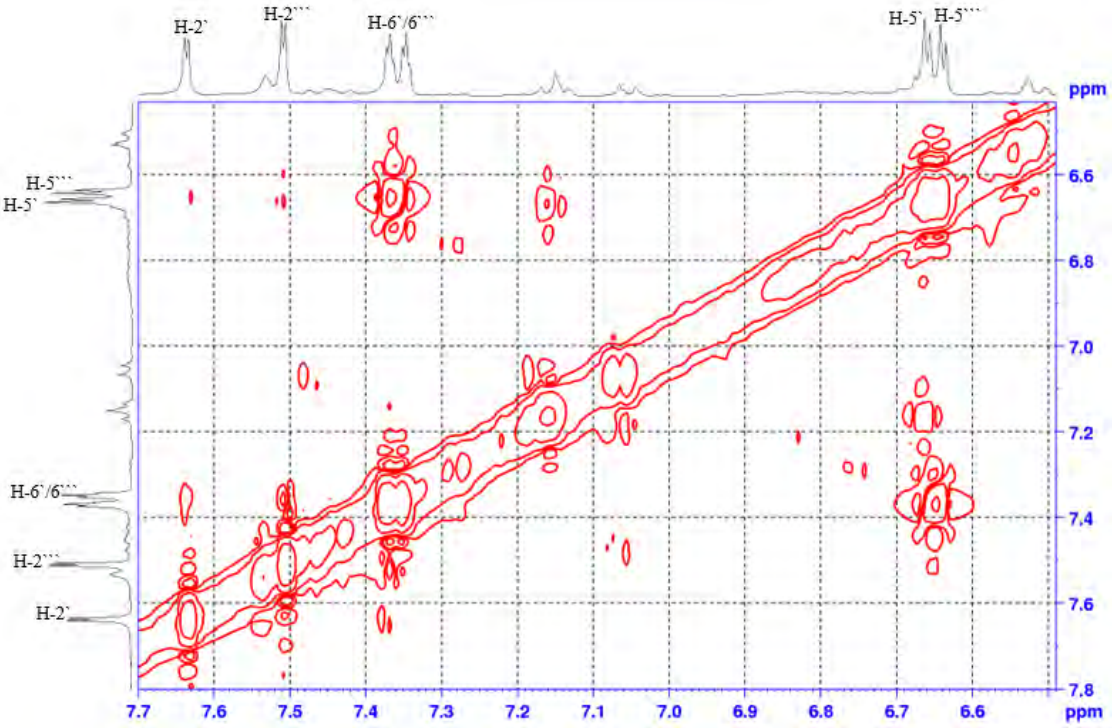

Plate 18D: ^{13}C-NMR spectrum (CD_3OD, 100 MHz) of compound **18**

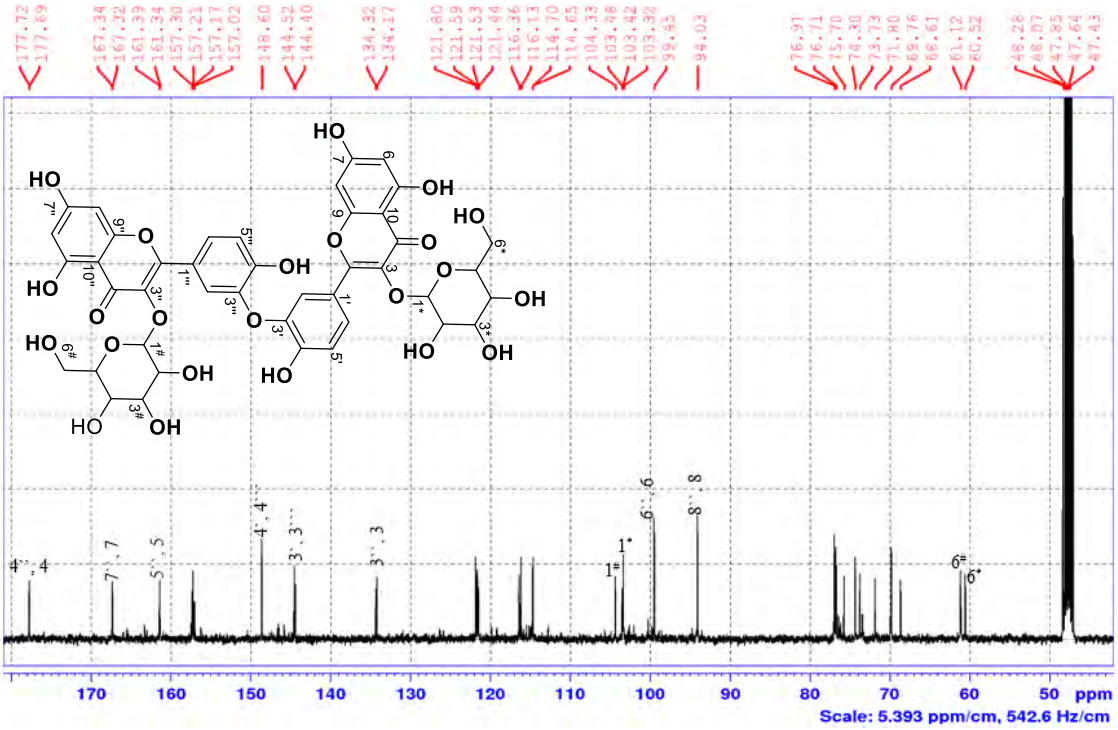

Plate 18E: DEPT-135 spectrum (CD_3OD) of compound **18**

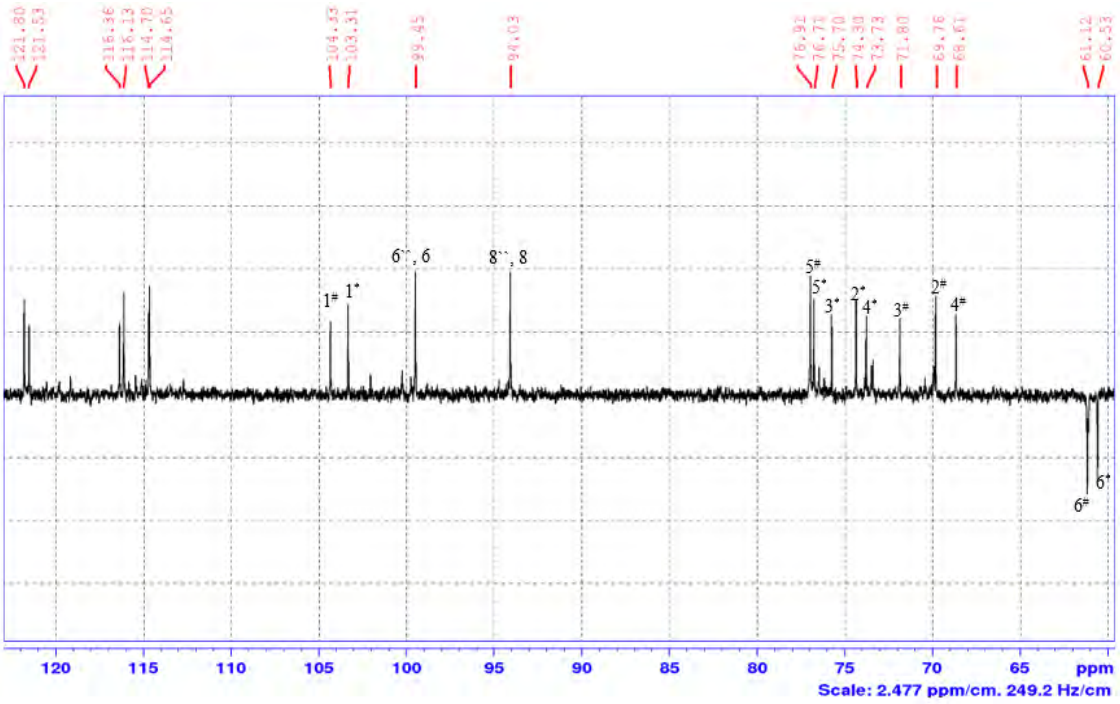

Plate 18E: HSQC spectrum (CD_3OD) of compound **18**

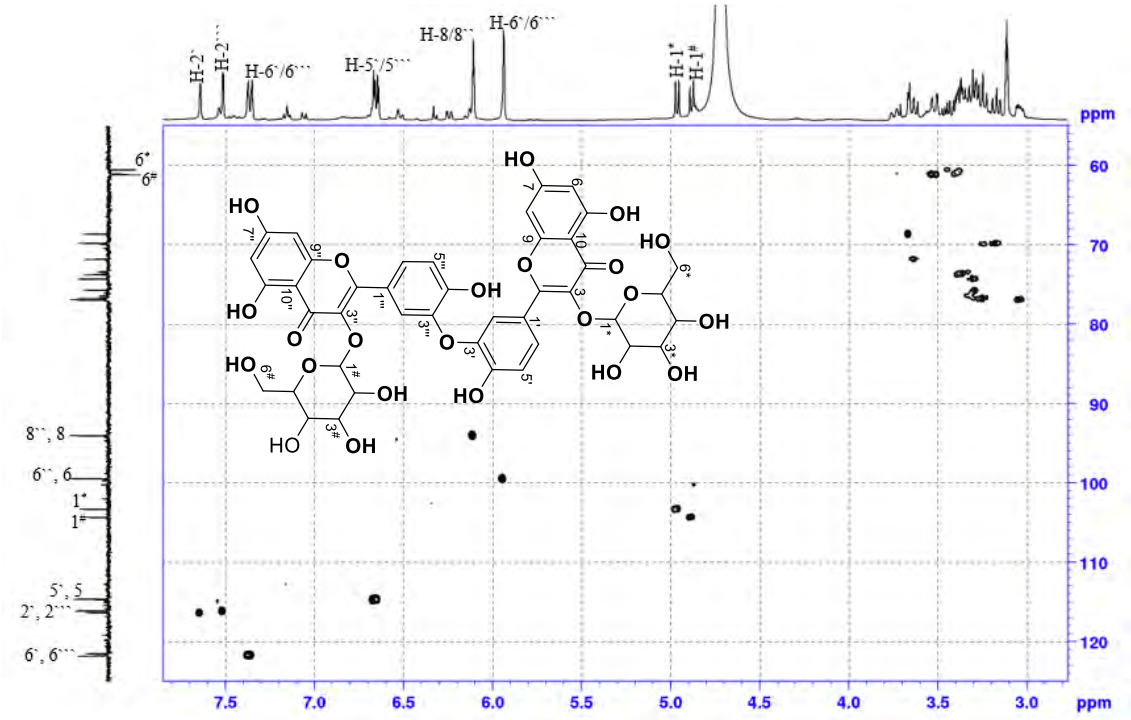

Plate 18F: HMBC spectrum (CD_3OD) of compound **18**

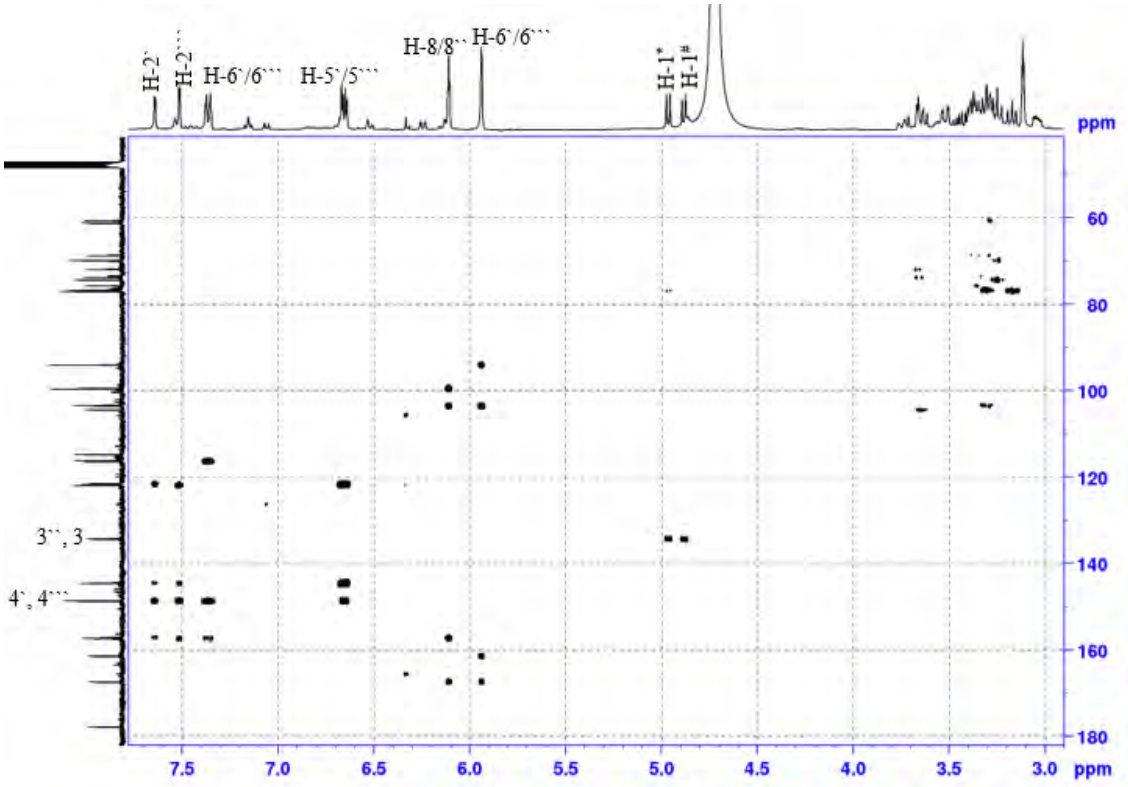

Plate 18G: LC-MS spectrum of compound **18**

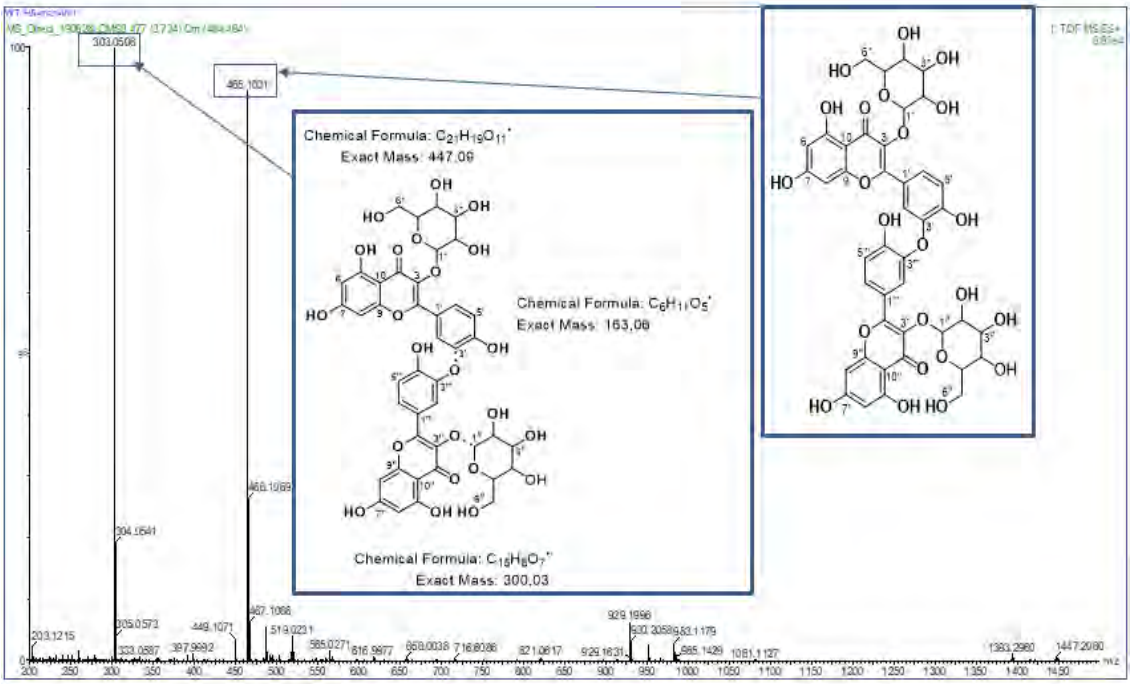

Plate 19A: ^{1}H-NMR spectrum (CD_3OD and $CDCl_3$, 400 MHz) of compound **19**

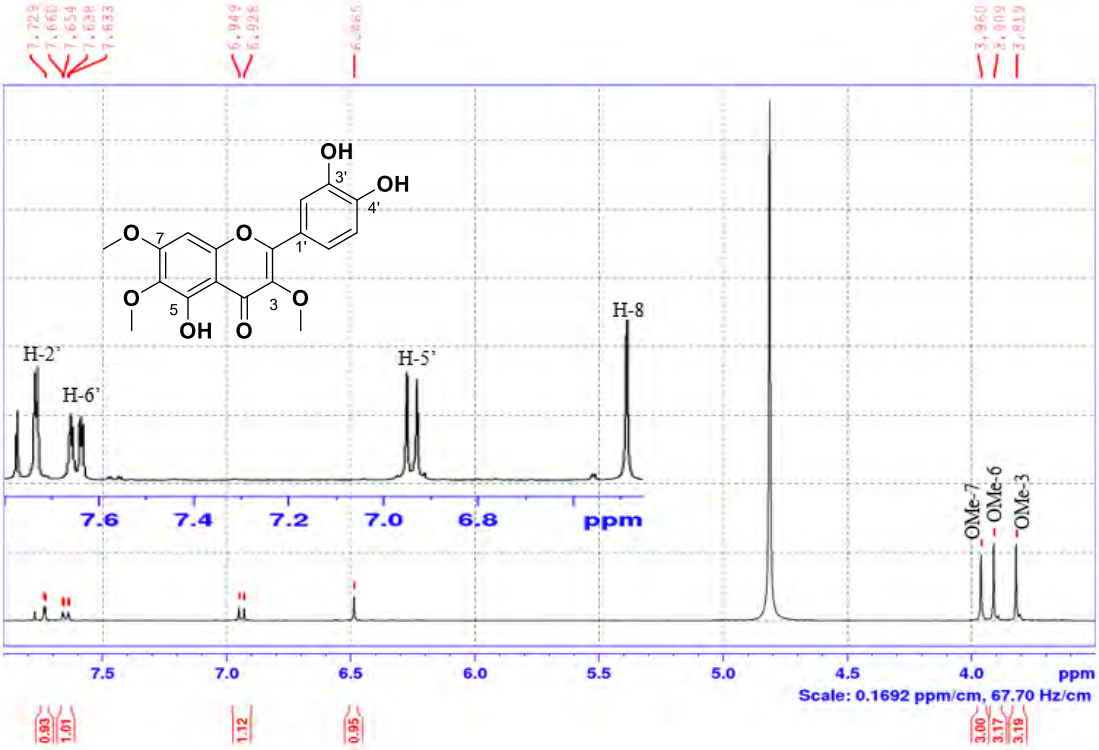

Plate 19B: COSY spectrum (CD_3OD and $CDCl_3$) of compound **19**

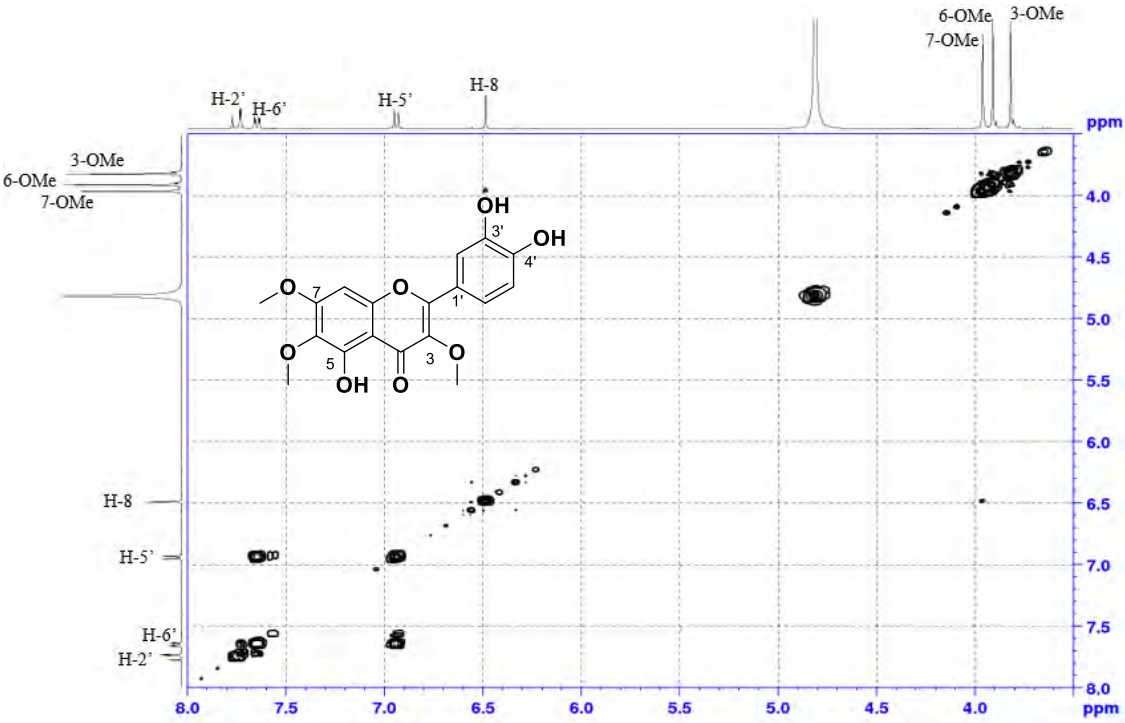

Plate 19C: ^{13}C-NMR spectrum (CD_3OD and $CDCl_3$, 100 MHz) of compound **19**

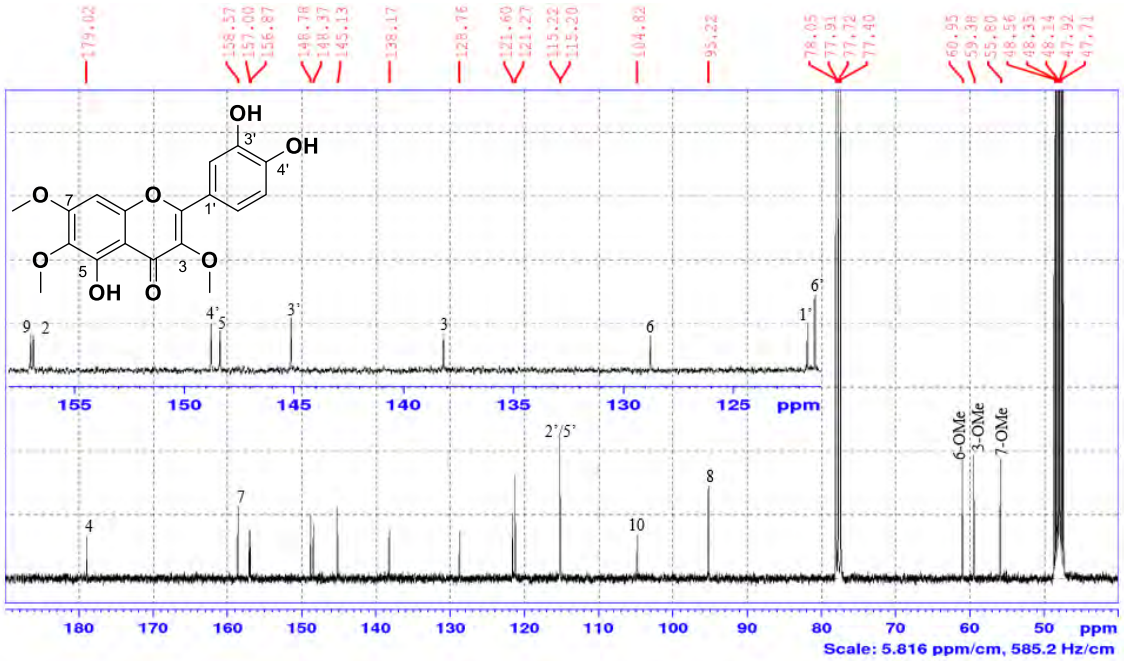

Plate 19D: DEPT-135 spectrum (CD_3OD and $CDCl_3$) of compound **19**

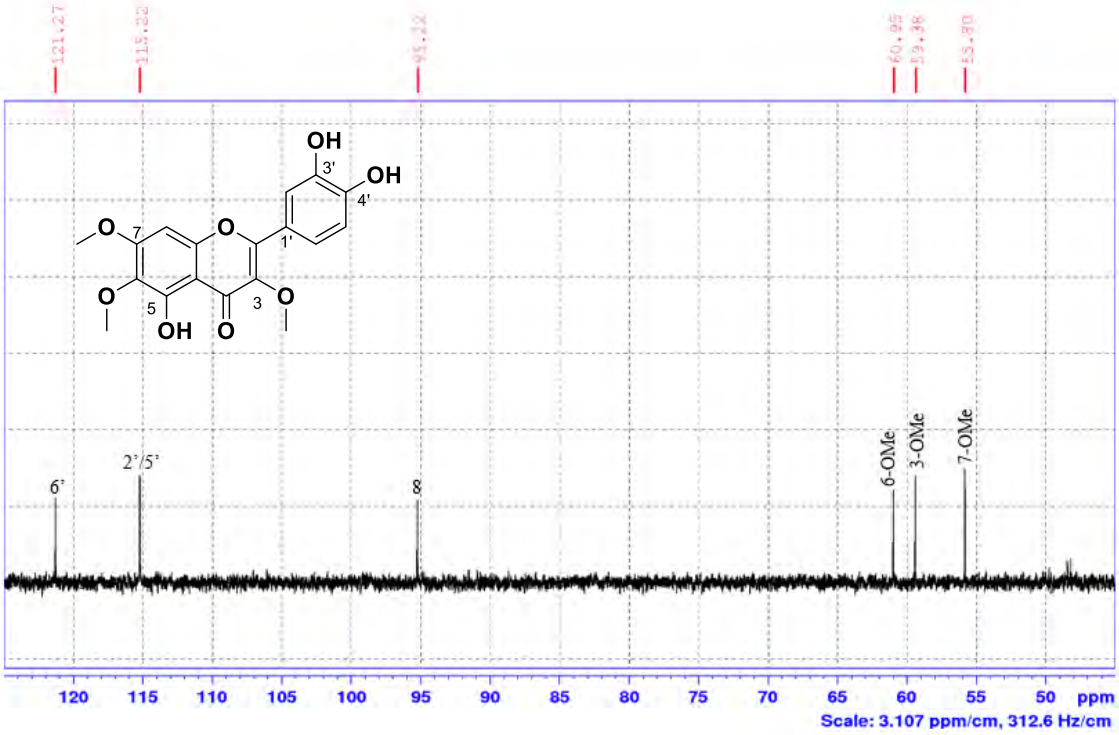

Plate 19E: HSQC spectrum (CD_3OD and $CDCl_3$) of compound **19**

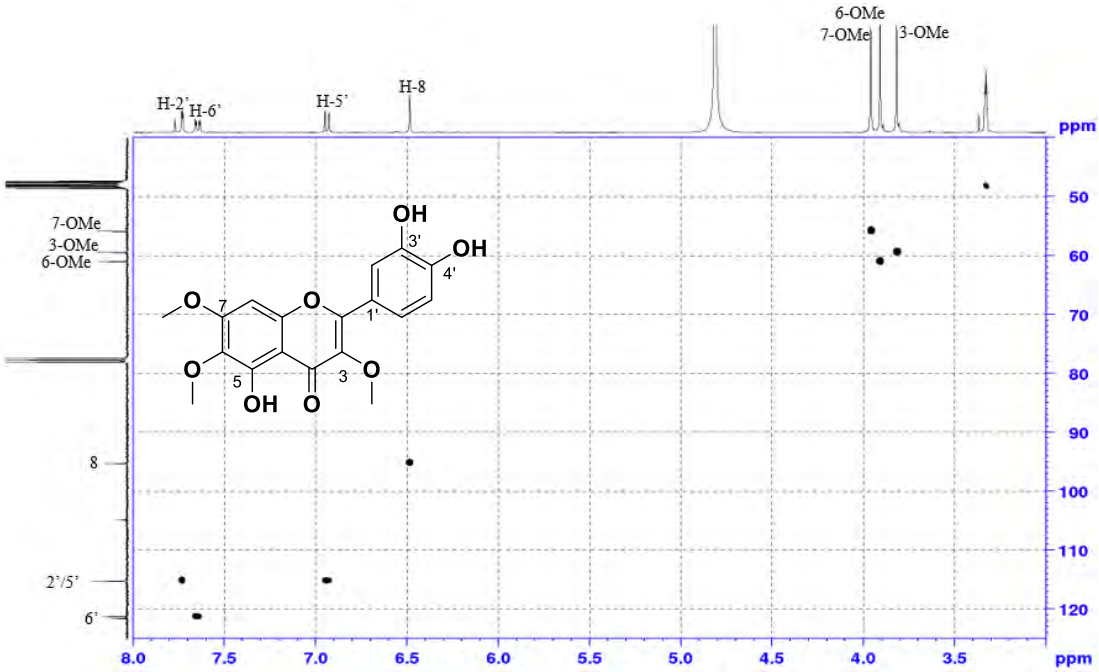

Plate 19F: HMBC spectrum (CD_3OD and $CDCl_3$) of compound **19**

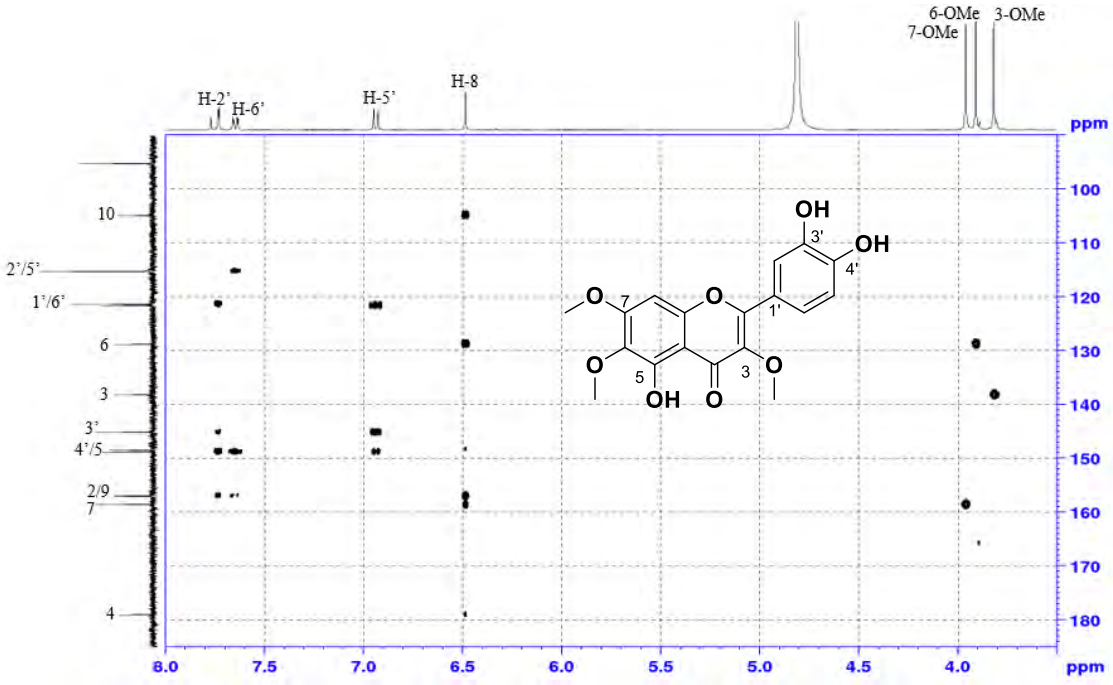

Plate 20A: ^{1}H-NMR spectrum (D_2O, 400 MHz) of compound **20**

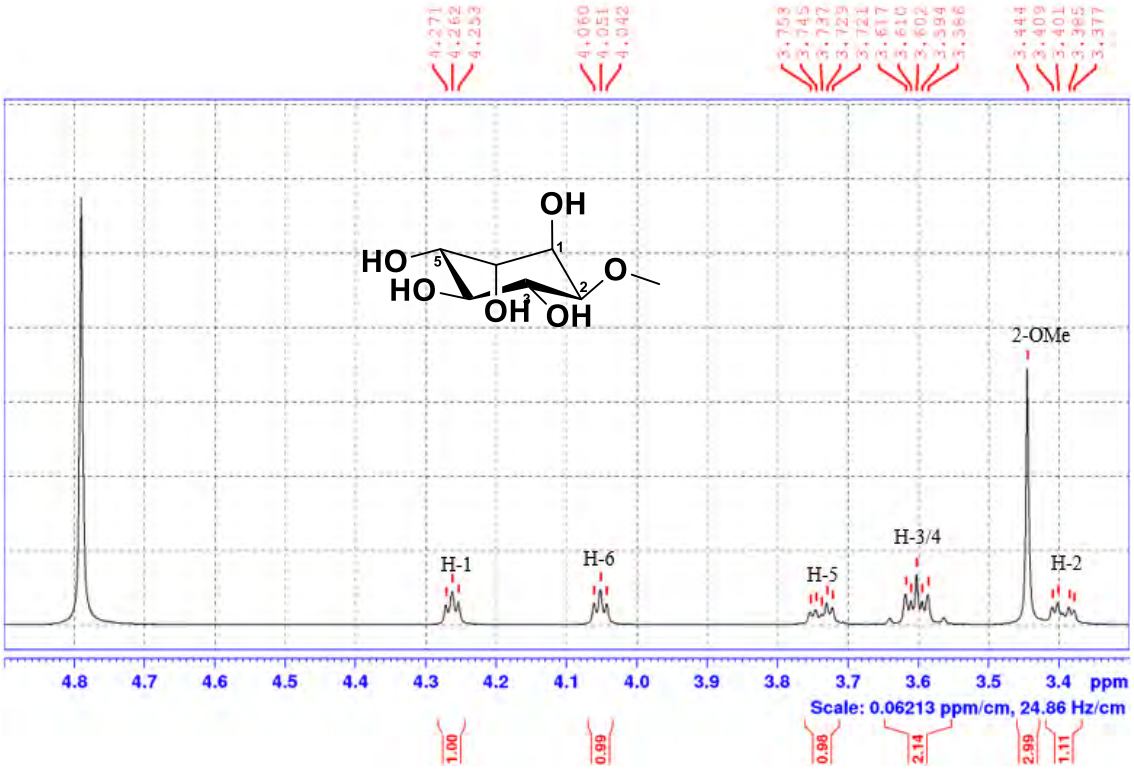

Plate 20B: COSY spectrum (D_2O) of compound **20**

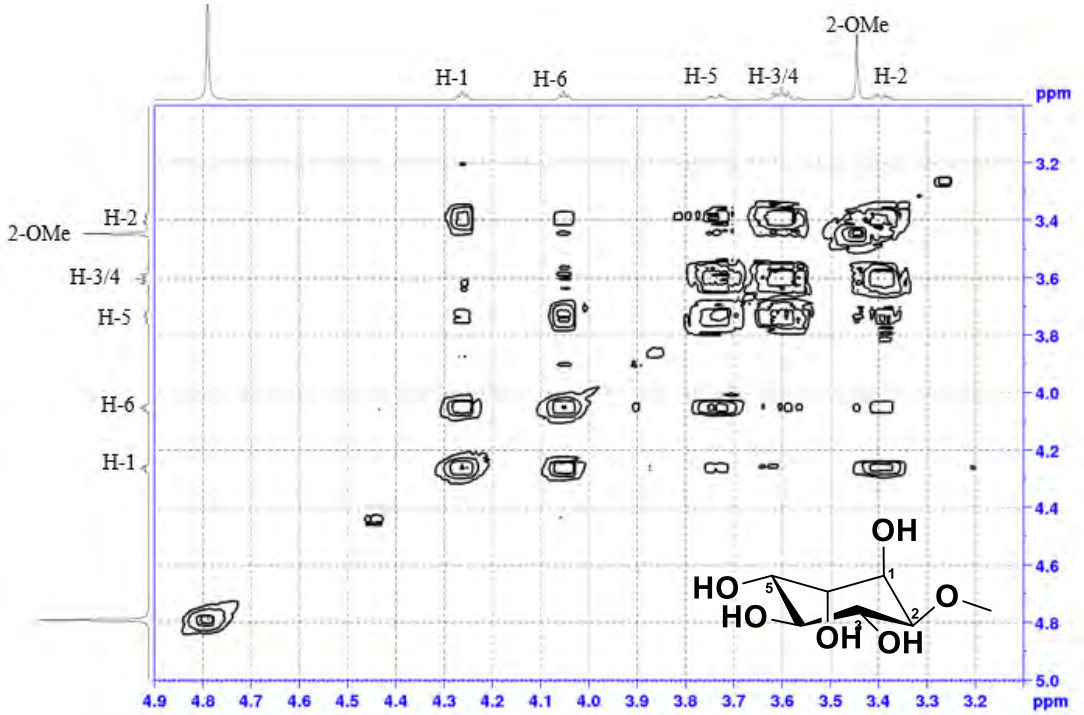

Plate 20C: ^{13}C (D_2O, 100 MHz) and DEPT-135 NMR (D_2O) spectra of compound **20**

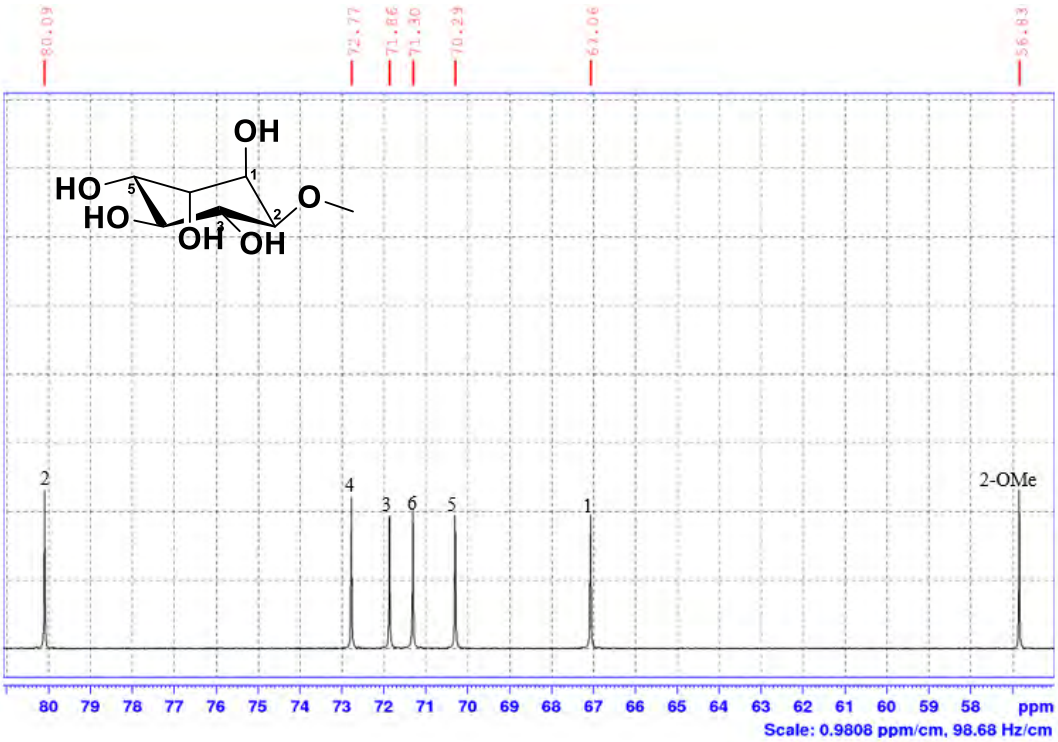

Plate 20D: HSQC spectrum (D_2O) of compound **20**

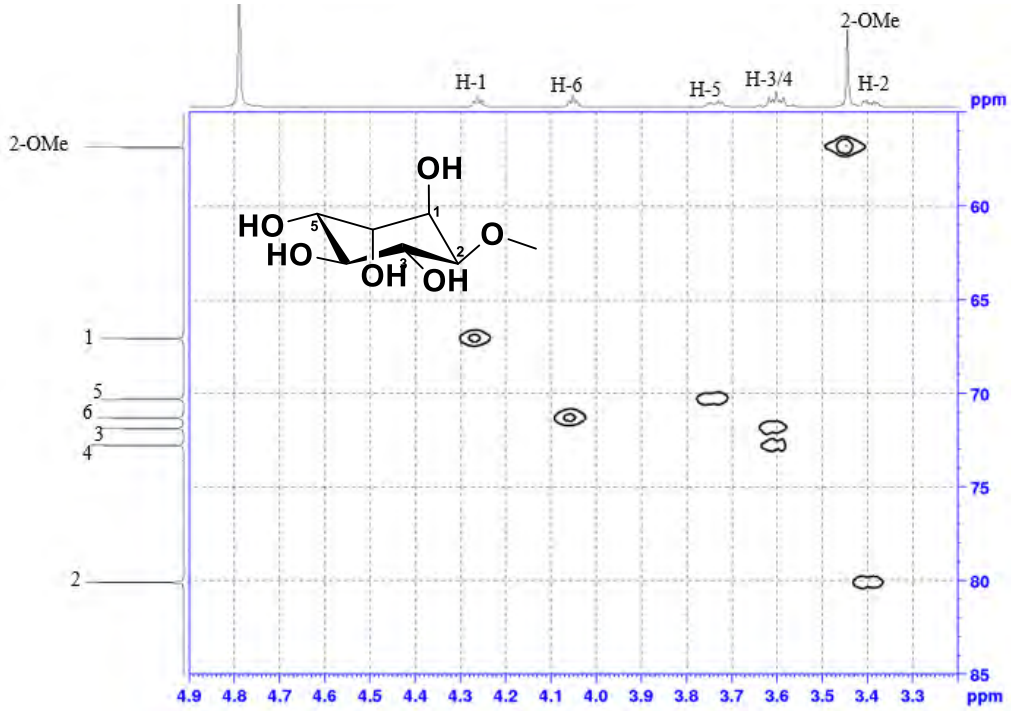

Plate 20E: HMBC spectrum (D_2O) of compound **20**

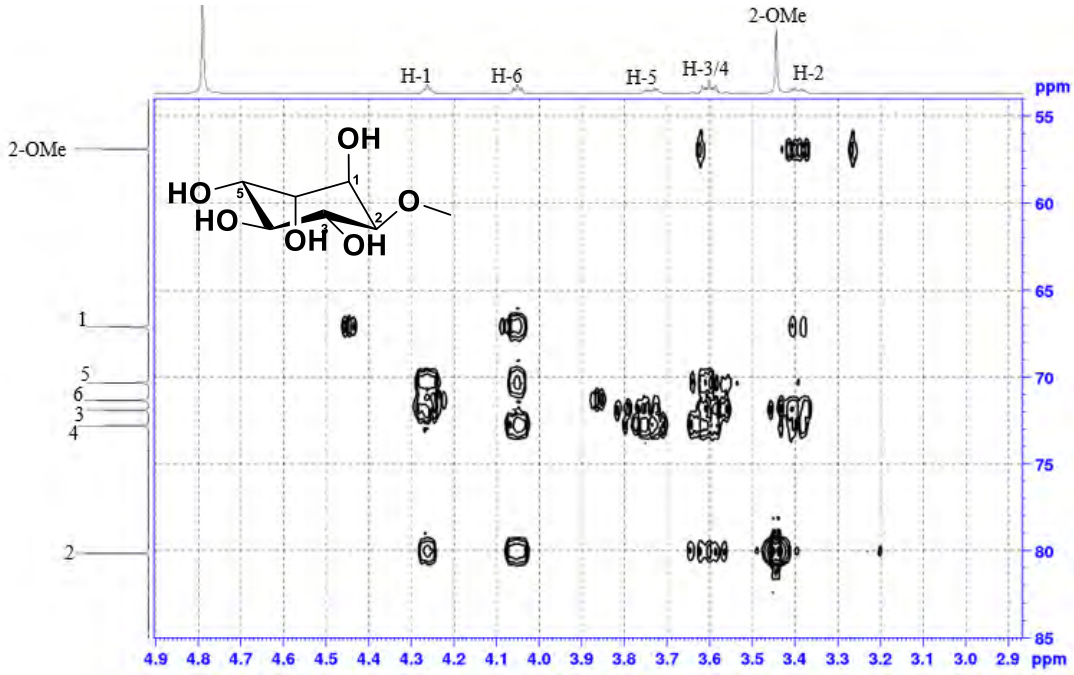

Plate 21A: ^{1}H-NMR spectrum (pyridine-d_5, 400 MHz) of compounds **21**[H1] and **22**[H2]

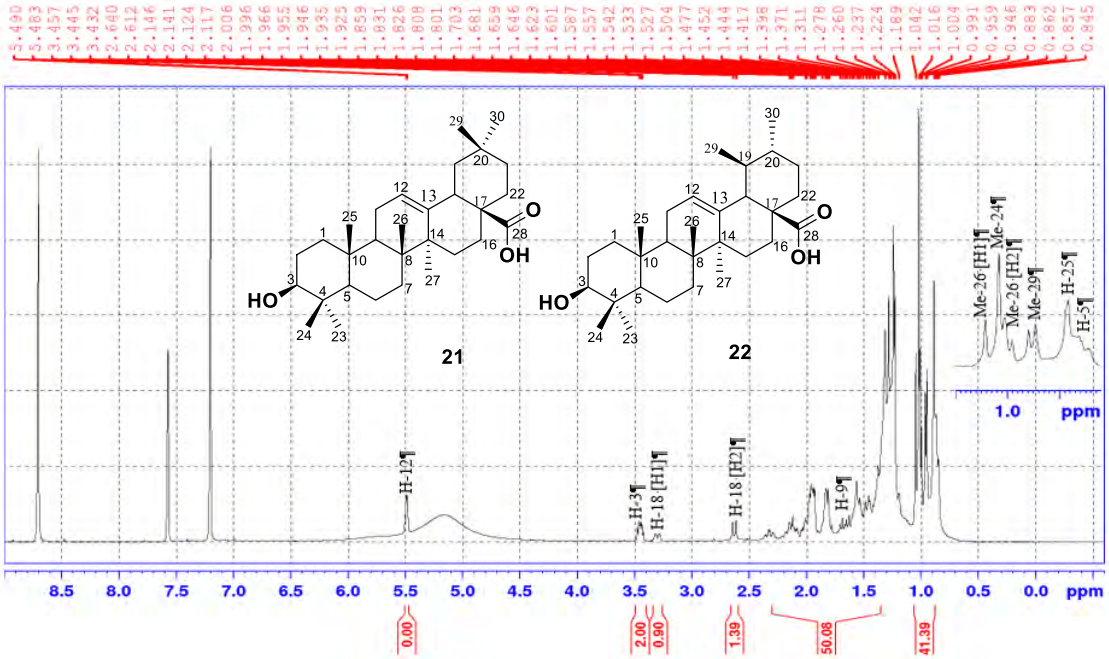

Plate 21B: COSY spectrum (pyridine-d_5) of compounds **21**[H1] and **22**[H2]

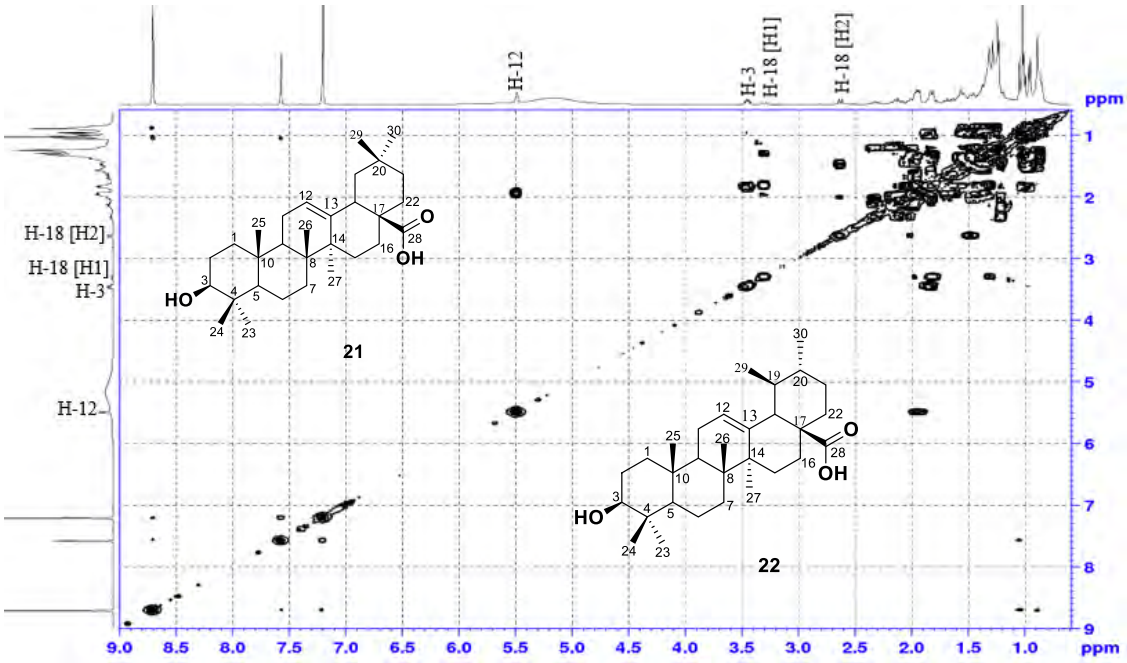

Plate 21C: ^{13}C-NMR spectrum (pyridine-d_5, 100 MHz) of compounds **21**[H1] and **22**[H2]

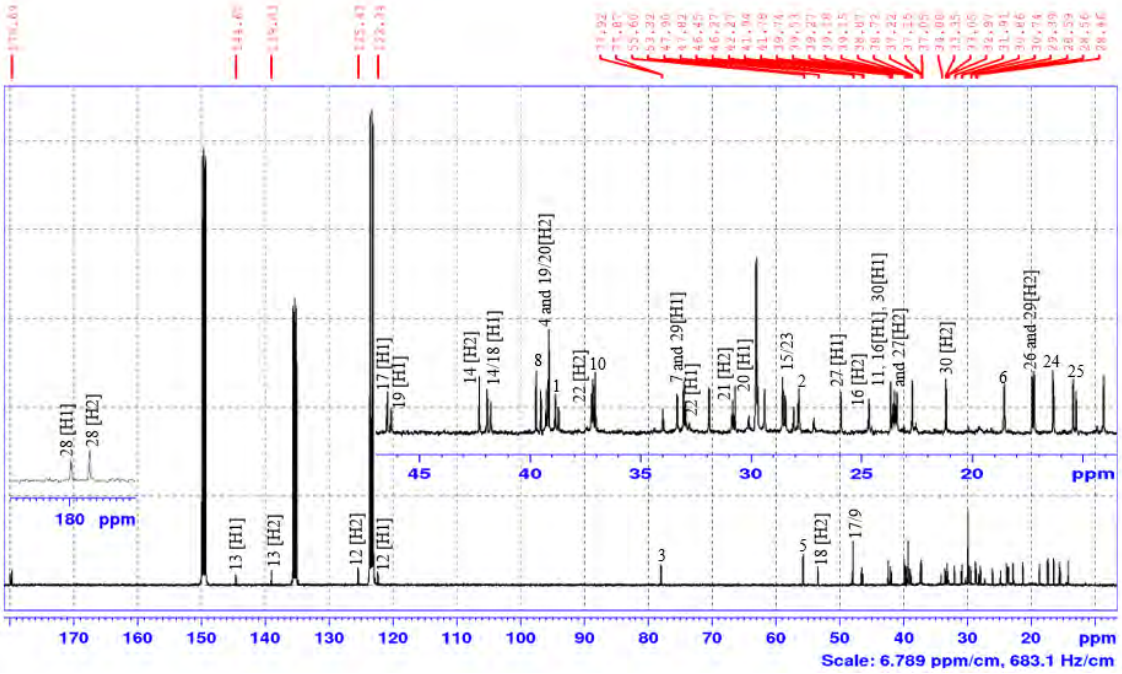

Plate 21D: DEPT-135 spectrum (pyridine-d_5) of compounds **21**[H1] and **22**[H2]

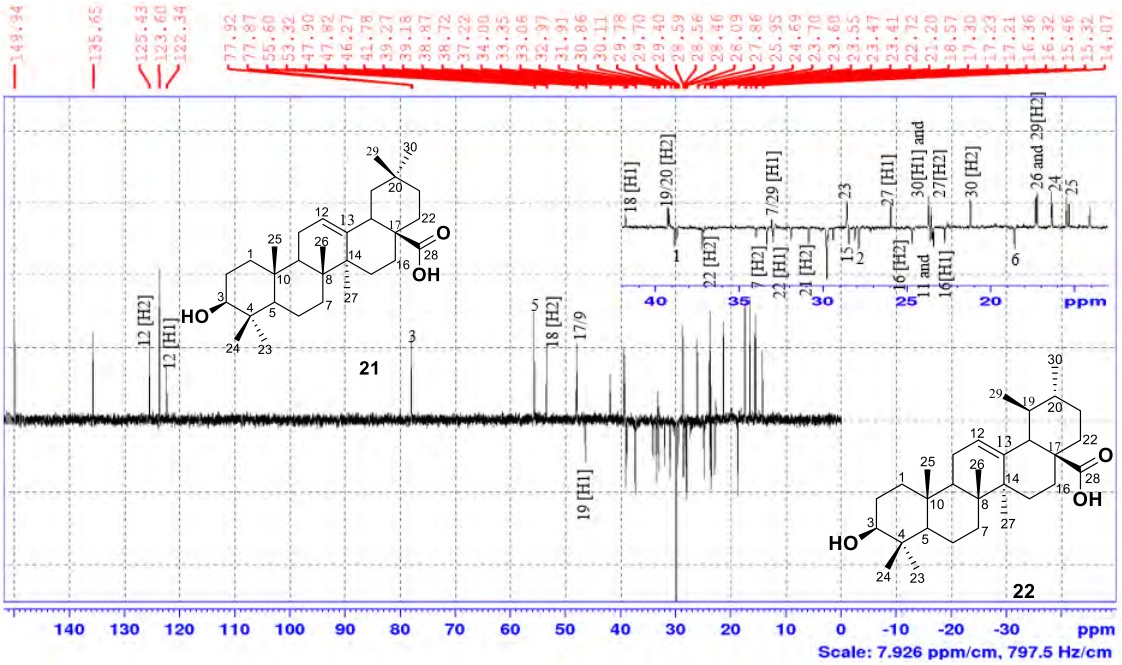

Plate 21E: HSQC spectrum (pyridine-d_5) of compounds **21**[H1] and **22**[H2]

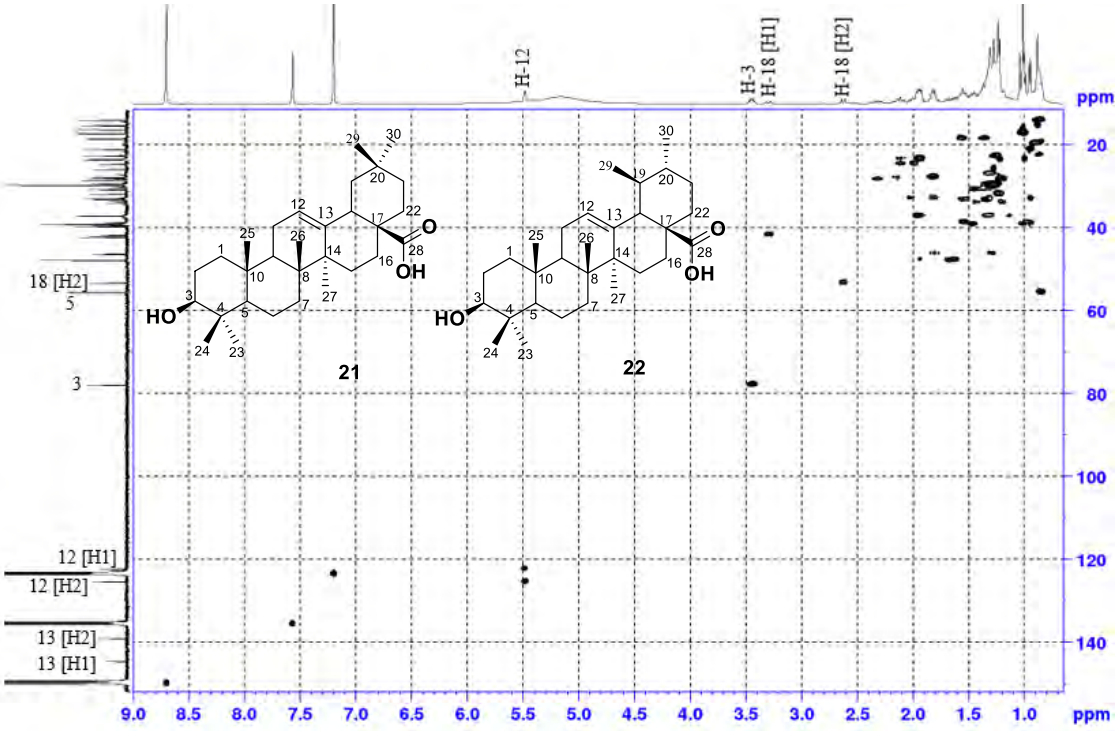

Plate 21F: HMBC spectrum (pyridine-d_5) of compounds **21**[H1] and **22**[H2]

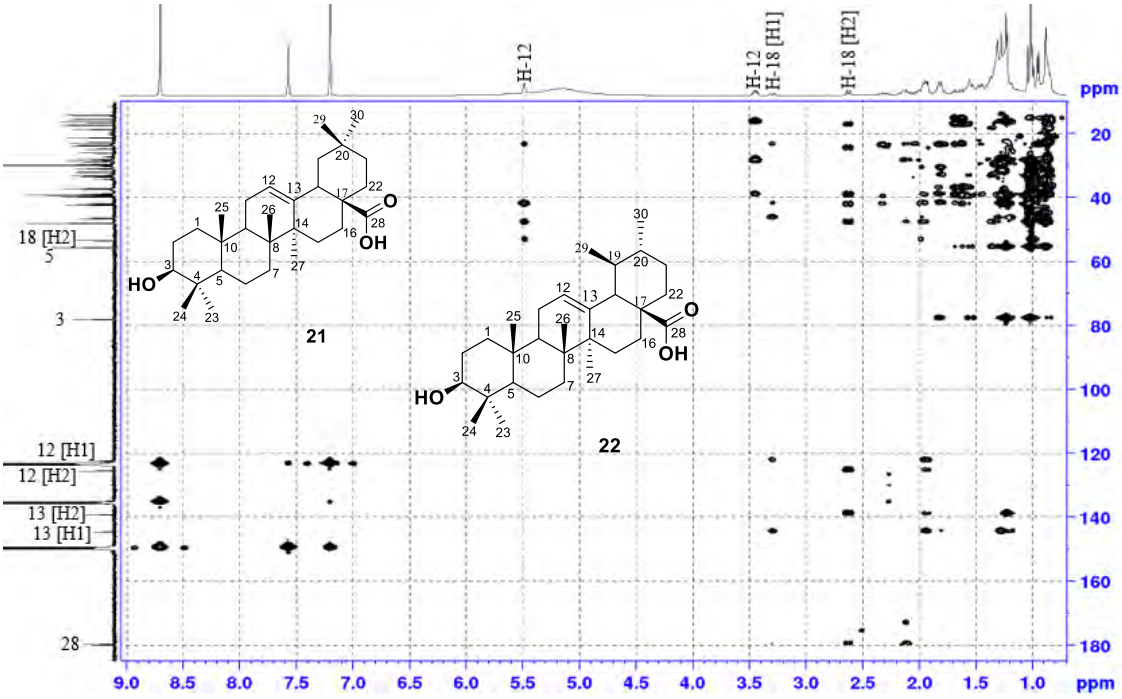

Appendix

Spectroscopic data of the isolated compounds from *Bulbine frutescens*

Plate 22A: ^{1}H NMR (DMSO-d_6, 400MHz) of compound **23**

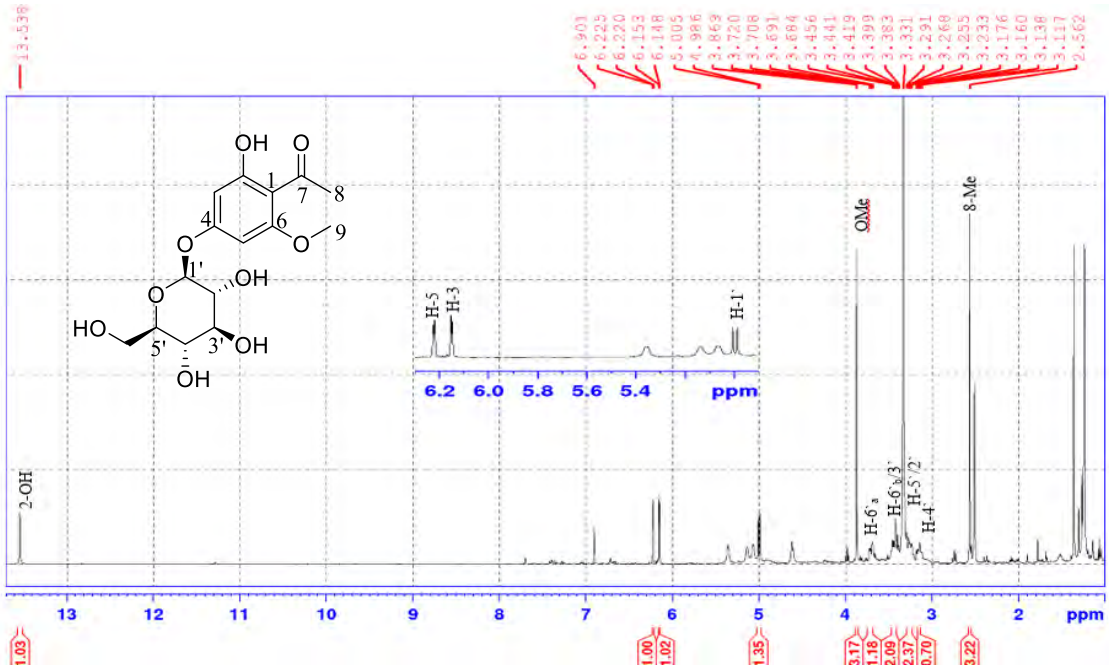

Plate 22B: COSY NMR spectrum (DMSO-d_6) of compound **23**

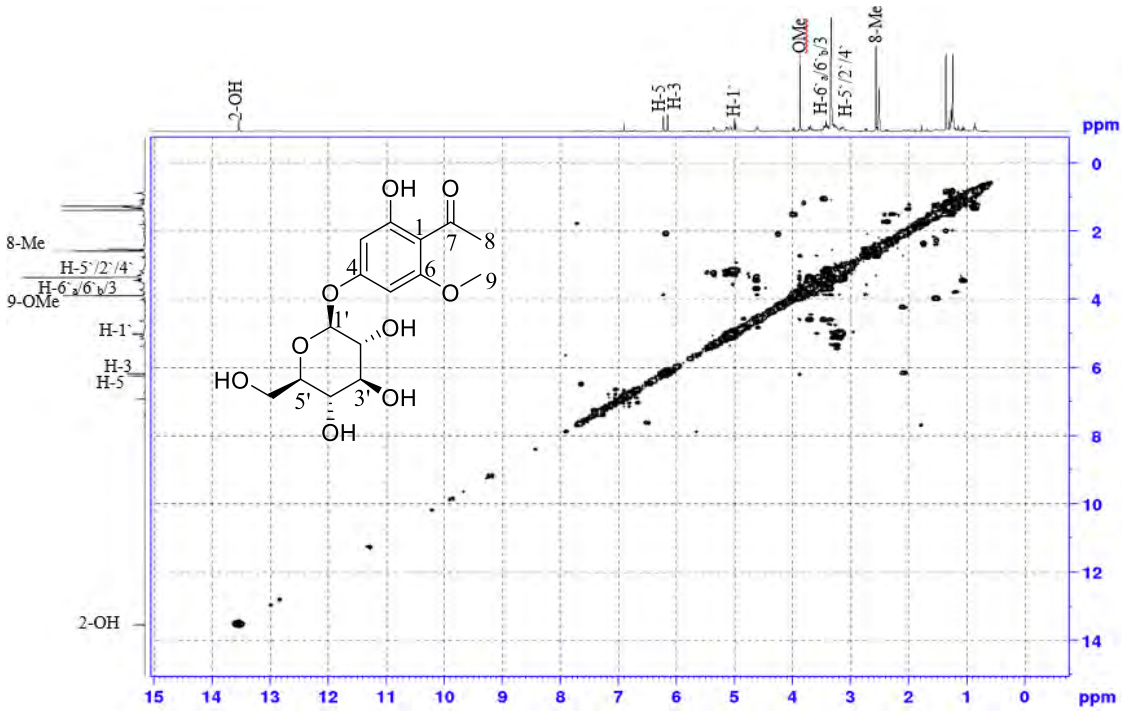

Plate 22C: ^{13}C NMR (DMSO-d_6, 100MHz) of compound **23**

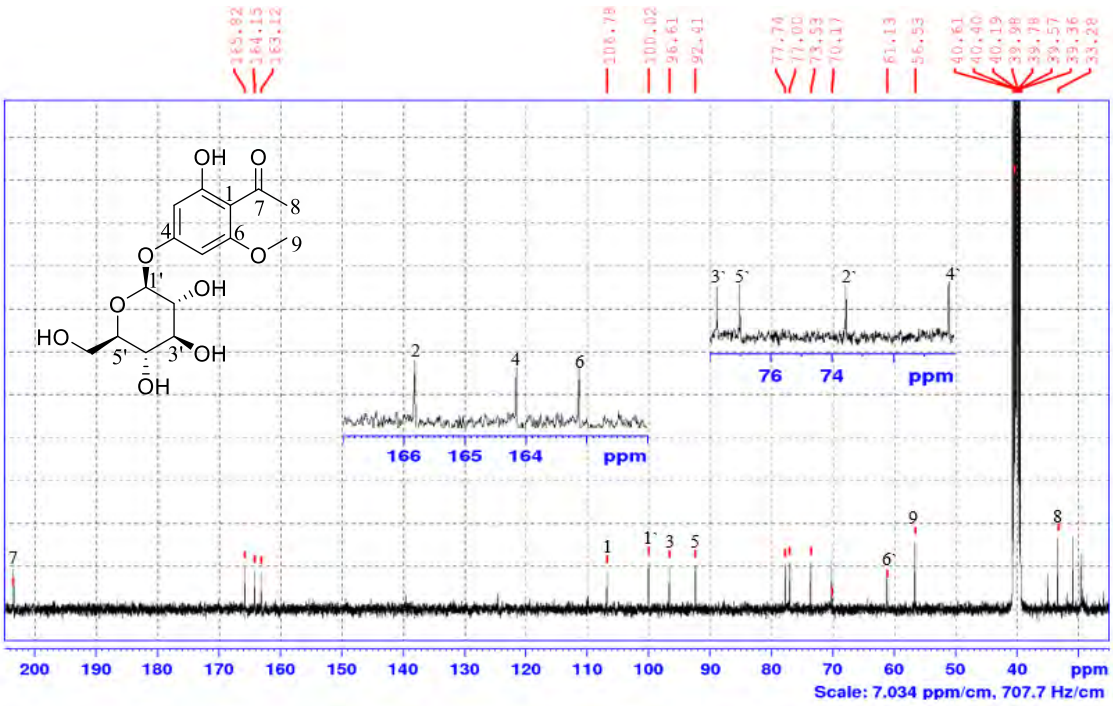

Plate 22D: DEPT-135 NMR spectrum (DMSO-d_6) of compound **23**

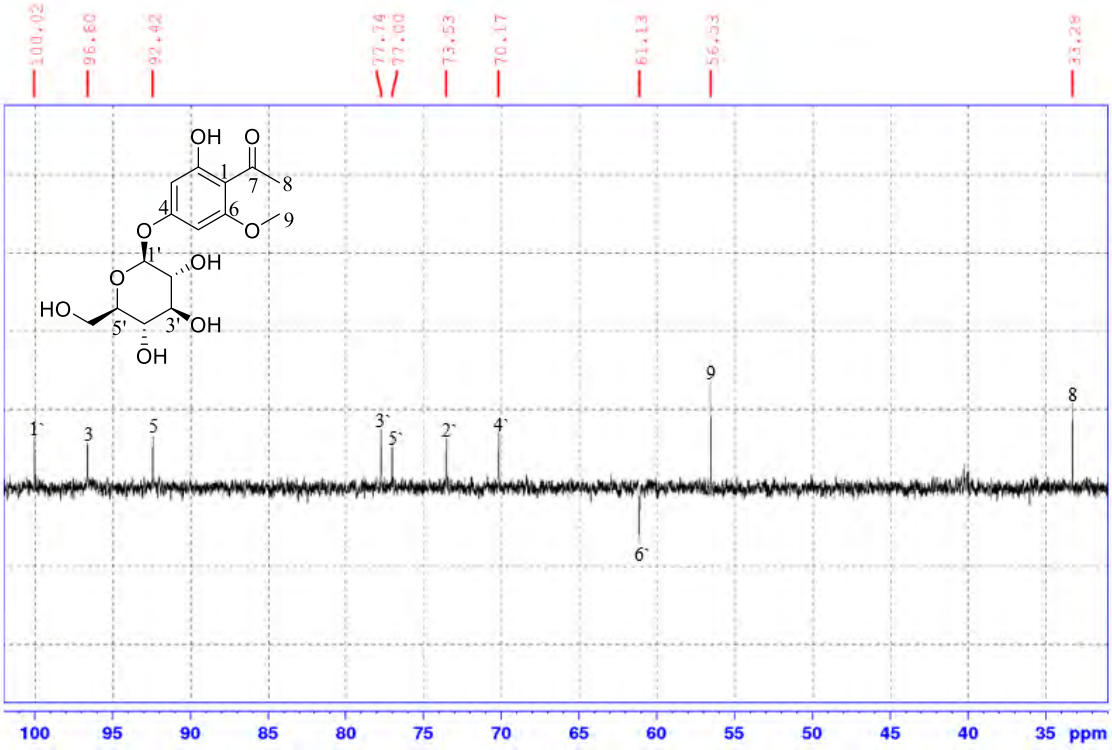

Plate 22E: HSQC NMR spectrum (DMSO-d_6) of compound **23**

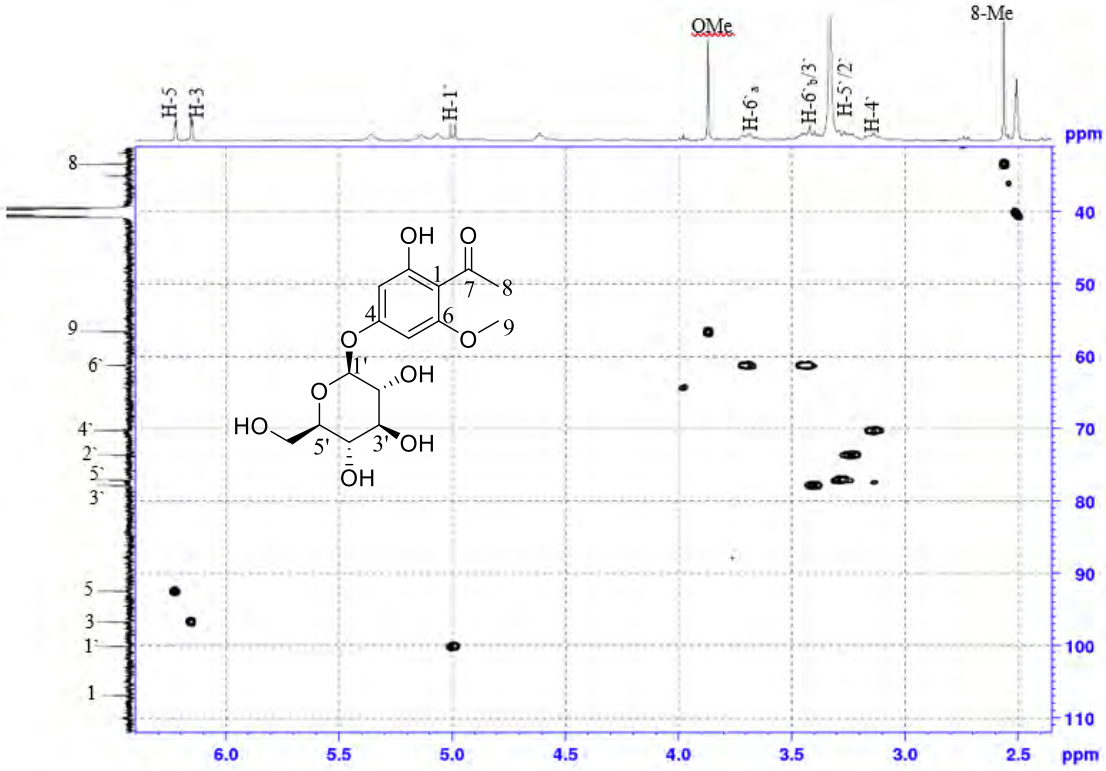

Plate 22F: HMBC NMR spectrum (DMSO-d_6) of compound **23**

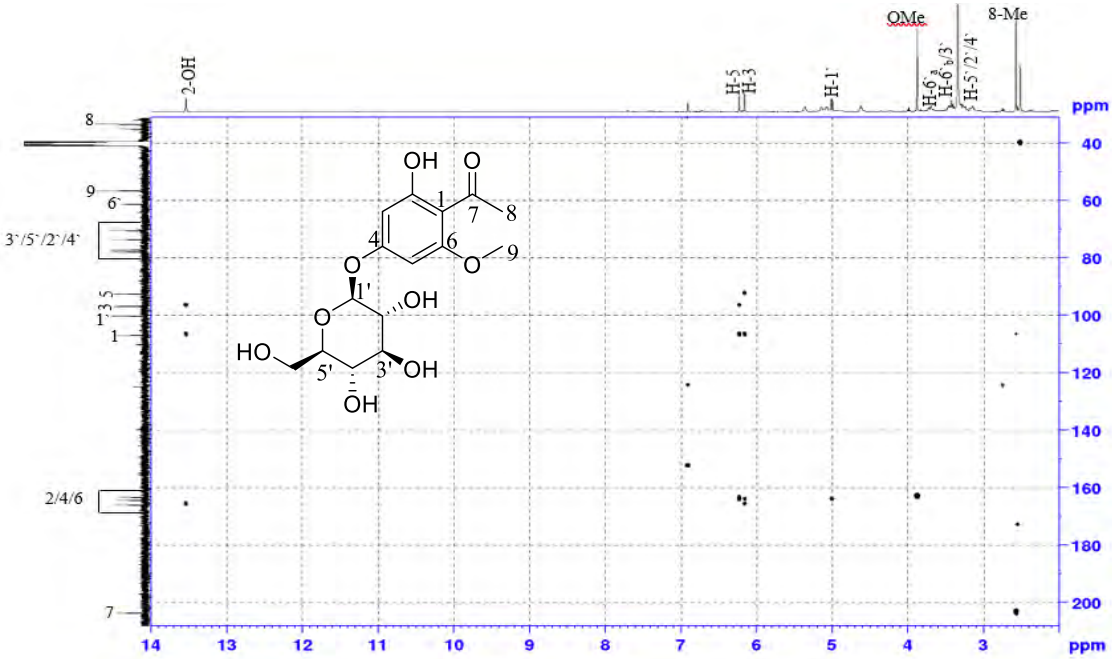

Plate 23A: ^{1}H NMR spectrum (D_2O, 400MHz) of compound **24**

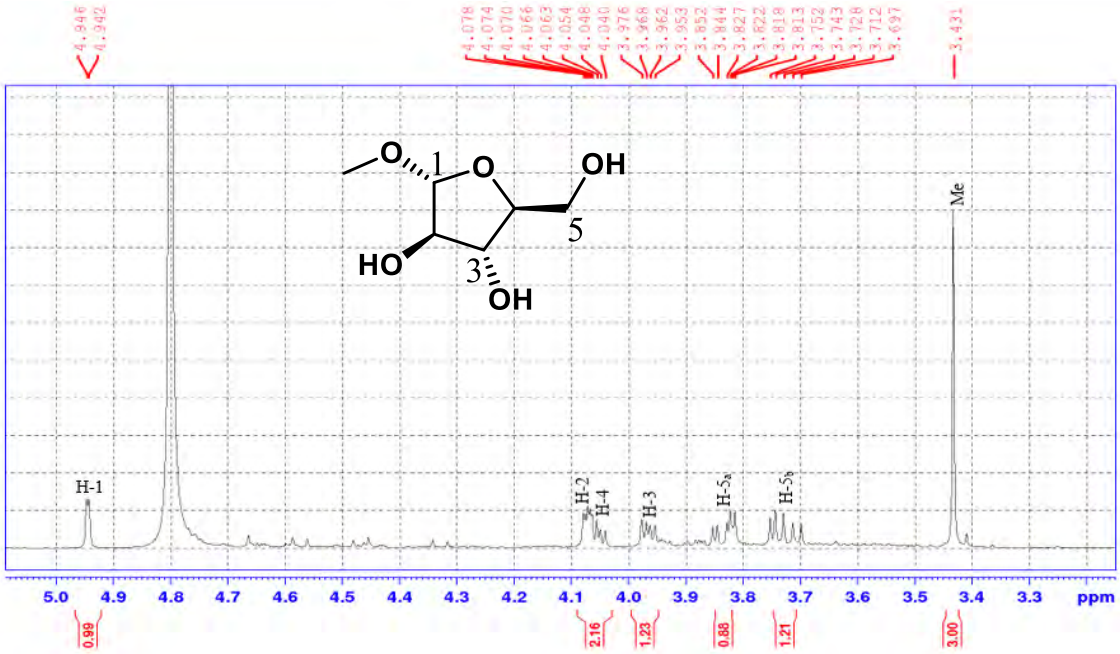

Plate 23B: COSY NMR spectrum (D_2O) of compound **24**

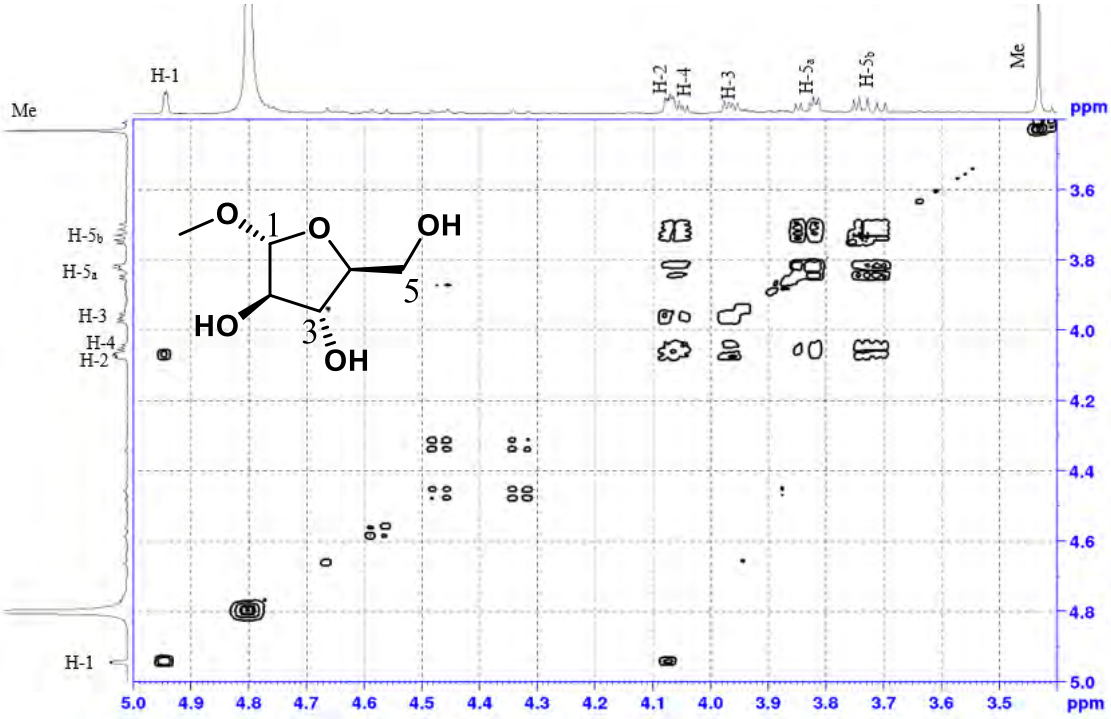

Plate 23C: ^{13}C NMR spectrum (D_2O, 100MHz) of compound **24**

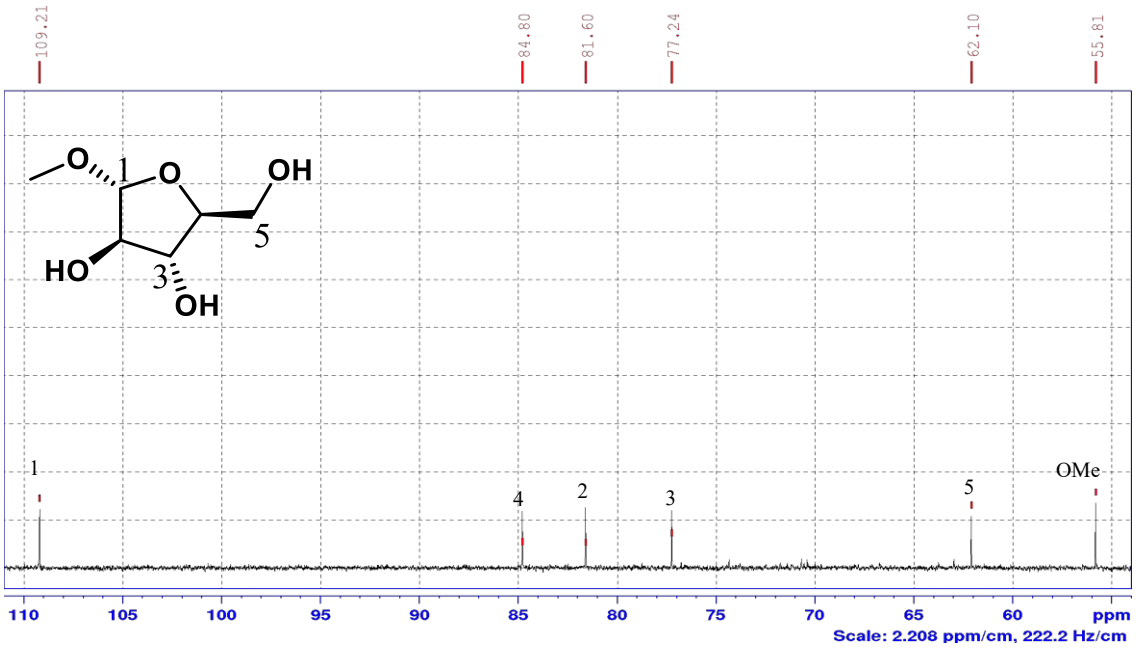

Plate 23D: DEPT-135 NMR spectrum (D_2O) of compound **24**

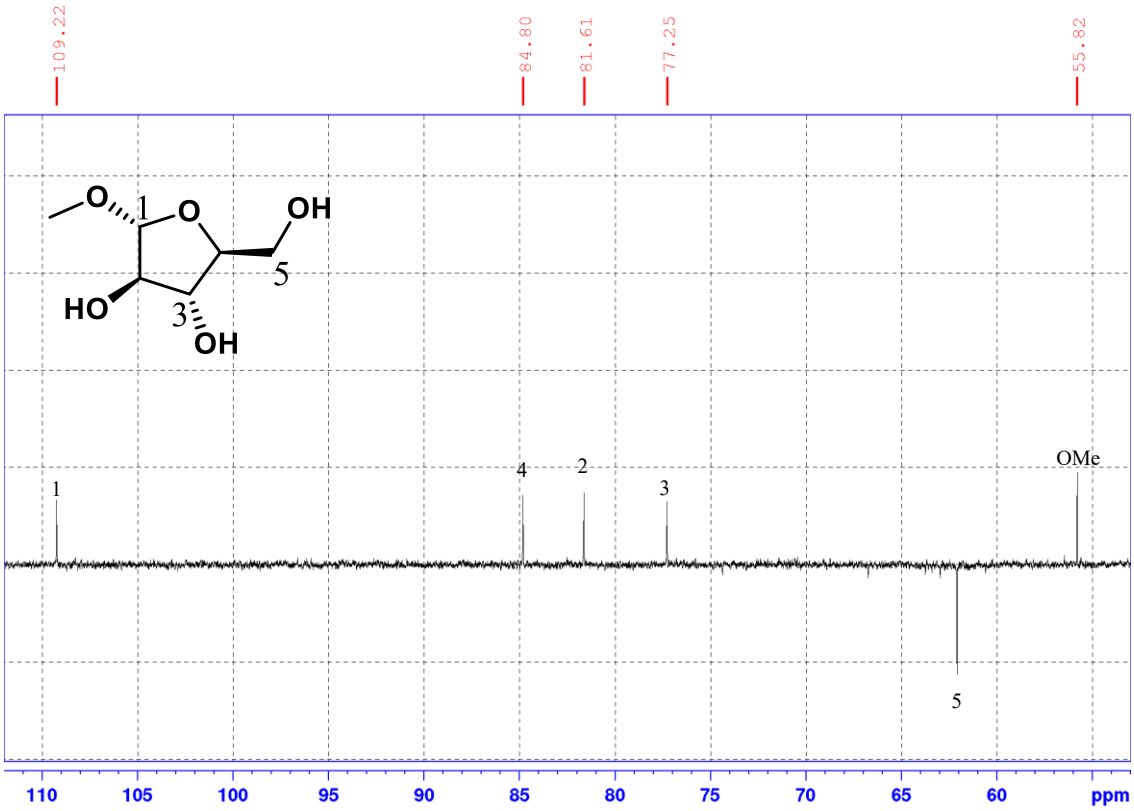

Plate 23E: HSQC NMR spectrum (D_2O) of compound **24**

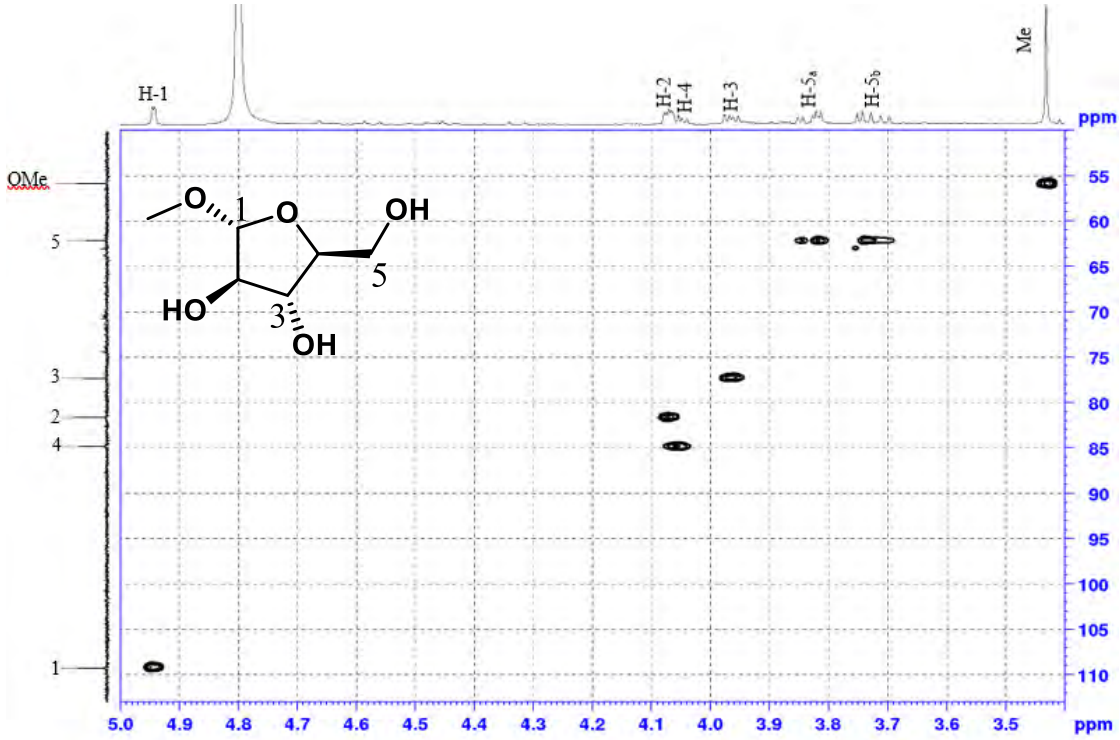

Plate 23F: HMBC NMR spectrum (D_2O) of compound **24**